Role of Aquaporin-Mediated Transport in Salinity Tolerance of Northern Grasses

by

Maryamsadat Vaziriyeganeh

A thesis submitted in partial fulfillment of the requirements for the degree of

Doctor of Philosophy

in

Land Reclamation & Remediation

Department of Renewable Resources
University of Alberta

Abstract

Although many aspects of salinity tolerance in plants have been thoroughly researched, some of the fundamental aspects of plant water relations remain unclear. The main objective of my thesis research was to examine the role of aquaporin-mediated water transport in salinity tolerance of three northern grass species varying in salt tolerance: salt-loving halophytic grass *Puccinellia nuttalliana,* salt tolerant *Poa juncifolia*, and relatively salt intolerant *Poa pratensis*. To achieve this objective, three studies were conducted under controlled-environment conditions.

In Chapter 2, I tested the hypothesis that Na^+ is the principal salt factor responsible for the enhancement of root water transport in halophytic plants, which enables the plants to maintain water balance, gas exchange, and growth under salinity conditions. I subjected plants to 150 mM NaCl, KCl, and Na_2SO_4 treatments to separate different salt factors that affect physiological and growth responses in *P. pratensis*, *P. juncifolia*, and *P. nuttalliana*. The study confirmed the hypothesis and demonstrated that sustained growth, chlorophyll concentrations, gas exchange, and enhanced root cell hydraulic conductivity in *P. nuttalliana* were associated with the presence of Na^+ in the salt treatments. The enhancement of cell hydraulic conductivity was abolished by 50 μM $HgCl_2$, confirming that the effect of Na^+ was on the aquaporin-mediated water transport. The observed increases in root Ca^{2+} and K^+ concentrations also likely played some role in the transcriptional and (or) posttranslational regulation of aquaporins that enhanced root water transport in *P. nuttalliana.*

To examine the molecular basis contributing to water balance maintenance in *P. nuttalliana* under salinity conditions, high-throughput RNA-sequencing and metabolome analyses were carried out in plants subjected to 0 (control) and 150 mM NaCl treatments

(Chapter 3). In RNAseq, a total of 31 Gb clean bases were generated and *de novo* assembled into 941,894 transcripts. The *PIP2;2* and *HKT1;5* transcript levels increased in response to the NaCl treatment implying their roles in water and ion homeostasis. The expression of several transcription factors, including *WRKY39*, *DEK3*, *HY5*, and *ABF2*, also increased in response to NaCl treatment. The metabolomic analysis revealed that the concentrations of proline and dopamine significantly increased under NaCl stress. Several phosphatidylcholines increased in roots suggesting their possible role in maintaining the functionality of cell membranes under salt stress conditions. In leaves, the TCA cycle was enriched pointing to enhanced energy metabolism to cope with salt stress. Microscopic examination of leaf and root structures revealed the presence of epidermal salt glands and enhanced cell wall lignification in the root cells in response to NaCl, which likely contribute to the salt tolerance strategy of *P. nuttalliana*.

In Chapter 4, I cloned *PIP1;1*, *PIP1;3*, *PIP2;1, PIP2;2, PIP2;3,* and *TIP1;1* aquaporins from *P. nuttalliana, P. juncifolia*, and *P. pratensis* to better understand their structure and function in relation to salt tolerance. I analyzed mRNA expression changes of the aquaporins in roots by exposing the plants to 0 (control) and 150 mM NaCl in hydroponic culture. The NaCl treatment upregulated several *PIP* transcripts and decreased the *PnuTIP1;1* expression in *P. nuttalliana*. The *PnuPIP2;2* transcripts increased by about six-fold in *P. nuttalliana* and by about two-fold in *P. juncifolia*, while no changes were observed in *P. pratensis*. I then expressed *PnuPIP2;2* in yeast (*Saccharomyces cerevisiae)* and examined the water fluxes in the absence and presence of 150 mM NaCl using a stopped-flow light-scattering spectrometer. The results demonstrated that the rate of water transport in yeast expressing *PnuPIP2;2* was enhanced by 150 mM NaCl compared to an empty vector control. *PnuPIP2,2* expression also resulted in a higher Na^+ uptake by yeast cells, suggesting its ion transporting function. Structural analysis

revealed relatively high hydrophilicity of *PnuPIP2;2* and the unique pore characteristics that likely affect its transporting properties.

The results of my PhD research clearly point to the importance of aquaporins in water balance maintenance of salt tolerant grasses under salinity conditions. A model based on the study results is proposed to explain the complex responses of *P. nuttalliana* to salt stress and the processes, which likely contribute to water homeostasis in these plants under salinity conditions.

Preface

This thesis is an original work by Maryamsadat Vaziriyeganeh. The work presented in this thesis is part of the research project of Dr. Janusz J. Zwiazek on the functions of aquaporins in plants. With the exceptions explained below, all experiments were carried out and the data were analyzed by Maryamsadat Vaziriyeganeh under the supervision of Dr. Janusz J. Zwiazek and Dr. Micaela Carvajal.

Chapter 2 of this thesis has been published as "Vaziriyeganeh M., Carvajal M., Du N., Zwiazek J.J. 2022. Salinity tolerance of halophytic grass *Puccinellia nuttalliana* is associated with enhancement of aquaporin-mediated water transport by sodium. International Journal of Molecular Sciences 23: 5732". I designed and performed the experiments, collected, and analyzed the data, and wrote the manuscript with the guidance of Dr. J.J. Zwiazek, Dr. M. Carvajal, and Dr. N. Du.

Chapter 3 has been published as "Vaziriyeganeh M., Khan S., Zwiazek J.J. 2021. Transcriptome and metabolome analyses reveal potential salt tolerance mechanisms contributing to maintenance of water balance by the halophytic grass *Puccinellia nuttalliana*". Frontiers in Plant Science 12: 760863". I designed and carried out the experiments with the guidance of Dr. J. J. Zwiazek. Dr. Shanjida Khan assisted with data collection and analysis.

Chapter 4 in this thesis has been submitted for publication to Plant, Cell & Environment as "Vaziriyeganeh M., Khan S., Zwiazek J.J. 2022. Analysis of aquaporins in northern grasses reveal their functional importance in salt tolerance". I designed and carried out the experiments with the guidance of Dr. J.J. Zwiazek. Dr. S. Khan assisted with data collection and analysis.

Acknowledgments

Financial support for the studies described in this thesis was provided by the Natural Sciences and Engineering Research Council of Canada in the form of the Discovery Grant to Dr. J.J. Zwiazek. I am grateful for the Graduate Research Assistantship provided to me by the University of Alberta during my PhD program and for the University of Alberta PhD Recruitment Scholarship.

I would like to thank my co-supervisors, Dr. Janusz Zwiazek and Dr. Micaela Carvajal as well as the supervisory committee member Dr. Stephen Strelkov for their guidance and advice throughout my PhD program. I would also like to extend my gratitude to the external examiners, including Dr. Juan Manuel Ruiz Lozano and Dr. Nadir Erbilgin, for reviewing my thesis.

I am indebted to Dr. Shanjida Khan for teaching me so many valuable molecular biology techniques. I also thank Dr Wenqing Zhang, Dr, Seonghee Lee and other members of the Plant Physiology group for their support and help in the lab.

Finally, I would like to thank my parents and my daughter for their encouragement and support throughout the many years of my university education in Iran and Canada.

Table of Contents

List of Tables

List of Figures

Chapter 1. Introduction and Literature Review

1.1 General Introduction

Salinity is among the most significant environmental factors affecting plants world-wide. Although the greatest economic impact of soil salinity is on agriculture, the primary and secondary soil salinization affects plants in many undisturbed natural ecosystems and in the areas impacted by human activities such as mine reclamation sites (Lalonde et al. 2020, Zhang et al. 2020) and urban areas (Equiza et al. 2017, Zwiazek et al. 2019). Although most of the terrestrial plant species are sensitive to salt, there is great diversity of plants with varying salt tolerance levels. While some of the most sensitive glycophytes may show growth and yield reductions when exposed to NaCl concentrations as low as 10 mM (Chinnusamy et al. 2005), the most salt-tolerant species of halophytes can tolerate soil NaCl concentrations exceeding 1,000 mM and require salt to grow and complete their life cycle (Moir-Barnetson et al. 2016). Not surprisingly, the salt-loving halophytes have received considerable attention of plant scientists, especially in agriculture, since understanding their mechanisms of salt tolerance could help improve salt tolerance of economically important crop plants. As a result, numerous studies have been carried out in the last decades focusing on halophytes and other salt-tolerant plants, and many review articles summarized over the years continuing advances in plant salt tolerance research (e.g., Chinnusamy et al. 2005, Flowers and Colmer 2008, Munns and Tester 2008, Shabala 2013, Mishra and Tanna 2017, Liang et al. 2018, Munns et al. 2020). Although many of these studies recognized the importance of water relations in plant responses to salt and in plant salt tolerance, some of the fundamental processes of salt tolerance involving water relations remain poorly understood. Continuing advances in plant water relations research also make it important to

revisit some of the earlier concepts of plant responses to salt factors. A combination of osmotic imbalance, ion toxicity, and reactive oxygen species generated by the exposure of plants to salt affects water transport into and/or within the plants (Munns and Tester 2008). It is now recognized that one of the initial plant responses to salt stress is an inhibition of root hydraulic conductivity (Martínez-Ballesta et al. 2003, 2008), due to the effect of salt on the aquaporin-mediated water transport in the root tissues (Lee et al. 2010, Lee and Zwiazek 2015). However, my earlier research (Vaziriyeganeh 2017, Vaziriyeganeh et al et al. 2018) showed that in the roots of a relatively salt tolerant grass species *Poa juncifolia*, cell hydraulic conductivity was either not affected or enhanced by NaCl. In the roots of the halophytic grass *Puccinellia nuttalliana*, cell hydraulic conductivity was enhanced even by high NaCl concentrations (Vaziriyeganeh 2017, Vaziriyeganeh et al. 2018). These findings laid the foundations for my PhD research program aimed at better understanding of the processes contributing to the maintenance of water balance in salt tolerant plants and the contribution of aquaporins to these processes. Understanding the effects of salinity on plant water relations is complicated by the presence of different types of salts in saline soils. However, the effects of salt composition on plant water relations and plant hydraulic responses are not well understood. Therefore, in my thesis research I also aimed at separating the effects of different types of ions on plant physiological responses and water transport.

The main objective of my PhD thesis was to contribute new knowledge concerning the processes that enable salt-tolerant plants to regulate their root aquaporin function and to maintain water balance when exposed to salt. I carried out three controlled-environment studies, which examined the role of water transport and aquaporins in the responses to salinity of three species of northern grasses that vary in salt tolerance levels: salt-tolerant halophyte *P.*, moderately salt-

tolerant *P. juncifolia*, and relatively salt-sensitive *P. pratensis*. In the study described in Chapter 2, I tested the hypothesis that sodium is the principal salt factor responsible for the enhancement of aquaporin-mediated water transport in the roots of salt tolerant grasses, and this enhancement plays a significant role in the maintenance of water balance, gas exchange, and growth of halophytic plants exposed to salinity. In the second study (Chapter 3), I carried out the high-throughput RNA-sequencing in roots and metabolome characterizations in roots and leaves of the NaCl-treated halophytic grass *P. nuttalliana* plants to unravel the processes enabling the plants to maintain the functionality of aquaporin-mediated water transport under salt stress conditions. I hypothesized that ion and osmotic homeostasis combined with changes in the aquaporin gene profiles are the key elements involved in the water balance maintenance of these halophytic plants under salinity conditions. Finally, in Chapter 4, I cloned several aquaporins from *P. nuttalliana, P. juncifolia*, and *P. pratensis* to better understand the structure and function of aquaporins in relation to salt tolerance, I tested the hypothesis that the differences in the responses of cell hydraulic conductivity to NaCl in the three grass species, including an enhancement of cell hydraulic conductivity in salt tolerant plants, involve changes in the expression patterns of *PIP* and *TIP* aquaporins as well as the direct effects of NaCl on gating properties.

In addition to the research component, I have included in this PhD dissertation a literature review (Chapter 1.2 – 1.11) to provide a reader with a general background information concerning the topics discussed in the thesis. Finally, Chapter 5 provides an overall synthesis of the thesis and recommendations for future research.

Progressing industrialization and population growth have created many global environmental concerns, not the least of which is increased salinization of soil and water.

Increasing human population and shrinking land availability for cultivation are the two major factors threatening agricultural sustainability (Shahbaz and Ashraf 2013). Elevated soil salinity is a challenging problem for plants in many natural ecosystems and in the areas affected by human activities. Salinity decreases soil fertility and significantly contributes to desertification processes in the world's drylands (Thomas and Middleton 1993). Soil salinization is considered the second most significant cause of land degradation after soil erosion (Zaman et al. 2018). These concerns are especially significant for agricultural crop production (FAO 2016) and explain why so much of our knowledge concerning salinity effects on plants comes from agricultural research. It was estimated that about 20% of the total cultivated land in the world is affected by salinity (Mustafa et al. 2019) and, unless preventive steps are taken, as much as 50% of this land will be salinized by the year 2050 (Ashraf 2009).

Soil salinity refers to the presence of elevated levels of different types of salts in soil water and is usually measured and expressed in units of electrical conductivity (EC). Elevated salinity may be due the presence of salts containing sodium, magnesium, potassium, calcium, and other cations that may be associated with different anions (Tanji 1990). However, the term salt is most commonly applied to sodium salts, especially when accompanied by chloride. NaCl is the most abundant and phytotoxic salt that affects plants worldwide (Franklin and Zwiazek 2004, Isayenkov and Maathuis 2019). The soils that are characterized by high concentration of Na^+ are known as sodic soils while those with high concentrations of NaCl are referred to as saline sodic soils. Sodic (alkaline) soils often contain $NaHCO_3$ and Na_2CO_3, which contribute to high soil pH in addition to elevated Na^+ content (Hu et al. 2015). These soils have usually a very poor structure that makes it difficult for plant roots to penetrate and absorb water and nutrients (Hu et al. 2015). Soil is considered saline when EC of the soil saturated paste extract exceeds 4

dS m^{-1} at 25°C (United States Laboratory Staff 1954) and this definition of soil salinity remains widely used at the present time.

1.2 Sources of Soil Salinity

The sources of soil salinity include both natural and anthropogenic factors (Brindha and Schneider 2019). Soil salinity can be caused by weathering of rocks or parent material. Natural saline areas are widely distributed across the world, especially since many land areas in the world used to be covered in the past by the oceans. They include solonetzic soils that are abundant in the prairie provinces in Canada, and which contain high Na^+ concentrations derived from the incorporation of marine shale into the parent sediments (Cairns and Bowser 1977). Salt can be also carried by wind and rainfall, especially in coastal areas (Sultana et al. 2001). Seawater contains on an average 3.5% salts, mostly NaCl, with EC of about 50 dS m^{-1}, while the EC of rainwater is about 0.01 dS m^{-1} (Yadav et al. 2011). However, of the greatest concern is salinity caused by human activities, such as improper irrigation. It was estimated that about a half of the agricultural lands is affected by salinity (Machado and Serralheiro 2017). Excessive use of fertilizers can also contribute to increasing soil salinity as more chemicals are added to the soil. Another important factor contributing to soil salinity is deforestation, which can lead to increased soil temperature and enhanced evaporation, resulting in salt build-up at the soil surface (Hastenrath 1991). When deforested sites are converted to agricultural areas, a gradual salt build-up due to irrigation makes the soil in many cases unsuitable for future afforestation (Jimenez-Casas and Zwiazek 2014). Similarly, overgrazing in arid and semi-arid areas can result in desertification and increased evapotranspiration may cause salt accumulation in the soil (Szaboles 1994). Other cause of salinity include contamination with chemicals, which mainly

occurs in industrial areas when industrial chemicals containing salts are discharged into the soil (Yadav et al. 2011) and the use of de-icing salts in urban areas (Equiza et al. 2017).

1.3 Types of Soil Salinity

1.3.1 Primary (natural) salinity

There are several different classifications of soil salinity and most of them are related to the processes involved in salt accumulation. Primary salinity is caused by natural processes such as accumulation of salts over many thousands of years through weathering of rocks or buildup of salt carried from the oceans by wind. Natural soil salinity is affected by the chemistry of the parent material and of the ground water. The movement of salts into and out of the soil depends on the movement of water which carries dissolved salts. When precipitation rates exceed evapotranspiration rates, water may infiltrate deeper soil layers and move salts into the ground water and, eventually, be discharged into lakes and oceans (Dehaan and Taylor 2002). Natural soil salinization, also referred to as the "primary salinization", takes place mainly in the areas where precipitation levels are low and evapotranspiration rates are high (Fitzpatrick et al. 2000). This causes an upward movement of salts from the groundwater and deeper soil layers to the soil surface where they accumulate. In the areas where vegetation is cleared, the amount of water taken up by plants from the soil decreases and more water is leached into the groundwater, causing the groundwater levels and salts to rise. When the water evaporates from the soil surface, salts are left behind. Dryland salinity can also occur in irrigated areas where deep-rooted trees are replaced with shallow-rooted agricultural crop plants causing excessive leaching and rising groundwater and salts (Pannell and Ewing 2006). Dryland salinity cannot be easily managed. One relatively effective method to deal with dryland salinity is to pump the saline ground water for safe disposal or further use for irrigation of deep-rooted trees or plants that are salt tolerant

and can accumulate the salt. This method is referred to as the bio- (or biological) drainage and may be considered as the type of phytoremediation (Pannell and Ewing 2006). Dryland salinity has a severe negative economic impact in many parts of the world including South-Western United States, Mexico, and Australia by affecting agricultural production and water quality (McFarlane et al. 2016).

1.3.2 Secondary soil salinity

Unlike natural salinity, secondary salinity occurs due to human activities such as agricultural irrigation in which water is reapplied to plants over many cycles. Each time when water is applied, some of it will evaporate and salt will remain behind and become more concentrated (Shahbaz and Ashraf 2013). Shortage of water in arid and desert areas requires the use of saline and brackish water (water with elevated salts, but less than in seawater) to meet the demand of crop plants in intensive agriculture. The unsuitable use of such poor-quality waters, especially in soils characterized by slow drainage, results in the capillary rise and evaporation of the soil water, which cause development of surface salinity (Sparks and Carey1995). A similar process is partly blamed for an elevated soil salinity of oil sands mine tailings in northeastern Alberta, Canada, where water that is used for bitumen extraction is recycled many times before being deposited in mining pits for reclamation and revegetation (Lalonde et al. 2020). There are several strategies that are used to manage irrigation salinity including facilitating consistent water distribution, draining excess salt from the soil surface into subsoil, mixing fresh and saline waters, and the use of salt tolerant plants such as halophytes (Machado and Serralheiro 2017).

1.4 Effects of Salinity on Plants

Soil salinity is one of the most challenging environmental factors affecting plant distribution, growth, and productivity because the majority of plants are salt-sensitive and are affected by even moderate concentrations of salts (Shrivastava and Kumar 2015). Plant responses to salinity and physiological processes involved in these responses have been thoroughly described in many reviews and in my MSc thesis (Vaziriyeganeh 2017). I will present here a general overview of literature to help the reader understand some of the concepts described in this thesis.

Salinity can affect plants in many ways and its negative impact is usually due to complex interactions between physiological and biochemical processes (Akbarimoghaddam et al. 2011). Salinity can affect all stages of plant vegetative and reproductive growth as well as seed germination (Shrivastava and Kumar 2015). The most phytotoxic salt is NaCl and its effects on plants include osmotic stress, ion toxicity, nutrient imbalance, especially N, Ca, K, P, Fe, and Zn, as well as oxidative stress (Munns and Tester 2008). Following an exposure of plants to salinity, the first and most detrimental effect that is observed is osmotic stress. Therefore, maintaining osmotic balance are essential for plants to tolerate salinity (Adem et al. 2014). Failure to maintain osmotic balance results in reduced water uptake, loss of turgidity, cell dehydration, as well as reductions of transpiration rates and photosynthesis (Munns and Tester 2008). Initial effects of NaCl, but not necessarily other salts, may include an inhibition of root water transport (Azaieh et al. 1992, López-Berenguer et al. 2006, Lee et al. 2010). Various physiological processes are affected including transport of photosynthates, ion and hormonal balance, and nutrient uptake (Ashraf 2004, Munns and Tester 2008). As with other environmental stresses, oxidative stress follows and the resulting accumulation of reactive oxygen species triggers

antioxidant defenses (Isayenkov and Maathuis 2019). Ion toxicity, that follows osmotic stress in plants exposed to salinity, develops over time as cations and anions accumulate in plant tissues. This stress can be delayed, or even prevented, in salt-tolerant plants by reducing salt uptake from the soil, salt sequestration in the vacuoles and cell walls, and (or) its secretion through special glands (Zhu 2002). For NaCl, Na^+ is considered more toxic to plants compared with Cl^- and it can compete with other cations, mainly K^+, and cause ion imbalance in cells (Isayenkov and Maathuis 2019). However, Cl^- can act synergistically with Na^+ and aggravate its effects on plants, likely due to its effect on the Na^+ membrane transport (Franklin and Zwiazek 2004).

1.5 Soil Salinity Monitoring

Soil salinity is commonly measured as electrical conductivity (EC) of the soil solution, soil saturated paste, or 1:1 (volume) mixture of soil and distilled water (Smith and Doran 1996). The Standard International (SI) unit of EC is Siemen per meter (S m^{-1}). However, other units, including dS m^{-1} (1 dS m^{-1} = 10 S m^{-1}), can be often found in the literature. Siemen replaces mho (representing the reciprocal of ohm) that was commonly used in the past (Smith and Doran 1996). Measuring salinity is an important analytical factor for determining suitability of soil for growing plants. Generally, EC values of saturated soil extracts of less than 2 dS m^{-1} are considered non-saline. Salt-sensitive plants can be affected by EC between 2 and 4 dS m^{-1} and most crops are affected by EC between 4 and 8 dS m^{-1}. Only a few species of the most salt tolerant crop plants can grow in soils with EC values higher than 16 dS m^{-1} (Zaman et al. 2018).

1.6 Halophytes

1.6.1 What are halophytes?

Over a century ago, von Marilaun described halophytes as the plant species that are adapted to saline environments (Cheeseman 2015). There is much interest in halophytes because understanding their mechanisms of salt tolerance is viewed as a potentially important step in improving salt tolerance of glycophytic plants through either conventional breeding or genetic engineering. True halophytes are plants that can attain their optimal growth at high NaCl concentrations and require salt to complete their life cycle. However, there is still some confusion as to what these concentrations should be for plants to be classified as the halophytes and often halophytes are referred to as highly salt-tolerant plants whether they require salt for survival. Some literature considers these concentrations to be 300 mM or higher (Flowers et al. 1977). However, other NaCl concentration thresholds have also been proposed ranging from as low as 70 mM (Greenway & Munns 1980) or 85 mM (Glenn et al. 1999) to 200 mM (Flowers and Colmer 2008). This lack of consensus demonstrates that there is a considerable difference in salt tolerance between various plant species. In late 1990s, about 600 plant species were listed as halophytes (Glenn et al.1999). However, in the 2014 eHALOPH Halophyte Database, this number increased to about 1,500 plant species (Flowers 2014), and in the same year, 1,653 halophyte species were listed by a different source (Saslis-Lagoudakis et al. 2014). This discrepancy may, possibly, be again due to the lack of a strictly defined threshold required for plants be considered halophytes. Halophytes probably evolved as the descendants of charophytic algae (Lewis and McCourt 2004). It was suggested that glycophytes were evolved before halophytic plants since environmental conditions around the freshwater pools of water were more suitable than saline waters for plants to grow (Flowers et al. 2010).

Despite the ability of halophytic plants to tolerate high salt concentrations, most studies on salt effects and salt tolerance in plants have been carried out in glycophytes since they include most of the economically important plant species. Glycophytes are salt-sensitive plants, although their salt tolerance widely varies between species, however, with the growing salinity concern and development of genetic engineering tools, potential economic importance of halophytes is gaining more attention as is the awareness that understanding salt tolerance mechanisms in halophytes may help with the efforts of improving salt tolerance in glycophytes. Several species of halophytes including as *Thellungiella salsuginea* (described initially as *T. halophila*), *Mesembryanthemum crystallinum*, and *Suaeda salsa* became model plants for the research aimed at understanding salt tolerance mechanisms (Inan et al. 2004). Unfortunately, although some studies observed enhanced salinity tolerance in transgenic plants (e.g., Munns et al. 2012), only a limited success has been achieved in improving salt tolerance of plants through biotechnology.

1.6.2 Classification of halophytes

Considering the problems with reaching a consensus of what constitutes a halophyte, or even a salt-tolerant plant, it should not come as a surprise that different classifications have been also proposed for halophytes. In one of the most widely used classifications, halophytes are divided into obligate, facultative, and habitat-indifferent categories (Cushman 2001). Obligate halophytes are plants that require salt to complete their life cycle and sodium is considered for them an essential element. Sometimes, obligate halophytes are considered the only true halophytic salt-loving plants and it was hypothesized that they developed in saline habitats to avoid competing with glycophytes (Grigore and Toma 2017). In the above classification, facultative halophytes avoid saline soils, but can tolerate moderately high salt concentrations. However, their optimum growth occurs in the absence of salt or in low-salinity soils. (Cushman

2001). Habitat-indifferent halophytes prefer to grow in a salt-free soil but can also grow in moderately saline soils that are too high for salt-sensitive plants to survive. The distinction between these different classes of halophytes, especially the facultative and habitat-indifferent halophytes, is rather unclear and often based on the salt tolerance level combined with ecophysiological characteristics (Cushman 2001). Similarly, in this classification, the distinction may be difficult to make between the salt-tolerant glycophytes and the facultative or habitat-indifferent halophytes. One of the more recent classifications of halophytes is based on integrating the anatomy with ecological factors. In this classification, halophytes are divided into extreme-halophytes and meso-halophytes (Grigore and Toma 2017). Extreme-halophytes are the plant species that are well adapted to salinity and grow only in saline soils while meso-halophytes display lower salt tolerance level (Grigore and Toma 2017). None of the proposed classifications is perfectly clear and inclusive, partly because there is still no consensus regarding the definition of a halophyte.

1.6.3 Salt resistance mechanisms in halophytes

According to Levitt (1972), stress resistance mechanisms in plants can be due to either stress avoidance or stress tolerance, (and in some cases also stress escape). While this terminology can be also applied to salt stress, it is often difficult to separate salt tolerance and salt avoidance mechanisms in plants and the terms tolerance and resistance have been commonly used interchangeably. Salt resistance is affected by plant growth and developmental stage. As plants grow, they usually develop more salt resistance mechanisms and, therefore, older plants are often more salt resistant compared with younger plants (Vicente et al. 2004). Like all other plants, halophytes may use various stress resistance mechanisms and, in addition to tolerating

high salt levels in their tissues, they can also avoid salt buildup in their cells and tissues by restricting salt uptake, sequestering, and (or) secreting it.

Compared to glycophytes, halophytic plants have acquired unique morphological, structural, and physiological strategies to cope with salt in their environment (Donohue et al. 2010). When salt tolerance is used as a term to describe the ability of plants to cope with high salt concentrations in the cytosol, if may refer to various processes, often involving complex enzymatic pathways that protect the cytoplasm against toxic effects of salt. Some of these processes may include signal transduction, ROS scavenging and detoxification pathways, osmotic adjustment, and maintenance of ion balance through an accumulation of ions such as K^+ and organic solutes, as well differential expression of salt responsive genes and transcription factors (Flowers and Colmer 2008, Khan et al. 2016).

Salt avoidance relies on the mechanisms, which prevent salt from accumulating in sensitive parts of the plant, such as the cytoplasm (Mishra and Tanna 2017). Some of these mechanisms include salt secretion, salt exclusion, some forms of salt sequestration, leaf shedding, and succulence (Shabala et al. 2014). There are some halophytes, referred to as recretohalophytes that can secrete salt from their leaves (Flowers et al. 2015). About 370 recretohalophytes have been identified all over the world mainly in seawaters and saline lands (Flowers et al. 2010). These plants develop unique structures such as salt glands, salt hairs or salt bladders that enable them to secrete salt out of the plants. Salt bladders and salt glands have different structures. Salt bladders consist of one balloon-shaped epidermal bladder cell that is about ten times bigger than neighboring epidermal cells (Shabala et al. 2014). In *Mesembryanthemum crystallinum*, salt bladders originate from a single trichome (epidermal hair). These structures form very fast and are unstable. Once the bladder accumulates certain

amount of salt, salt bladders easily break up and release salt to the surrounding area (Shabala et al. 2014).

Salt glands are two- or multicellular structures. These structures can store large amounts of salt inside them. Salt glands form more stable structures compared with salt bladders (Yuan et al. 2016). Some of the earliest studies on salt secretion were performed on the salt bladders of *Hormosira banksii* (Bergquist 1959). However, more recent studies aimed at understanding secretion mechanisms and salt transport pathways in salt bladders and salt glands focused on *Chenopodium quinoa* and *Limonium bicolor* (Shabala et al. 2014). In addition to forming unique structures such as salt bladders and salt glands, some halophytes are able to secrete salt as a liquid through the leaf edges and once in contact with the air, water evaporates and salt turns into crystals. Shedding of the old leaves is another salt avoidance strategy in some halophytic plants that helps remove excessive salt (Grigore and Toma 2017).

Salt exclusion is an adaptation of halophytes that allows them to minimize an uptake of sodium and chloride from soil and their transfer to the shoots. In this way, salt concentration in the shoots can remain low and the damage produced by salt is minimized (Munns 2005). Due to this unique feature, the concentration of salt in the shoots of salt-excluding halophytes is much lower than in the roots. A similar strategy of Na^+ accumulation in roots and restricting its transfer to shoots has been also described for many glycophytes and is especially effective in woody plants (Apostol and Zwiazek 2003, Franklin and Zwiazek 2004, Hussain at al. 2004).

There are several enzymatic and metabolic pathways involved in salt exclusion mechanisms. Maintaining high concentration of K^+ and low concentration of Na^+ in the cytoplasm through ion homeostasis is crucial for plant survival in both halophytes and glycophytes under salinity conditions. Sodium can reach toxic levels faster than chloride,

resulting in severe damage to cell structures. Plants attempt to maintain the balance between of Na^+ influx and efflux (Tester and Davenport 2003). The salt overly signaling (SOS) pathway is considered an essential pathway for Na^+ exclusion and ion homeostasis control at the cellular level (Shi et al. 2000). The SOS pathway includes three protein complexes known as SOS1, SOS2, and SOS3. Each complex has a specific function, and they all depend on each other. After roots perceive salt stress and Na^+ enters the cells, a spike of Ca^{2+} in cells activates the SOS signal transduction (Yi et al. 2013). SOS3 encodes a calcium-binding protein that activates the serine/threonine protein kinase SOS2. The SOS3–SOS2 interactions recruit SOS2 to the plasma-membrane leading to the activation of SOS1, a Na^+/H^+ plasma membrane antiporter, which facilitates Na^+ efflux from the cell (Shi et al. 2000, Fuglsang et al. 2007, Ji et al. 2013, El Mahi et al. 2019). The function of SOS1 in Na^+ efflux is linked to H^+-ATPase activity (Fuglsang et al. 2007) and is an active mechanism that requires energy input. The hydrolysis of H^+-ATPase, located in the plasma membrane, releases the energy that is used to generate H^+ gradient across the membrane (Palmgren 2001) and its activity commonly increases after exposure to salt in salt-tolerant plants (López-Pérez et al. 2009). The H^+-ATPase is considered an essential housekeeping enzyme in plants and, in addition to salt stress, it can be regulated by various internal and environmental factors including light, temperature, mineral nutrients, and water availability (Morsomme and Boutry 2001).

1.6.4 Oxidative stress and salinity tolerance of halophytes

Oxidative stress signaling and ROS detoxification are important processes contributing to salt tolerance in plants. Formation of ROS is a consequence of exposure of living organisms to oxygen and cannot be completely avoided. However, excessive accumulation of ROS often takes place in plants exposed to salinity and other environmental stresses and leads to oxidative stress,

which can severely damage lipids, proteins, and nucleic acids (Pan et al. 2006). There are numerous highly reactive radical and non-radical species of oxygen, including superoxide anion (O_2^-), hydroxyl radical (HO•), hydrogen peroxide (H_2O_2), and singlet oxygen ($^1O_2$) that may accumulate in plants during stress events (Waszczak et al. 2018). To protect cells against the consequences of oxidative stress, plants have developed various enzymatic and non-enzymatic systems to scavenge the ROS produced from the electron transport chains in mitochondria and chloroplasts. There are numerous enzymes in plants that are credited with ROS scavenging properties including different peroxidases, peroxiredoxins, and catalase (Foyer and Shigeoka 2011, Dumont and Rivoal 2019). Enhanced enzymatic scavenging of ROS has been proposed as a probable mechanism contributing to salt tolerance in several halophytic grasses including *Puccinellia* sp. (Roy and Chakraborty 2014). Ascorbic acid, tocopherols, carotenoids, flavonoids, polyamines, and glutathione are among the common non-enzymatic scavengers of ROS in plants (Foyer and Shigeoka 2011, Dumont and Rivoal 2019). Similarly, to all other plants, early sensing and signaling of salinity stress are the key elements of salt tolerance mechanisms in halophytes (Bose et al. 2014, Nikalje et al. 2019). However, it was argued that halophytes and other highly salt-tolerant plant species possess efficient Na^+ exclusion mechanisms and do not require a high level of antioxidant activity since effective salt exclusion prevents excessive ROS production (Bose et al. 2014).

Although excessive production and accumulation of ROS leads to oxidative stress, ROS also act as important regulatory molecules in plants and play major roles in early signaling events affecting many different plant functions (Das and Strasser 2013, Nikalje et al. 2018, Waszczak et al. 2018). These signaling pathways can play a crucial role in plant growth, development, gravitropism, hormonal action, and many other physiological responses (Miller at

al. 2008, Ray et al. 2012, Waszczak et al. 2018). The balance, between the formation of ROS and their scavenging by the enzymatic and non-enzymatic means in plants defines their role in plant growth and development (Foyer and Noctor 2005, Nikalje et al. 2018).

1.6.5 Salt tolerance and accumulation of compatible solutes in halophytes

Accumulation of compatible solutes is one of the strategies that halophytes use to enable them cope with high concentrations of salt. These osmolytes include low molecular weight neutral organic molecules, sugars, polyols, polyphenols, glycine betaine, proline, and other amino acids that accumulate in cells (Flowers and Colmer 2008). In addition to their osmotic properties, organic solutes help protect the integrity of cell organelles by stabilizing proteins and other macromolecules (Baturin et al. 2014, Patel et al. 2016). These molecules generally have a net neutral charge so their accumulation does not affect charge balance in the cell that would negatively affect the cell function (Jogawat 2019). Osmolytes play an important role in balancing the low osmotic potential of the vacuoles and the apoplast that develops as a result of Na^+ and Cl^- accumulation. Therefore, similarly to drought stress, osmotic adjustment by compatible solute accumulation is an important factor in preventing cell dehydration and maintaining cell turgor and physiological functions (Turner et al. 2007). Osmolyte accumulation is among the earliest responses of plants exposed to salinity and other environmental stresses that affect osmotic balance in plants such as drought and temperature stress (Burg and Ferraris 2008). In addition to maintaining osmotic balance, osmolytes may act as antioxidants, photosynthesis protectants, macro-biomolecule stabilizers, and protein folding enhancers (Szabados et al. 2011, Jogawat 2019). Polyamines, amino acids, and their derivatives have been reported to protect DNA, and enzyme function in plants (Paul et al. 2017, Jogawat 2019). The osmolytes that are

likely to serve the most prominent role in salt tolerance of halophytic grasses include proline, glycine betaine (Roy and Chakraborty), and inositols (Sengupta et al. 2008).

1.7 Water Relations

1.7.1 Importance of water for plant growth

Although water is the most abundant molecule on the Earth's surface, the availability of water is considered the most limiting factor to plant growth and productivity in most parts of the world (McElrone et al. 2013). Water plays a crucial role in all physiological processes and large amounts of water are required for most plants to reach their maximum growth potential. Water constitutes about 70–95% of fresh weight in the non-woody plant tissues (Kramer and Boyer 1995). Among many diverse roles that it plays it plays in plants, water functions as a universal solvent, as a reactant in many biochemical reactions, it is essential for cell expansion, and is responsible for maintaining turgor (Wheeler 2005).

The concentration of solutes in plant cells is usually high, producing low osmotic potential, which drives water influx into the cells and creates a positive pressure (turgor) when the swollen protoplasts push against the cell walls. Turgor pressure is largely responsible for providing mechanical support to non-woody tissues and it usually ranges between 1.0 and 5.0 MPa in plants with an adequate water supply (Kramer and Boyer 1995). Plant growth and functionality is affected by the loss of turgor since the pressure on the cell walls is required for cells to expand as the key element of growth processes (Chavarria and dos Santos 2012). Although different plants may vary in their water use efficiency, they all require large amounts of water since most of it is lost through transpiration. Studies showed that while more than 90% of absorbed nitrogen, potassium and phosphorus are incorporated into the plant tissues, only less

than 1% of the absorbed water is used for biomass production (Lambers et al. 2008). A large individual tree can lose as much as 2,000 liters of water by transpiration on a hot summer day (Forest Research 2020).

1.7.2 Root water transport pathways

Water is mostly absorbed by plants from the soil through the root system. The root system usually has a complex network of fine absorbing roots with hairs that increase the root absorption area (McCully 1999). The roots of most plants growing under natural conditions are colonized by mycorrhizal fungi, which form a hyphal network extending into the soil and aid with the uptake of water and mineral nutrients (Smith and Read 2008). Once water is absorbed by roots, it must be radially transported into the vascular cylinder through a combination of apoplastic, symplastic and transmembrane pathways. With the exception of tall trees, this is the site of the greatest resistance to water flow in plants (Steudle and Peterson 1998).

Water moves as a result of osmotic and hydrostatic (transpiration-driven) forces through the places of least resistance (Steudle and Peterson 1998). Root apoplastic pathway refers to the transport of water from the root surface to the xylem through the cell walls and intercellular spaces. This is often the lowest resistance pathway in roots until water reaches the exodermis, and (or) the endodermis, in the outer and inner parts of the cortex, respectively. Radial cell walls of the exo- and endodermis contain suberized Casparian strips, and become lignified with age, which forces water with dissolved solutes to cross the plasma membrane into the protoplast (Enstone et al. 2002).

In symplastic pathway, water moves between adjacent cells through plasmodesmata, which interconnect neighboring cells and allow water to be transported between the cells without crossing the plasma membranes. In this pathway, water moves slowly since it must pass through

the living cell components (Caldeira et al. 2014). Since water movement through this pathway is difficult to study, its significance and overall contribution to radial water movement in roots is little understood.

In the transcellular (transmembrane) pathway, water moves from cell to cell across cell membranes. This transport is facilitated by aquaporins, which can regulate resistance of the membranes to water flow. Since the symplastic and transmembrane pathways are difficult to separate experimentally, they are commonly referred to as cell-to-cell pathway (Steudle and Peterson 1998, Javot and Maurel 2002).

1.7.3 Driving forces for water movement in plants

The movement of water takes place as a result of water potential gradients. These gradients are commonly created by local differences in osmotic and turgor potentials (osmotic forces) and through the chain of events that involve transpirational water loss from the leaves (transpiration-driven or hydrostatic forces) (McElrone et al. 2013). The high cohesive forces make water molecules move together in the water column inside the water-conducting xylem elements. They are aided by the adhesive forces between water molecules and the molecules of the inner walls of the water-conducting elements (vessels or tracheids) (Kramer and Boyer 1995). During the transpiration, water is lost from the leaf creating a water potential gradient that continues inside the leaf tissues all the way to the xylem. The tension created by this transpirational water loss pulls water up in the in the xylem, which draws water from the root tissues next to the xylem elements. The resulting water potential gradient across the root tissues is responsible for radial water flow in the roots and for water uptake from the soil (Kramer and Boyer 1995). This continuous water movement from the soil to the plant and from the plant to the air is referred to as the Soil Plant Atmosphere Continuum (SPAC) (Goldsmith 2013). In

slowly transpiring plants, the main forces responsible for water movement in roots are generated by local differences in solute concentrations. In the composite root water transport model (Steudle and Peterson 1998), water flow is switched between the different pathways depending on transpiration intensity with aquaporins mainly involved in regulation of water flow when osmotically driven forces predominate in plants. However, more recent evidence points to the importance of root water transport by aquaporins regardless of transpiration intensity (Lee et al. 2009, Maurel et al. 2016).

1.8 Challenges in Studying Plant Water Transport

The studies of water relations at the tissues and organ levels are complex and there is still a large gap in understanding the contributions of the different pathways to an overall water transport (Kapilan et al. 2018). The measurements of cell-to-cell pathway commonly involve cell pressure probes that require considerable skill and experience to use (Tomos and Leigh 1999, Lee et al. 2012). Additionally, aquaporin transport inhibitors that are used to determine the contribution of aquaporins to water flow are usually not highly specific (Maurel et al. 2015). To measure relative contributions of cell-to-cell and apoplastic pathways, apoplastic dyes that are unable to pass across cell membranes are sometimes used, but there are concerns that dye molecules are much larger than those of water (Liu et al. 2020). Hydraulic conductance of the apoplastic pathway can be changed by altering the properties of the cell walls, development of air spaces between the cells, and deposition of hydrophobic substance such as suberin in the root tissues (Lambers et al. 2008). Therefore, examining root structure may provide additional important clues concerning the properties of apoplast and its potential modifications. Since the development of molecular biology has provided an array of relatively simple laboratory techniques, most of the studies that are aimed at understanding the properties of cell-to-cell

pathway have focused on the expression of aquaporin genes and its regulation. When combined with the analysis of aquaporin proteins as well as their properties, localization, and posttranslational regulation, these studies provide an important insight into the role of aquaporins in water transport (Ahmed et al. 2020). The molecular approaches, collectively with the functional studies carried out at the cell, tissue, organ, and plant levels, have provided a wealth of information concerning regulation of water transport in plants in responses to various environmental factors including salinity, drought, temperature, hypoxia, and mineral nutrition (Tyerman et al. 2021).

Interpreting the results of studies involving excised roots is also challenging. The properties of root water transport have been usually studied in excised roots, which has been the subject of criticism since this eliminates shoots as a driving force for water transport, but also a likely source of signals that can affect root water flow (Lee et al. 2009, Knipfer and Fricke, 2010, Liu et al. 2014). However, measurements of water flow in individual detached roots or root systems (Carvajal et al. 1996, Wan and Zwiazek 1999) combined with the cell pressure probe (Tomos and Leigh 1999) provide many important clues concerning relative contributions of the different root water transport pathways. In the root pressure probe technique, measurements are carried out in excised roots attached to the probe after root pressure develops in the xylem as a result of solute accumulation. Once the root pressure becomes constant, hydrostatic and osmotic pressure can be measured. Generally, for this technique, root tips, root segments or entire root systems of smaller plants can be used (Steudle and Meshcheryakov 1996). There are several advantages of using the pressure probes. The main advantage of using this technique is that it can be used to measure different transport components at the same time, and both water and solute flows can be precisely measured. In addition, the active accumulation of ions in the root xylem

(active pumping) and of the metabolic state of roots can be monitored throughout the experiment. However, as mentioned above, the main disadvantage is that root water potential and preferred routes of water transport may be different in excised, compared with intact roots (Lee et al. 2009). Although some studies considered roots to be similar to an osmotic system, the root cell membranes as well as the exo-and endodermal layers, which function as barriers to apoplastic water flow, make the conventional osmotic model difficult to apply to roots (Kramer and Boyer 1995). Therefore, there is a huge variation in the hydraulic conductivity of roots due to the nature of driving forces and the osmotic forces are usually much smaller than the hydrostatic forces (Steudle and Meschcheryakov 1996, Knipfer and Fricke 2010).

With the advances in plant water relations research, new findings may put in question the validity of some of the widely accepted concepts. An example is a simple model in which the exo- and endodermal layers prevent apoplastic flow of water with dissolved solutes into the stele. This has been challenged by the studies which demonstrated that these apoplastic barriers are leaky and cannot completely prevent the transport of water and solutes (Kim et al. 2018). The composite water flow model (Steudle and Peterson 1998) may also require some future refinements as we learn more about plant water transport from an ongoing research and new measurement techniques are being developed and employed for the plant water relations studies.

1.9 Plant Aquaporins

Aquaporins are small membrane channel proteins that belong to the large family of major intrinsic proteins (MIPs). Although the main role of aquaporins is to transport water, they also contribute to the transport of other small molecules including gases and ions (Maurel et al. 2015, Zwiazek et al. 2017, Tyerman et al. 2021). Aquaporins have been found in all organisms

including ancient primitive forms of archaebacteria. Initially, the term “aquaporin” was referred only to the water transporting MIPs, however, it is presently recognized that not all members of this PIP family of proteins are specifically involved in water transport (Groszmann et al. 2017).

All aquaporins consist of six packed helical domains with N and C termini facing the cytosol. Five loops (A–E) also joins to transmembrane helices. Loops B and D are extremely hydrophobic and face the cytosol and they play an important role in aquaporin gating while loops A and C and E are extracytoplasmic (Kapilan et al. 2018). Aquaporins form tetramers through hydrogen bounds and interactions between the monomers (Fig. 1.1). Loops B and E contain an internal repeat of three amino acids including Asparagine-Proline-Alanine residues that form NPA motif. NPA can be extended to both sides of the pore across the membrane and is considered an important feature in all aquaporins since it determines aquaporin selectivity (Afzal et al. 2016). The connection between the loop C with loops B and E is also important for the functionality and water permeability of aquaporins (Murata et al. 2000).

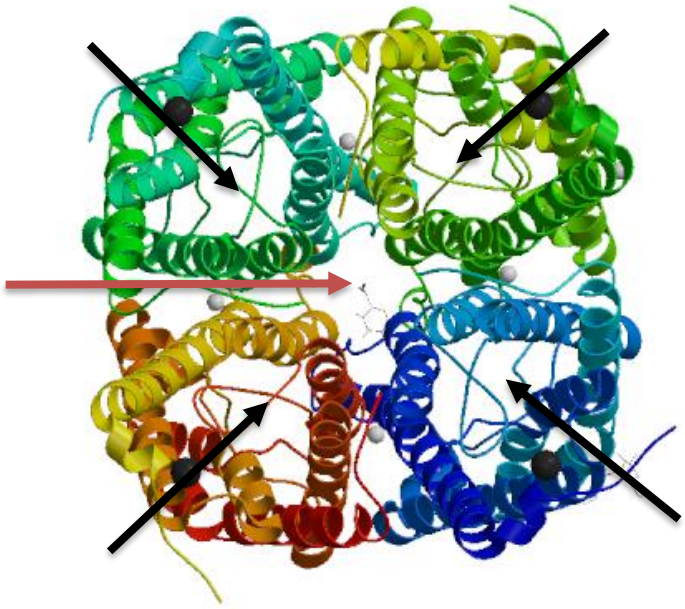

Fig. 1.1. Top view of *Puccinellia nuttalliana* PIP2;2 homotetramer. The black arrows point to the pores in individual monomers and the red arrow points to the central pore (www.swissmodel.expasy.org).

The discovery of aquaporins opened a whole new era in plant biology since water transport plays a vital role in all aspects of plants' life and clear understanding of water transport regulation mechanisms may be key to improving the productivity and stress resistance of plants (Kapilan et al. 2018). Just as important may be more recent findings that aquaporins may also be involved in the transmembrane transport of CO_2 (Uechlein et al. 2003), O_2 (Zwiazek et al. 2017) and other small molecules including glycerol (Biela, et al. 1999), urea (Gerbeau et al. 1999), methylammonium (Holm et al. 2005), boric acid (Takano et al. 2006), silicic acid (Ma et al. 2006), ammonia (NH_3), and CO_2 (Holm et al. 2005). It was also proposed that some of the plant aquaporins including *Arabidopsis thaliana* AtPIP2;1 may act as dual water and ion channels (Byrt et al. 2017, Tyerman et al. 2021). Numerous studies have been carried out to identify molecular and cellular properties of aquaporins as well as their regulation and selectivity. These

studies pointed to the importance of aquaporins in plant growth and development and in plant responses to different environmental conditions (Maurel 2007, Maurel et al. 2015, Ding et al. 2022).

1.9.1 The plant aquaporin family

Plant aquaporins consist of a wide variety of different isoforms. Commonly, *in silico* methods are used to identify the plant aquaporin genes. Based on the molecular cloning efforts together with bioinformatics, homology sequence, and membrane localization, plant aquaporins have been divided into five subfamilies including plasma membrane intrinsic proteins (PIPs), tonoplast intrinsic proteins (TIPs), nodulin-26 like intrinsic proteins (NIPs), small basic intrinsic proteins (SIPs) and X intrinsic proteins (XIPs) (Sakurai et al. 2005). The PIPs and TIPs are localized to the plasma membranes and tonoplasts, respectively, while SIP's have been implicated in solute transport and are localized to the endoplasmic reticulum (Johanson et al. 2001, Johanson and Gustavsson 2002, Ishikawa et al. 2005). NIPs are named due to the similarity with soybean (*Glycine max*) GmNOD26 and other nodulin 26-like intrinsic proteins that are expressed at the symbiosome membrane in roots of legume plants infected by rhizobacteria. NIPs are the first plant aquaporins that were classified on the basis of their subcellular localization (Sakurai et al. 2005). They are expressed mostly in the peribacteroid membrane of N_2-fixing symbiotic root nodules but were also found in many non-legume plants. They transport a wide range of molecules including silicon and are involved in developmental processes and stress tolerance (Ma et al. 2006, Zhang et al. 2022). Finally, the most recently described XIPs were discovered first in the moss *Physcomitrella patens* (Danielson and Johanson 2008). XIPs may be localized in the internal and plasma membranes (Ampah-Korsah et al. 2016) and were demonstrated to be involved in the

transport of glycerol, urea, hydrogen peroxide (Bienert et al. 2011), and boric acid (Ampah-Korsah et al. 2016), but do not appear to be major water transporters (Bienert et al. 2011)

The comparison of homology of aquaporins in plants suggests that they can have divergent sequences and functions. For example, PIP subfamily is divided into the PIP1 and PIP2 subgroups. These subgroups may function independently as monomers or together by forming heterotetramers to increase water permeability of the plasma membrane (Fetter et al. 2004). PIP1 and PIP2 aquaporins were also shown to interact in maize (*Zea mays*) as a requirement for PIP1 trafficking to the plasma membrane (Zelazny et al. 2007) as discussed below.

1.9.2 Subcellular localization and trafficking of aquaporins

Plant aquaporins localize mostly to the cell membranes that are derived from the secretory pathways. This extensive localization pattern suggests the importance of plant cell compartmentation as well as the need of cells to control water and solute transport across intracellular and plasma membranes (Ma et al. 2006). The classification of plant aquaporins is partly based on their subcellular localization, however, in general, the subcellular localization of plant aquaporin family seems to be complex and highly regulated. The localization and abundance of aquaporin proteins are usually examined using isoform-specific aquaporin (especially PIP and TIP) antibodies and the binding regions of the antibodies are examined against recombinant aquaporin proteins expressed in yeast cells (Sakurai et al. 2008). Most of the studies on plant aquaporin regulation and trafficking were carried out with PIPs and demonstrated a multilevel control of their contributions to water permeability of the membranes (Hachez et al. 2013). The interactions between different plant aquaporins can affect their subcellular localization as plant aquaporins are able to form both homotetramers and heterotetramers that affects their function (Zelazny et al. 2007). For instance, it was shown in

maize that when ZmPIP1s were expressed alone, they were stored in the ER, however, when they were expressed with ZmPIP2s, they were transferred to the plasma membrane. This demonstrates the importance of aquaporin interactions in their localization (Zelazny et al. 2007). In addition to the interactions between PIPs (Zelazny et al. 2007, Yaneff et al. 2014, Bienert et al. 2018, Vaipai et al. 2018), water permeability of PIPs can be regulated by the interactions with other membrane proteins, including receptor-like kinase (RLK) and FERONIA (Bellati et al. 2016). PIPs were also found to contain the specific motif in their N-terminal part of the aquaporins that acts as an ER export signal for membrane trafficking (Souriel et al. 2011). A study with transgenic Arabidopsis containing a mutated diacidic motiff in AtPIP2;1 showed that root water transport capacity decreased since the ER-retained AtPIP2;1 interacted with other PIPs to inhibit their trafficking to the plasma membrane (Sorieul et al. 2011).

Localization of aquaporins in response to salt and osmotic stresses is a crucial process to change their levels in the target membrane (Luu et al. 2012). For example, in osmotically stressed ice plant (*Mesembryanthemum crystallinum*), McTIP1;2 was re-localized from the tonoplast to endosomal compartments as it could be important in the homeostatic process and maintaining cellular osmolarity (Vera-Estrella et al. 2004). In Arabidopsis, salinity caused re-localization of TIP1;1 into intracellular structures that were referred to as intravacuolar invaginations (Boursiac et al. 2005). In addition, phosphorylation of the carboxy-terminal Ser-283 of AtPIP2;1 was found to regulate the salt- or H_2O_2-induced internalization (Prak et al. 2008). These findings suggested that H_2O_2 acts as a signaling molecule to induce internalization of PIP proteins in response to environmental stresses by changing their phosphorylation status to regulate the cell membrane water permeability (Li et al. 2013).

1.9.3 Posttranslational regulation of plant aquaporins

Although determining aquaporin gene expression levels provides useful information concerning gene regulation by environmental factors, posttranslational regulation of aquaporins is just as important for transport regulation as the aquaporin membrane abundance and membrane trafficking (Hachez and Chaumont 2010, Tyerman et al. 2021). The opening and closing of water channels, referred to as gating, provides a rapid response mechanism to changes in environmental factors that require an adjustment of membrane water permeability. (Vandeleur et al. 2014). Methods such as mass spectrometry, 2D gel electrophoresis, mass spectrometry, interaction analyses, protein crystallography and structure-function predictions approaches, have been used for studying aquaporin proteins and their posttranslational modifications under various environmental conditions (Prak et al. 2008). These studies demonstrated that plant aquaporins undergo different posttranslational changes including heteromerization, phosphorylation, ubiquitylation, deamidation, N-glycosylation, and methylation. All these modifications affect the folding of aquaporin proteins and their trafficking from the ER to the target membranes as well as their gating (Moeller at al. 2011, Sutka et al. 2017).

1.9.4 Pore structure of aquaporins and gating

X-ray crystallography of plant aquaporins has been commonly used to examine their potentially important structural features including the structure of aquaporin pores in their opened and closed states (Maurel et al. 2015). The central pore of aquaporins consists of transmembrane domains and loops B and E, which both have a specific conserved region with the asparagine-proline-alanine sequences that is referred to as NPA motif. NPA motif plays an essential role in water transport and selectivity of aquaporins. In addition to NPA motif, aquaporins develop another unique structure called ar/R selectivity filter. This region plays an

important role in aquaporin substrate specificity (Maurel et al. 2015). The characteristics of different aquaporins are mainly determined by interactions between the aromatic/arginine (Ar/R) and NPA as well as by H-bonding and hydrophobic regions within the pore. The water permeability of aquaporins is thought to be the result of the hydrogen bond competition between water and the few polar groups which are present in the pore of the aquaporin that drives water molecules to pass through the pore (Fujiyoshi et al. 2002). Although the hourglass shape of the pore is most commonly found in aquaporins, other more complex shapes may be formed and affect aquaporin transporting properties as discussed in Chapter 4 of this thesis.

1.9.5. Transport assays and aquaporin transport inhibitors

Different functional assays have been employed to demonstrate that aquaporins significantly contribute to the transport of water and other molecules. Heterologous expression of plant aquaporins in the oocytes of *Xenopus laevis* (African clawed frog) or yeast are the most common methods that are used to demonstrate their functions as channels (Ishikawa et al. 2005, Xu et al. 2015, Tyerman et al. 2021). The rate of volume change of oocytes or yeast protoplasts in response to osmolarity of the external solution can be measured with a microscope (oocytes) or a stopped-flow spectrometer (yeast protoplasts) and the rate of water transport calculated from the rate of volume change (Fischer and Kaldenhoff 2008, Almeida-Rodriguez et al. 2010, Xu et al. 2015). The large size of *X. laevis* oocytes makes them easy to use, however, despite the advantages of using *X. laevis* oocytes due to their large size, there are also some disadvantages of using this system. The main drawback is that the natural conditions which the plant cells are normally exposed to are very different from those of the *X. laevis* oocytes and the results derived from this assay must be interpreted with caution (Deshmukh et al. 2016). Aquaporins can be also expressed in yeast for transport assays or purified aquaporins can be reconstituted into

liposomes. For example, the liposomes were used to demonstrate the water channel activity of the GmNOD26 aquaporin purified from native peribacteroid membranes (Dean et al. 1999) and hydrogen peroxide transport through various aquaporins (Wang et al. 2020). More commonly, these transport assays are carried out by measuring fluxes of water and other studied molecules into and out of the transformed yeast cells overexpressing aquaporins (Uehlein et al. 2003, Fischer and Kaldenhoff 2008, Israel et al. 2021). To demonstrate oxygen transport by the *Nicotiana tabacum* NtPIP1;3, the rate of oxygen binding to myoglobin was measured in transformed yeast (Zwiazek et al. 2017). Sometimes, indirect measurement can be used to demonstrate the transport of molecules by aquaporins, e.g., by measuring the accumulation of ions in aquaporin-transformed yeast cells (Qiu et al. 2020) or performing survival assays with aquaporin-transformed yest cells treated with hydrogen peroxide (Liu and Zwiazek 2022).

Mercury salts have been long used to inhibit water transport through aquaporins in membrane vesicles and intact cells (Gerbeau et al. 1999, Wan and Zwiazek 1999). Mercury can bind the thiol group in cysteine residues in aquaporins and block water transport, but it can also affect the functions of other proteins and in higher concentrations it inhibits respiration (Wan and Zwiazek 1999, Lee et al. 2012). Nevertheless, in very low concentrations (50 - 100 μM), mercury is considered to be a reliable tool for demonstrating aquaporin-mediated water transport and for inhibition of cell and root hydraulic conductivities (Wan and Zwiazek 1999, Kamalludin and Zwiazek 2001, Vaziriyeganeh et al. 2018). Mercury attaches to the thiol group of cysteine residues since has a higher affinity to these residues than other ionized groups such as NH_2 or the imidazole group of histidine. Using mutagenesis in specific sites of AQP1, it was demonstrated that the binding site for mercury is Cys189 at the constriction region (Hasegawa et al. 1993). However, some mercury-resistant PIPs have been identified in Arabidopsis and tobacco (Biela et

al. 1999). Other inhibitors of aquaporin gating were also tried with some success. Gold and silver can inhibit aquaporin activities by biding to specific residue, but they have been used less frequently as the aquaporin blockers compared with mercury and less is known about their mode of action (Yukutake et al. 2008, Liu et al. 2020).

Chapter 2. Salinity tolerance of halophytic grass *Puccinellia nuttalliana* is associated with enhancement of aquaporin-mediated water transport by sodium.

2.1. Introduction

Salinity is among the most challenging problems faced by terrestrial plants in many parts of the globe due to the accumulation of salts in the soil through natural process and human activities. Although soil salinity may refer to the presence of elevated concentrations of different salts, sodium salts, especially when accompanied by chloride, are the most common and detrimental salts affecting plants worldwide (Munns and Tester 2008). However, sulphates, carbonates and bicarbonates, as well as calcium, magnesium and potassium ions often contribute to soil salinity (Volkov and Flowers 2019).

The majority of terrestrial plants are salt-sensitive glycophytes and only about 2% of plants have been classified as halophytes that can tolerate high salt concentrations (Flowers and Colmer 2008). Although salt tolerance levels widely vary between glycophytes, these plants have evolved by adapting to soils with low soil sodium levels and maintain low Na^+ concentrations in their aboveground tissues (Cheesman et al. 2015). Halophytic plants also vary in their level of salt tolerance and in one of the most commonly used classifications, these salt tolerant plants are divided into obligate, facultative, and habitat-indifferent halophytes (Grigore and Toma 2017). Obligate halophytes (euhalophytes) require salt for their survival and usually show the optimum growth and development in NaCl concentrations exceeding 200 mM (Flowers and Colmer 2008). In contrast, facultative halophytes can survive without salt, but their growth is enhanced by moderate salinity and is reduced by both low and high salt concentrations. The habitat indifferent

halophytes are plants that prefer salt-free soils but can also cope with relatively high salt concentrations (Mishra and Tana 2017).

The salt tolerance of halophytes has attracted considerable attention and many processes contributing to salt tolerance have been described for various species of halophytic plants. However, some of the fundamental aspects of salt tolerance in halophytes related to water relations remain obscure. The ability of plants to cope with salinity is largely determined by their ability to maintain the acquisition of water and mineral nutrients and protecting the tissues against direct ion toxicity, oxidative stress, and osmotic effects of salts (Tester and Davenport 2003, Sun et al. 2009). Maintenance of plant water balance requires complex and precise control and coordination of the processes of water uptake, water movement within the plant, and water loss. Water flow in most plants encounters the most resistance when crossing the root tissues between the epidermis and the root xylem (Steudle and Peterson 1998). A sharp increase in the root water flow resistance (decreased root hydraulic conductivity) is among the earliest responses to salt observed in glycophytes (Martinez-Ballesta et al. 2003, Nguyen et al. 2006, Lee et al. 2010). The root water flow resistance is dynamically controlled by root aquaporins that are an integral part of the cell-to-cell pathway (Kapilan et al. 2018) and are sensitive to NaCl (Carvajal et al. 2000, Martinez-Ballesta et al. 2008, Lee and Zwiazek 2015). The decrease of root hydraulic conductivity triggers stomatal closure and a decrease of transpiration rates (Vitali et al. 2015), which reduces the relative contribution of hydrostatic forces and increases the significance of osmotic forces that are altered by salt.

In salt-sensitive plants, the inhibition of aquaporin function is rapid and strong (Boursiac et al. 2005, Horie et al. 2011, Lee and Zwiazek 2015). The aquaporin-mediated root water transport and cell hydraulic conductivity were inhibited by about three-fold in Arabidopsis

within several minutes following root exposure to concentrations of NaCl as low as 10 mM (Lee and Zwiazek 2015). However, in the halophytic grass *Puccinellia nuttalliana*, cell hydraulic conductivity was enhanced by the treatments with 50 and 150 mM NaCl leading to the hypothesis that NaCl may enhance the aquaporin-mediated transport in roots of halophytic plants (Vaziriyeganeh at al. 2018). A subsequent study demonstrated that the six-day treatment with 150 mM NaCl triggered an increase in gene expression of *PnuPIP2;2*, suggesting that this aquaporin in *P. nuttalliana* may be key to maintaining efficient root water transport under salinity conditions (Vaziriyeganeh et al. 2021).

Salt affects plants through a combination of osmotic, ionic, nutritional, and oxidative factors (Munns 2002, Tester and Davenport 2003, Munns and Tester 2008, Silva et al. 2008, Isayenkov and Maathuis 2019), which can potentially alter plant water transport and water relations (Maurel et al. 2015). Amelioration of root hydraulic conductivity (Carvajal et al. 2000), root cell hydraulic conductivity (Lee and Zwiazek 2015), and osmotic water permeability in plasma membrane vesicles (Martínez-Ballesta et al. 2008) by Ca^{2+} in NaCl-treated plants point to a direct ion effect on the aquaporin-mediated water transport. However, treatments of barley (*Hordeum vulgare*) with the same osmolarity solutions of NaCl and sorbitol had an almost identical effect on root hydraulic conductivity (Kaneko et al. 2015). Salinity tolerance of halophytic plants is often attributed to their efficient Na management (Flowers and Colmer 2008). NaCl secretion through salt glands by some halophytes and more efficient compartmentalization of Na^+ compared with K^+ in the vacuoles (Wang et al. 2001, Ramos et al. 2004, Fatemi et al. 2019) may partly explain greater toxicity of high treatment concentrations with potassium salts compared with similar concentrations of NaCl. However, the difference in

ion management do not fully explain growth enhancement by NaCl that has also been reported for some halophytic plants (Wang et al. 2001, Vaziriyeganeh et al. 2018).

Since the exact signals triggering an enhancement of root hydraulic conductivity in *P. nuttalliana* by NaCl (Vaziriyeganeh et al. 2018) are unclear, the present study was designed to separate different ionic factors in their effects on the root water transport properties and physiological processes in three related northern grass species varying in salt tolerance. The grasses included relatively salt-sensitive Kentucky bluegrass (*Poa pratensis*), moderately salt-tolerant alkali bluegrass (*Poa juncifolia*), and the salt-loving halophytic Nuttall's alkaligrass (*P. nuttalliana*) (Harivandi et al. 1992, Vaziriyeganeh et al. 2018). Plants were treated for up to ten days with 150 mM NaCl, 150 mM KCl, and 150 mM Na_2SO_4 and their growth and physiological responses, including water relations and the aquaporin-mediated cell-to-cell root water transport, were examined. I tested the hypothesis that Na^+ is the principal factor responsible for the enhancement of cell hydraulic conductivity in the roots of halophytic grasses and this enhancement plays a significant role in the maintenance of water balance, gas exchange, and growth of halophytic plants exposed to salinity.

2.2 Materials and Methods

2.2.1 Plant material and treatments

Seeds of Kentucky bluegrass (*Poa pratensis* L.), alkali bluegrass [*Poa juncifolia* Scribn.), and Nuttall's alkali bluegrass [*Puccinellia nuttalliana* (Schult.) Hitchc.] were collected in central Alberta, Canada. The seeds were surface sterilized with 70% ethanol for 2 min followed by 1% sodium hypochlorite for 1 min. Sterilized seeds were washed several times with the autoclaved

distilled water and germinated on the sterile half-strength Murashige & Skoog (MS) solid medium without sucrose and hormones (Grant et al. 2017).

Several days after seed germination, the germinant were transferred to 500 cm^3 pots filled with commercial growing mix (Sunshine® Mix #4 Professional Growing Mix, Sun Gro Horticulture, Seba Beach, Alberta). The plants were grown for eight weeks in a controlled-environment growth room set to 22/18° C (day/night) temperature, 65 ± 10% relative humidity, and 16-h photoperiod with 300 μmol m^{-1} s^{-1} photosynthetic photon flux density (PPFD) provided by the full-spectrum fluorescent bulbs (Philips high output, Markham, ON, Canada). They were fertilized weekly with half-strength modified Hoagland's solution (Epstein 1972) and watered three times per week to runoff.

After eight weeks of growth, seedlings were removed from the soil and placed in 12 L plastic containers filled with 50% Hoagland's solution. Styrofoam boards were floated on the top of nutrient solution with holes cut in each board through which seedling roots were slipped into the solution and the stems secured to the board with foam stoppers. There were three repeated experiments for different sets of measurements. In each experiment, there were three plants per species randomly placed in each of the 12 replicated containers (four containers per treatment with twelve plants in total in each container). The mineral solution was aerated with an air pump to provide O_2 concentration of approximately 8 mg L^{-1}. After one-week of acclimation to hydroponic conditions, plants were treated with 150 mM NaCl, 150 mM Na_2SO_4, or 150 mM KCl for six days. The salts were gradually added to nutrient solution in 50 mM increments over 24 h. Providing plants with the same salt concentrations enabled us to compare the osmotic and ionic effects of salts as well as the effects of different Na^+ concentrations in the presence of different anions (NaCl *vs* Na_2SO_4). The salts were gradually added during the day (3 x 50 mM)

to reduce osmotic shock. The control group consisted of plants growing in 50% Hoagland's solution with no added salts. For all measurements, plants were randomly picked from the containers.

2.2.2 Plant morphology and dry weights (DW)

After six days of treatments, plants were inspected for the visible impact of salts. Six plants from each treatment were harvested and their shoots and roots separated. The shoots and roots were placed in an oven at 70^{o}C for 72 h and weighed for the DW determinations.

2.2.3 Net photosynthesis (Pn) and transpiration (E) rates

The measurements of Pn and E were carried out three, six and nine days of treatments from approximately 5 to 9 hours following the onset of photoperiod and by alternating plants from the different treatments. Three fully expanded uppermost leaves from each plant were marked and used for the measurements using a LI-6400 portable photosynthesis system with a 2×3 cm^2 leaf chamber (LI-COR Biosciences, Lincoln, NB, USA). The reference CO_2 concentration was 400 μmol mol^{-1}, the flow rate was 200 μmol s^{-1}, and the relative humidity (RH) level was set to 50% in the cuvette. The leaf chamber temperature was maintained at 20°C, and PPFD was 400 μmol m^{-2} s^{-1} provided by the red-blue light spectrum of the light attachment. To determine leaf areas, the parts of the leaves that were inserted into the leaf chamber were excised after the last measurement and scanned. The leaf areas were calculated using the Sigmascan Pro 5.0 computer software (Systat Software, San Jose, CA, USA).

2.2.4 Leaf chlorophyll concentrations

Chlorophyll-a (chl-a), chlorophyll-b (chl-b) and total chlorophyll concentrations were determined in six randomly selected seedlings per treatment (n = 6) after six days of treatments.

Fully expanded leaves were freeze-dried and grinded in a Thomas Wiley Mini-Mill (Thomas Scientific, NJ, USA). Chlorophyll was extracted from the leaf samples (10 mg dry weight) with 8 ml dimethyl sulfoxide (DMSO) at 65°C for 22 h. Chlorophyll concentrations were measured in DMSO extracts with a spectrophotometer (Genesys 10S-UV-VIS, Thomas Scientific, NJ, USA) at 648 nm and 665 nm for chlorophyll-a and chlorophyll-b, respectively. Total chlorophyll concentrations (chlorophyll a + b) were calculated using the Arnon's equation (Šesták et al. 1971).

2.2.5 Leaf water potentials (ψ_w) and shoot water contents (WC)

The measurements of (ψ_w) were carried out after six days of treatments in six plants per treatment (n = 6) using a Scholander pressure chamber (PMS instruments, Corvallis, OR, USA) as previously described (Vaziriyeganeh et al. 2018). The measurements were carried out from approximately 5 to 9 hours following the onset of photoperiod. The same leaf that was marked and used for the gas exchange measurements was excised and immediately placed in a Scholander pressure chamber with the cut end of the leaf protruding through the lid. Chamber pressure was increased until xylem sap was released from the excised leaf and balance pressure was recorded.

Shoot water contents were determined after six days of treatments in six plants per treatment (n = 6). The shoots were excised from each plant and weighed to establish their fresh weight (FW). They were then dried in an oven at 70°C for 72 h and weighed to determine the dry weights (DW). The shoot WC was calculated using the following equation:

$$WC\ (\%) = [(FW - DW) / FW] \times 100$$

2.2.6 Cell hydraulic conductivity (L_{pc})

Cell pressure probe was used to determine L_{pc} of the root cortex cells in plants subjected to six days of treatments with 150 mM NaCl, 150 mM Na_2SO_4, 150 mM KCl, and in untreated control. Six plants per treatment were taken for the measurements (n = 6). The roots were placed on a metal sledge covered with a paper towel and the respective treatment solutions were flown along the roots. Micro capillaries used with the cell pressure probe were pulled to a fine point using a pipette puller (Kopf Vertical puller, Model 72, Tujunga, California, USA) and subsequently ground to openings ranging from 8-10 µm. The micro capillaries were filled with silicone oil (Type AS4, Wacker, Munich, Germany). The tip of the micro-capillary was inserted 20 mm above the root apex into the cortical layer of plant roots. When the cell was punctured, half-time of water exchange ($T_{1/2}$), turgor pressure (Pt), and cell elasticity (ε) were determined as earlier described (Lee and Zwiazek 2015, Vaziriyeganeh et al. 2018) to calculate cell hydraulic conductivity. Once the hydraulic parameters were recorded, $HgCl_2$ was added to the treatment solutions to the final concentration of 50 µM and the parameters recorded again (Lee and Zwiazek 2019). Mercury inhibits aquaporin activity by selectively binding to Cys residues within the pore and $HgCl_2$ has been commonly used in low concentrations to block water transport across aquaporins (Wan and Zwiazek 1999, Hirano et al. 2010). Following the measurements, thin sections of roots were examined under the microscope to determine cell dimensions and the cell volume for the L_{pc} calculations (Lee and Zwiazek 2019).

2.2.7 Tissue elemental analyses

The elemental analyses were carried out in the Natural Resources Analytical Laboratory of the University of Alberta, Edmonton, Canada. For the analyses, root and shoot samples (0.2 g dry weight) of six plants per species (n = 6) were collected after six days of the different salt

treatments. The roots were quickly rinsed in deionized water and blotted dry. To determine tissue concentrations of Na, K, and Ca, the samples were digested with 70% HNO_3 and heated for 10 minutes at 185℃ in a microwave oven (Mars 5 Microwave Accelerated Reaction System, CEM, Matthews, NC, USA). The extracts were diluted with Milli-Q water, filtered, and analyzed by with the inductively coupled plasma – optical emission spectrometer (iCap 6000, Thermo Fisher Scientific Inc, Waltham, MA, USA). Tissue Cl was analyzed in hot water extracts using the EPA 325.2 ferric thiocyanate method (US Environmental Protection Agency 1983) with the Thermo Gallery Plus Beermaster Autoanalyzer (Thermo Fisher Scientific, Vantaa, Finland).

2.2.8 Statistical analyses

Statistical analyses were carried out using the SPSS 18.0 statistical package (SPSS Inc., Chicago, IL, USA). One-way ANOVA was carried out followed by the Tukey's test to detect significant differences between the treatments for each plant species ($p \leq 0.05$). The L_{pc} data were analyzed for significant differences between the treatments and species as the main factors. The data for each measurement were obtained from the same experiment with each replicate representing one plant. The data that did not meet the ANOVA assumptions of normality of distribution and homogeneity of variance were transformed with a log10 function.

2.3 Results

2.3.1 Plant morphology and dry weights (DW)

Stunted roots and shoots as well as extensive leaf chlorotic and leaf necrotic lesions were observed in *P. pratensis* plants after six days of treatments with 150 mM NaCl, 150 mM Na_2SO_4, and 150 mM KCl (Supplementary Fig. 2.1). Stunted growth, but relatively less extensive leaf necrosis compared with *P. pratensis*, were also observed in *P. juncifolia* in all salt treatments

(Supplementary Fig. 2.1). Control plants of *P. nuttalliana* and the plants treated with 150 mM KCl exhibited leaf chlorosis and necrosis and were smaller compared with the plants treated with 150 mM NaCl and 150 mM Na_2SO_4, which showed no visible signs of salt injury (Supplementary Fig. 2.1).

Root and shoot DW of *P. pratensis* were sharply reduced in plants treated for six days with 150 mM NaCl and 150 mM Na_2SO_4 and these reductions were several-fold greater compared with the plants treated with 150 mM KCl (Fig. 2.1A, B). Similar trends to root and shoot DW were observed for the total DW (Fig. 2.1C) and all three salt treatments reduced to a similar extent the shoot: root DW ratios (Fig. 2.1D).

The root DW in *P. juncifolia* was significantly reduced by the 150 mM Na_2SO_4 treatment (Fig. 2.1A). The shoot (Fig. 2.1B) and total (Fig. 2.1C) DW were significantly decreased by all salt treatments, but the reductions were greater in plants treated with the Na salts compared with KCl. There was no significant effect of any of the salt treatments on shoot: root DW rations (Fig. 2.1D).

In *P. nuttalliana*, the root DW was not affected by 150 mM NaCl but was reduced by the 150 mM KCl and 150 mM Na_2SO_4 treatments compared with the untreated control (Fig. 2.1A). A reduction in shoot DW was observed in plants treated with 150 mM KCl, while the shoot DW was enhanced by 150 mM NaCl (Fig. 2.1B). There was no effect of 150 mM Na_2SO_4 treatment on the shoot DW (Fig. 2.1B). Only the 150 mM KCl treatment had a negative effect on the total DW *P. nuttalliana* (Fig. 2.1C). The shoot: root DW ratios were enhanced by all salt treatments (Fig. 2.1D).

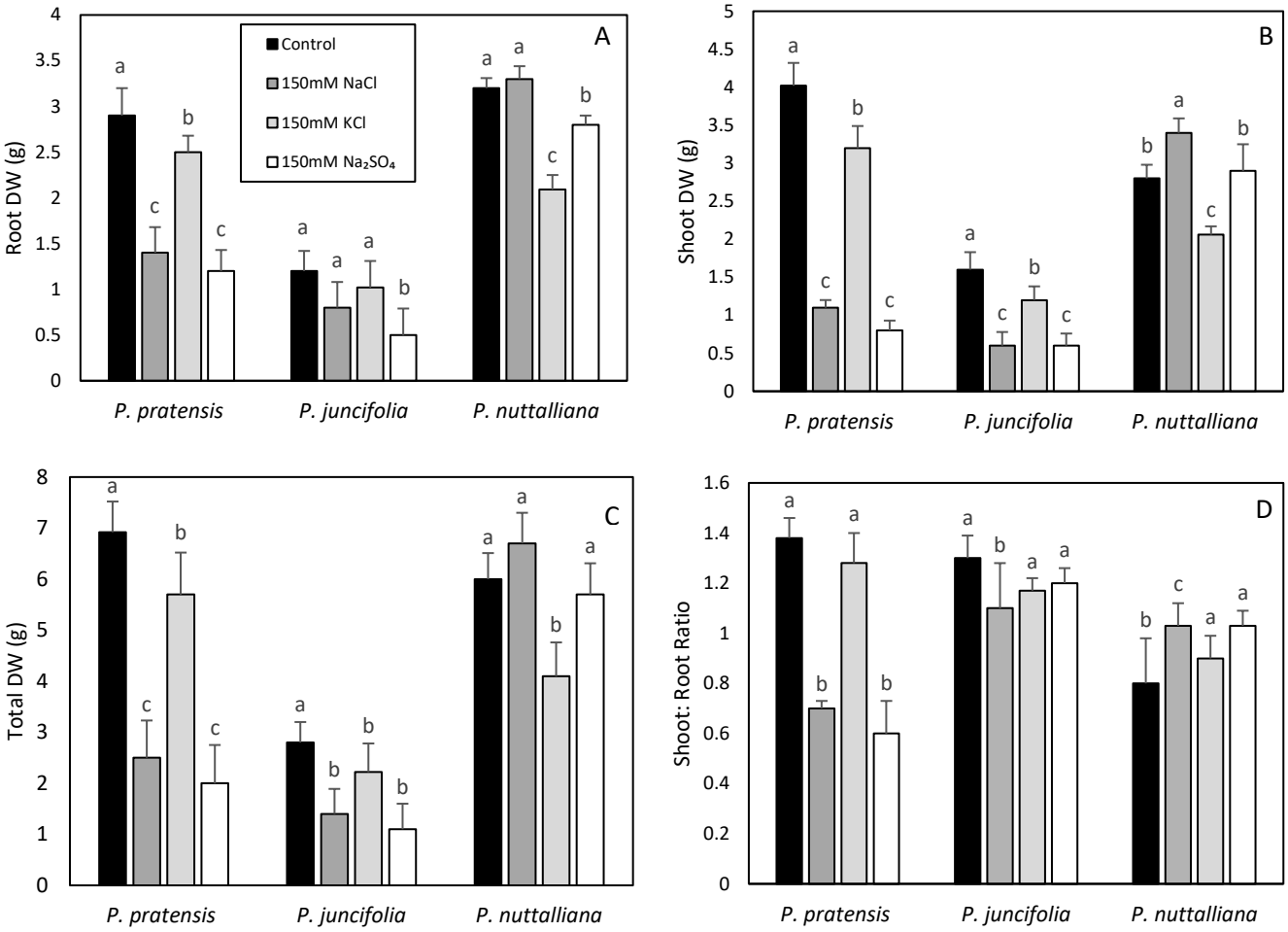

Fig. 2.1. Root (A), shoot (B), and total dry weights (DW) (C) and shoot to root DW ratios (D) in *Poa pratensis*, *Poa juncifolia* and *Puccinellia nuttalliana* treated for six days with 150 mM NaCl, 150 mM KCl, 150 mM Na_2SO_4 and in control (untreated) plants. Different letters or numbers above the bars indicate significant differences ($p \leq 0.05$) between treatments within each species as determined by the Tukey's test. Means (n = 6) and SE are shown.

2.3.2 Net photosynthesis (Pn) and transpiration (E) rates

Compared with control plants, Pn was sharply reduced in *P. pratensis* and *P. juncifolia* by all salt treatments after three, six and nine days. (Fig. 2.2A, C, E). In *P. nuttalliana*, there was no effect of 150 NaCl and 150 Na_2SO_4 on Pn. However, Pn declined compared with control in plants treated with 150 mM KCl on all measurement days (Fig. 2.2A, C, E).

In *P. pratensis* and *P. juncifolia*, E decreased compared with their respective controls in all salt treatments and on all treatment days (Fig. 2.2B, D, F). In *P. nuttalliana*, after 3 and 6 days of treatments, E decreased in plants treated with 150 mM KCl and 150 mM Na_2SO_4 (Fig. 2.2B, D). After 9 days, all salt treatments resulted in a significant decrease of E in *P. nuttalliana* (Fig. 2.2F).

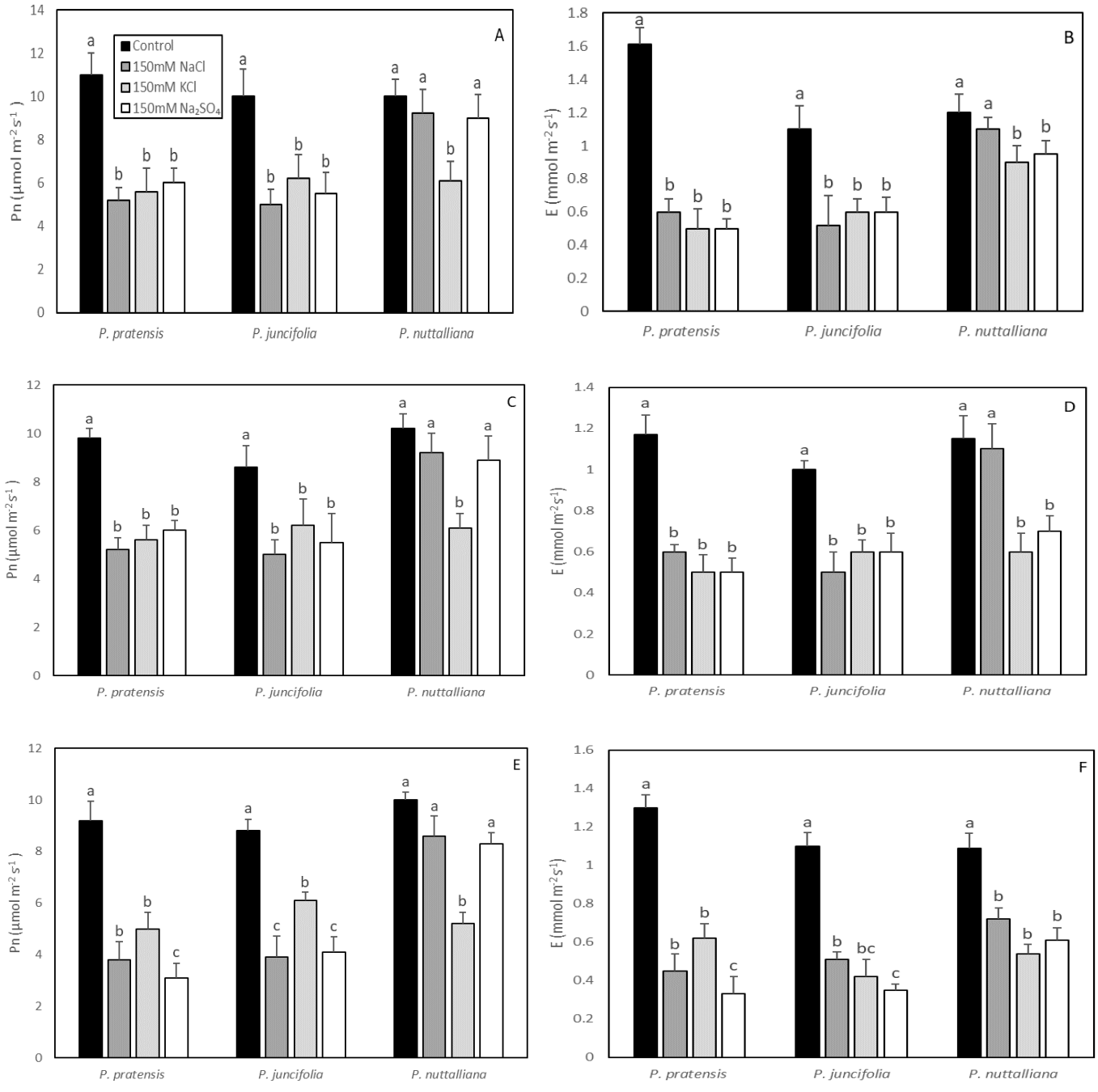

Fig. 2.2. Net photosynthesis (Pn) (A, C, E) and transpiration (E) (B,D,F) rates in *Poa pratensis*, *Poa juncifolia*, and *Puccinellia nuttalliana* after three (A,B), six (C,D) and nine (E,F) days of treatments with 150 mM NaCl, 150 mM Na_2SO_4, 150 mM KCl, and in untreated control plants. Different letters above the bars indicate significant differences ($p \leq 0.05$) between treatments within each species as determined by the Tukey's test. Means (n = 6) and SE are shown.

2.3.3 Leaf chlorophyll concentrations

After six days of treatments, chlorophyll a, chlorophyll b, and total leaf chlorophyll concentrations decreased in *P. pratensis* exposed to 150 mM NaCl, 150 mM KCl and 150 mM Na_2SO_4 compared with control plants (Fig. 2.3A, B, C). Chlorophyll a:b ratios increased in *P. pratensis* as a result of 150 mM NaCl and 150 mM Na_2SO_4 treatments (Fig. 2.3D).

In *P. juncifolia*, leaf chlorophyll a concentration decreased in the 150 mM Na_2SO_4 treatment and increased in the leaves treated with 150 mM NaCl (Fig. 2.3A). There was no significant treatment effect on the chlorophyll b concentrations (Fig. 2.3B). The total chlorophyll concentrations increased in the 150 mM NaCl treatment and decreased in plants treated with 150 mM KCl and 150 mM Na_2SO_4 (Fig. 2.3C). The chlorophyll a:b ratios also decreased in the 150 mM KCl and 150 mM Na_2SO_4 treatments (Fig. 2.3D).

In *P. nuttalliana*, there was a large increase in the leaf chlorophyll a, chlorophyll b, and total chlorophyll concentrations in plants treated with 150 mM NaCl and 150 mM Na_2SO_4, but there was no effect of KCl on the leaf chlorophyll concentrations (Fig. 2.3A, B, C). The leaf chlorophyll a:b ratios decreased in *P. nuttalliana* in all salt treatments (Fig. 2.3D).

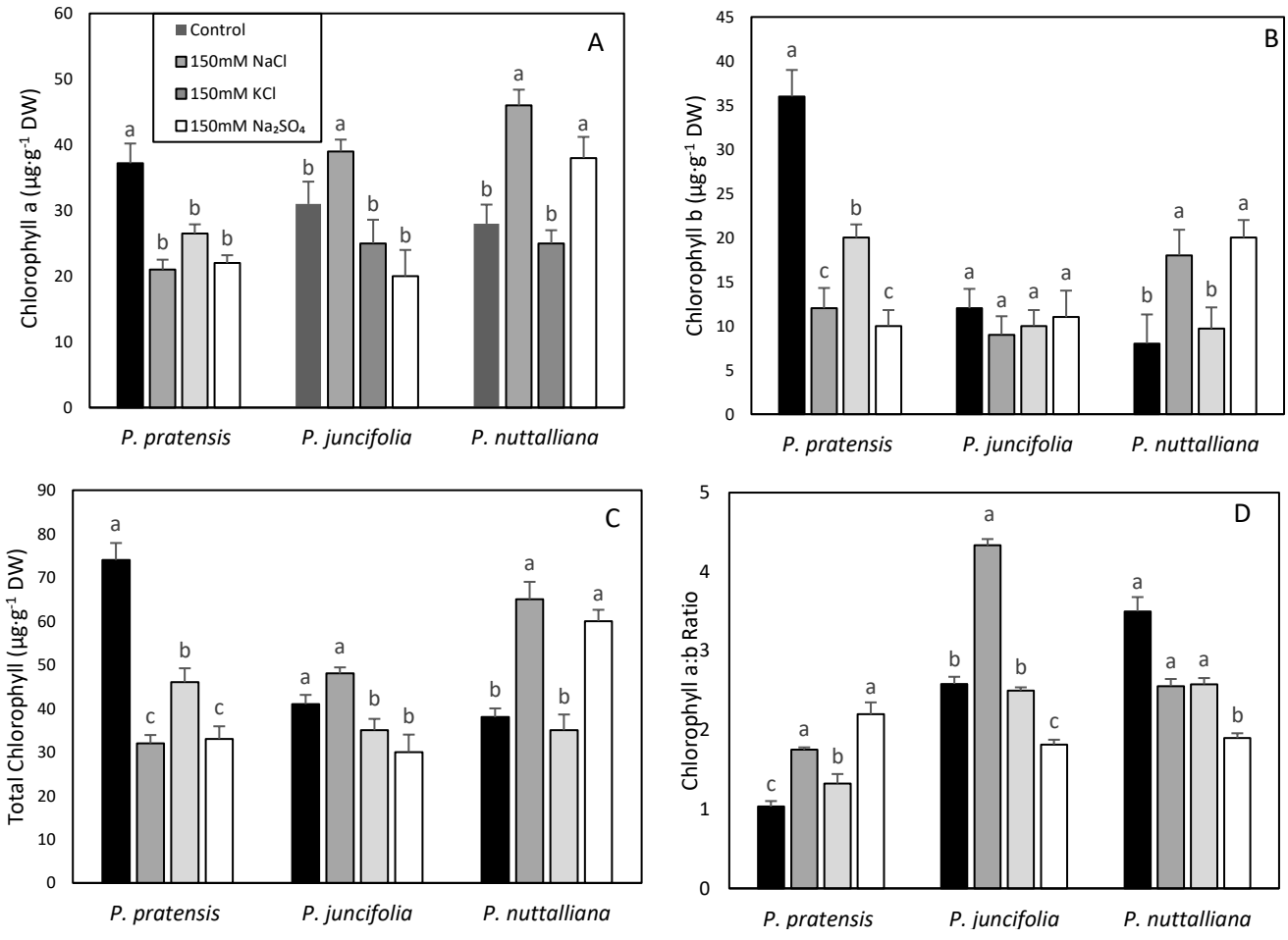

Fig. 2.3. Leaf chlorophyll a (A), chlorophyll b (B), and total chlorophyll (C) concentrations, and chlorophyll a:b ratios (D) in *Poa pratensis*, *Poa juncifolia*, and *Puccinellia nuttalliana* subjected to six days of treatments with 150 mM NaCl, 150 mM KCl, 150 mM Na_2SO_4 and in untreated control plants. Different letters above the bars indicate significant differences ($p \leq 0.05$) between treatments within each species as determined by the Tukey's test. Means (n = 6) and SE are shown.

2.3.4 Leaf water potentials (ψ_w) and shoot water contents (WC)

After six days of 150 mM NaCl, 150 Na_2SO_4, and 150 mM KCl treatments, ψ_w sharply decreased in *P. pratensis* and *P. juncifolia* and the greatest decrease was observed in plants treated with 150 mM Na_2SO_4 (Fig. 2.4A). In *P. nuttalliana*, there was no significant effect of NaCl and KCl treatments on ψ_w, but the ψ_w values were significantly lower in plants treated with 150 mM Na_2SO_4 (Fig. 2.4A).

The shoot WC decreased in *P. pratensis* and *P. juncifolia* subjected to six days of 150 mM NaCl, 150 mM KCl, and 150 mM Na_2SO_4 treatments compared with untreated control and the greatest decrease was measured in plants treated with 150 mM Na_2SO_4 (Fig. 2.4B). In *P. nuttalliana,* WC of plants treated with NaCl and Na_2SO_4 was similar to the untreated control plants; however, WC was significantly reduced by the 150 mM KCl treatment compared with control (Fig. 2.4B).

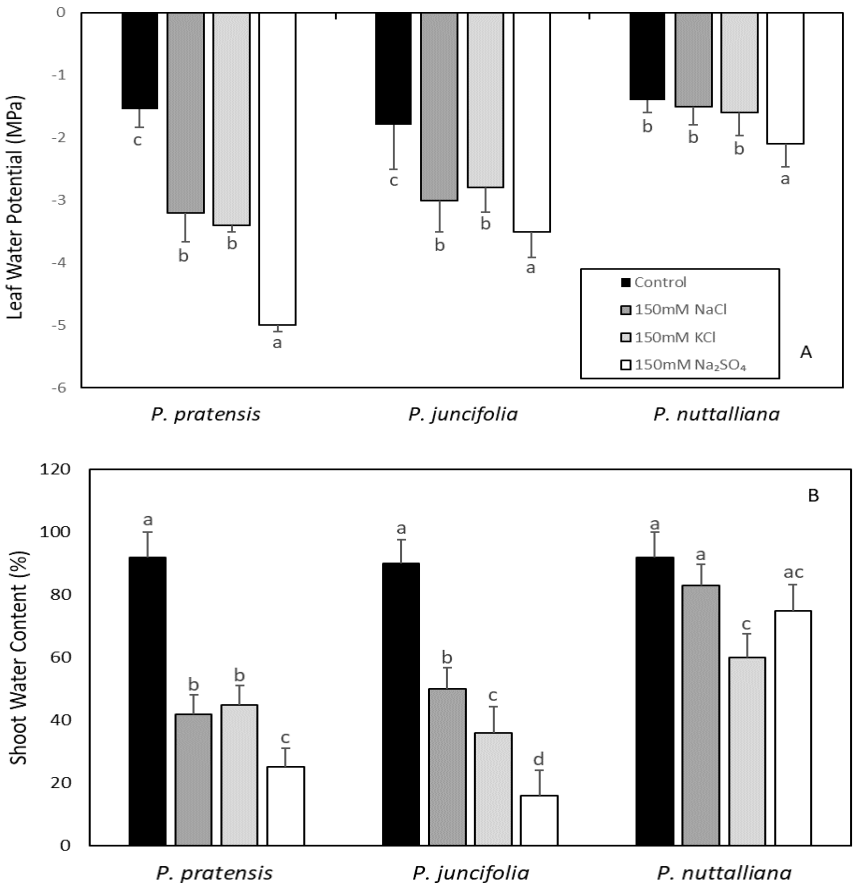

Fig. 2.4. Leaf water potentials (A) and shoot water contents (B) in *Poa pratensis*, *Poa juncifolia*, and *Puccinellia nuttalliana* treated with 150 mM NaCl, 150 mM KCl, and 150 mM Na_2SO_4 and in untreated control plants. The measurements of leaf water potentials and shoot water content were carried out after six days of treatments. Different letters above the bars indicate significant differences ($p \leq 0.05$) between treatments within each as determined by the Tukey's test. Means (n = 6) and SE are shown.

2.3.5 Cell hydraulic conductivity (L_{pc})

The L_{pc} in *P. pratensis* treated with 150 mM NaCl and 150 mM Na_2SO_4 decreased by two- to three-fold and only a relatively smaller decrease was measured in plants treated with 150 mM KCl compared with control plants (Fig. 2.5). Lower magnitude decreases of L_{pc} compared with *Poa pratensis* were also observed in the roots of *P. juncifolia* treated with 150 mM NaCl, 150 mM Na_2SO_4, and 150 mM KCl (Fig. 2.5). In *P. nuttalliana*, the L_{pc} values increased by approximately three-fold in the 150 mM NaCl and 150 mM Na_2SO_4 treatments and were not affected by 150 mM KCl (Fig. 2.5). Treatments with 50 µM $HgCl_2$ decreased the L_{pc} values to similar levels in all plant species regardless of the treatment (Fig. 2.5).

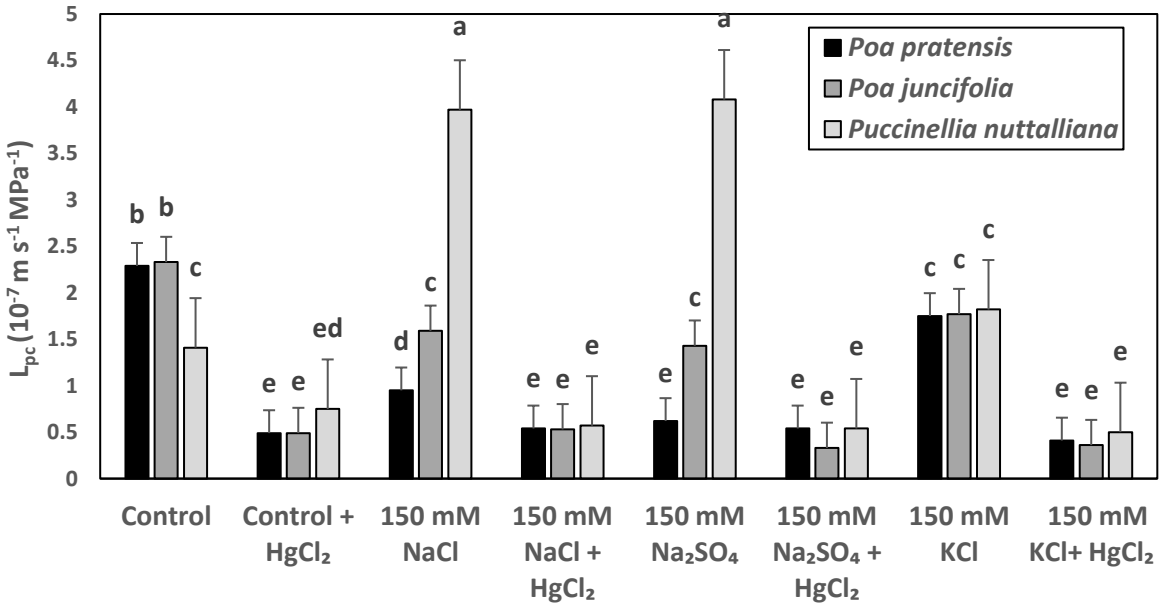

Fig. 2.5. Cell hydraulic conductivity (L_{pc}) of root cortex cells in *Poa pratensis*, *Poa juncifolia*, and *Puccinellia nuttalliana* plants treated with 150 mM NaCl, 150 mM Na_2SO_4, and 150 mM KCl for six days and in untreated control. The roots were exposed to their respective salt treatments in 50% Hoagland's solutions (no salt for controls) followed by 50 µM $HgCl_2$. Means (n = 6) and SE are shown. Different letters above the bars indicate significant differences ($p \leq 0.05$) between treatments and species as determined by the Tukey's test.

2.3.6 Root and shoot elemental concentrations.

Root Na^+ concentrations increased to similar levels in the three plant species after six days of 10 mM NaCl and 150 mM Na_2SO_4 treatments (Fig. 2.6A). Shoot Na^+ concentrations increased by approximately the same magnitude in *P. pratensis* and *P. juncifolia* treated with 150 mM NaCl. However, the Na^+ shoot concentrations in *P. nuttalliana* treated with 150 mM NaCl was less than a half of the concentrations measured in the two other plant species (Fig. 6B). The shoot Na^+ concentrations in all three species of plants treated with 150 mM Na_2SO_4 were higher compared with the plants treated with 150 mM NaCl (Fig. 2.6B).

The concentrations of K^+ in roots and shoots of all plant species increased by about three-fold compared with untreated control as a result of the 150 mM KCl treatment (Fig. 2.6C, D). Both the 150 mM NaCl and 150 mM Na_2SO_4 treatments decreased root and shoot K^+ concentrations in *P. pratensis*. There was no effect of 150 mM NaCl on the K^+ root and shoot concentrations and no effect of 150 mM Na_2SO_4 on shoot K^+ concentrations in *P. juncifolia* (Fig. 2.6C, D). However, the 150 mM Na_2SO_4 treatment decreased K^+ root concentrations in *P. juncifolia* compared with control plants (Fig. 2.6C). In *P. nuttalliana* treated with 150 mM NaCl and 150 mM Na_2SO_4, root and shoot K^+ concentrations increased compared with the untreated control and the increase was especially pronounced in shoots (Fig. 2.6C, D).

All three salt treatments decreased root and shoot Ca concentrations in *P. pratensis* (Fig. 2.6E, F). In *P. juncifolia*, root Ca concentrations were also reduced by all salt treatments (Fig. 2.6E). However, there was no significant effect of 150 mM NaCl and 150 mM Na_2SO_4 and a small increase in Ca shoot concentration as a result of the 150 mM KCl treatment (Fig. 2.6F). The 150 mM KCl treatment decreased Ca root concentrations and increased Ca shoot

concentrations in *P. nuttalliana* (Fig. 2.6E, F). Both 150 mM NaCl and 150 mM Na_2SO_4 triggered increases in root and shoot Ca concentrations in *P. nuttalliana* (Fig. 2.6E, F).

Root Cl^- concentrations increased by several-fold in all three species of plants subjected to 150 mM NaCl and 150 mM KCl treatments (Fig. 2.6G). The shoot Cl^- concentrations sharply increased in the three examined plant species treated with 150 mM NaCl and 150 mM KCl compared with control and the concentrations were higher compared with the roots in the same treatments (Fig. 2.6H).

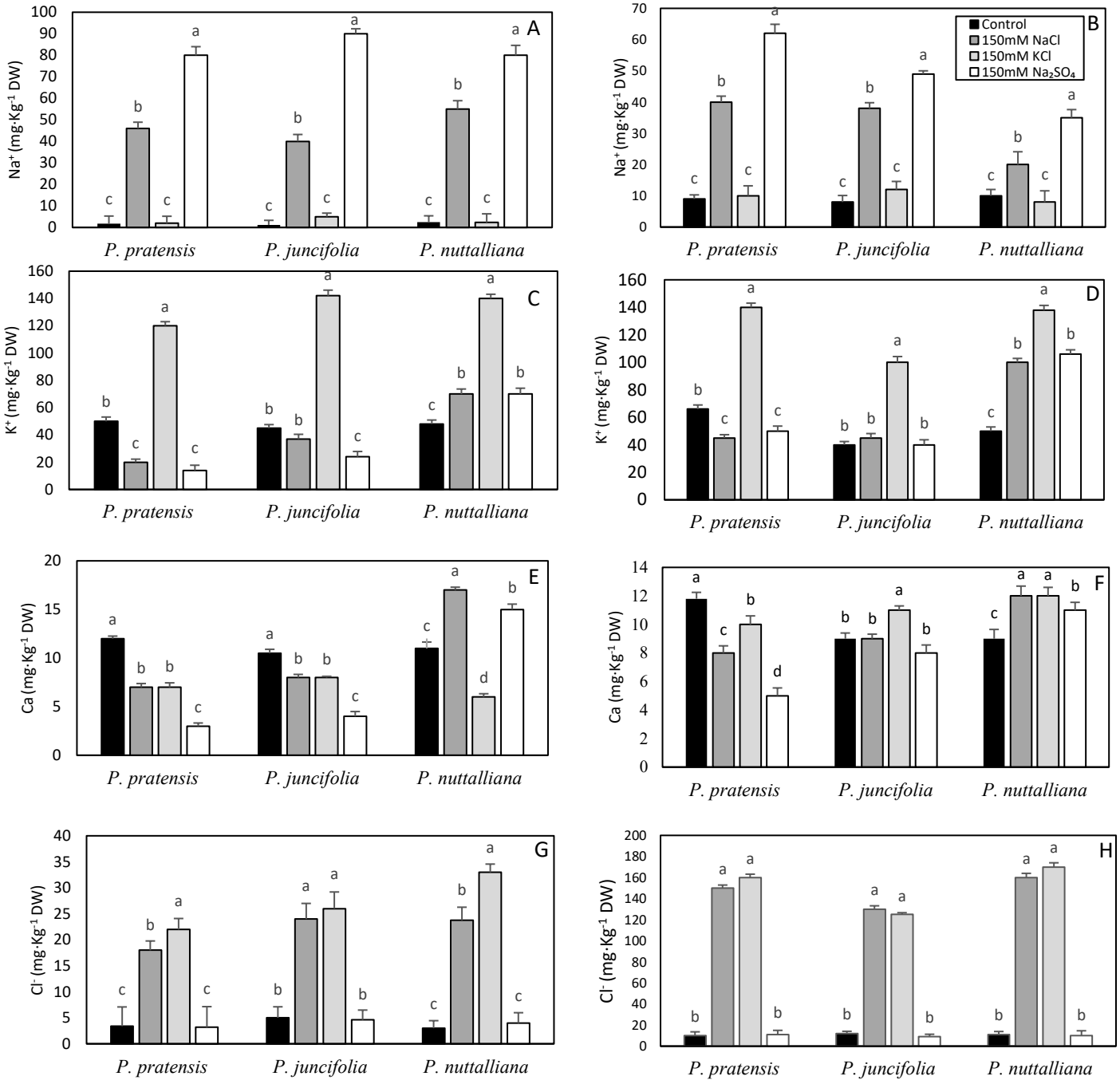

Fig. 2.6. Concentrations of Na^+, K^+, Ca, and Cl^+ in roots (A, C, E, G) and shoots (B, D, F, H) of *Poa pratensis*, *Poa juncifolia*, and *Puccinellia nuttalliana* after six days of treatments with 150 mM NaCl, 150 KCl, 150 mM Na_2SO_4 and in untreated control plants. Different letters above the bars indicate significant differences ($p \leq 0.05$) between treatments within each plant species as determined by the Tukey's test. Means (n = 6) and SE are shown.

2.4 Discussion

The present study aimed at understanding how the different salt factors affect root water transport properties and physiological responses in three species of northern grasses varying in salt tolerance. Signs of visible injuries were apparent in the glycophytic grass *P. pratensis* in all salt treatments and the effects of these treatments on *P. juncifolia* included largely stunted growth. The magnitude of these growth reductions was greater in *P. pratensis* compared with a moderately salt tolerant *P. juncifolia* which, similarly to the earlier study (Vaziriyeganeh et al. 2018), showed slow growth compared with the other two plant species, also under control conditions. A different pattern was observed in the halophytic *P. nuttalliana* plants, which were visibly larger in the two Na-salt treatments compared with control plants and the plants treated with KCl. These observations were corroborated by the plant dry biomass measurements, which demonstrated no effects of 150 mM NaCl and 150 mM Na_2SO_4 on the total dry weight of *P. nuttalliana* and the reduction of the total dry weight by the 150 mM KCl treatment. Although Na^+ is considered to be the main cause of ion toxicity in salt-sensitive plants (Tester and Davenport 2003), deleterious effects of salinity also involve osmotic factors as well as accompanying anions (Isayenkov and Maathuis 2019). Since osmotic potentials of 150 mM NaCl are by about one-third higher (less negative) compared with 150 mM Na_2SO_4 and NaCl and KCl contain the same Cl^- concentrations, the results point to Na^+ as a likely direct factor contributing to salinity tolerance in *P. nuttalliana* and the main detrimental factor to *P. pratensis*.

Sodium salts reduced shoot dry weights in *P. pratensis* more than root dry weights resulting in a decrease in shoot: root DW ratios while all salt treatments increased shoot:root DW ratios in *P. nuttalliana* and had no significant effect on shoot:root DW ratios in *P. juncifolia*. A decrease in the shoot to root ratios is a common response to salinity in salt-sensitive plants and

was proposed to be the consequence of the osmotic effect rather than the ion toxicity (Hsiao and Xu 2000). However, in my study, only NaCl and Na_2SO_4, and not KCl, significantly reduced shoot to root ratios in *P. pratensis* pointing to ion toxicity as the principal factor contributing to changes in growth allocations, as also reported for soybean (Wang et al. 2005).

Both Pn and E significantly decreased in *P. pratensis* and *P. juncifolia* after 3, 6, and 9 days of treatments with 150 mM NaCl, 150 mM KCl, and 150 mM Na_2SO_4. However, only the 150 mM KCl treatment inhibited Pn in *P. nuttalliana* despite the reductions in E by all salts after 9 days of treatments. The decreases in Pn and E in all three plant species treated with 150 mM KCl suggest little differences between halophytic and glycophytic grasses in their abilities to cope with K^+ excess. Potassium is the principal ion used to control osmotic balance and stomatal opening (Andrés et al. 2014). However, some halophytic plants can substitute K^+ with Na^+ to promote stomatal opening since the availability of K^+ may be affected by the salinity conditions (Hedrich and Shabala 2018, Rasouli et al. 2021). Although elevated concentrations of K^+ in the root medium alters osmotic balance in plants, it was also demonstrated that 50 mM KCl treatments of drought stressed *P. pratensis* promoted stomatal reopening and rapid resumption of photosynthesis during drought recovery (Hu et al. 2013).

The responses of Pn in plants exposed to salinity can involve multiple processes including reductions in photosynthetic pigments, electron transport, and enzymatic reactions that are involved in photosynthesis as well as reductions in CO_2 uptake due to stomatal closure (Chaves et al. 2009, Kwon et al. 2019). Leaf chlorophyll concentration can be an important biochemical indicator of salt tolerance in plants since it significantly contributes to Pn and plant growth responses under salinity conditions (Ashraf and Harris 2013, Acosta-Motos et al. 2015). While longer-term effects of salinity on Pn involve severe damage to the photosynthetic

apparatus by salt accumulation in leaves (Chaves et al. 2009, Stepien and Johnson 2009), short-term effects have been often attributed to the reduced CO_2 uptake due to stomatal closure (Parida and Das 2005). In *P. pratensis*, six days of treatments with all salts triggered large decreases in leaf chlorophyll concentrations, while relatively minor changes were observed in *P. juncifolia* and more than two-fold increases in chlorophyll concentrations were measured in *P. nuttalliana* treated with 150 M NaCl and Na_2SO_4. Interestingly, chlorophyll a:b ratios increased as a result of salt treatments in *P. nuttalliana* while they decreased in *P. pratensis*. Maintenance of high chlorophyll a level is thought to be essential for plant for survival. Therefore, when chlorophyll is degraded under stress, chlorophyll b may be converted to chlorophyll a resulting in high chlorophyll a:b ratios (Ashraf and Harris 2013).

Sodium appears to be a crucial element for the chloroplast development and its function in halophytes and, unlike K^+, Na^+ can increase both the number of chloroplasts and chlorophyll concentrations in the leaves of halophytic plants (Bose et al. 2017). In *Atriplex vesicaria*, low concentration of Na^+ triggered chlorosis even when the concentration of K^+ was high (Bose et al. 2017). In isolated chloroplasts of halophytic quinoa (*Chenopodium quinoa*) and pigface (*Carpobrotus rosii*) plants, Pn could be maintained under high concentrations of Na^+ (100 mM) and low concentration of K^+ (50 mM) (Percey et al. 2016). It was also demonstrated that in the chloroplasts of halophytic plants, Na^+ concentrations could be 20 times higher compared with the glycophytes (Müller et al. 2014).

In the present study, the rapidity of the Pn responses to salts and its close correlation with E indicated that stomatal limitations were among the key factors contributing to the Pn declines in *P. pratensis* and *P. juncifolia*. Leaf water potentials in both plant species sharply decreased when measured after six days of treatments with all salts while in *P. nuttalliana*, leaf water

potentials significantly decreased only in the 150 mM Na_2SO_4 treatment. The decreases of water potentials in *P. pratensis* and *P. juncifolia* are likely a combination of the reduced water uptake and the accumulation of salts and organic solutes in the leaf tissues resulting in decreased osmotic potentials. Glycophytes have a limited ability to reduce an entry of salts to roots or to exclude them from leaves (Munns 2002). Reductions in water uptake due to decreased osmotic potential of the root medium and decreased root hydraulic conductivity are major factors contributing to reduced water contents in salt-affected plants (Muhsin and Zwiazek 2002, Apostol and Zwiazek 2003, Calvo-Polanco et al. 2008). Similarly, to stomatal regulation, root hydraulic conductivity is dynamically regulated and affected by various environmental factors, which may alter water delivery to the transpiring areas and upset water balance (Nardini et al. 2007; Liu et al. 2015). Studies on purified plasma membrane vesicles of *Beta vulgaris* demonstrated their high water permeability, suggesting that efficient cell-to-cell water transport under salt stress plays a significant role in water balance maintenance (Alleva et al. 2006). Enhanced cell hydraulic conductivity in NaCl-treated *P. nuttalliana* was also proposed to play a major role in salt tolerance of this halophytic grass (Vaziriyeganeh et al. 2018) and likely involves the reported increase in gene expression of the *PIP2;2* aquaporin (Vaziriyeganeh et al. 2021).

Leaf water potentials and shoot water contents of *P. nuttalliana* were not altered by the 150 mM NaCl demonstrating the ability of plants to maintain water balance. Salt exclusion, sequestration, and secretion as well as accumulation of organic solutes are important mechanisms contributing to the maintenance of osmotic balance in halophytes (Mishra and Tana 2017). Halophytic turfgrasses can exclude salt from the root cortex (Abideen et al. 2014) and to secrete salt through the salt glands or salt bladders in the leaf epidermis (Tada et al. 2014, Flower

and Colmer 2015, Vaziriyeganeh et al. 2021). Some halophytes also maintain osmotic potential by accumulating salt in the vacuoles (Acosta-Motos et al. 2017). The Na^+ concentrations in roots of *P. nuttalliana* treated with NaCl and Na_2SO_4 increased to the similar levels as in the other two grass species. However, the shoot Na^+ concentrations in these treatments in *P. nuttalliana* were only approximately one-half of the concentrations measured in *P. pratensis* and *P. juncifolia*, suggesting restricted root-to-shoot transport or (and) salt secretion. Extensive salt secretion through the leaves was observed in the earlier study in NaCl-treated *P. nuttalliana* (Vaziriyeganeh et al. 2021). Similarly to other plants (White and Broadley 2001), roots of the three studied grass species accumulated only a relatively small fraction of Cl^- compared with shoots and there were no significant differences in Cl^- concentrations of roots and shoots between the species.

Contrary to *P. pratensis*, in which root K^+ concentrations decreased and shoot concentrations remained unchanged in the NaCl and Na_2SO_4 treatments, shoot and root K^+ concentrations in *P. nuttalliana* increased in plants treated with sodium salts. Interestingly, in the intermediate salt tolerant species, *P. juncifolia*, the root and shoot K^+ concentrations remained little changed compared with control plants. Salinity can disrupt the K^+ balance in the cytosol and disrupt metabolic pathways since, in addition to its role in regulating osmotic balance, K^+ is required for the activation of various cytosolic enzymes (Shabala and Cuin 2008). Strong correlations between the tissue K^+ concentration and salt tolerance have been frequently reported for many plants (Chen et al. 2007, Cuin et al. 2008, Hauser and Horie 2010). High K^+/Na^+ ratio is essential for maintaining cell metabolism including protein biosynthesis (Roy and Chakraborty 2014). A high K:Na ratio in mesophyll cells was suggested to be the principal factor contributing to salt tolerance in *Thellungiella halophila* while the lack of this feature contributed

to salt sensitivity in *Arabidopsis* (Volkov et al. 2004). Sustained root water uptake by the NaCl-treated halophytic grasses was also attributed to the maintenance of stable K^+ levels in the roots (Vaziriyeganeh et al. 2018), likely involving the high affinity K^+ transporter PnHKT1;5, which was upregulated by NaCl in *P. nuttalliana* (Vaziriyeganeh et al. 2021). High salt concentrations trigger K^+ efflux through the depolarization-activated outward-rectifying K^+ channels (Shabala et al. 2006). The Na influx and K^+ efflux cause activation of ATPase pumps and hyperpolarization of the membranes. As a result, K^+ uptake is increased by the activation of two specific K^+ channels including voltage-dependent hyperpolarization-activated (KIR) and depolarization-activated (KOR) Shaker-type K channels (Roy and Chakraborty 2014). The increased activity of H^+ATPase pumps can also provide driving force for the activation of high affinity K^+ transporters and increase K^+ concentration during salinity (Shabala et al. 2006).

Maintenance of water balance requires efficient water delivery to leaves. In the present study, both sodium salts enhanced L_{pc} in *P. nuttalliana* by about two-fold compared with the untreated control but decreased L_{pc} in *P. juncifolia* and *P. pratensis*. It is noteworthy that 150 mM KCl had no significant impact on L_{pc} in *P. nuttalliana* and trigerred relatively minor decreases of L_{pc} in *P. pratensis* and *P. juncifolia*. An inhibition of root hydraulic conductivity is among the most sensitive initial responses of plants to salt stress (Carvajal et al. 1999, Lee et al. 2010, Sutka et al. 2011) and involves rapid reductions in the aquaporin-mediated cell-to-cell water transport. In the wild-type *Arabidopsis*, NaCl concentration as low as 10 mM decreased L_{pc} by three-fold within 30 minutes following its application to roots and there was no effect on NaCl on L_{pc} in the *AtPIP2;5* overexpression lines (Lee and Zwiazek 2015).

The results of the present study clearly demonstrated that Na^+ was the main factor contributing to the inhibition of L_{pc} in *P. pratensis* and *P. juncifolia* subjected to the sodium salts

and it was the factor responsible for the enhancement of L_{pc} in *P. nuttalliana*. Despite the differences in osmotic potentials between 150 mM Na_2SO_4 and 150 mM NaCl, their effects on L_{pc} in this halophytic grass were similar. Also, the KCl treatment had no significant effect on L_{pc} while the NaCl treatment enhanced L_{pc} in *P. nuttalliana*. It also appears that despite the two-fold higher Na^+ concentration in the Na_2SO_4 compared with NaCl treatment solutions, the effects of both salts on L_{pc} were similar, which could possibly be attributed to the contributions of the associated anions (Franklin and Zwiazek 2004, Nguyen et al. 2006).

Although NaCl effects include direct ion toxicity and osmotic imbalance that can both contribute to root hydraulic conductivity reductions (Horie et al. 2011, Qian et al. 2015, Ranganathan et al. 2017), the two stresses may vary in their modes of action on the aquaporin-mediated water transport (Qian et al. 2015). Since the treatments with 50 µM $HgCl_2$ brought the L_{pc} values in all three plant species and in all salt treatments to a similar level, the treatment effects can be attributed to the mercury-sensitive aquaporin-mediated water transport. Although $HgCl_2$ is not a specific aquaporin inhibitor, in low concentrations, as used in the present study, it inhibits the functionality of most of the aquaporins in the absence of other effects such as respiration (Wan and Zwiazek 1999, Hirano et al. 2010). Mercury changes the conformation of Ar/R region by attaching to the Cys residues (Wan and Zwiazek 1999, Hirano et al. 2010). Therefore, the enhancement of L_{pc} in *P. nuttalliana* by NaCl and Na_2SO_4 points to the effects of Na on the aquaporin-mediated water transport.

Aquaporins are proteins forming water channels in cell membranes to facilitate the transport of water and other small molecules including gases and some ions across the membranes (Madeira et al. 2016, Zwiazek et al. 2017, Liu et al. 2020, Tyerman et al. 2021). Therefore, maintaining the functionality of aquaporins under salinity conditions could have

important consequences to the transport of these molecules in halophytic plants. With typically between 30 and 70 aquaporin genes that are present in various plant species and many possible transcriptional and posttranscriptional regulations (Kapilan et al. 2018), the enhancement of aquaporin-mediated water transport in *P. nuttalliana* by Na^+ may involve complex regulation mechanisms. Links between the inhibition of root water transport by NaCl and aquaporin function have been studied in various glycophytic plants and attributed to changes in the aquaporin abundance (Katsuhara and Hanba 2008), gene expression (Katsuhara et al. 2011, Lee and Zwiazek 2015, Knipfer et al. 2021), aquaporin phosphorylation and (or) dephosphorylation (Martínez-Ballesta et al. 2008, Horie et al. 2011, Lee and Zwiazek 2015), membrane trafficking (Luu et al. 2012), pH, and Ca^{2+} (Alleva et al. 2006, Martínez-Ballesta et al. 2008). It appears that the strategy of *P. nuttalliana* plants to maintain water homeostasis in the presence of NaCl involves large increases in root transcript levels of the fast water transporting *PIP2;2* aquaporin, while decreasing gene expression levels of the tonoplast *TIP* aquaporins (Vaziriyeganeh et al. 2021). The increased *PIP2;2* gene expression could be a major factor contributing to the enhancement of cell hydraulic conductivity by the sodium salts reported in the present study. It is possible that, in addition to its role as a fast water transporter (Chapter 4 of this thesis), PIP2;2 could be involved in the transport of ions, including Na^+ and K^+ as reported for several plant PIP2s including PIP2;1 and PIP2;2 from *Arabidopsis thaliana* (Kourghi et al. 2017) and PIP2;8 from *Hordeum vulgare* (Tran et al. 2020). However, this is not likely the case in the present study since the cation conductance of these aquaporins is to different degrees blocked by Ca^{2+} (Tyerman et al. 2021), and there were also no significant differences in Na^+ root concentrations between *P. nuttalliana* and the two other studied plants. The lower Na^+ shoot concentrations in *P. nuttalliana* compared with the less salt-tolerant grasses were found to be facilitated by its

secretion through salt glands present in the leaves (Vaziriyeganeh et al., 2021), as also reported for other halophytes (Barzegargolchini et al., 2017; Pardo et al., 2017). It was proposed that the increased transcript levels of several cyclic nucleotide-gated channels by NaCl in *P. nuttalliana* could be associated with the enhanced Na^+ loading into the xylem as part of the salt tolerance mechanisms (Vaziriyeganeh et al. 2021).

Low pH of the cytoplasm is among the common factors inhibiting aquaporin activity in plants subjected to environmental stresses (Fischer and Kaldenhoff 2008). There is mounting experimental evidence that salinity increases the apoplastic pH and decreases pH of the cytosol (Geilfus and Muchling 2011, Morgan et al. 2014, 2017), which may be reversed by treatments of plants with Ca (Morgan et al. 2017). This may partly explain the alleviating effect of Ca on salt stress and aquaporin function in plants (Morgan et al. 2017). The observed increase in tissue K^+ concentration in *P. nuttalliana* in this and the earlier study (Vaziriyeganeh et al. 2018) could be expected to affect H^+ fluxes leading to an increase in cytosolic pH and an enhancement of aquaporin activity. Although the KCl treatment also enhanced the accumulation of K+ in roots in all three studied plant species, the presence of Na^+ could differently affect K^+ fluxes and its intracellular concentrations.

It is also noteworthy that, contrary to *P. pratensis* and *P. juncifolia*, in which salt treatments decreased root Ca concentrations and as opposed to the KCl treatment, which reduced root Ca concentrations in *P. nuttalliana*, the NaCl and Na_2SO_4 treatments increased root concentrations of Ca in this halophytic grass. It was reported that under salinity stress, the concentrations of Ca in halophytes can be several-fold higher compared with glycophytes in which elevated salinity commonly inhibits Ca uptake by roots (Hadi et al. 2008). Calcium accumulates in Golgi and ER soon after an exposure of plants to salt stress and before it is

transported to other organelles and the cytosol (Demidchik et al. 2018). The increase in Ca^{2+} in the cytoplasm of halophytes exposed to salt results in the activation of the salt overly sensitive (SOS) signaling pathway (Nikalje et al. 2017). The SOS complex regulates specific transporters, including the NHX exchangers and Na^+/H^+ antiporters, to exclude Na^+ from the cytosol (Hadi and Karimi 2012).

The present results together with an earlier reported up-regulation of several SOS pathway genes in the NaCl-treated roots of *P. nuttalliana* (Vaziriyeganeh et al. 2021) demonstrate that maintenance of high root Ca concentrations in *P. nuttalliana* is likely an important factor contributing to its tolerance of the sodium salts. However, they do not directly explain the enhancement of the aquaporin-mediated transport by the sodium salts. High cytosolic Ca^{2+} is commonly associated with aquaporin closure (Alleva et al. 2006, Martínez-Ballesta et al. 2008). However, treatments of plants with calcium salts were also demonstrated to alleviate NaCl (Martínez-Ballesta et al. 2008) and low root temperature (Lee at al. 2012) stresses by up-regulating the activities of aquaporins. This enhancement was explained as a likely effect of Ca^{2+} on the calcium-dependent phosphorylation and depohosphorylation (Martínez-Ballesta et al. 2008, Lee et al. 2012). The effect of Ca^{2+} on maintaining cell membrane integrity under stress conditions (Zhao et al. 2007) could also be an important factor supporting water transport activities. Clearly, the role of Ca^{2+} in regulation of the aquaporin-mediated water transport in plants exposed to salinity deserves further attention.

In conclusion, the study demonstrated that sustaining growth, chlorophyll concentrations, gas exchange, and water transport in *P. nuttalliana* requires the presence of sodium in the applied salt treatments. The maintenance of high Pn in this halophytic grass could be explained by a combination of stomatal and non-stomatal factors, including leaf chlorophyll

concentrations. The enhanced L_{pc} in *P. nuttalliana* by Na (150 mM NaCl and 150 mM Na_2SO_4) treatments was due to the mercury-sensitive aquaporin-mediated water transport that could reflect the earlier reported enhancement of gene expression of some of the PIP2 aquaporins by NaCl in *P. nuttalliana*. The Ca and K^+ accumulation in roots that was triggered by sodium likely played a role in regulating the aquaporin gating properties and (or) aquaporin gene activity in this halophytic plant.

2.5 References

Abideen, Z., Koyro, H.W., Huchzermeyer, B., Ahmed, M.Z., Gul, B. and Khan, M.A. 2014. Moderate salinity stimulates growth and photosynthesis of *Phragmites karka* by water relations and tissue specific ion regulation. Environmental and Experimental Botany 105: 70-76.

Acosta-Motos, J.R., Diaz-Vivancos, P., Alvarez, S., Fernandez-Garcia, N., Sanchez-Blanco, M.J. and Hernandez, J.A. 2015. Physiological and biochemical mechanisms of the ornamental *Eugenia myrtifolia* L. plants for coping with NaCl stress and recovery. Planta 242: 829-846.

Acosta-Motos, J.R., Ortuño, M.F., Bernal-Vicente, A., Diaz-Vivancos, P., Sanchez-Blanco, M.J. and Hernandez, J.A. 2017. Plant responses to salt stress: adaptive mechanisms. Agronomy 7: 18.

Alleva, K., Niemietz, C.M/, Sutka, M., Maurel, C., Parisi, M., Tyerman, S.D. and Amodeo, G. 2006. Plasma membrane of *Beta vulgaris* storage root shows high water channel activity regulated by cytoplasmic pH and a dual range of calcium concentrations. Journal of Experimental Botany 57: 609-621.

Alshammary, S.F. 2012. Effect of salinity on water relations of four turfgrasses. African Journal of Agricultural Research 7: 5498-5505.

Andrés, Z., Pérez-Hormaeche, J., Leidi, E.O., Schlücking, K., Steinhorst, L., McLachlan, D.H., Schumacher, K., Hetherington, A.M., Kudla, J., Cubero, E. and Pardo, J.M. 2014. Control of vacuolar dynamics and regulation of stomatal aperture by tonoplast potassium uptake. Proceedings of the National Academy of Sciences of the United States of America 111: E1806-E1814.

Apostol, K.G. and Zwiazek, J.J. 2003. Hypoxia affects root sodium and chloride concentrations and alters water conductance in salt-treated jack pine (*Pinus banksiana*) seedlings. Trees – Structure and Function 17: 251-257.

Ashraf, M. and Harris, P.J.C. 2013. Photosynthesis under stressful conditions: an overview. Photosynthetica 51: 163-190.

Barzegargolchini, B., Movafeghi, A., Dehestani, A. and Mehrabanjoubani, P. 2017. Increased cell wall thickness of endodermis and protoxylem in *Aeluropus littoralis* roots under salinity: The role of LAC4 and PER64 genes. Journal of Plant Physiology 218: 127-134.

Bose, J., Munns, R., Shabala, S., Gilliham, M., Pogson, B. and Tyerman, S.D. 2017. Chloroplast function and ion regulation in plants growing on saline soils: lessons from halophytes. Journal of Experimental Botany 68: 3129-3143.

Boursiac, Y., Chen, S., Luu, D.T., Sorieul, M., van den Dries, N. and Maurel, C. 2005. Early effects of salinity on water transport in Arabidopsis roots. Molecular and cellular features of aquaporin expression. Plant Physiology 139: 790-805.

Calvo-Polanco, M.C., Zwiazek, J.J., Voicu, M.C, 2008. Responses of ectomycorrhizal American elm (*Ulmus americana*) seedlings to salinity and soil compaction. Plant and Soil 308: 189-200.

Carvajal, M., Cerda, A. and Martinez. 2000. Does calcium ameliorate the negative effect of NaCl on melon root water transport by regulating aquaporin activity? New Phytologist 145: 439-447.

Carvajal, M., Martínez, V. and Alcaraz, C.F. 1999. Physiological function of water channels as affected by salinity in roots of paprika pepper. Physiologia Plantarum 105: 95-101.

Chaves, M.M., Flexas, J. and Pinheiro, C. 2009. Photosynthesis under drought and salt stress: regulation mechanisms from whole plant to cell. Annals of Botany 103: 551-560.

Cheesman, J.M. 2015. The evolution of halophytes, glycophytes and crops, and its implications for food security under saline conditions. New Phytologist 206: 557-570.

Chen, Z., Pottosin, II., Cuin, T.A., Fuglsang, A.T., Tester, M., Jha, D., Zepeda-Jazo, I., Zhou, M., Palmgren, M.G., Newman, I.A. and Shabala, S. 2007. Root plasma membrane transporters controlling K^+/Na^+ homeostasis in salt-stressed barley. Plant Physiology 145: 1714-1725.

Cuin, T.A., Betts, S.A., Chalmandrier, R. and Shabala, S. 2008. A root's ability to retain K^+ correlates with salt tolerance in wheat. Journal of Experimental Botany 59: 2697-2706.

Demidchik, V., Shabala, S., Isayenkov, S., Cuin, T.A. and Pottosin, I. 2018. Calcium transport across plant membranes: mechanisms and functions. New Phytologist 220: 49-69.

Epstein, E.X. 1972 Mineral nutrition of plants: principles and perspectives. Wiley, New York.

Fatemi, F., Hashemi-Petroudi, S.H., Nematzadeh, G., Askari, H. and Abdollahi, M.R. 2019. Exploiting differential gene expression to discover ionic and osmotic-associated transcripts in the halophyte grass *Aeluropus littoralis*. Biological Procedures Online 21: 14.

Fischer, M. and Kaldenhoff, R. 2008. On the pH regulation of plant aquaporins. Journal of Biological Chemistry 283: 33889-33892.

Flowers, T.J. and Colmer, T.D. 2008. Salinity tolerance in halophytes. New Phytologist 179: 945-963.

Franklin, J.A. and Zwiazek, J.J. 2004. Ion uptake in *Pinus banksiana* treated with sodium chloride and sodium sulphate. Physiologia Plantarum 120: 482-490.

Geilfus, C.M. and Muehling, KH. 2012. Transient alkalinization in the leaf apoplast of *Vicia faba* L. depends on NaCl stress intensity: an *in situ* ratio imaging study. Plant, Cell & Environment 35: 578-587.

Grant, J.N., Burris, J.N., Stewart, C.N. and Lenaghan, S.C. 2017. Improved tissue culture conditions for the emerging C4 model *Panicum hallii*. BMC Biotechnology 17: 39.

Grigore, M.-N. and Toma, C. 2017. Anatomical adaptations of halophytes. A review of classic literature and recent findings. Springer, Cham, Switzerland.

Hadi, M.R. and Karimi, N. 2012. The role of calcium in plant's salt tolerance. Journal of Plant Nutrition 35: 2037-2054.

Hadi, M.R., Khiyam-Nekoie, S.M., Khavarinejad, R., Khosh, K., Sima, N.A. and Yavari, P. 2008. Accumulation and role of ions (Ca^{2+}, Mg^{2+}, SO_4^{-2}) on salt tolerance in *Triticum turgidum* L. Journal of Biological Sciences 8: 143-148.

Harivandi, M.A., Butler, J.D. and Wu, L. 1992. Salinity and turfgrass culture. In Waddington, D.V., Carrow, R.N., Shearman, R.C. (Eds), Turfgrass. American Society of Agronomy, Madison, WI, Series No. 32., pp. 207-229.

Hauser, F. and Horie, T. 2010. A conserved primary salt tolerance mechanism mediated by HKT transporters: a mechanism for sodium exclusion and maintenance of high K^+/Na^+ ratio in leaves during salinity stress. Plant, Cell & Environment 33: 552-565.

Hedrich, R. and Shabala, S. 2018. Stomata in a saline world. Current Opinion in Plant Biology 46: 87-95.

Hirano, Y., Okimoto, N., Kadohira, I., Suematsu, M., Yasuoka, K. and Yasui, M. 2010. Molecular mechanisms of how mercury inhibits water permeation through aquaporin-1: understanding by molecular dynamics simulation. Biophysical Journal 98: 1512-1519.

Horie, T., Kaneko, T., Sugimoto, G., Sasano, S., Panda, S.K., Shibasaka, M. and Katsuhara, M. 2011. Mechanisms of water transport mediated by PIP aquaporins and their regulation via phosphorylation events under salinity stress in barley roots. Plant, Cell & Physiology 52: 663-675.

Hsiao, T.C. and Xu, L.K. 2000. Sensitivity of growth of roots versus leaves to water stress: biophysical analysis and relation to water transport. Journal of Experimental Botany 51: 1595-616.

Hu. L., Wang, Z. and Huang, B. 2013. Effects of cytokinin and potassium on stomatal and photosynthetic recovery of Kentucky bluegrass from drought stress. Crop Science 53: 221-231.

Huang, C., Wei, G., Jie ,Y., Wang, L., Zhou, H., Ran, C., Huang, Z., Jia, H. and Anjum, S.A. 2014. Effects of concentrations of sodium chloride on photosynthesis, antioxidative

enzymes, growth and fiber yield of hybrid ramie. Plant Physiology and Biochemistry 76: 86-93.

Isayenkov, S.V. and Maathuis, F.J. 2019. Plant salinity stress: many unanswered questions remain. Frontiers in Plant Science 10: 80.

Jaleel, C.A., Manivannan, P., Sankar, B., Kishorekumar, A., Gopi, R., Somasundaram, R. and Panneerselvam, R. 2007, Water deficit stress mitigation by calcium chloride in *Catharanthus roseus*: Effects on oxidative stress, proline metabolism and indole alkaloid accumulation. Colloids and Surfaces B: Biointerfaces 60: 110-116.

Kaneko, T., Horie, T., Nakahara, Y., Tsuji, N., Shibasaka, M. and Katsuhara, T. 2015. Dynamic regulation of root hydraulic conductivity of barley plants in response to salinity/osmotic stress. Plant, Cell & Physiology 56: 875-882.

Kapilan, R., Vaziri, M. and Zwiazek, J.J. 2018. Regulation of aquaporins under stress. Biological Research 51: 4.

Katsuhara, M. and Hanba, Y.T. 2008 Barley plasma membrane intrinsic proteins (PIP aquaporins) as water and CO_2 transporters. Pflugers Archiv European Journal of Physiology 456: 687-691.

Katsuhara, M., Rhee, J.Y., Sugimoto, G. and Chung, G.C. 2011. Early response in water relations influenced by NaCl reflects tolerance or sensitivity of barley plants to salinity stress via aquaporins. Soil Science and Plant Nutrition 57: 50-60.

Kourghi, M., Nourmohammadi, S., Pei, J.V., Qiu, J., McGaughey, S., Tyerman, S.D., Byrt, C.S, and Yool, A. 2017. Divalent cations regulate the ion conductance properties of diverse classes of aquaporins. International Journal of Molecular Sciences 16: 2323.

Knipfer, T., Danjou, M., Vionne, C. and Fricke, W. 2021. Salt stress reduces water uptake in barley (*Hordeum vulgare* L.) through modification of the transcellular path. Plant, Cell & Environment 44: 458-475.

Kwon, O.K., Mekapogu, M. and Kim, K.S. 2019. Effect of salinity stress on photosynthesis and related physiological responses in carnation (*Dianthus caryophyllus*). Horticulture, Environment, and Biotechnology 60: 831-839.

Lalonde, R.S., Pinno, B.D., MacKenzie, D. and Utting, N. 2020. Capping dewatered oil sands fluid fine tailings with salvaged reclamation soils at varying depths to grow woody plants. Canadian Journal of Soil Science 100: 546-557.

Lee, S.H. and Zwiazek, J.J. 2015. Regulation of aquaporin-mediated water transport in Arabidopsis roots exposed to NaCl. Plant and Cell Physiology 56: 750-758.

Lee, S.H. and Zwiazek, J.J. 2019. Regulation of water transport in Arabidopsis by methyl jasmonate. Plant Physiology and Biochemistry 139: 540-547.

Lee, S.H., Calvo-Polanco, M., Chung, G.C. and Zwiazek, J.J. 2010. Role of aquaporins in root water transport of ectomycorrhizal jack pine (*Pinus banksiana*) seedlings exposed to NaCl and fluoride. Plant, Cell & Environmrnt 33: 769-780.

Lee, S.H., Chung, G.C., Jang, J.Y., Ahn, S.J., Hong, S.-W. and Zwiazek, J.J. 2012. Overexpression of PIP2;5 aquaporin alleviates effects of low root temperature on cell hydraulic conductivity and growth in Arabidopsis. Plant Physiology 159: 479-488.

Liu, J., Equiza, M.A., Navarro-Rodenas, A., Lee, S.H. and Zwiazek, J.J. 2014. Hydraulic adjustments in aspen (*Populus tremuloides*) seedlings following defoliation involve root and leaf aquaporins. Planta 240: 553-564.

Liu, S.Y., Fukumoto, T., Gena, P., Feng, P., Sun, Q., Li, Q., Matsumoto, T., Kaneko, T., Zhang, H., Zhang, J., Zhong, S., Zeng, W., Katsuhara, M., Kitagawa, Y., Wang, A., Calamita, G. and Ding, X. 2020. Ectopic expression of a rice plasma membrane intrinsic protein (OsPIP1;3) promotes plant growth and water uptake. Plant Journal 102: 779–796.

Luu, D.T., Martiniere, A., Sorieul, M., Runions, J. and Maurel, C. 2012. Fluorescence recovery after photobleaching reveals high cycling dynamics of plasma membrane aquaporins in *Arabidopsis* roots under salt stress. Plant Journal 69: 894–905.

Madeira, A., Moura, T.F. and Soveral, G. 2016. Detecting aquaporin function and regulation. Frontiers in Chemistry 4: 3.

Martinez-Ballesta, M.C., Aparicio, F., Pallas, V., Martinez, V. and Carvajal, M. 2003. Influence of saline stress on root hydraulic conductance and PIP expression in Arabidopsis. Journal of Plant Physiology 160: 689-697.

Martinez-Ballesta, M.C., Cabanero, F., Olmos, E., Periago, P.M., Maurel, C. and Carvajal, M. 2008. Two different effects of calcium on aquaporins in salinity-stressed pepper plants. Planta 228: 15-25.

Maurel, C., Boursiac, Y., Luu, D.T., Santoni, V., Shahzad, Z. and Verdoucq, L. 2015. Aquaporins in plants. Physiological Reviews 95: 1321-1358.

Mishra, A. and Tana, B. 2017. Halophytes: potential resources for salt stress tolerance genes and promoters. Frontiers in Plant Science 8: 829.

Morgan, S.H., Lindberg, S., Maity, P.J., Geilfus, C.M., Plieth, C. and Mühling, K.H. 2017. Calcium improves apoplastic - cytosolic ion homeostasis in salt-stressed *Vicia faba* leaves. Functional Plant Biology 44: 515-524.

Morgan, S.H., Maity, P.J., Geilfus, C.M, Lindberg, S. and Mühling, K.H. 2014 Leaf ion homeostasis and plasma membrane H^+-ATPase activity in *Vicia faba* change after extra calcium and potassium supply under salinity. Plant Physiology and Biochemistry 82: 244-253.

Muhsin, T.M. and Zwiazek, J.J. 2002. Ectomycorrhizae increase water conductance and protect white spruce (*Picea glauca*) seedlings against salt stress. Plant and Soil 238: 217-225.

Müller, M., Kunz, H.H., Schroeder, J.I., Kemp, G., Young, H.S. and Neuhaus, H.E. 2014. Decreased capacity for sodium export out of Arabidopsis chloroplasts impairs salt tolerance, photosynthesis, and plant performance. Plant Journal 78: 646-658.

Munns, R. 2002. Comparative physiology of salt and water stress. Plant, Cell & Environment 25: 239-250.

Munns, R. 2005. Genes and salt tolerance: bringing them together. New Phytologist 167: 645-663.

Munns, R. and Tester, M. 2008. Mechanisms of salinity tolerance. Annual Review of Plant Biology 59: 651-681.

Nardini, A., Gasco, A., Trifilo, P., Lo Gullo, M.A. and Salleo, S. 2007. Ion-mediated enhancement of xylem hydraulic conductivity is not always suppressed by the presence of Ca^{2+} in the sap. Journal of Experimental Botany 58: 2609-2615.

Nguyen, H., Calvo-Polanco, M. and Zwiazek, J.J. 2006. Gas exchange and growth responses of ectomycorrhizal *Picea mariana*, *Picea glauca*, and *Pinus banksiana* seedlings to NaCl and Na_2SO_4. Plant Biology 8: 646-652.

Nikalje, G.C., Nikam, T.D. and Suprasanna, P. 2017. Looking at halophytic adaptation to high salinity through genomics landscape. Current Genomics 18: 542–552.

Parida, A.K. and Das, A.B. 2005. Salt tolerance and salinity effects on plants: a review. Ecotoxicology and Environmental Safety 60: 324-349.

Percey, W.J., McMinn, A., Bose, J., Breadmore, M.C., Guijt, R.M. and Shabala, S. 2016. Salinity effects on chloroplast PSII performance in glycophytes and halophytes. Functional Plant Biology 43: 1003-1015.

Pardo, F.E., Hilal, M.B., Albornoz, P.L., Gallardo, M.G. and Ruiz, V.E. 2017. Anatomical and physiological responses of four quinoa cultivars to salinity at seedling stage. Indian Journal of Science and Technology 10: 1-12.

Qian, Z.-J., Song, J.-J., Chaumont, F. and Ye, Q. 2015. Differential responses of plasma membrane aquaporins in mediating water transport of cucumber seedlings under osmotic and salt stresses Plant, Cell & Environment 38: 461-473.

Ramos, J., Lopez, M.J. and Benlloch, M. 2004. Effect of NaCl and KCl salts on the growth and solute accumulation of the halophyte *Atriplex nummulari*a. Plant and Soil 259: 163-168.

Rasouli, F., Kiani-Pouya, A., Tahir, A., Shabala, L., Chen, Z. and Shabala, S. 2021. A comparative analysis of stomatal traits and photosynthetic responses in closely related halophytic and glycophytic species under saline conditions. Environmental and Experimental Botany 181: 104300.

Ranganathan, K., Cooke, J.E., El Kayal, W., Equiza, M.A., Vaziriyeganeh, M. and Zwiazek, J.J. 2017. Over-expression of PIP2; 5 aquaporin alleviates gas exchange and growth inhibition in poplars exposed to mild osmotic stress with polyethylene glycol. Acta Physiologiae Plantarum 39: 1-9.

Roy, S. and Chakraborty, U. 2014. Salt tolerance mechanisms in salt tolerant grasses (STGs) and their prospects in cereal crop improvement. Botanical Studies 55: 31.

Šesták, Z., Catský, J. and Jarvis, P.G. 1971. Plant photosynthetic production. Manual of methods. Dr. W. Junk n.v. Publishers, The Hague, Netherlands.

Shabala, S. and Cuin, T.A. 2008. Potassium transport and plant salt tolerance. Physiologia Plantarum 133: 651-669.

Shabala, S., Demidchik, V., Shabala, L., Cuin, T.A., Smith, S.J., Miller, A.J., Davies, J.M. and Newman, I.A. 2006. Extracellular Ca^{2+} ameliorates NaCl-induced K^+ loss from Arabidopsis root and leaf cells by controlling plasma membrane K^+-permeable channels. Plant Physiology 141: 1653-1665.

Silva, C., Martínez, V. and Carvajal, M. 2008. Osmotic versus toxic effects of NaCl on pepper plants. Biologia Plantarum 52: 72-79.

Stepien, P. and Johnson, G.N. 2009. Contrasting responses of photosynthesis to salt stress in the glycophyte Arabidopsis and the halophyte *Thellungiella*: role of the plastid terminal oxidase as an alternative electron sink. Plant Physiology 149: 1154-1165.

Steudle, E. and Peterson, C.A. 1998. How does water get through roots? Journal of Experimental Botany 49: 775-788.

Sun, J., Chen, S.L., Dai, S.X., Wang, R.G., Li, N.Y., Shen, X. and Zhang, Z.K. 2009. Ion flux profiles and plant ion homeostasis control under salt stress. Plant Signaling & Behavior 4: 261-264.

Tada, Y., Komatsubara, S. and Kurusu, T. 2014. Growth and physiological adaptation of whole plants and cultured cells from a halophyte turf grass under salt stress. AoB Plants plu041.

Tarasoff, C.S., Ball, D.A. and Mallory-Smith, C.A. 2007. Extreme ionic and temperature effects on germination of weeping alkaligrass (*Puccinellia distans*), Nuttall's alkaligrass

(*Puccinellia nuttalliana*) and Kentucky bluegrass (*Poa pratensis*). Weed Science 55: 305-310.

Tester. M. and Davenport, R. 2003. Na^+ tolerance and Na^+ transport in higher plants. Annals of Botany 91: 503-527.

Tran, S.T.H., Imran, S., Horie, T., Qiu, J., McGaughey, S., Byrt, C.S., Tyerman, S.D. and Katsuhara, M. 2020. A survey of barley PIP aquaporin ionic conductance reveals Ca^{2+}-sensitive *HvPIP2;8* Na^+ and K^+ conductance. International Journal of Molecular Sciences 21: 7135.

Tyerman, S.D., McGaughey, S.A., Qiu, J., Yool, A.J. and Byrt, C.S. 2021. Adaptable and multifunctional ion-conducting aquaporins. Annual Review of Plant Biology 72: 8.1-8.34.

Vaziriyeganeh, M., Khan, S. and Zwiazek, J.J. 2021. Transcriptome and metabolome analyses reveal potential salt tolerance mechanisms contributing to maintenance of water balance by the halophytic grass *Puccinellia nuttalliana*. Frontiers in Plant Science 12: 760863.

Vaziriyeganeh, M., Lee, S.H. and Zwiazek J.J. 2018. Water transport properties of root cells contribute to salt tolerance in halophytic grasses *Poa juncifolia* and *Puccinellia nuttalliana*. Plant Science 276: 54-62.

Vitali, V., Bellati, J., Soto, G., Ayub, N.D. and Amodeo, G. 2015. Root hydraulic conductivity and adjustments in stomatal conductance: hydraulic strategy in response to salt stress in a halotolerant species. AoB Plants 7: plv136.

Volkov, V. and Flowers, T.J. 2019, Mechanisms of ion transport in halophytes: from roots to leaves. In Gul, B., Böer, B., Khan, A., Clüsener-Godt, M., Hameed, A. (Eds). Tasks for Vegetation Science – 49. Shabkha Ecosystems, Volume VI: Asia/Pacific. Springer Nature Switzerland AG, Cham, Switzerland, pp. 125-150.

Volkov V., Wang, B., Dominy, P.J., Fricke, W. and Amtmann, A. 2004. *Thellungiella halophila*, a salt-tolerant relative of *Arabidopsis thaliana*, possesses effective mechanisms to discriminate between potassium and sodium. Plant, Cell & Environment 27: 1-14.

Wan, X. and Zwiazek, J.J. 1999. Mercuric chloride effects on root water transport in aspen (*Populus tremuloides*) seedlings. Plant Physiology 121: 939-946.

Wang, B., Lüttge, U. and Ratajczak, R. 2001. Effects of salt treatment and osmotic stress on V-ATPase and V-PPase in leaves of the halophyte *Suaeda salsa*. Journal of Experimental Botany 52: 2355-2365.

Wang, D., Grieve, C.M. and Suarez, D.L. 2005. Composition of irrigation water salinity affects growth characteristics and uptake of selenium and salt ions by soybean. Journal of Plant Nutrition 28: 1073-1088.

White, P.J. and Broadley, M.R. 2001. Chloride in soils and its uptake and movement within the plant: a review. Annals of Botany 88: 967-988.

Zhao. F., Song, C.-P., He, J. and Zhu, H. 2007. Polyamines improve K^+/Na^+ homeostasis in barley seedlings by regulating root ion channel activities. Plant Physiology 145: 1061-1072.

Zwiazek, J.J., Tan, X., Xu, H., Navarro-Ródenas, A. and Morte, A. 2017. Significance of oxygen transport through aquaporins. Scientific Reports 17: 40411.

2.6 Supplementary Material

Supplementary Fig. 2.1. *Poa pratensis*, *Poa juncifolia*, and *Puccinellia nuttalliana* plants after 10 days of treatments with 150 mM NaCl, 150 mM KCl, and 150 mM Na_2SO_4. Control plants were in 50% Hoagland's solution without added salts.

Chapter 3. Transcriptome and metabolome analyses reveal potential salt tolerance mechanisms contributing to maintenance of water balance by the halophytic grass *Puccinellia nuttalliana*

3.1 Introduction

Soil salinity is a challenging problem that affects plants in many natural ecosystems and in areas affected by human activities. The concerns of primary salinization due to the factors such as seawater intrusion and volcanic bedrock weathering (Alfarrah and Walraevens 2018, Mirzavand et al. 2020) have been grossly aggravated by secondary salinization due to anthropogenic manipulation of the hydrologic cycle (Herbert et al. 2015). Rising mean temperatures in many parts of the world enhance secondary salinization by increasing evapotranspiration, leading to salt buildup in the soil (Pankova and Konyushkova 2014, Okur and Örcen 2020). According to the 2013 estimate, current annual economic losses due to salt-induced land degradation could be as much as $27 billion (Shahid et al. 2018).

High salinity areas are dominated by salt-tolerant halophytic plant species, which can survive NaCl concentrations exceeding 300 mM (Flowers and Colmer 2008, Al Hassan et al. 2016). Halophytes constitute only a tiny fraction of all higher plant species, comprising approximately 2% of the world's flora (Sairam and Tyagi 2004). Halophytic plants have developed unique structural and physiological strategies to cope with salt (Shabala et al. 2014, Flowers et al., 2015). Despite the ability of halophytic plants to tolerate high salt concentrations, most studies on salt effects and salt tolerance in plants have been carried out in glycophytes since they include most of the economically important plant species. However, with the growing

salinity concerns, halophytes are gaining more attention due to their successful salt tolerance strategies.

Numerous efforts have been made to understand salinity effects on plants and the mechanisms of plant salt tolerance for crop improvement and development of vegetation management strategies in salt-affected areas (Bushman et al. 2016, Nikalje et al. 2017, Aliakbari et al. 2020). Salinity affects all stages of plant development including seed germination, vegetative, and reproductive growth (Shrivastava and Kumar 2015). It affects plants through a combination of osmotic factors, direct ion toxicity, nutrient imbalance, and reactive oxygen species (ROS) accumulation (Munns and Tester 2008, Flowers et al. 2015). Plant survival in soils with elevated salinity requires an efficient water-transporting system, which can overcome osmotic effects of salt and direct ion toxicity that affect water transport in salt-sensitive plants. Water transport is partly regulated by the aquaporins (Voicu et al. 2009, Groszmann et al. 2017). Aquaporin proteins form water channels, which facilitate the passive transport of water and a range of neutral solutes and gasses across the cell membranes (Maurel et al. 2008, Zwiazek et al. 2017, Tan et al. 2018). It has been demonstrated that the aquaporin-mediated water transport is rapidly inhibited in glycophytic plants by NaCl concentrations as low as 10 mM (Lee and Zwiazek 2015). However, cell hydraulic conductivity was enhanced in *Puccinellia nuttalliana* by 50 and 150 mM NaCl (Vaziriyeganeh et al. 2018). A subsequent study showed that Na^+ was the factor responsible for the enhancement of aquaporin-mediated root water transport in this halophytic grass resulting in higher cell hydraulic conductivity (Vaziriyeganeh et al. 2022). However, the exact processes contributing to this enhancement, including those at the molecular level, remain unknown.

Plant molecular responses to NaCl involve complex gene regulatory networks that may directly and indirectly affect the function of aquaporins and, ultimately, plant water transport. As soon as plants perceive salt stress, signaling molecules such as ROS, Ca^{2+}, and various phytohormones are activated. Transcription factor (TF) families play important roles in plant responses to abiotic stress. TFs such as MYB, NAC, WRKY, bHLH, bZIP, AP2/ERF, and ERF/DREB may be involved in plant stress responses (Baillo et al. 2019, Das et al. 2019). The salt overly sensitive (SOS) signal transduction cascade consisting of SOS3 (CBL calcium sensor), SOS2 (CIPK protein kinase), and SOS1 (Na^+/H^+ antiporter) genes encode proteins that are involved in Na^+ extrusion (Zhu et al. 1998, Ji et al. 2013) to regulate plant ion homeostasis. Salt stress triggers cytosolic Ca^{2+} signaling (Hasegawa et al. 2000, Parre et al. 2007). Ca^{2+} binds to SOS3 and forms a SOS3-SOS2 complex by activating SOS2 leading to the activation of the downstream SOS1, a $Na^{+/}H^+$ antiporter. Several other ion transporters function as pumps for the sequestration of Na^+ into vacuoles of both roots and shoots (Nikalje et al. 2017). Exposure of plants to salt also triggers changes in the aquaporin expression (Lee and Zwiazek 2015, Braz et al. 2019). However, gene expression data alone cannot unravel complex responses that are triggered by salt and lead to altered hydraulic responses in plants.

Since salinity tolerance is a complex trait that involves multi-gene responses, only a comprehensive study approach involving different methods can provide the best platform for the efforts aimed at improvement of salt tolerance in plants. Recent advances in metabolomics and transcriptomics (Cavill et al. 2016, Ren et al. 2019) have created an opportunity to examine a wide spectrum of these complex plant responses contributing to salt tolerance. While transcriptomics can provide useful information concerning the functional elements of the genome and associated pathways related to salt stress, combining the transcriptomic and

metabolomic data can be a powerful tool to better characterize the molecular and functional traits involved in the salt tolerance processes.

In the present study, plants of the halophytic northern grass *Puccinellia nuttalliana* were exposed to the 150 mM NaCl treatment for six days and root transcriptome as well as root and leaf metabolome analysis were performed to understand the mechanisms underlying salt tolerance. It was of particular interest to unravel the processes enabling *P. nuttalliana* to maintain the functionality of aquaporin-mediated water transport under salt stress conditions that were earlier reported (Vaziriyeganeh et al. 2018, 2022). I hypothesized that ion and osmotic homeostasis combined with changes in the aquaporin gene profile are the key elements involved in water balance maintenance under salinity conditions. The transcriptomic and metabolomic analyses were supplemented with the measurements of plant growth parameters, root and leaf structure, and tissue ion concentrations to obtain a more complete view of the processes contributing to salt tolerance in this halophytic plant.

3.2 Materials and Methods

3.2.1 Growth conditions and NaCl treatment

Seeds of *Puccinellia nuttalliana* (Schult.) Hitchc. were surface sterilized for 2 min with 70% ethanol followed by 1% sodium hypochlorite for 1 min. The sterilized seeds were washed by autoclaved water and spread on plates containing half-strength Murashige and Skoog (MS) solid medium (Murashige and Skoog, 1962) with no added sugar or hormones. Three days after germination, the seedlings were transferred to plastic containers filled with horticultural soil and grown in the controlled-environment growth room with 22/18ºC (day/night) temperature, 16-h photoperiod with 300 µmol m^{-2} s^{-1} photosynthetic photon flux density (PPDF), and 50-60%

relative humidity. Plants were fertilized once a week with half-strength modified Hoagland's solution (Epstein 1972) and were watered twice a week to runoff. After eight weeks of growth in the soil, the seedlings were removed from pots, their roots washed, and placed in six 12 L containers filled with aerated 50% Hoagland's mineral solution. The containers with seedlings were placed in a controlled-environment growth room with the growth conditions as described above and grown for one week prior to the commencement of NaCl treatment. The plants in three containers (nine plants per container) were treated for six days with 0 mM NaCl (control) and those in the remaining three containers (nine plants per container) were treated with 150 mM NaCl, which was gradually added in 50 mM increments over the course of one day to the nutrient solution. The NaCl treatment concentration and duration were selected based on the previous study, (Vaziriyeganeh et al. 2018) that showed an enhancement of growth and root cell hydraulic conductivity in *P. nuttalliana*. The experiment was arranged in the randomized complete block design with plants placed in three replicated containers per treatment (control and 150 mM NaCl). Four (n = 4) plants per treatment were randomly taken from the three replicated containers for metabolomic analysis and transcriptome sequencing, respectively, and six plants (n = 6) for dry weight determinations and elemental analysis.

3.2.2 Plant dry weights and tissue elemental analysis

After six days of treatments, shoot and root dry weights were determined in six seedlings per treatment (n = 6). Plants were harvested, and their shoots and roots separated and placed in an oven at 70^{o}C for 72 h and weighed. The total plant dry weights were obtained by combining shoot and root dry weights. For the elemental analyses, root and shoot samples (0.2 g dry weight) of six plants per treatment (n = 6) were collected after six days of treatments. To determine shoot and root concentrations of sodium and potassium, the samples from six plants per treatment (n =

6) were digested with 70% HNO_3 and heated for 10 minutes at 185℃ in a microwave oven (Mars 5 Microwave Accelerated Reaction System, CEM, Matthews, NC, USA). The extracts were diluted with Milli-Q water, filtered, and analyzed with the inductively coupled plasma – optical emission spectrometer (iCap 6000, Thermo Fisher Scientific Inc, Waltham, MA, USA). Tissue chloride was analyzed in hot water extracts using the EPA 325.2 ferrothiocyanate method (US Environmental Protection Agency 1983) with the Thermo Gallery plus Beermaster Auto analyzer (Thermo Fisher Scientific, Vantaa, Finland). The analyses were carried out in the Natural Resources Analytical Laboratory of the University of Alberta, Edmonton, Canada.

3.2.3 RNA extraction

Total RNA was extracted from the roots of *Puccinellia nuttalliana* using the RNeasy Plant Mini Kit (QIAGEN, Venlo, Netherlands). The quality of total RNA was determined by gel electrophoresis, and the concentration of the extracted total RNA was determined using a NanoDrop 2000c spectrophotometer (Thermo Fisher Scientific Inc., Waltham, MA, USA). The RNA quality control (RNA concentration, RIN value, 28S/18S, and the fragment length distribution) was performed using a 2100 Bioanalyzer (Agilent, Mississauga, ON, Canada). The RNA Integrity Number (RIN) values were greater than 7.0.

3.2.4 cDNA library preparation and RNA sequencing

The mRNA was fragmented, and then poly(A) + mRNA was isolated using oligo dT. Double-stand cDNA (dscDNA) was synthesized from the fragmented RNA by the N6 random primer. The synthesized cDNA was subjected to end-repair and then was 3’ adenylated. Successively, DNA oligonucleotides adaptors were ligated to the ends of these 3’ adenylated cDNA fragments. The ligation products were purified, and several rounds of PCR amplification were performed to enrich the purified cDNA template. The double-strand PCR products were

denatured by heat, and the single-strand DNA was cyclized by splint oligo and DNA ligase. The sequencing of each cDNA library was carried out in the BGISEQ-500 system with the paired-end sequencing length of 100 bp according to the manufacturer's instructions at the Beijing Genomics Institute (BGI-Shenzhen, China).

3.2.5 Sequencing reads filtering, *de novo* assembly and functional annotation

The sequencing reads containing low quality, adaptor-polluted, and high content of unknown base (N) reads were processed to be removed before downstream analyses. The raw data filtering component statistics and clean reads quality metrics are provided in the Supplementary Table 3.1. The Trinity (Grabherr et al. 2011) was used to perform de novo assembly with clean reads and Tgicl (Pertea et al. 2003) on cluster transcripts to remove abundance and obtain unigenes. Functional annotation of the unigenes was performed by a BLASTx search with an E-value of 10−5 against seven protein databases included non-redundant (NR) protein database, non-redundant nucleotide sequence (Nt) database, Gene ontology (GO), euKaryotic Orthologous Group database (KOG), Kyoto Encyclopedia of Genes and Genomes protein database (KEGG), SwissProt, and InterPro. Additionally, Blast2GO (Conesa et al. 2005) was used to obtain the GO. The ratio of different unigene annotations was calculated based on the NR database functional annotation results.

3.2.6 Unigene simple sequence repeats detection

The MISA version v1.0 was used, with the parameters 1-12,2-6,3-5,4-5,5-4,6-4 100 150, to detect simple sequence repeats (SSRs) in unigenes, then designed primers for each SSR with the Primer3 software (https://primer3.ut.ee/) using the default parameters.

3.2.7 Unigene expression and differentially expressed genes detection

Bowtie2 (Langmead et al. 2012) version: v2.2.5 was used to map clean reads to unigenes and then calculate the gene expression level with RSEM (Li et al. 2011) version: v1.2.12 using the default parameters. The fragments per kilobase per transcript per million mapped reads (FPKM) method was used (Trapnell et al. 2010) to compare the gene expression differences among different samples. Ddifferentially Expressed Genes (DEGs) were detected with DEseq2 using the parameters: fold change ≥ 2.00 and adjusted P value ≤ 0.05. GO and KEGG pathway and enrichment analysis were performed on the DEGs.

3.2.8 Validation of expression changes by quantitative real-time PCR

To confirm the gene expression data obtained from the RNA-seq data, a subset of differentially expressed genes was validated by quantitative real-time PCR (qRT-PCR). Four plants per treatment and three technical replications were used. The genes included HKT1;5 (Unigene42482_All), PIP2;2 (Unigene159054_All), TIP4;4 (Unigene43183_All), WRKY17 (CL11112.Contig4_All), DUF4220 (Unigene37730_All), CBL10 (Unigene160802_All), MYB77 (Unigene25779_All), and HAK9 (CL646.Contig7_All). Roots were washed in distilled water and blot-dried with a paper towel. The collected tissues were immediately flash-frozen in liquid nitrogen and stored in -80^{o}C freezer until used. The roots were homogenized by grinding in liquid nitrogen with a pestle and mortar and total RNA was extracted from roots using QIAGEN RNeasy Plant Mini Kit (Qiagen, Germantown, MD, USA. The RNA concentration and purity were assessed using a Thermo Scientific™NanoDrop™ One Microvolume UV-Vis Spectrophotometer (Thermo Fisher Scientific, Waltham, MA, USA). RNA quality was also checked on a 1% (w/v) agarose gel. The removal of genomic DNA contamination and first strand cDNAs were generated using the Qiagen QuantiTect Reverse Transcription Kit with 500 µg total

RNA according to the manufacturer's instructions. The qRT-PCR was performed using SYBR Green I dye reagent in an Applied Biosystems 7500 Fast system with 10-fold diluted cDNA. The relative expression of all genes was calculated using the $2^{-\Delta\Delta CT}$ method (Livak and Schmittgen 2001). Melting curve analysis and gel electrophoresis were performed for the specificity of the PCR amplification product for each primer pair. Two reference genes, *ACT* (Actin) and *ADP* (ADP-ribosylation factor 1) were used for normalization. The primers used for the qRT PCR analysis are listed in Supplementary Table 3.2. For validation of primers, serial dilutions of the cDNA were used to create a standard curve by plotting the log value of starting templet quantity against the Ct values obtained for each dilution. Amplification efficiency (E) was calculated using slope from linear regression of the standard curve according to the equation $E = (10^{-1/slope} - 1) \times 100$ (Supplementary Table 3.2).

3.2.9 DI/LC-MS/MS

The individual freeze-dried and grinded plant root and leaf tissue samples were placed in screw vials and sent to The Metabolomics Innovation Centre (TMIC), AB, Canada for further sample preparation and analysis. A targeted quantitative metabolomics approach was applied to analyze root and shoot samples using a combination of direct injection (DI) mass spectrometry and a reverse-phase LC-MS/MS custom assay. This custom assay, in combination with an ABSciex 4000 QTrap (Applied Biosystems/MDS Sciex) mass spectrometer, was used for the targeted identification and quantification of different endogenous metabolites including amino acids, acylcarnitines, biogenic amines and derivatives, organic acids, glycerophospholipids, and sugars (Foroutan et al. 2009, 2020). The method combines the derivatization and extraction of analytes, and the selective mass-spectrometric detection using multiple reaction monitoring (MRM) pairs. Isotope-labeled internal standards and other internal standards were used for

metabolite quantification. The custom assay contained a 96 deep-well plate with a filter plate attached with sealing tape, and reagents and solvents used to prepare the plate assay. First 14 wells were used for one blank, three zero samples, seven standards and three quality control samples. For all metabolites except organic acids, samples were thawed on ice and were vortexed and centrifuged at 13,000 x g. Each 10 µL sample was loaded onto the center of the filter on the upper 96-well plate and dried with a stream of nitrogen. Subsequently, phenyl-isothiocyanate was added for derivatization. After incubation, the filter spots were dried again using an evaporator. Extraction of the metabolites was then achieved by adding 300 µL of extraction solvent. The extracts were obtained by centrifugation into the lower 96-deep well plate, followed by a dilution step with the MS running solvent. For the organic acid analysis, 150 µL of ice-cold methanol and 10 µL of isotope-labeled internal standard mixture were added to 50 µL of each sample for overnight protein precipitation and then centrifuged at 13,000 x g for 20 min. The supernatant (50 µL) was loaded into the center of wells of a 96-deep well plate, followed by the addition of 3-nitrophenylhydrazine (NPH) reagent. After incubation for 2 h, butylated hydroxytoluene (BHT) stabilizer and water were added before LC-MS injection. Mass spectrometric analysis was performed using an ABSciex 4000 Qtrap® tandem mass spectrometry instrument (Applied Biosystems/MDS Analytical Technologies, Foster City, CA, USA) equipped with an Agilent 1260 series UHPLC system (Agilent Technologies, Palo Alto, CA, USA). The samples were delivered to the mass spectrometer by the LC method followed by the direct injection (DI) method.

3.2.10 Metabolome data analysis

Metabolites were searched using Analyst software (V.1.6.2) from AB SCIEX (Concord, ON, Canada). Principle component analysis (PCA) and statistical analyses were performed using

MetaboAnalyst 5.0 (Pang et al. 2021). Venn diagrams were created using Venny 2.0.2 interactive tool (Oliveros 2007 -2015).

3.2.11 Root anatomy and leaf morphology

Distal root segments (n = 5) from each treatment were prepared for microscopy according to Roschzttardtz et al. (2009). Distal 3-5-cm root segments were fixed in formalin-acetic acid-alcohol (FAA) solution. After fixation, the root segments were dehydrated in an ethanol series followed by toluene, embedded in paraffin, and sectioned with a microtome (model RM2125 RTS, Leica; Solms, Germany). The sections were mounted on slides and examined under the light microscope (Olympus SZ61 TR Stereo Light Microscope equipped with SeBaCam 5.1MP Camera). Lignin auto fluorescence was visualized using green light (Filter Wheel Setting = 3, Green Image, Leica Filter cube: I3), following UV excitation at 330 nm to 380 nm with a fluorescent microscope (Carl Zeiss; Jena, Germany) (Donaldson and Radotic 2013). The light intensity of lignification was determined with Image J software (https://imagej.nih.gov/ij/) (n = 5 images per group) and quantified as previously described (Yamaguchi et al. 2010).

3.2.12 Sample preparation for scanning electron microscopy (SEM)

Approximately 5-mm-long leaf segments were excised from the control *Puccinellia nuttalliana* plants and from plants treated for six days with 150 mM NaCl. The leaf samples were immediately placed in the FAA fixative and dehydrated using a series of increasing ethanol concentrations followed by hexamethyldisilazane and air-dried. The samples were then placed on metal SEM stubs, attached with a double-sided carbon tape, sputter-coated with Au/Pd, and mounted. The samples were viewed using the ZEISS EVO 10 Scanning Electron Microscope (Carl Zeiss Microscopy, Köln, Germany) at the University of Alberta Microscopy Facility.

3.3.13 Statistical analyses

Statistical analyses were carried out using the SPSS 18.0 statistical package (SPSS Inc., Chicago, IL, USA). One-way ANOVA was carried out followed by the Tukey's test to detect significant differences between the treatments for each plant species ($p \leq 0.05$).

3.3 Results

3.3.1 Plant dry weights and Na^+, K^+, and Cl^- tissue concentrations

The six-day 150 mM NaCl treatment had no significant effect on the root, shoot, and total plant dry weights as well as the shoot:root dry weight ratios (Fig. 3.1A). *Puccinellia nuttalliana* accumulated less K^+ and more Na^+ in roots compared with shoots, resulting in about three-fold higher Na^+/K^+ ratio in roots than shoots under salt stress (Fig. 3.1B). The concentration of Cl^- in shoots relative to roots was six times higher under NaCl treatment (Fig. 3.1C).

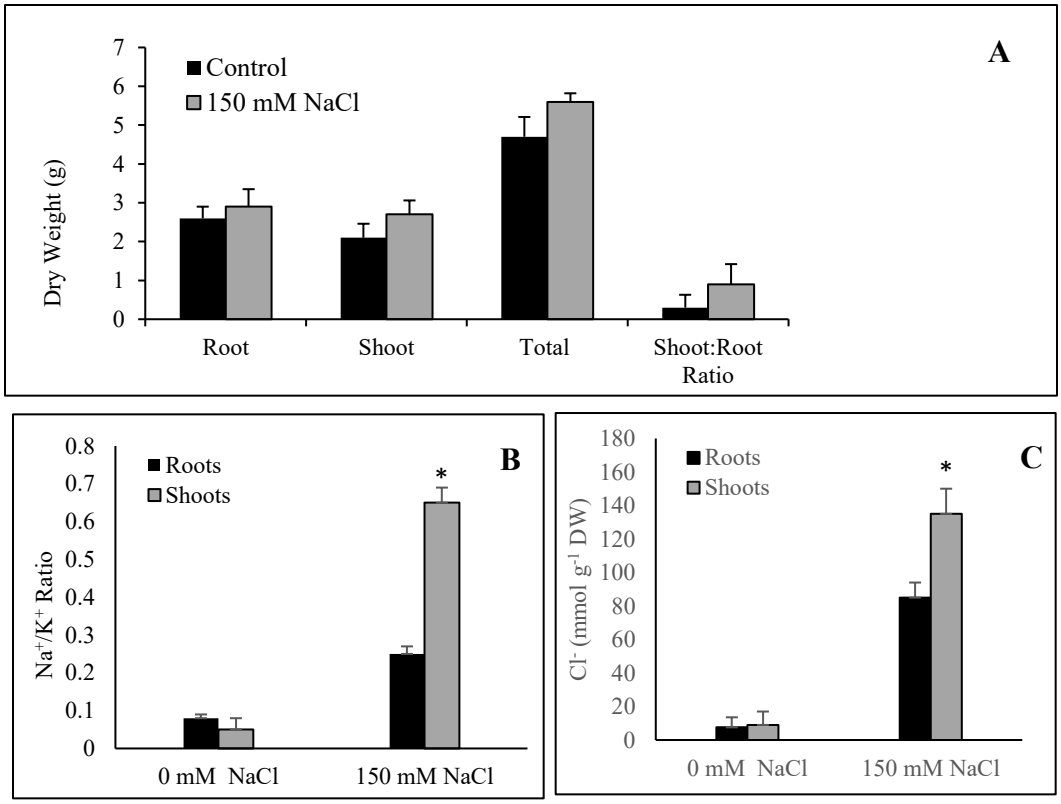

Fig. 3.1. Root, shoot, total dry weights, and shoot: root dry weight ratios (A), Na^+/K^+ ratios (B) and Cl^- concentrations (C) in roots and shoots of *Puccinellia nuttalliana* treated with 0 mM and 150 mM NaCl for six days. Asterisks above the bars indicate significant differences ($p \leq 0.05$) between treatments as determined by the Tukey's test. Means (n = 6) and SE are shown.

3.3.2 Sequencing and *de novo* assembly

Transcriptome sequencing generated 52.47 million paired-end reads per sample and in total about 30.91 Gb clean bases. Raw reads were filtered for low-quality, adaptor-polluted, and high content of unknown base (N) reads. The statistics of the assembled sequence and Trinity based *de novo* assembly statistics from each assembly are presented in Table 3.1. The raw reads were deposited in the Sequence Read Archive (SRA) of the National Center for Biotechnology Information (NCBI) database. The BioSample accessions are Pnu_RNAseq_Control (SRX8289102) and Pnu_RNAseq Treated (SRX8289103).

Table 3.1. Output statistics for *Puccinellia nuttalliana* transcriptome sequencing and de novo assembly. Trinity statistics for quality metrics of transcripts of each *Puccinellia nuttaliana* sample

Filter summary

Sample	Total raw reads (M)	Total clean reads (M)	Total clean bases (Gb)	Clean reads Q20 (%)	Clean reads Q30 (%)	Clean reads ratio (%)
C1	52.47	51.69	5.17	97.94	91.46	98.52
C2	52.47	51.49	5.15	97.96	91.61	98.12
C3	52.47	51.56	5.16	98.08	91.94	98.26
T1	52.47	51.38	5.14	97.98	91.84	97.92
T2	52.47	51.34	5.13	97.69	90.73	97.84
T3	52.47	51.56	5.16	97.86	91.41	98.25

***De novo* assembly Trinity statistics**

Sample	Total number	Mean length	N50	N70	N90	GC (%)
C1	180284	565	873	445	232	46.9
C2	187042	576	886	465	237	46.78
C3	192381	587	914	477	240	46.1
T1	152132	575	929	459	230	49.15
T2	108930	691	1228	635	261	49.7
T3	121125	598	961	512	240	50.33

C = control, T = 150 mM NaCl treatment, and 1–3 = replications.

3.3.3 Functional annotation of unigenes and unigene SSR detection

After assembly, a total of 242833 unigenes were identified. The clustering quality metrics are shown in Supplementary Table 3.2, and the unigene length distribution is shown in Fig. 3.2A. All unigenes were blast-searched against the public databases, including non-redundant protein (Nr) database, non-redundant nucleotide (Nt) database, InterPro, Swiss-Prot, Gene Ontology (GO), Kyoto Encyclopedia of Genes and Genomes (KEGG), and Clusters of Orthologous Groups (KOG). The number and percentage of unigenes annotated by each database are summarized in Table 3.2. Results of functional annotation showed that 156208 (64.33%) of 242833 unigenes were successfully annotated by the databases. The Venn diagram was used to show the annotation results of NR, KOG, KEGG, SwissProt, and InterPro in Fig. 3.2B. The Venn diagram showed that all five databases simultaneously annotated 67221 unigenes. In functional annotation, 54.38% aligned unigenes in the NR database were used to calculate their distribution and frequency in different species. Based on the NR database, ~34% of unigenes matched sequences from only three grass species including *Aegilops tauschii* (18.03%),

Brachypodium distachyon (8.92), and *Hordeum vulgare* (7.11%) (Fig. 3.2C). The unigenes annotated by the Nr database were assigned into three gene sub-ontologies: biological process (26 subcategories), cellular component (16 subcategories), and molecular functions (14 subcategories) (Supplementary Fig. 3.1) using the Blast2GO program (Conesa et al. 2005).

Table 3.2. Annotation summary for unigenes of *Puccinellia nuttalliana* using public databases

Values	Total	Nr	Nt	SwissProt	KEGG	KOG	InterPro	GO	Intersection	Overall
Number	242,833	132,055	65,723	90,860	101,589	112,069	114,638	77,665	23,491	156,208
Percentage	100%	54.38%	27.07%	37.42%	41.83%	46.15%	47.21%	31.98%	9.67%	64.33%

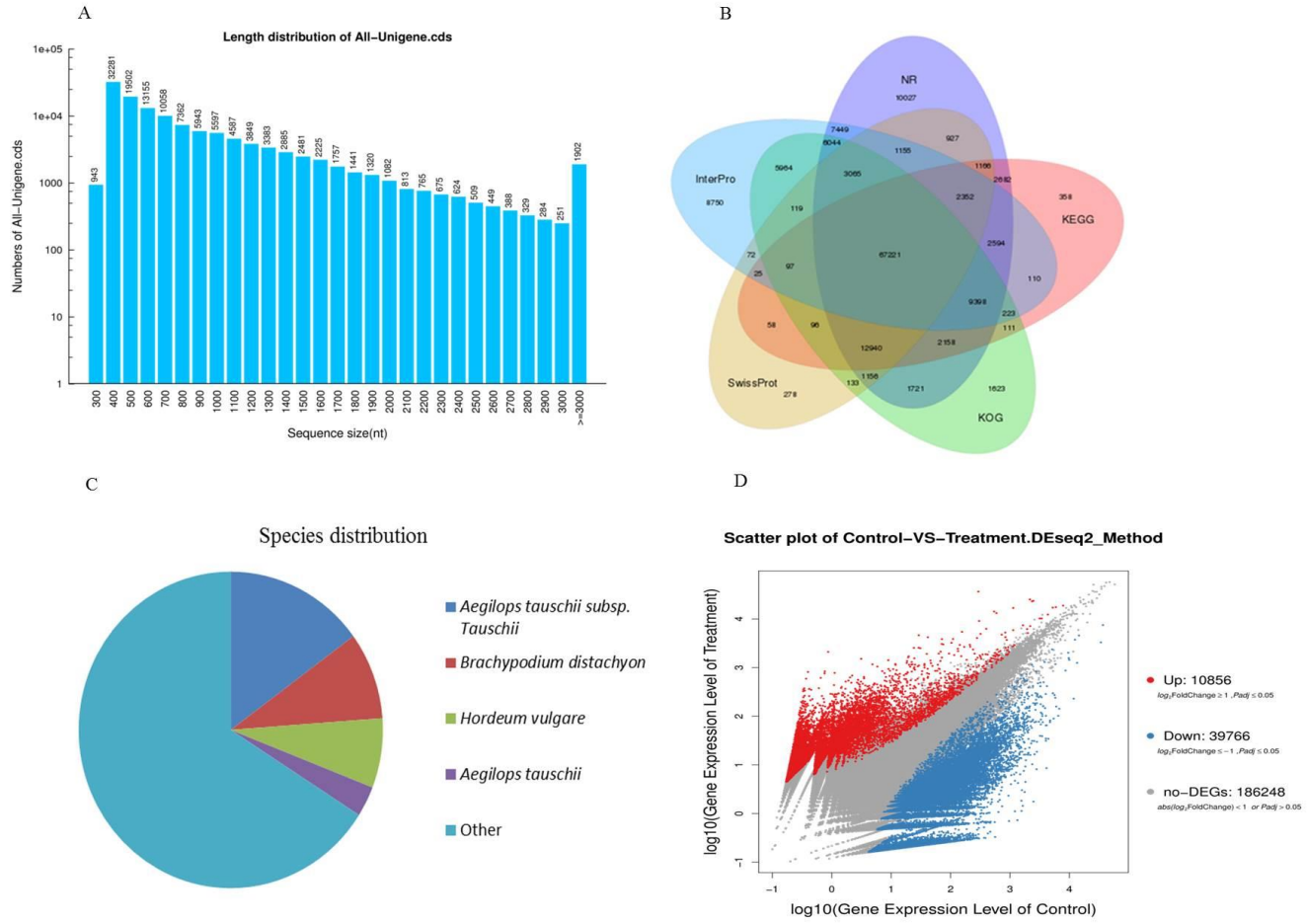

Fig. 3.2. The length distribution of unigenes of *Puccinellia nuttalliana* transcriptome (A), venn diagram showing functional annotation between NR, KOG, KEGG, Swissprot and Interpro databases (B), distribution and frequency of non-redundant (NR) annotated species (C), scatter plot of differentially expressed genes (DEGs) in roots of NaCl-treated *Puccinellia nuttalliana* plants compared to the controls. Red color represents the upregulated genes, blue color represents the downregulated genes, grey color represents the non-significant differential genes (D).

Simple sequence repeats (SSRs) or microsatellites are short, tandemly repeated DNA motifs used to evaluate population genetic diversity and structure and genetic linkage mapping. *De novo* screening of large sets of SSR detection was performed for *Puccinellia nuttalliana*. The size summary of SSR is shown in Fig. 3.3. Trinucleotide repeats were predominant (17,613). Five and six tandem repeats were found for 560 and 602 motifs, respectively. The prominent trinucleotide repeat was identified as CCG/CGG (3227) and AAC/GTT (3210).

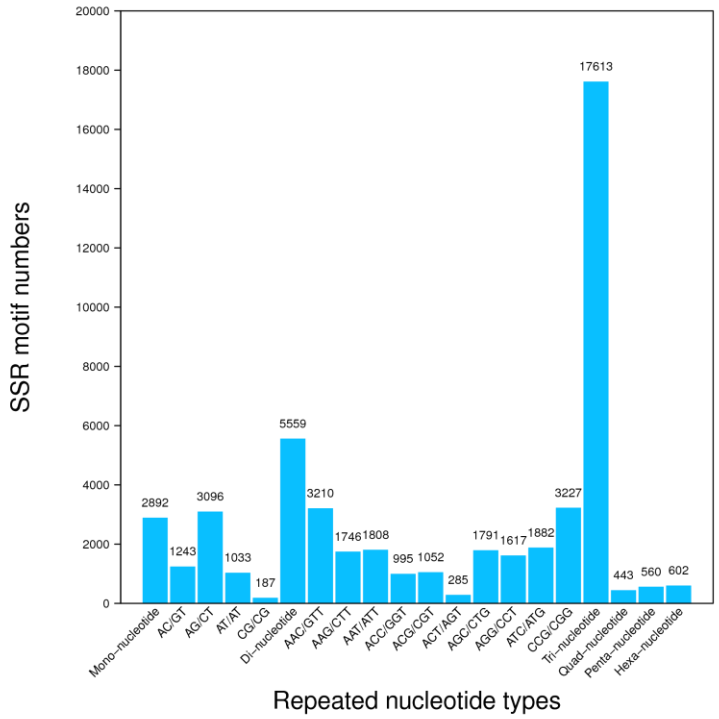

Fig. 3.3. Frequency distribution of simple sequence repeats (SSR). The x-axis indicates the type of SSR and the y-axis indicates the number of SSR.

3.3.4 Validation of RNA-seq results by quantitative real-time PCR

To validate the RNA-Seq transcriptome profiling, eight differentially expressed genes including *HKT1;5*, *PIP2;2*, *TIP4;4*; *WRKY17*, *DUF4220*, *CBL10*, *MYB77*, and *HAK9* were randomly selected for qRT-PCR analysis. The results demonstrated similar gene expression trends using the qRT-PCR analysis to those obtained through the RNA-seq data (Fig. 3.4).

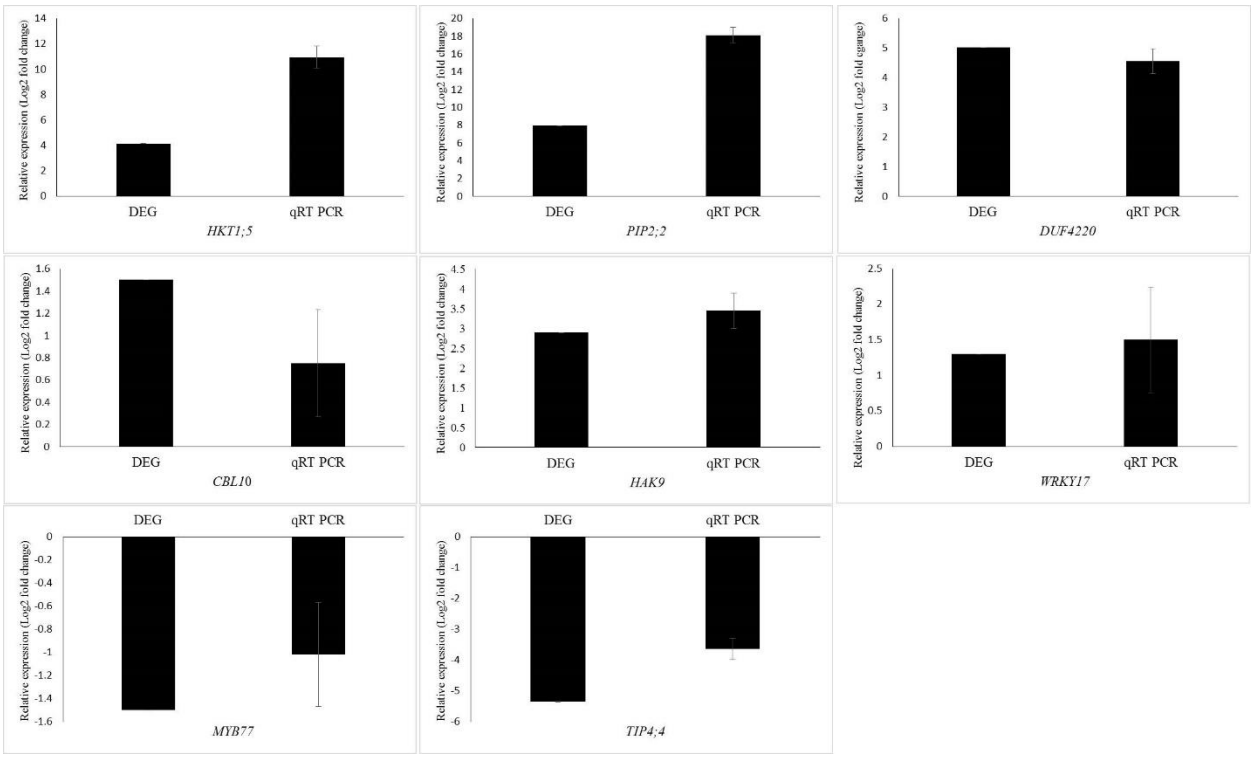

Fig. 3.4. Validation of transcriptional changes of eight randomly selected genes from the DEGs using qRT-PCR of *Puccinellia nuttalliana* under NaCl stress. Values are means + SE of four biological replicates. Each biological replicate was comprised of three technical replicates.

3.3.5 Differences in transcript profiles between NaCl-treated and control plants

A total of 50,622 genes were differentially expressed between the NaCl-treated and control *Puccinellia nuttalliana* root samples (Fig. 3.2D). Among these DEGs, 10,856 and 39766 were up-and downregulated under salt stress. Gene Ontology (GO) classification was performed of the differentially expressed genes in *Puccinellia nuttalliana*. The GO classification of differentially expressed genes is shown in Fig.3.5. The most enriched biological process terms were cellular process, metabolic process, biological regulation, regulation of biological process, response to stimulus, and signaling. In the category of cellular components, cell, cell part, organelle, membrane, and membrane parts were highly represented. In the category of molecular functions, binding, catalytic activity, structural molecular activity, transporter activity, and

transcription regulation activity were enriched. KEGG pathway classification with DEGs was performed to identify the major active biological pathways in *Puccinellia nuttalliana* in response to salt stress.

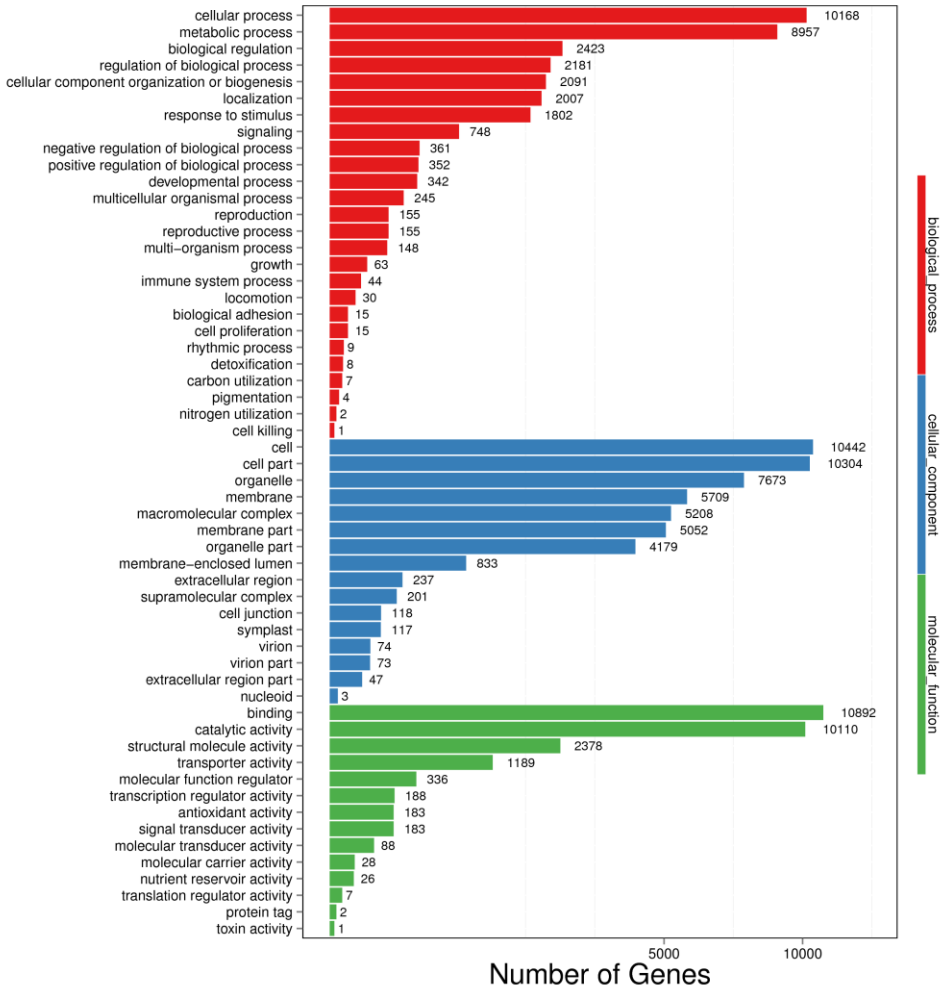

Fig. 3.5. Gene ontology enrichment analysis of differentially expressed genes between 0 (control) and 150 mM NaCl- treated *Puccinellia nuttalliana*.

The pathway classification results are shown in Fig. 3.6A and the pathway functional enrichment results are shown in Fig. 3.6B. The DEGs were assigned to 21 KEGG terms under five primary categories: cellular processes, environmental information processing, genetic information

processing, metabolism, and organismal systems. Most of the DEGs included carbohydrate metabolism (1674), amino acid metabolism (1067), energy metabolism (1073), lipid metabolism (1012), and nucleotide metabolism (866). Genetic information processing exhibited the second highest DEGs, followed by environmental information processing. The differentially expressed genes (DEGs) were subjected to the KEGG pathway enrichment analysis. Significantly enriched KEGG pathways included the ribosome, RNA transport, arachidonic acid metabolism, fatty acid elongation, butanoate metabolism, biotin metabolism, and cholesterol metabolism categories (Fig. 3.6B).

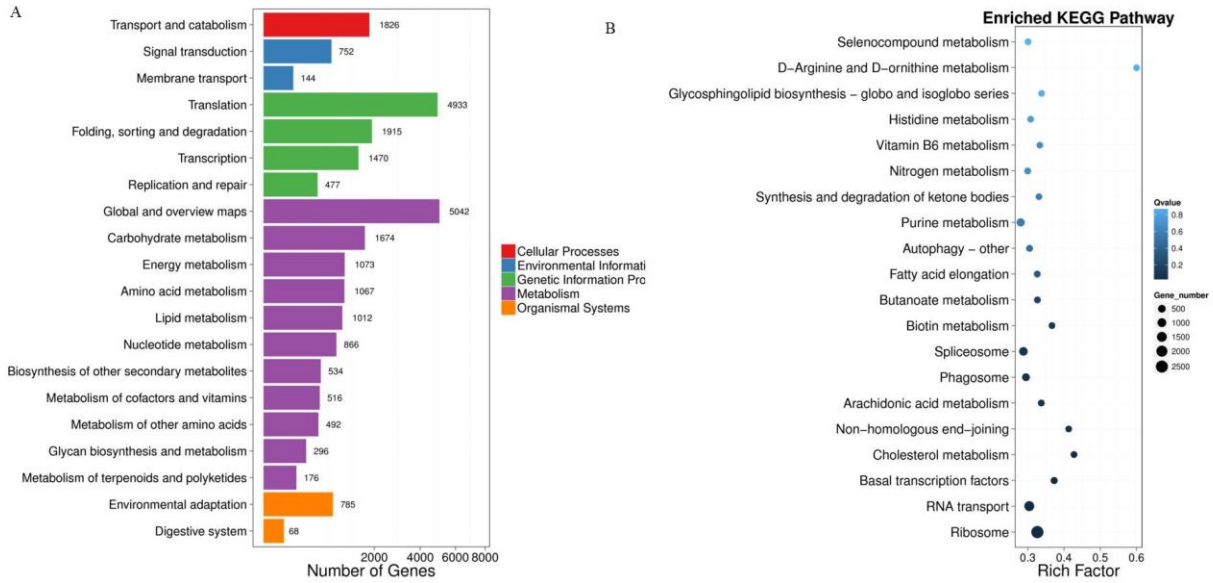

Fig. 3.6. KEGG pathway classification of differentially expressed genes in roots of NaCl treated *Puccinellia nuttalliana* plants compared to the untreated control. The five branches for KEGG pathways: cellular processes, environmental information processing, genetic information processing, metabolism, organismal systems, and drug development (A), top 20 KEGG pathways of differentially expressed genes in roots of salt treated *Puccinellia nuttalliana* plants compared to the controls (B). *X* axis represents enrichment factor. *Y* axis represents pathway name. The *q* value is indicated by the colors (high: white, low: blue), the lower *q* value indicates the more significant enrichment. Point size indicate DEG number (The bigger dots refer to larger amount). Rich Factor refers to the value of enrichment factor, which is the quotient of foreground value (the number of DEGs) and background value (total Gene amount). The larger the value, the more significant enrichment.

3.3.6. Activation of signals and signal transduction pathways in response to NaCl stress

Multiple modifying enzymes comprising MAPKs, CIPKs, and CBLs, that are involved in the signal transduction processes, were induced by salt stress. Increased levels of transcript abundance were found for these proteins under salt stress compared to control plants Several genes involved in Ca^{+2} signaling were differentially expressed, such as calcium-transporting ATPases (*Ca^{2+} -ATPase,* Unigene24255_All) and Ca^{+}/H^{+} exchangers (*CAXs*, Unigene78000_All, Unigene33268_All, and CL20809.Contig7_All) were upregulated in

response to salt stress (Table 3.3). Increased calcium ions signals are sensed by several calcium sensor proteins such as calcium-dependent protein kinases (*CDPK*) and calcineurin B-like (CBL) proteins. In this study, three *CBLs* (Unigene42846_All, CL2596, Contig5_All and CL16803.Contig1_All), and 19 *CDPK* genes were upregulated in response to salt stress. SOS3 activates SOS2 (CIPK) and forms a SOS3-SOS2 complex that triggers downstream SOS1. Under salt stress, 11 *CIPKs* were upregulated. All differentially expressed *SOS1* (*NHE*) were downregulated in response to NaCl stress. DEGs showed that the mitogen-activated protein kinase (MAPK) signaling pathway was perturbed due to salinity stress. MAPK cascades comprised of three kinases, MAPK, MAPK kinase (MAPKK, or MEK), and MAPKK kinase (MAPKKK, or MEKK (Joo et al., 2008). In this study, two transcripts orthologous to Arabidopsis *MAPK5* (Unigene36765_All; log2 FC= 5.23), *MAPK6* (CL2073.Contig1_All; log2 FC=1.34) increased in abundance due to salt stress (Table 3.3). *MEKK* (CL288.Contig3_All; log2 FC= 6.45) and *MAPKKK3* (Unigene32660_All; log2 FC= 3.69) transcripts, involved in MAPK signaling pathway, were also upregulated in response to NaCl (Table 3.3). Transcript orthologous to Arabidopsis *ACS2* (Unigene4173_All; log2 FC= -5.28) was downregulated due to salt stress (Table 3.3). Other crucial signaling moieties are phospholipase C, and phospholipase D. Two phospholipase C-like transcripts Unigene76877_All (log2 FC= 4.70) and Unigene89254_All (log2 FC= 6.18) and one phospholipase D (Unigene80611_All; log2 FC= 5.37)-like transcripts were upregulated in response to salt stress (Table 3.3).

Table 3.3. Fold changes of differentially expressed genes under salt stresses in the roots of *Puccinellia nuttalliana*

Query_ID	Regulated	log2 Fold Change	P-value	Annotation
Signal transduction pathway genes				
Unigene24255_All	Up	5.30	9.23E-05	Calcium transporting ATPase
CAX				
CL17973.Contig1_All	Down	-3.75	2.29E-05	Vacuolar cation/proton exchanger CAX2.
Unigene5119_All	Down	-5.33	1.04E-06	Vacuolar cation/proton exchanger CAX2
CL17973.Contig2_All	Down	-5.08	0.0046	Vacuolar cation/proton exchanger CAX2
Unigene42846_All	Up	7.09	9.99E-06	Calcineurin B-like protein 1
CL2596.Contig5_All	Up	5.23	0.0030	Calcineurin B-like protein 4
Unigene42846_All	Up	7.09	9.99E-06	Calcineurin B-like protein 1
CL2596.Contig5_All	Up	5.21	0.0030	Calcineurin B-like protein 4
Unigene160802_All	Up	5.41	0.0026	Calcineurin B-like protein 6
CL16803.Contig1_All	Up	5.76	0.0008	CBL-interacting protein kinase 28
Unigene36765_All	Up	5.23	0.0031	MAPK5; mitogen-activated protein kinase 5
CL2073.Contig1_All	Up	1.34	0.0080	MAPK6; mitogen-activated protein kinase 6
CL288.Contig3_All	Up	6.45	8.80E-05	mitogen-activated protein kinase kinase kinase
Unigene32660_All	Up	3.69	0.0064	Mitogen-activated protein kinase kinase kinase 3
Unigene4173_All	Down	-5.29	0.0026	ACS2, 1-aminocyclopropane-1-carboxylate synthase 2
Unigene76877_All	Up	4.70	0.0106	Phospholipase C
Unigene89254_All	Up	6.18	0.0003	Phospholipase C
Unigene80611_All	Up	5.38	0.0037	Phospholipase D
Unigene20698_All	Up	5.95	0.000182	Calcium-dependent protein kinase 2
Unigene80242_All	Up	3.96	0.004923	Calcium-dependent protein kinase 12
CL19105.Contig2_All	Up	3.72	0.002681	Calcium-dependent protein kinase 7
Unigene88181_All	Up	5.70	0.002045	Calcium-dependent protein kinase 3
CL21144.Contig1_All	Up	7.46	3.02E-06	Calcium-dependent protein kinase 29
Unigene48040_All	Up	4.88	0.006771	Calcium-dependent protein kinase 2
Unigene93001_All	Up	5.09	0.006859	Calcium-dependent protein kinase 11

Unigene73511_All	Up	4.70	3.92E-07	Calcium-dependent protein kinase 29
CL21144.Contig2_All	Up	5.50	1.19E-05	Calcium-dependent protein kinase 29
Unigene24112_All	Up	5.58	0.001833	Calcium-dependent protein kinase 1;
Unigene23838_All	Up	5.57	0.000261	Calcium-dependent protein kinase 20
Unigene80411_All	Up	5.27	0.004867	Calcium-dependent protein kinase 23
Unigene139659_All	Up	4.93	0.008305	Calcium-dependent protein kinase 21
Unigene27820_All	Up	5.06	8.57E-05	Calcium-dependent protein kinase 5
Unigene165516_All	Up	3.84	0.009487	Calcium-dependent protein kinase 19
Unigene35719_All	Up	4.31	0.001686	Calcium-dependent protein kinase 29-like
Unigene53868_All	Up	4.81	0.000465	Calcium-dependent protein kinase 2
Unigene160926_All	Up	5.26	0.002987	Calcium-dependent protein kinase 15
Unigene87392_All	Up	4.95	0.006536	Calcium-dependent protein kinase SK5
Ion transporter				
Unigene42482_All	Up	4.13	1.41E-06	HKT8-like Na+/K+ transporter
Unigene20014_All	Up	5.77	1.09E-05	CDK protein kinase
Unigene62798_All	Up	5.48	0.0020	Cyclin-dependent kinase CDK5
Unigene63446_All	Down	-4.41	0.0011	NHX5 Sodium/hydrogen exchanger 5
Unigene64682_All	Down	-4.50	9.54E-07	NHX6 Sodium/hydrogen exchanger 6
Unigene167080_All	Up	5.38	0.0032	Choline dehydrogenase
CL11886.Contig2_All	Up	1.84	0.0048	HAK23 Potassium transporter 23
Unigene24263_All	Up	5.61	0.0013	Potassium channel AKT1
CL14368.Contig2_All	Up	2.02	0.0035	Cyclic nucleotide-gated ion channel 1
CL11034.Contig2_All	Up	6.66	1.65E-06	Cyclic nucleotide-gated ion channel 20
CL3751.Contig3_All	Up	3.023	8.89E-05	S-type anion channel SLAH1-like
Unigene158776_All	Up	4.52	0.0043	Chloride channel
Transcription factors				
Unigene159865_All	Up	5.00	0.0064	Transcription factor MYB119
CL10257.Contig5_All	Up	2.88	0.0069	Transcription factor MYB59
Unigene25216_All	Up	1.41	0.0047	Transcription factor MYB12
Unigene167936_All	Up	5.09	0.0056	Transcription factor MYB3R-4
CL3152.Contig6_All	Up	4.63	5.50E-07	Transcription factor MYB37

CL8099.Contig1_All	Up	7.80	7.04E-07	bZIP9 basic leucine zipper 9
CL19018.Contig6_All	Up	4.24	0.0004	bZIP transcription factor 27
CL1946.Contig4_All	Up	1.42	0.0041	bZIP transcription factor 23
Unigene158885_All	Up	5.16	0.0063	Transcription factor HY5
CL17434.Contig2_All	Down	-3.83	0.0023	WRKY transcription factor 26
CL19887.Contig2_All	Down	-4.81	0.0003	WRKY transcription factor 19
Unigene41823_All	Down	-7.87	3.24E-07	WRKY transcription factor 9
CL17890.Contig3_All	Up	2.98	0.0034	WRKY transcription factor 74
Unigene54941_All	Down	-5.27	0.0043	Ethylene-responsive transcription factor RAP2-2
CL3748.Contig7_All	Down	-5.94	0.0010	Ethylene-responsive transcription factor RAP2-3
Unigene24458_All	Up	5.12	0.0048	Ethylene-responsive transcription factor RAP2-10
Unigene12659_All	Up	7.06	1.64E-05	Nascent polypeptide-associated complex subunit alpha-like protein 3
Unigene100143_All	Up	5.24	0.0052	Nascent polypeptide-associated complex subunit alpha-like protein 3
Unigene68164_All	Up	4.80	0.0009	Nascent polypeptide-associated complex subunit alpha-like protein 1
CL18756.Contig2_All	Up	7.18	4.78E-05	NAC domain-containing protein 78
CL1250.Contig12_All	Up	4.19	0.0034	NAC domain-containing protein 13
Unigene59213_All	Down	-6.94	1.63E-14	Nascent polypeptide-associated complex subunit alpha-like protein 2
Unigene167020_All	Up	3.98	0.0100	ABF2-like
Aquaporins				
Unigene159054_All	Up	7.92	2.80E-12	Aquaporin PIP2-2
Unigene76130_All	Down	-6.56	5.22E-10	Aquaporin TIP1-1
Unigene134545_All	Down	-4.99	0.0052	Aquaporin TIP2-1
Unigene19900_All	Down	-5.43	1.50E-05	Aquaporin TIP2-3
CL9482.Contig2_All	Down	-3.69	1.65E-06	Aquaporin TIP3-1
Unigene1799_All	Down	-5.72	1.04E-07	Aquaporin TIP4-1
CL11639.Contig2_All	Down	-6.94	2.12E-05	Aquaporin TIP4-2
Unigene43183_All	Down	-5.26	0.0027	Aquaporin TIP4-4
Unigene66763_All	Down	-6.39	0.0001	Aquaporin NIP1-1
Unigene71932_All	Down	-3.28	0.0014	Aquaporin NIP2-2
Genes involved in ROS defences				
Unigene17356_All	Up	6.03	0.0008	Superoxide dismutase
Unigene71422_All	Up	4.34	0.0052	Superoxide dismutase
Unigene78951_All	Up	5.78	0.0010	superoxide dismutase
Unigene43908_All	Up	4.49	0.0009	superoxide dismutase
CL14042.Contig2_All	Up	5.37	0.0029	superoxide dismutase
CL21164.Contig1_All	Up	5.53	0.0030	Peroxidase
Unigene45372_All	Up	4.08	0.0006	Peroxidase
Unigene49792_All	Up	1.98	0.0061	Peroxidase
CL3980.Contig1_All	Up	4.58	0.0032	Catalase

Unigene5188_All	Up	6.40	0.0002	Catalase
Unigene27478_All	Up	3.24	0.0049	Catalase
Unigene5399_All	Up	4.71	0.0096	Catalase
Genes involved in glycerophospholipid biosynthesis				
Unigene54315_All	Down	-4.98	0.0077	Phospholipase D beta 1
Unigene67197_All	Down	-3.83	0.0014	Phospholipase D
Unigene35739_All	Down	-3.18	0.0001	N-acyl-phosphatidylethanolamine-hydrolysing phospholipase D
CL17819.Contig2_All	Down	-3.06	0.0067	Phospholipase D1
Unigene50422_All	Down	-5.81	0.0006	Phospholipase D1
Unigene34512_All	Down	-4.48	0.0002	Phospholipase D
Unigene80611_All	Up	5.37	0.0037	Phospholipase D
Unigene29494_All	Down	-3.13	0.0043	Phospholipase D
Genes involved in lignin biosynthesis				
Unigene2227_All	Down	-4.09	0.0003	Caffeoyl-CoA O-methyltransferase
Unigene50175_All	Down	-4.26	4.09E-07	4-coumarate--CoA ligase 2-like
Unigene165035_All	Up	5.92	4-coumarate--CoA ligase 2	4-coumarate--CoA ligase 2
CL6032.Contig6_All	Up	1.47	0.0029	LAC17, Laccase-17
Unigene64739_All	Up	1.72	0.0046	PER39, PEROXIDASE 39
CL14735.Contig1_All	Up	5.12	0.0056	PRX34 Peroxidase 34
Genes involved in proline biosynthesis				
Unigene18828_All	Up	2.43	2.46E-06	P5CS2, Delta-1-pyrroline-5-carboxylate synthase 2
Unigene2907_All	Up	7.46	7.06E-06	P5CS, Delta-1-pyrroline-5-carboxylate synthase

3.3.7 Ion transporters

Transcript orthologous to *Brachypodium distachyon HKT1;5* (Unigene42482; log2 FC= 4.13) increased in abundance in salt-treated plants (Table 3.3). Two *CDKs* genes, Unigene20014 (log2 FC= 5.77) and Unigene62798 (log2 FC= 5.48), were found significantly upregulated in response to salt stress. CDKs are a large family of serine/threonine protein kinases regulating the cell cycle. Three transcripts orthologous to Arabidopsis *NHX5*, *NHX6*, and *NHX1* were downregulated in NaCl-treated plants. *HAK9* (CL646.Contig7_All; log2 FC= 2.90) and *HAK23* (CL11886.Contig2_All; log2 FC= 1.84) transcripts from HAK/KUP/KT family significantly

increased in NaCl-treated plants. *AKT1* (Unigene24263_All, log2 FC= 5.61), two cyclic nucleotide-gated cation channels (CNGCs) (CL14368.Contig2_All and CL11034.Contig2_All) ion transporters like genes were also upregulated under NaCl stress (Table 3.3). Transport of Na^+ and K^+ ions across the plasma membrane are driven by transport protons across the H^+ gradient mediated by H^+-ATPase and V-ATPase. In this study, several vacuolar ATPases and plasma membrane H^+-transporting ATPases were upregulated in NaCl-treated plants. Under NaCl conditions, Cl^- membrane transport can be conducted via the membrane transporters of multiple protein families, including CCC, cation/chloride cotransporter, and SLASH, anion channel associated homolog 1. In the present study, one SLASH1-like (CL3751.Contig3_All; log2 FC= 3.02) and one Cl^- channel-like (Unigene158776_All; log2 FC= 4.51) transcripts were upregulated under salt stress.

3.3.8 Transcription factors and regulators

Multiple transcription factor (TF) families were differentially expressed in response to NaCl treatment. Myeloblastosis oncogene (MYB) is a large, functionally diverse protein family of which a small number are directly related to salt stress response. Unigene annotation identified 408 MYB genes of which only small members were upregulated by NaCl. *MYB119* (Unigene159865_All; log2 FC= 5.00), *MYB59* (CL10257.Contig5_All; log2 FC= 2.88), *MYB12* (Unigene25216_All; log2 FC= 1.41), *MYB3R-4* (Unigene167936_All; log2 FC= 5.09) *MYB37* (CL3152.Contig6_All; log2 FC=4.63) showed highly increased transcript abundance compared to control plants. The basic leucine zipper (bZIP) represents another most diverse transcription factor family. bZIP9 (CL8099.Contig1_All; log2 FC= 7.8) showed the highest increase in transcript abundance from this family in response to NaCl treatment. The other bZIPs that were upregulated include *bZIP27* (CL19018.Contig6_All; log2 FC= 4.24), *bZIP9*

(CL8099.Contig1_All; log2 FC= 7.79), *bZIP23* (CL1946.Contig4; log2 FC= 1.42), and *bZIP17* (Unigene158885_All; log2 FC=5.15) (Table 3.3). Four *WRKY* TFs showed a decrease in transcript abundance compared to control plants under salt stress: *WRYK26* (CL17434.Contig2_All; log2 FC=-3.83), *WRYK70* (CL2822.Contig1_All, log2 FC= -2.60), *WRYK19* (CL19887.Contig2_All; log2 FC= -4.81), and *WRYK9* (Unigene41823_All; log2 FC= -7.87). Six *WRYK* genes were upregulated, but only *WRKY39* (CL17890.Contig3_All; log2 FC= 2.99) showed greater than two log2 fold increased than control plants (Table 3.3). A total of 26 drebrins and related actin-binding proteins (*DREB*) were differentially expressed in response to NaCl. Among them, 15 were upregulated with large log2 fold changes (4-7) compared to control plants. The APETALA2/ethylene-responsive element binding protein (AP2/EREBP) family transcription factors *RAP2.2* (Unigene54941_All) and *RAP2-3* (CL3748.Contig7_All) showed greater than five-fold (log2) downregulation, whereas *RAP2-10* (Unigene24458_All) showed greater than five-fold (log2) upregulation compared to control plants. A total of 112 NAC (NAM/ATAF1/CUC2) TFs were identified in this study. Many of the identified NAC TFs were expressed differentially in response to NaCl. *NAC3* (Unigene12659_All; log2 FC= 7.06), *NACA3* (Unigene100143_All; FC= 5.24), *NAC* (Unigene68164), *NAC107* (CL18756.Contig2_All; FC= 7.18) and *NAC48* (CL1250.Contig12_All; FC= 4.19) associated with the high upregulations of transcript levels whereas *NACA2* (Unigene59213_All; FC= -6.93) were significantly downregulated under salt stress. Additionally, one abscisic acid-responsive (ABA) transcription factor gene, *ABF2* (Unigene167020_All; log2 FC=3.98), was upregulated in response to salt stress (Table 3.3).

3.3.9 Aquaporins

Several aquaporin genes were differentially expressed in the roots of *Puccinellia nuttalliana* as a result of the NaCl treatment. *PIP2;2* transcript (Unigene159054_All; log2 FC=7.92) orthologus to *Hordeum vulgare HvPIP2;2*, was uregulated in salt-treated plants. Transcript abundance of the tonoplast aquaporins *TIP1;1* (Unigene76130_All; FC = -6.56), *TIP2;1* (Unigene134545_All; FC = -4.99), *TIP2;3* (Unigene19900_All; FC = -5.43), *TIP3;1* (CL9482.Contig2_All; FC = -3.69), *TIP4;1* (Unigene1799_All; FC = -5.72), *TIP4;2* (CL11639.Contig2_All; FC = -6.94) and *TIP4;4* (Unigene43183_All; FC = -5.27) were significantly downregulated by the NaCl treatment. Two nodulin-26 like intrinsic protein (NIP) genes, *NIP1;1* (Unigene66763_All; FC = -6.39) and *NIP4;2* (Unigene71932_All; FC=-3.28), were also significantly downregulated (Table 3.3).

3.3.10 Expression of genes involved in ROS defenses

The NaCl treatment significantly induced the expression of genes involved in ROS defenses. Various enzymatic antioxidants, such as peroxidase (*POD*), superoxide dismutase (*SOD*), and catalase (*CAT*), were significantly upregulated by NaCl (Table 3.3).

3.3.11 Metabolite abundance changes in response to NaCl treatment

In total, 103 metabolites were identified in leaf and root extracts of *Puccinellia nuttalliana* by liquid chromatography-mass spectrometry (LC-MS) including different amino acids, organic acids, sugars, amines, and glycerophospholipids. The principal component analysis (PCA) showed clear separations among the control and NaCl-treated plants (Fig. 3.7). The analysis also showed no outliers and significant changes in the metabolite profiles due to the NaCl treatment. The differential abundance of metabolites evaluated by log2 fold change (Fig. 3.8) showed that 34 metabolites were upregulated in roots, including proline, transhydroxy

proline, dopamine, histidine, serine, aspartic acid 28 glycerophospholipids. Significantly increased metabolites from the glycerophospholipids family included LYSOC16:0, LYSOC18:1, LYSOC18:2, PC36:0AA, PC36:6AA, PC aa C32:3, PC ae C34:3, PC ae C34:3, PC aa C34:4, PC ae C34:3, PC aa C34:4, PC aa C34:3, PC aa C34:2, PC aa C34:1, PC ae C36:4, PC ae C36:2, PC aa C36:5, PC aa C36:4, PC aa C36:3, PC aa C36:1, PC ae C38:4, PC ae C38:3, PC aa C38:4, PC aa C38:3, PC ae C40:3, PC ae C42:4, PC ae C42:3, PC aa C42:4, PC aa C42:2 and PC ae C44:3. In contrast, no metabolites from the glycerophospholipid family were significantly different in leaves between the control and NaCl-treated plants. Only proline, dopamine, and methylhistidine concentrations were significantly increased in leaves.

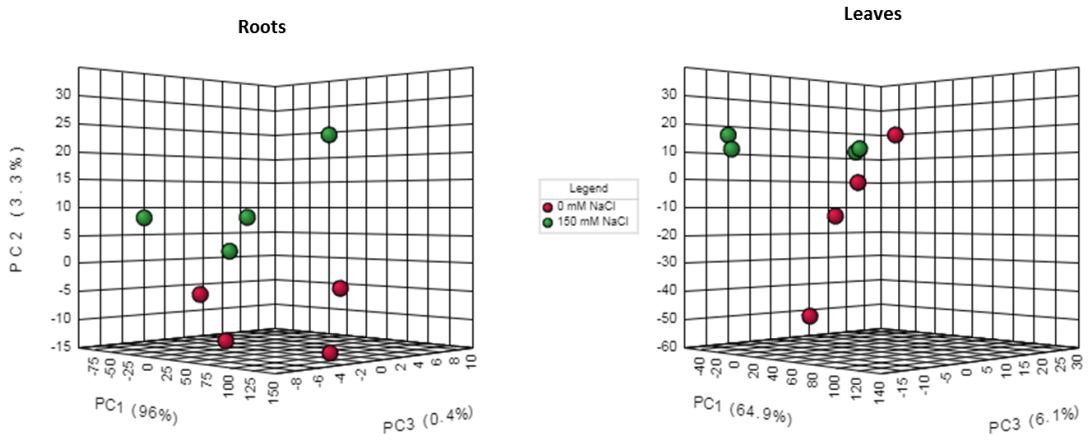

Fig. 3.7. Three-dimensional principal component analysis score plot between individual samples for 0 mM NaCl and 150 mM NaCl six-day treatments.

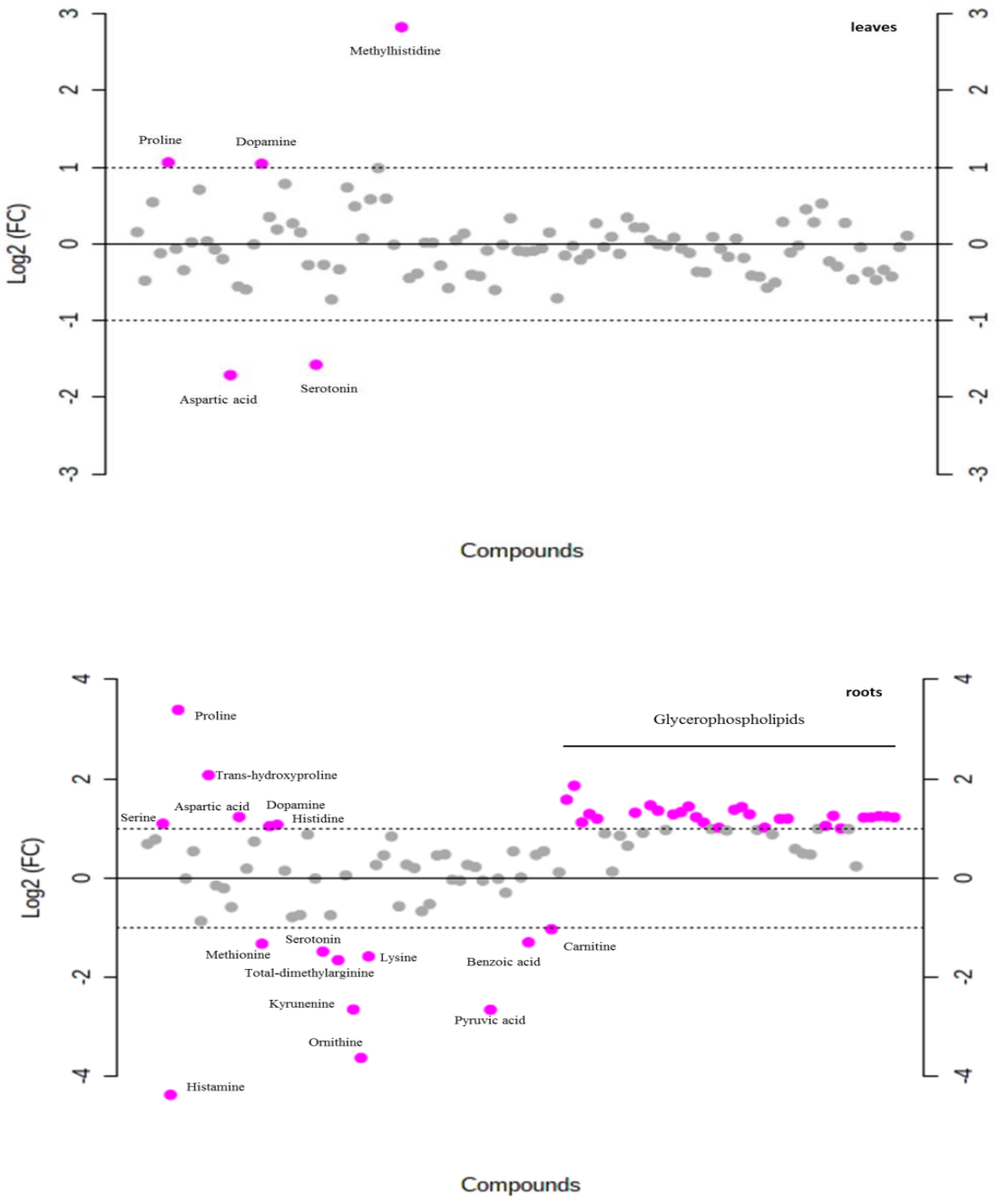

Fig. 3.8. Fold-change analysis with threshold 2 of each metabolite in roots and leaves of *Puccinellia nuttalliana* treated with 150 mM NaCl for six days compared with the plants treated with 0 mM NaCl. The values are on a log scale, so that both upregulated and downregulated features are plotted in a symmetrical way. Gray circles represent metabolites with no significant difference.

3.3.12 Proline and dopamine biosynthesis pathways

Two transcripts of 1-delta-pyrroline-5-carboxylate synthase (*P5CS*) (Unigene18828_All and Unigene2907_All) and a Pyrroline-5-carboxylate reductase (*P5CR*), the key enzyme of proline biosynthesis, were found to be upregulated by the NaCl treatment. DEGs also revealed that two ornithine d-aminotransferase transcripts were significantly upregulated. The predicted proline biosynthesis pathway in *Puccinellia nuttalliana* is shown in Supplementary Fig. 3.2. There are two reported dopamine synthesis pathways in plants, either via hydroxylation of tyramine or L-DOPA's decarboxylation. A decrease in the concentration of tyrosine and an increase in the concentration of tyramine in response to the NaCl treatment revealed that dopamine was produced via the hydroxylation pathway (Supplementary Fig. 3.2).

3.3.13 Metabolic pathways altered by NaCl treatment

The metabolomics data were subjected to the Kyoto Encyclopedia of Genes and Genomes (KEGG) pathway enrichment analysis for differentially expressed metabolites induced by salt stress. The top 20 perturbed pathways in the roots and leaves of *Puccinellia nuttalliana* is shown in Fig. 3.9. Ten metabolic pathways were significantly activated in both roots and leaves (Fig. 3.10), including arginine and proline metabolism, cysteine and methionine metabolism, glycine, serine and threonine metabolism, carbon fixation in photosynthetic organisms, seleno compound metabolism and beta-alanine metabolism. The perturbation of metabolites involved in the pathways in roots included pyruvate metabolism, histidine metabolism, betalain biosynthesis, tyrosine metabolism, ubiquinone and other terpenoid-quinone biosynthesis, lysine degradation and thiamine metabolism. In leaves, the altered pathways include the TCA cycle, butanoate metabolism, porphyrin and chlorophyll metabolism, alanine, aspartate and glutamate

metabolism, arginine biosynthesis, glyoxylate and dicarboxylate metabolism and sulfur metabolism.

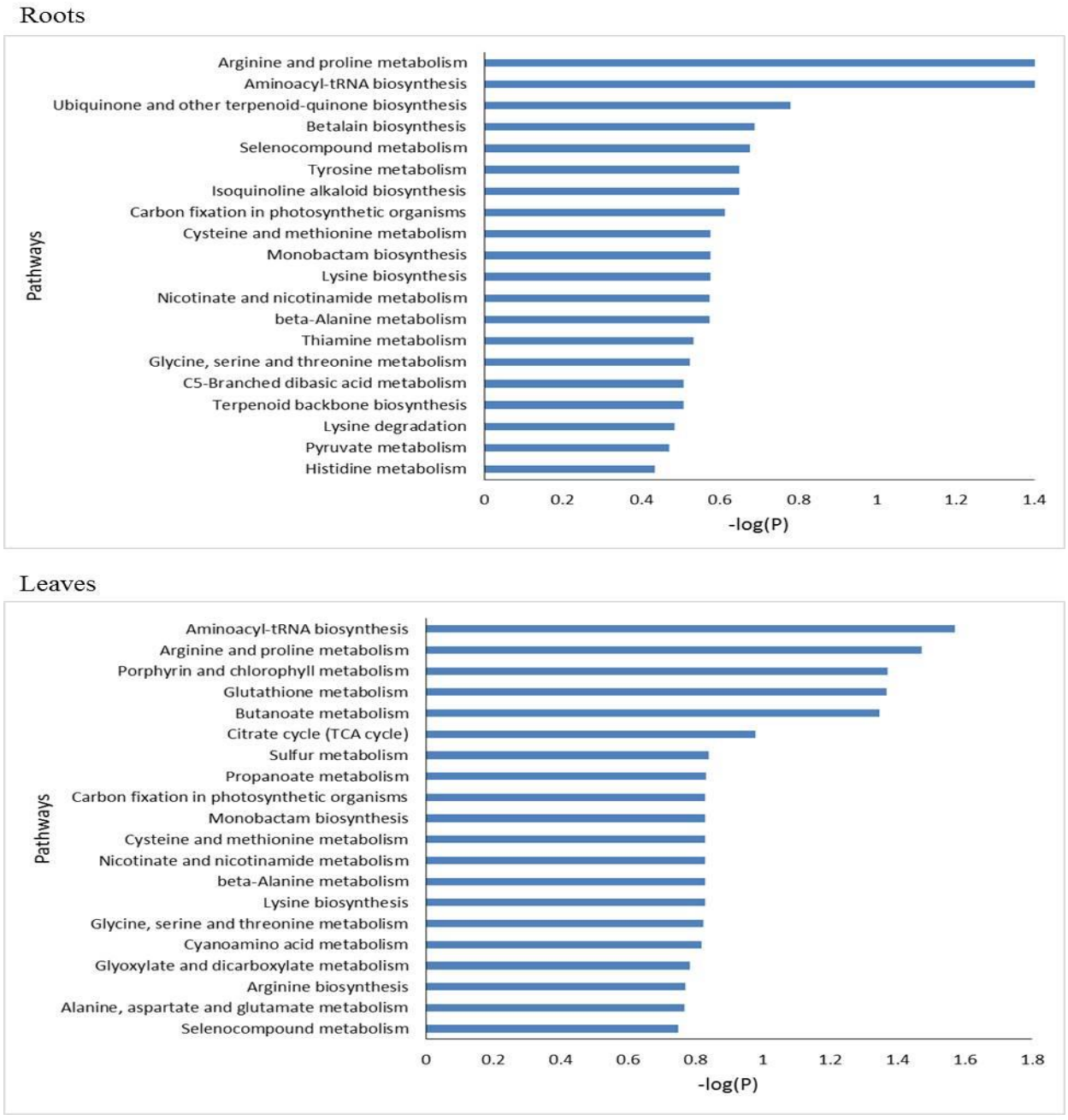

Fig. 3.9. The top 20 enriched pathway analysis of differentially accumulated metabolites in roots and leaves of *Puccinellia nuttalliana* between 0 mM and 150 mM NaCl treatments.

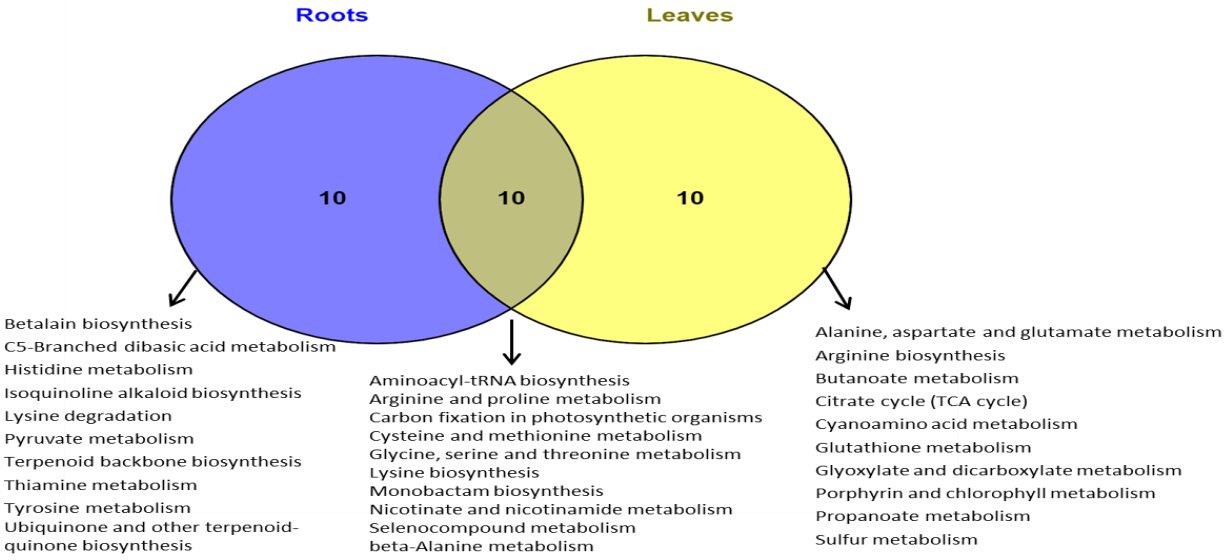

Fig. 3.10. Venn diagram of KEGG pathways in which differentially accumulated metabolites were involved in roots and leaves o*f Puccinellia nuttalliana* plants treated with 150 mM NaCl for six days.

3.3.14 Salt secretion by leaves and cell wall lignification in roots in response to NaCl

Scanning electron microscopy demonstrated globular materials deposited on the unwashed leaf surfaces of 150 mM NaCl-treated plants that were absent in control plants (Fig. 3.11A, B). However, the details of salt glands were not visible in the scanning electron micrographs since they were covered by the globular materials. There were no globular materials deposited on leaf surfaces of the control plants. Salt deposition on the leaf surfaces was observed in the NaCl-treated plants (Fig. 3.11C).

Light microscopy observations revealed the presence of aerenchyma in the root cortex of *Puccinellia nuttalliana* plants. In addition, extensive sclerification in the root vascular region was observed after six days of the 150 mM NaCl treatment and was accompanied by thickening of the endodermal cell walls. Six to eight protoxylem vessels surrounded one to two large central

metaxylem vessels (Fig. 3.11D, E). In most of the examined specimens, there were two metaxylem vessels in control plants and one metaxylem vessel in plants treated with 150 mM NaCl (Fig. 3.11D, E). Lignin distribution, which was examined in root sections by the fluorescence microscopy, demonstrated that the exposure to NaCl resulted in thickening of the root endodermal cell walls and the walls of the metaxylem vessels (Fig. 3.11F, G).

DEGs identified that caffeoyl-CoA O-methyltransferase (*CCoAOMT*), a key enzyme in the lignin biosynthesis pathway, was significantly downregulated (Unigene2227_All; FC = -4.09) in response to salt stress. Also, DEG encoding *4-coumarate-CoA ligase* (Unigene165035_All; FC = 5.92), which participates in monolignol biosynthesis, was induced by the treatment. The levels of other transcripts related to lignin biosynthesis, including *LAC17* (CL6032.Contig6_All), *PER39* (Unigene64739_All), *PRX34* (CL14735.Contig1_All), also increased in plants treated with NaCl (Table 3.3).

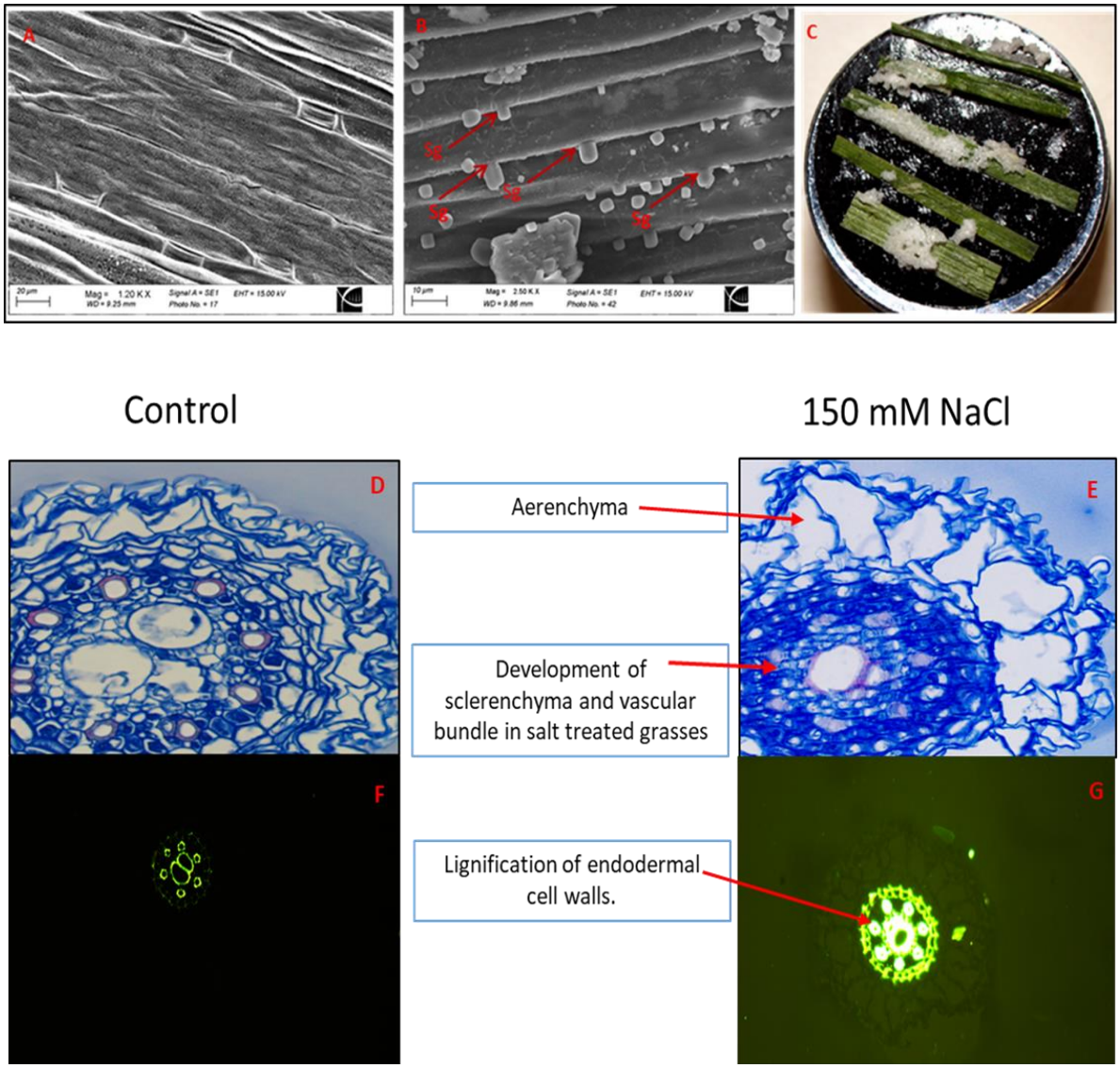

Fig. 3.11. Scanning electron micrographs of the abaxial leaf surfaces from control (A) and 150 mM (B) NaCl-treated *Puccinellia nuttalliana* plants for six days, Sg: salt gland; leaves showing salt crystals on their surfaces after the plants were treated with 150 mM NaCl treated for 6 days (C); root cross sections of plants treated for six days with 0 mM NaCl (D) and 150 mM (E) NaCl; lignification of the endodermal cell walls visualized by fluorescence after six days of 0 mM (F) and 150 mM NaCl (G) treatments.

3.4 Discussion

In the present study, 242,833 unigenes were identified with an average length of 742 bp. A large number of trinucleotide SSRs was found, which have been implicated in other plants to be involved in various cellular and metabolic processes including stress and defense responses (Ahmadi and Ahmadikhah 2022). A high percentage of *P. nuttalliana* sequences closely matched the sequences in *Aegilops tauschii*, which tolerates salinity through an effective Na^+ homeostasis strategy (Wei et al., 2008; Abbas et al., 2021). Appropriate salt concentrations are required for optimal growth of true halophytes (Yuan et al., 2019). For example, the optimal NaCl concentration for the growth of *Suaeda salsa* was 200 mM (Yang et al., 2010), while 100 mM NaCl was found to be optimal for *Cakile maritima* (Debez et al., 2004). A previous study showed that the NaCl treatments with the concentrations as high as 150 mM enhanced shoot and root growth of *P. nuttalliana* while no growth enhancement was observed in plants treated with 300 mM NaCl (Vaziriyeganeh et al., 2018).

3.4.1 Aquaporins are involved in salt tolerance in *Puccinellia nuttalliana*

A previous study demonstrated that the aquaporin-mediated transport was enhanced by Na^+ since similar effects were observed in plants treated for six days with 150 mM NaCl and 150 mM Na_2SO_4, but not with 150 mM KCl (Vaziriyeganehet al. 2022). In all studied species of glycophytic plants, cell hydraulic conductivity and aquaporin-mediated root water transport were inhibited by NaCl (Martinez-Ballesta et al. 2003, Boursiac et al. 2005, Sutka et al. 2011, Vaziriyeganeh et al. 2018). The NaCl concentration that inhibited cell hydraulic conductivity in roots of Arabidopsis was as low as 10 mM (Lee and Zwiazek 2015). Maintenance of water balance in plants exposed to salinity requires a coordinated effort that may involve a combination of salt exclusion and salt tolerance processes to minimize direct ion toxicity and osmotic effects

of salt. Contrary to the tonoplast intrinsic proteins (TIPs), NOD26-like intrinsic proteins (NIPs), and to most of the plasma membrane intrinsic proteins (PIP) groups of aquaporins, NaCl triggered a significant increase in root *PIP2;2* transcripts in *P. nuttalliana*, which could contribute to the earlier observed increases in root cell hydraulic conductivity by NaCl (Vaziriyeganeh et al. 2018, 2022). It cannot be excluded that PIP2;2 may also play a dual role under salt stress by facilitating Na^+ translocation since some of the aquaporins were demonstrated to function as ion transporters. Studies in Arabidopsis demonstrated that PIP2;1 and PIP2;2 function as water and ion channels in heterologous systems suggesting their role as non-selective cation channels (NSCC) responsible for Na^+ entry into plant roots (Byrt et al., 2017, McGaughey et al. 2018). However, the possibility that PIP2;2 may also act as an ion transporter needs to be further examined. It also remains unclear how the function of PIP2;2 can be maintained in *P. nuttalliana* in the presence of Na^+ and what specific properties of the PIP2;2 protein make it more desirable under NaCl stress conditions compared with the other PIPs, which had their transcripts downregulated by the NaCl treatment. Transcriptome profiling of a halophytic plant *Kochia sieversiana* revealed that 10-12 aquaporin genes were upregulated by mild salinity, while only two aquaporins were upregulated by high salinity, and it was suggested that these aquaporins contribute to salinity and osmotic tolerance (Zhao et al., 2017). However, the authors did not specify which aquaporins were upregulated by salt stress. Downregulation of several *TIPs* in *P. nuttaliana* by the NaCl treatment may also have important consequences to water homeostasis by regulating water fluxes across the tonoplast. Several studies revealed that TIP aquaporins, which are primarily located in the tonoplast (Maurel et al. 2008), play important roles under salt stress (Afzal et al. 2016, Liu et al. 2020b). In addition to the intracellular water movement, TIPs are involved in transporting small solutes and gases (Nozaki et al. 2008). A

study with a succulent halophyte *Mesembryanthemum crystallinum* also showed that the transcript abundance of *TIP1;2* decreased in response to salt stress, suggesting that TIPs may play a role in salt responses of halophytes (Kirch et al. 2000). On the other hand, higher expression levels of both *PIPs* and *TIPs* were observed in the shoots of the mangrove tree *Avicennia officinalis* treated with 500 mM NaCl (Tan et al. 2013). The increased expression levels of *TIPs* by NaCl in *A. officinalis* and the decreased expression of *TIPs* in *P. nuttalliana* are likely related to the differences in plant salt tolerance strategies of these two halophytes.

It is noteworthy that two NIPs were also upregulated in *P. nuttalliana* by NaCl, pointing to their possible roles in the salt tolerance mechanisms. The NIP2 homolog aquaporin was identified as a Si transporter (Ma and Yamaji 2006). Under salinity stress, Si uptake by the NIP aquaporins may reduce Na^+ conglomeration in cell membranes and improve water transport (Rios et al., 2017). Overexpression of a wheat NIP aquaporin (TaNIP) in Arabidopsis was also demonstrated to improve plant salt stress tolerance, which was associated with an increase in K^+/Na^+ ratios in roots of salt-stressed overexpression plants compared with the wild-type plants (Gao et al. 2010).

3.4.2 Osmoprotectants in salt tolerance of *Puccinellia nuttalliana*

The metabolomic analysis demonstrated that proline accumulation is among salt stress tolerance mechanisms in *P. nuttalliana*. There was a significant increase in the leaf and root proline concentrations after six days of the NaCl treatment. The RNAseq data suggest that the glutamate and ornithine pathways contributed to proline biosynthesis. The significance of the glutamate and the ornithine pathways in proline biosynthesis in salt-treated plants is not clear. However, proline is synthesized mainly from glutamate and plants use ornithine as an alternative pathway for proline biosynthesis (An et al. 2013, Szabados and Savouré 2010). In *P. nuttalliana*,

PROT2 expression was upregulated in roots by the NaCl treatment. PROT2 is presumed to be involved in xylem-to-phloem transfer and long-distance transport of proline (Zhang et al. 2010, Yao et al., 2020). The concentrations of free amino acids were higher in *P. nuttalliana* leaves compared with roots under both control and salt stress conditions. Free amino acids are used for osmotic adjustment in numerous plant species (Jiménez-Arias et al. 2021). Several amino acid transporters may be involved in the distributions of amino acids in different plant parts (Yao et al. 2020). Two members of the amino acid permease (AAP) family, *AAP3* and *AAP7* were upregulated in *P. nuttalliana* in response to NaCl treatment indicating their involvement in the redistribution of root-derived amino acids to leaves. AAP3 is preferentially expressed in the root phloem (Okumoto et al. 2004).

The results of this study demonstrate that *P. nuttalliana* is a dopamine- (3-hydroxytyramine or 3,4-dihydroxyphenethylamine) and serotonin-rich plant species, which likely contribute to its ability to withstand high salt concentrations. In mammals, dopamine and serotonin have been characterized as neurotransmitters. The absence or deficiency of dopamine in humans can cause Parkinson's disease, depression, and impaired motor control (Belujon and Grace 2017). In plants, dopamine contributes to abiotic stress tolerance, including drought and salt stress, by affecting the expression of many stress-related genes (Liu et al. 2020a). Dopamine is also a strong antioxidant (Kulma and Szopa 2007) and it can alleviate oxidative damage through direct scavenging of oxidants and enhancing antioxidative enzyme activities in plants affected by salt (Li et al. 2015). Dopamine was also suggested to alleviate salt-induced stress by regulating SOS pathway (Li et al. 2015) through its effect on the expression of Na^+/H^+ antiporters, including SOS1 (Gao et al. 2020, Marchiosi et al. 2020). Dopamine may also play a role in regulating water transport in plants affected by salinity. In rice plants, the *OsPIP1-3*

transcript was upregulated by salt stress, whereas exogenous application of dopamine decreased the *OsPIP1-3* expression under salt stress (Abdelkader et al. 2012). There are two reported dopamine production pathways in plants, either via hydroxylation of tyramine or decarboxylation of L-DOPA. In *P. nuttalliana*, tyrosine decarboxylase's upregulation and decreased concentration of tyrosine increased concentration of tyramine under salt stress revealing that dopamine is synthesized via hydroxylation of tyramine. Understanding the underlying molecular mechanisms of dopamine biosynthesis is vital for stabilizing the metabolic processes by modifying the dopamine metabolic pathway to improve salt tolerance in glycophytes. Serotonin was identified in both leaves and roots of *P. nuttalliana* and was significantly downregulated by the NaCl treatment in roots, but not in leaves. Serotonin is a neurotransmitter in mammals (Belujon and Grace 2017). In plants, serotonin may serve multiple functions that have not yet been well characterized. It was reported to be involved in plant growth and development processes, as well as in responses to biotic and abiotic stresses (Erland et al. 2016). A recent study showed that an application of exogenous serotonin increased leaf chlorophyll concentrations in salt-stressed *Brassica napus* plants and activated antioxidant enzyme systems including CAT, SOD, and POD (Liu et al. 2021).

3.4.3 Signal transduction and activation of salt signaling pathways

Salt stress tolerance of halophytes is modulated by multiple sensors and signaling pathways, including Ca^{2+}, salt overly sensitive (SOS) pathway and mitogen-activated protein kinase (MAPK) cascades, ROS, and hormones (Yang and Guo 2018, Isayenkov and Maathuis 2019). Ca^{2+} accumulation in cells can be triggered through the phospholipase C mechanism (Putney and Tomita 2012). In *P. nuttalliana*, two phospholipase C and one phospholipase D transcripts were upregulated in response to NaCl stress. Phospholipase D (PLD) and

phosphoinositide-specific phospholipase C (PLC) pathways are involved in the production of phosphatidic acid (PA), a signaling lipid, which rapidly increases in response to drought and salinity stresses (Mueller-Roeber and Pical 2002, Hong et al. 2010, McLoughlin and Testerink 2013). PA interacts with MPK6 and activates the phosphorylation of SOS1 (Yu et al. 2010, Yang and Guo 2018). The increase in cytosolic Ca^{2+} in response to salt stress results in the activation of CBL/CIPKs in the SOS signaling pathway to control Na^{+} transport in halophytes (Nikalje et al. 2017). In *P. nuttalliana*, several SOS pathway genes, *CBLs* and *CIPKs* were differentially expressed in response to NaCl. *CBL1*, *CBL3*, *CBL10*, *CIPK32*, *CIPK26*, *CIPK18*, *CIPK8*, *CIPK11*, *CIPK21*, *CIPK23*, *CIPK28 CIPK1*, and *CIPK9* were upregulated, demonstrating that SOS was active in response to NaCl. CBL1 and CBL10 were identified as positive regulators of salt stress in Arabidopsis plants (Quan et al. 2007), and OsCPK21 was demonstrated to improve salt stress tolerance in rice (Asano et al. 2011). The present study identified multiple transcripts of the three MAPK kinases, which participate in mitogen-activated protein kinase pathway. These kinases, including *MAPKKK*, *MAPKK*, and *MAPK*, were upregulated by NaCl. A *MPK6* transcript that was upregulated in this study was reported to be involved in ethylene biosynthesis via phosphorylation of ACS2/ACS6 (Liu and Zhang 2004).

3.4.4 ROS scavengers

Salt stress triggers excessive ROS accumulation resulting in oxidative stress. Plants have effective non-enzymatic and enzymatic antioxidant defense systems for scavenging ROS including superoxide dismutase (SOD), catalase (CAT), and peroxidase (POD). SOD converts the superoxide radical into the less toxic H_2O_2, which is then scavenged by POD, CAT, and other scavenging enzymes (Nikalje et al. 2018, Xiong et al. 2019). In the present study, five *Cu, Zn-SODs*, five *Fe-SODs*, four *Mn-SODs*, four *CATs* and six *PODs* were upregulated by NaCl. These

enzymes likely contributed to salt tolerance of *P. nuttalliana* by alleviating oxidative damage via ROS scavenging activity.

3.4.5 Ion homeostasis

Similarly to other studies in salt tolerant plants (Cuin et al. 2008, Reddy et al. 2017), and the earlier study with *P. nuttalliana* (Vaziriyeganeh et al. 2018), high K^+/Na^+ ratios were measured in plants subjected to the 150 mM NaCl treatment. The high K^+/Na^+ ratio indicates low Na^+ selectivity in the presence of NaCl, which is important for plants to survive in saline environments. Several ion transporters are known to control K^+/Na^+ ratio. The high-affinity K^+ transporter (HKT) protein family protects plants by controlling excess Na^+. In rice, OsHKT1;5 was found to be involved in Na^+ exclusion from xylem to regulate K^+/Na^+ homeostasis during salt stress (Kobayashi et al. 2017). *Thellungiella halophila* and *Puccinellia tenuiflora* halophytic plants exhibit strong selectivity for K^+ over Na^+ via HKT proteins (Taji et al. 2004, Wang et al. 2004, Ren et al. 2005, Volkov and Amtmann, 2006). In the present study, differential gene expression (DEGs) analysis of RNAseq data revealed that *HKT1;5* was significantly upregulated in *P. nutalliana* by NaCl. Based on these finding, I hypothesized that *P. nuttalliana* relies on HKT1;5 to maintain balance between Na^+ and K^+ in the cytoplasm upon NaCl stress by controlling the Na^+ efflux and distribution into various organs. Several antiporters including *HAK9*, *HAK23*, *AKT1*, and *AKT3* were also induced by NaCl in *P. nuttalliana*. These genes might function as an effective pathway for K^+ and Na^+ uptake under NaCl stress. Several *CNGCs* (The cyclic nucleotide-gated channels) were significantly upregulated by NaCl. It is possible that these genes, in addition to participating in K^+ and Na^+ acquisition, might be involved in Na^+ loading into the xylem to maintain the ionic balance when exposed to NaCl. Plasma membrane Na^+/H^+ antiporter SOS1 and vacuolar Na^+/H^+ antiporters NHX help maintain high K^+/Na^+ ratio

in the cytosol and sequestration of Na^+ (and Cl^-) in the vacuoles, a key salt resistance features of halophytes (Nikalje et al. 2017). Surprisingly, all vacuolar *NHXs* were downregulated by NaCl in *P. nuttalliana*. This indicates that these genes in *P. nuttalliana* may have different functions or that the stress triggered the upregulation of *NHX1* transcript to increase active accumulation of K^+ in the vacuoles to reduce the Na^+ sequestering into the vacuoles and enhance Na^+ loading into the xylem of roots by other antiporters. Halophytes use Na^+ as an energy-efficient source of osmolytes to maintain their maximum growth under saline conditions (Nikalje et al. 2017). The stress that is induced in salt-loving plants by the lack of adequate salt in the root medium triggers plant responses that obscure the mechanisms involved in their salt tolerance. Another possibility is that *P. nuttalliana* does not depend on NHX to compartmentalize Na^+ and K^+ and, instead, relies on the synthesis of compatible organic solutes (Yokoi et al. 2002). All of the differentially expressed *SOS1* genes were downregulated in control (0 mM NaCl) *P. nuttalliana* plants compared with NaCl-treated plants. In a salt-free environment, the plants likely suffered from stress that led to the upregulation of *SOS1* genes to transport more Na^+ from roots to shoots through the xylem. In *Thellungiella halophila*, *SOS1* transcript was also more strongly induced in control plants compared with salt-treated plants (Kant et al. 2006). The authors suggested that SOS1 is involved in xylem loading of Na^+ under control conditions. Similarly, transcriptome profiling of a halophytic plant *Kochia sieversiana* showed that the expression of *NHX* genes was not induced by salinity stress (Zhao et al. 2017). The authors suggested that the genes known to be involved in salinity tolerance in glycophytic plants may play different roles and may not be involved in salinity tolerance mechanisms of *Kochia sieversiana.*

The concentration of Cl^- was significantly higher in shoots compared with roots of *P. nuttalliana* treated with NaCl. Halophytic plants can accumulate Cl^- in shoot tissues in

concentrations as high as 1.5 M (Bazihizina et al. 2019). Accumulation of Cl^- is less energy demanding compared with its exclusion and halophytes are thought to require high concentrations of Cl^- for optimal photosynthetic activity (Bazihizina et al. 2019).

3.4.6 Activation of salt-responsive transcription factors regulating gene responses to NaCl

Transcription factors (TFs) play an essential role in plant stress tolerance by regulating the transcription of the downstream genes via binding to a cis-regulatory specific sequence of the target genes. Various families of TFs such as AP2/ERF, bZIP, MYB, WRKY, NAC, with the links to salt tolerance (Nikalje et al. 2017) were differentially expressed in this study. Four WRKY transcription factors (*WRKY11*, *WRKY57*, *WRKY42*, and *WRKY39*) were significantly upregulated in *P. nuttalliana* by the NaCl treatment. It has been reported that WRKY11 responds to various environmental stresses. Overexpression of alfalfa WRKY11 improved salt tolerance in soybean (Wang et al., 2018b). The chromatin-associated protein DEK3, upregulated in *P. nuttalliana* in response to NaCl, was identified as a salt-tolerant protein in the earlier studies (Waidmann et al. 2014). Several *bZIP* genes were differentially expressed in response to the NaCl treatment. In transcriptome profiling of the halophytic turf grass *Sporobolus virginicus*, five *bZIP* genes were differentially expressed in roots in response to salt stress (Yamamoto et al. 2015). The Long Hypocotyl 5 (*HY5*) TF, that was upregulated by NaCl in *P. nuttalliana*, was reported to regulate several stress-responsive genes, including *MYB59* and *DREB2A* (Maxwell et al. 2003, Du et al. 2019, Skalak et al. 2021). These genes were also upregulated in *P. nuttalliana*. ABF2 functions as a positive regulator of the ABA signaling pathway in drought and salt stresses (Wu et al. 2020). A previous report of the halophyte *Salicornia persica* transcriptome profiling identified that the *ABF2* gene was upregulated under salinity conditions (Aliakbari et al. 2020).

In the present study, an *ABF2*-like transcript was upregulated by NaCl, indicating that ABF2 plays a regulatory role in ABA signaling *in P. nuttalliana*.

3.4.7 Pathways involved in salt tolerance responses

The pathways linked to salinity tolerance in *P. nuttalliana* were explored based on differential metabolites. In leaves, the salt-induced metabolites were associated with the TCA cycle, butanoate metabolism, as well as porphyrin and chlorophyll metabolism. Butanoate metabolism is closely associated with the phosphatidic acid (PA) pathway involved in salt stress signaling (Yu et al. 2010, Zhang et al. 2014). Butanoate metabolism pathway was also identified in salinity responses of salt tolerant wheat (Xiong et al. 2017). TCA cycle intermediates including citric acid, succinate, pyruvate, and 2-oxoglutarate significantly increased in leaves. Since TCA cycle is essential for energy production and maintaining various physiological processes (Fernie et al. 2004), these increases point to a boost of ATP production in *P. nuttalliana* by the NaCl treatment. Several pathways were preferably enriched with differential metabolites in roots, including pyruvate, histidine, thiamine and tyrosine metabolism. In both roots and leaves, salt-induced pathways included glycine, serine and threonine metabolism, arginine and proline metabolism, cysteine and methionine metabolism, and beta-alanine metabolism. Although some of these alterations of the amino acid metabolism pathways may be directly linked to the salt-tolerance mechanisms, more studies are required to clarify their significance in salt responses of this halophytic plant.

3.4.8 Involvement of glycerophopholipids in salt tolerance responses

Salt tolerance of *P. nuttalliana* likely involves the alterations in membrane lipids as evidenced by a significant increase in the metabolites of the glycerophopholipid family in roots. In addition to their functional role as structural constituents of membranes, glycerophospholipids

are involved in the plant hormone signal transduction (Bruntz et al. 2014). Several *PLD*-like transcripts were repressed by salt stress in *P. nuttalliana*. Phospholipase D regulates the intercellular signaling and metabolic pathways under stress conditions (Bruntz et al. 2014). It hydrolyses the phosphodiester bond of the glycerolipid phosphatidylcholine (PC) to form phosphatidic acid (PA) and choline (Brown et al. 2017). PLD and PA play significant roles in plants under drought and salinity stress (Hong et al. 2010).

3.4.9 Changes in plant structure in response to NaCl

The scanning electron microscopy demonstrated globular materials covering the salt glands on unwashed leaf surfaces. Salt glands are commonly present in halophytic plants (Oi et al. 2013). Light microscopy observations of *P. nuttalliana* root sections also revealed increased cell wall lignification of the endodermis and root metaxylem vessels of the NaCl-treated plants. Lignin biosynthesis pathway includes the monolignol biosynthesis step. The 4-coumarate-CoA ligase enzyme catalyses the first step to provide precursors for downstream metabolites (Fraser and Chapple 2011), and its transcript was differentially expressed in the present study. A caffeoyl-CoA O-methyltransferase (*CCoAOMT*) transcript, which works downstream of *4CL* (Xie et al. 2018) was significantly downregulated in *Puccinellia nuttalliana* in response to NaCl treatment. Downregulation of *CCoAOMT* gene was predicted to increase wood density in *Populus trichocarpa* by affecting lignin biosynthesis (Wang et al. 2018a). Enhanced cell wall lignification in root cells of halophytes is considered to be a salt tolerance feature (Barzegargolchini et al. 2017). In addition, root aerenchyma structures that were formed in *P. nuttalliana* in response to NaCl may play a role in improving root aeration under stress. Increased formation of aerenchyma was reported for maize (Zhu et al. 2010) and rice (Karahara et al. 2012) roots under osmotic stress conditions. Root sclerification, which was observed in *P.*

nuttalliana, has been commonly reported for plants exposed to salinity and other environmental stresses and plays a key role in regulating nutrient uptake and radial water flow in roots (Lux et al. 2004). This feature together with the thickening of endodermal cell walls in *P. nuttalliana* following salt treatment may serve as a cellular barrier reducing salt uptake into the stele through apoplastic pathway under salinity conditions (Chen et al. 2011).

In conclusion, the present study provides a comprehensive overview of transcriptomic and metabolomic changes in *P. nuttalliana* exposed to 0 and 150 mM NaCl. The study revealed important salt tolerance strategies that shed new light on the complex processes contributing to the maintenance of water balance in this halophytic plant. A model is proposed for salt tolerance mechanisms in *P. nuttalliana* based on the DEGs and deregulated metabolites as well as structural modifications (Fig. 3.12). Several ion transporters were identified, including HKT1;5 and the aquaporin PIP2;2 that likely play major roles in ion homeostasis, water balance, and water transport under salt stress. The study also identified *P. nuttalliana* as a dopamine-rich plants and NaCl induced an additional increase of dopamine concentrations in the root tissues. Overall, both metabolomic and transcriptomic analyses revealed that *P. nuttalliana* responds to salt stress by complex alterations in the nucleotide and amino acid metabolism, TCA cycle, and porphyrin and chlorophyll metabolism. Further studies of these genes and metabolites will provide additional insight into their functional significance.

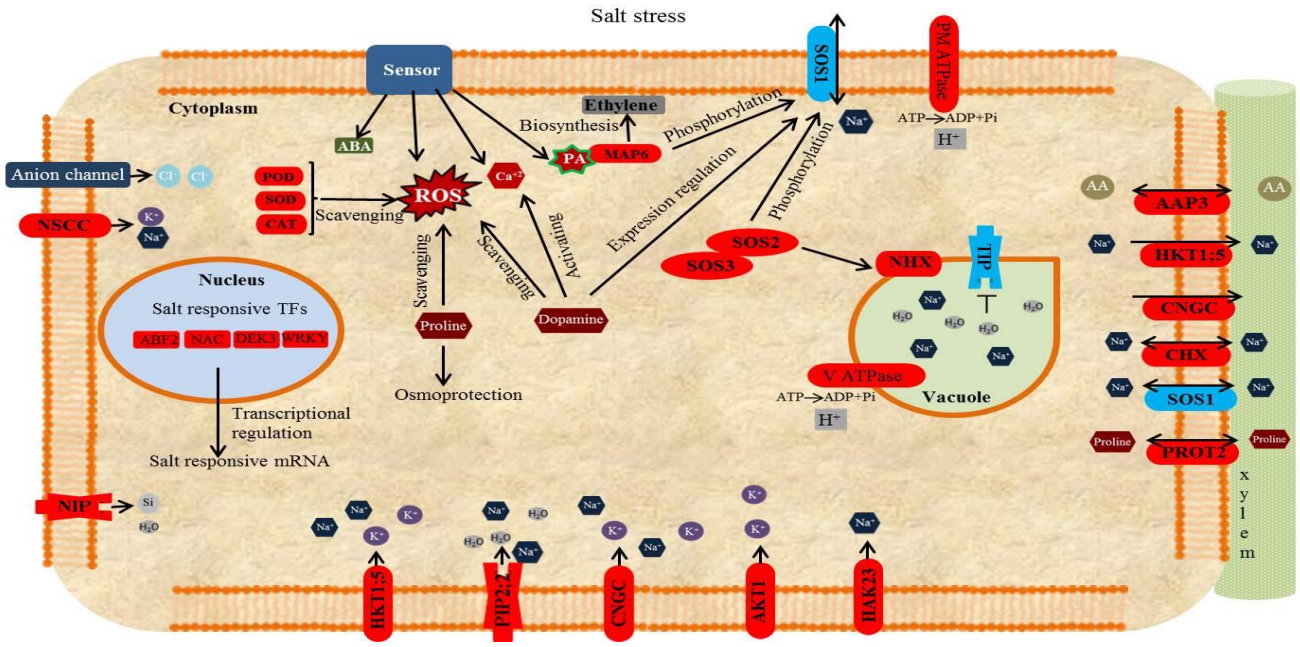

Fig. 3.12. A model proposed for the responses of *Puccinellia nuttalliana* to NaCl based on root transcriptomic and metabolomic analyses. NaCl is sensed by the salt sensors which triggers cytosolic Ca^{2+} accumulation in the cytosol. Ca^{2+} activates SOS3 leading to the formation of SOS3-SOS2 complex. This complex triggers the activation of downstream SOS1. Salt stress induces the activation of NaCl-responsive TFs, important regulators of salt responsive genes. TIPs are downregulated to slow down water efflux from vacuoles. PIP2;2 is upregulated to lower resistance of plasma membrane to water influx into the cytoplasm and transport of Na^+ ions. Several antiporters, NHX, HKT, SOS1, PIP2;2, AKT, HAK, CNGG, and NSCC are differentially expressed to facilitate intra- and intercellular K^+ and Na^+ homeostasis in *Puccinellia nuttalliana* under salt stress. Na^+ transport across the plasma membrane driven by the H^+ gradient occurred by plant proton pumps, H^+-ATPase and V-ATPase. Na^+ is sensed by sensors leading to the enhanced accumulation of ROS. The function of proline accumulation under salt stress is to provide osmotic adjustment and scavenging of ROS. Dopamine improves the antioxidant capacity by scavenging ROS, regulate the expression of SOS1 and activating Ca^{2+} signaling pathway. Phosphatidylcholines increased for membrane lipid remodeling to regulate fluid and ion permeability and maintain membrane integrity under saline environment. Salt stress elevates the level of PA, a direct activator of MPK6. MPK6 e is involved in regulating ethylene biosynthesis and phosphorylation of SOS1. Amino Acid Permease3 (AAP3) plays a potential role in the uptake and distribution of amino acids. L-Proline transport through plasma membrane is achieved L-proline transporter (ProT2). SOS—salt overly sensitive, PIP-Plasma membrane intrinsic protein, NHX - sodium/proton antiporters, PM-ATPase - plasma membrane ATPase, V-ATPase - vacuolar H ATPase, V-PPase - vacuolar pyrophosphatase, HKT - high affinity potassium transporter, HAK - high affinity K^+ transporter, AKT - Arabidopsis K^+ Transporter, ROS - reactive oxygen species, ATP - adenosine tryphosphate, ADP - adenosine diphosphate, TF - transcription factor. CNGC - cyclic nucleotide-gated cation channel; NSCC - non-selective cationic channel, PIP - plasma membrane intrinsic protein, ROS - reactive oxygen species. PA - phosphatidic acid, ABA - Abscisic acid. Phosphatidylcholines increased for membrane lipid remodeling to regulate fluid and ions permeability and maintain membrane integrity. Transcript upregulation denoted by red and downregulation by blue.

3.5 References

Abbas, A., Yu, H., Cui, H. and Li, X. 2021. Genetic diversity and synergistic modulation of salinity tolerance genes in *Aegilops tauschii* Coss. Plants 10: 10071393.

Abdelkader, A.F., El-khawas, S., El-Din El-Sherif, N.A.S., Hassanein, R.A., Emam, M.A. and Hassan, R.E.-S. 2012. Expression of aquaporin gene (Os PIP1-3) in salt-stressed rice (*Oryza sativa* L.) plants pre-treated with the neurotransmitter (dopamine). Plant Omics 5: 532–541.

Afzal, Z., Howton, T.C., Sun, Y. and Mukhtar, M.S. 2016. The roles of aquaporins in plant stress responses. Journal of Developmental Biology 4: db4010009.

Ahmadi, A.J. and Ahmadikhah, A. 2022. Occurrence of simple sequence repeats in cDNA sequences of safflower (Cartamus tinctorius) reveals the importance of SSR-containing genes for cell biology and dynamic response to environmental cues. Frontiers in Plant Science 13: 991107.

Al Hassan, M., Chaura, J., Lopez-Gresa, M.P., Borsai, O., Daniso, E., Donat-Torres, M.P., Mayoral, O., Vicente, O. and Boscaiu, M. 2016. Native-invasive plants vs. halophytes in Mediterranean salt marshes: stress tolerance mechanisms in two related species. Frontiers in Plant Science 7: 473.

Alfarrah, N. and Walraevens, K. 2018. Groundwater overexploitation and seawater intrusion in coastal areas of arid and semi-arid regions. Water 10: 143.

Aliakbari, M., Razi, H., Alemzadeh, A. and Tavakol, E. 2020. RNA-seq transcriptome profiling of the halophyte *Salicornia persica* in response to salinity. Journal of Plant Growth Regulation 40: 707-721.

An, Y., Zhang, M., Liu, G., Han, R. and Liang, Z. 2013. Proline accumulation in leaves of *Periploca sepium* via both biosynthesis up-regulation and transport during recovery from severe drought. PLoS One 8: e69942.

Asano, T., Hakata, M., Nakamura, H., Aoki, N., Komatsu, S., Ichikawa, H., Hirochika, H. and Ohsugi, R. 2011. Functional characterisation of OsCPK21, a calcium-dependent protein kinase that confers salt tolerance in rice. Plant Molecular Biology 75: 179-191.

Baillo, E.H., Kimotho, R.N., Zhang, Z. and Xu, P. 2019. Transcription factors associated with abiotic and biotic stress tolerance and their potential for crops improvement. Genes 10: 771.

Barzegargolchini, B., Movafeghi, A., Dehestani, A. and Mehrabanjoubani, P. 2017. Increased cell wall thickness of endodermis and protoxylem in *Aeluropus littoralis* roots under salinity: The role of LAC4 and PER64 genes. Journal of Plant Physiology 218: 127-134.

Bazihizina, N., Colmer, T.D., Cuin, T.A., Mancuso, S. and Shabala, S. 2019. Friend or foe? Chloride patterning in halophytes. Trends in Plant Science 24: 142-151.

Belujon, P. and Grace, A.A. 2017. Dopamine system dysregulation in major depressive disorders. International Journal of Neuropsychopharmacology 20: 1036-1046.

Boursiac, Y., Chen, S., Luu, D.T., Sorieul, M., van den Dries, N. and Maurel, C. 2005. Early effects of salinity on water transport in Arabidopsis roots. Molecular and cellular features of aquaporin expression. Plant Physiology 139: 790-805.

Braz, L.C.C., Fernandes, P.D., Barbosa, D.D., Dutra, W.F. Silva, C.R.C., Lima, L.M., Cavalcanti, J.J.V., Farias, F.J.C. and Santos, R.C. 2019. Expression of aquaporin subtypes (GhPIP1;1, GhTIP2;1 and GhSIP1;3) in cotton (*Gossypium hirsutum*) submitted to salt stress, AoB Plants 11: plz072.

Brown, H.A., Thomas, P.G. and Lindsley, C.W. 2017. Targeting phospholipase D in cancer, infection and neurodegenerative disorders. Nature Reviews Drug Discovery16: 351-367.

Bruntz, R.C., Lindsley, C.W. and Brown, H.A. 2014. Phospholipase D signaling pathways and phosphatidic acid as therapeutic targets in cancer. Pharmacological Reviews 66, 1033-1079.

Bushman, B.S., Amundsen, K.L., Warnke, S.E., Robins, J.G. and Johnson, P.G. 2016. Transcriptome profiling of Kentucky bluegrass (*Poa pratensis* L.) accessions in response to salt stress. BMC Genomics 17: 48.

Byrt, C.S., Zhao, M., Kourghi, M., Bose, J., Henderson, S.W., Qiu, J., Gilliham, M., et al. 2017. Non-selective cation channel activity of aquaporin AtPIP2;1 regulated by Ca^{2+} and pH. Plant, Cell & Environment 40: 802-815.

Cavill, R., Jennen, D., Kleinjans, J. and Briede, J.J. 2016. Transcriptomic and metabolomic data integration. Briefings in Bioinformatics 17: 891-901.

Chen, T., Cai, X., Wu, X., Karahara, I., Schreiber, L. and Lin, J. 2011. Casparian strip development and its potential function in salt tolerance. Plant Signaling and Behavior 6: 1499-1502.

Conesa, A., Gotz, S., Garcia-Gomez, J.M., Terol, J., Talon, M. and Robles, M. 2005. Blast2GO: a universal tool for annotation, visualization, and analysis in functional genomics research. Bioinformatics 21: 3674-3676.

Cuin, T.A., Betts, S.A., Chalmandrier, R. and Shabala, S. 2008. A root's ability to retain K^+ correlates with salt tolerance in wheat. Journal of Experimental Botany 59: 2697-2706.

Das, A., Pramanik, K., Sharma, R., Gantait, S. and Banerjee, J. 2019. In-silico study of biotic and abiotic stress-related transcription factor binding sites in the promoter regions of rice germin-like protein genes. PLoS One 14: e0211887.

Debez, A., Hamed, K.B, Grignon, C. and Abdelly, C. 2004. Salinity effects on germination, growth, and seed production of the halophyte *Cakile maritima*. Plant and Soil 262: 179-189.

Donaldson, L.A. and Radotic, K. 2013. Fluorescence lifetime imaging of lignin autofluorescence in normal and compression wood. Journal of Microscopy 251: 178-187.

Du, X.-Q., Wang, F.-L., Hong, L., Jing, S., Yu, M., Li, J., Wu, W-H., Kudla, J. and Wanf, Y. 201). The transcription factor MYB59 regulates K^+/NO_3^- translocation in the Arabidopsis response to low K^+ stress. Plant Cell. 31: 699–714.

Epstein, E. 1972. Mineral nutrition of plants: principles and perspectives. John Wiley and Sons, Inc., New York.

Erland, L.A., Turi, C.E. and Saxena, P.K. 2016 Serotonin: An ancient molecule and an important regulator of plant processes. Biotechnology Advances 34: 1347-1361.

Fernie, A.R., Carrari, F. and Sweetlove, L.J. 2004. Respiratory metabolism: glycolysis, the TCA cycle and mitochondrial electron transport. Current Opinion in Plant Biology 7: 254-261.

Flowers, T.J. and Colmer, T.D. 2008. Salinity tolerance in halophytes. New Phytologist 179: 945–963.

Flowers, T.J., Munns, R. and Colmer, T.D. 2015. Sodium chloride toxicity and the cellular basis of salt tolerance in halophytes. Annals of Botany 115: 419-431.

Foroutan, A., Guo, A.C., Vazquez-Fresno, R., Lipfert, M., Zhang, L., Zheng, J., et al. 2009. Chemical composition of commercial cow's milk. Journal of Agricultural and Food Chemistry 67: 4897–4914

Foroutan, A., Fitzsimmons, C., Mandal, R., Piri-Moghadam, H., Zheng, J., Guo, A., Li, C., Guan, L.L. and Wishart, D.S. 2020. The bovine metabolome. Metabolites 10: 233.

Fraser, C. M. and Chapple, C. 2011. The phenylpropanoid pathway in Arabidopsis. Arabidopsis Book. 9: e0152.

Gao, T., Zhang, Z., Liu, X., Wu, Q., Chen, Q., Liu, Q., van Nocker, S., Ma, F. and Li, C. 2020. Physiological and transcriptome analyses of the effects of exogenous dopamine on drought tolerance in apple. Plant Physiology and Biochemistry 148: 260-272.

Gao, Z., He, X., Zhao, B., Zhou, C., Liang, Y., Ge, R., Shen, Y. and Huang, Z. 2010. Overexpressing a putative aquaporin gene from wheat, TaNIP, enhances salt tolerance in transgenic Arabidopsis. Plant and Cell Physiology 51: 767-775.

Grabherr, M.G., Haas, B.J., Yassour, M., Levin, J.Z., Thompson, D.A., Amit, I., Adiconis, X., et al. 2011. Full-length transcriptome assembly from RNA-Seq data without a reference genome. Nature Biotechnology 29: 644-652.

Groszmann, M., Osborn, H.L. and Evans, J.R. 2017. Carbon dioxide and water transport through plant aquaporins. Plant, Cell & Environment 40: 938-961.

Hasegawa, P.M., Bressan, R.A., Zhu, J.K. and Bohnert, H.J. 2000. Plant cellular and molecular responses to high salinity. Annual Review of Plant Physiology and Plant Molecular Biology 51: 463-499.

Herbert, E.R., Boon, P., Burgin, A.J., Neubauer, S.C., Franklin, R.B., Ardo´n, M., Hopfensperger, K.N., Lamers, P.M. and Gell, P. 2015. A global perspective on wetland salinization: ecological consequences of a growing threat to freshwater wetlands. Ecosphere 6: 206.

Hong, Y., Zhang, W. and Wang, X. 2010. Phospholipase D and phosphatidic acid signalling in plant response to drought and salinity. Plant, Cell & Environment 33: 627-635.

Isayenkov, S.V. and Maathuis, F.J.M. 2019. Plant salinity stress: many unanswered questions remain. Frontiers in Plant Science 10: 80.

Ji, H., Pardo, J.M., Batelli, G., Van Oosten, M.J., Bressan, R.A. and Li, X. 2013. The salt overly sensitive (SOS) pathway: established and emerging roles. Molecular Plant 6: 275-286.

Jiménez-Arias, D., García-Machado, F.J., Morales-Sierra, S., García-García, A.L., Herrera, A.J., Valdés, F., Luis, J.C. and Borges, A.A. 2021. A beginner's guide to osmoprotection by biostimulants. Plants 10, 363.

Joo, S., Liu, Y., Lueth, A. and Zhang, S. 2008. MAPK phosphorylation-induced stabilization of ACS6 protein is mediated by the non-catalytic C-terminal domain, which also contains the cis-determinant for rapid degradation by the 26S proteasome pathway. Plant Journal 54: 129-140.

Kant, S., Kant, P., Raveh, E. and Barak, S. 2006. Evidence that differential gene expression between the halophyte, *Thellungiella halophila*, and *Arabidopsis thaliana* is responsible for higher levels of the compatible osmolyte proline and tight control of Na^+ uptake in *T. halophila*. Plant, Cell & Environment 29: 1220-1234.

Karahara, I., Umemura, K., Soga, Y., Akai, Y., Bando, T., Ito, Y., Tamaoki, D., et al. 2012. Demonstration of osmotically dependent promotion of aerenchyma formation at different

levels in the primary roots of rice using a 'sandwich' method and X-ray computed tomography. Annals of Botany 110: 503-509.

Kirch, H.H., Vera-Estrella, R., Golldack, D., Quigley, F., Michalowski, C.B., Barkla, B.J. and Bohnert, H.J. 2000. Expression of water channel proteins in *Mesembryanthemum crystallinum*. Plant Physiology 123: 111-124.

Kobayashi, N.I., Yamaji, N., Yamamoto, H., Okubo, K., Ueno, H., Costa, A., Tanoi, K., et al. 2017. OsHKT1;5 mediates Na^+ exclusion in the vasculature to protect leaf blades and reproductive tissues from salt toxicity in rice. Plant Journal 91: 657-670.

Kulma, A. and Szopa, J. 2007. Catecholamines are active compounds in plants. Plant Science 172: 433–440.

Langmead, B. and Salzberg, S.L. 2012. Fast gapped-read alignment with Bowtie 2. Nature Methods 9: 357–359.

Lee, S.H. and Zwiazek, J.J. 2015. Regulation of aquaporin-mediated water transport in Arabidopsis roots exposed to NaCl. Plant and Cell Physiology 56: 750-758.

Li, C., Sun, X., Chang, C., Jia, D., Wei, Z., Li, C. and Ma, F. 2015. Dopamine alleviates salt-induced stress in *Malus hupehensis*. Physiologia Plantarum 153, 584-602.

Li, H.W., Zang, B.S., Deng, X.W. and Wang, X.P. 2011. Overexpression of the trehalose-6-phosphate synthase gene OsTPS1 enhances abiotic stress tolerance in rice. Planta 234: 1007-1018.

Liu, Q., Gao, T., Liu, W., Liu, Y., Zhao, Y., Liu, Y., Li, W., Ding, K., Ma, F. and Li, C. 2020a. Functions of dopamine in plants: a review. Plant. Signaling and Behavior 15: 1827782.

Liu, X., Cheng, J., Jiang, F., Liang, M., Han, J., Zhang, J., Zhang, H. and Tang, X. (2020b). The tonoplast intrinsic protein gene KvTIP3 is responsive to different abiotic stresses in *Kosteletzkya virginica*. BioMed Research International 2020: 2895795.

Liu, Y. and Zhang, S. 2004) Phosphorylation of 1-aminocyclopropane-1-carboxylic acid synthase by MPK6, a stress-responsive mitogen-activated protein kinase, induces ethylene biosynthesis in Arabidopsis. Plant Cell 16: 3386-3399.

Liu, Y., Ding, X., Lv, Y., Cheng, Y., Li, C., Yan, L., Tian, S. and Zou, X. 2021. Exogenous serotonin improves salt tolerance in rapeseed (*Brassica napus* L.) seedlings. Agronomy. 11: 400.

Livak, K.J. and Schmittgen, T.D. 2001. Analysis of relative gene expression data using real-time quantitative PCR and the $2^{-\Delta\Delta C}_{\mathrm{T}}$ method. Methods 25: 402-408.

Lux, A., Luxova, M., Abe, J. and Morita, S. 2004. Root cortex: structural and functional variability and responses to environmental stress. Root Research 13: 117-131.

Ma, J.F. and Yamaji N. 2006. Silicon uptake and accumulation in higher plants. Trends in Plant Science 11: 392–397.

Marchiosi, R., Soares, A.R., Abrahão, J., dos Santos, W.D. and Ferrarese-Filho, O. 2020. L-DOPA and dopamine in plant metabolism. In Neurotransmitters in plant signaling and communication. Signaling and communication in plants. Baluška F., Mukherjee S. and Ramakrishna A. (Eds). Cham: Springer.

Martinez-Ballesta, M.C., Aparicio, F., Pallas, V., Martinez, V. and Carvajal, M. 2003. Influence of saline stress on root hydraulic conductance and PIP expression in Arabidopsis. Journal of Plant Physiology 160: 689-697.

Maurel, C., Verdoucq, L., Luu, D.T. and Santoni, V. 2008. Plant aquaporins: membrane channels with multiple integrated functions. Annual Review of Plant Biology 59: 595-624.

Maxwell, B.B., Andersson, C.R., Poole, D.S., Kay, S.A. and Chory, J. 2003. HY5, Circadian Clock-Associated 1, and a cis-element, DET1 dark response element, mediate DET1 regulation of chlorophyll a/b-binding protein 2 expression. Plant Physiology 133: 1565-1577.

McGaughey, S.A., Qiu, J., Tyerman, S.D., Caitlin, S. and Byrt, C.S. 2018. Regulating root aquaporin function in response to changes in salinity. Annual Plant Reviews 1: ar0626.

McLoughlin, F. and Testerink, C. 2013. Phosphatidic acid, a versatile water-stress signal in roots. Frontiers in Plant Science 4: 525.

Mirzavand, M., Ghasemieh, H., Sadatinejad, S.J. and Bagheri, R. 2020. An overview on source, mechanism and investigation approaches in groundwater salinization studies. International Journal of Environmental Science and Technology 17: 2463-2476.

Mueller-Roeber, B. and Pical, C. 2002. Inositol phospholipid metabolism in Arabidopsis. Characterized and putative isoforms of inositol phospholipid kinase and phosphoinositide-specific phospholipase C. Plant Physiology 130: 22-46.

Munns, R. and Tester, M. 2008. Mechanisms of salinity tolerance. Annual Review of Plant Biology 59: 651-681.

Murashige, T. and Skoog, F. 1962. A revised medium for rapid growth and bio assays with tobacco tissue cultures. Physiologia Plantantarum 15: 473-497.

Nikalje, G.C., Mirajkar, S.J., Nikam, T.D. and Suprasanna, P. 2018. Multifarious role of ROS in halophytes: Signaling and defense. In: Abiotic stress-mediated sensing and signaling in

plants: an omics perspective. Zargar S.M. and Zargar M.Y. (Eds). Singapore: Springer Singapore. 207–223.

Nikalje, G.C., Nikam, T.D. and Suprasanna, P. 2017. Looking at halophytic adaptation to high salinity through genomics landscape. Current Genomics 18: 542-552.

Nozaki, K., Ishii, D., and Ishibashi, K. (2008). Intracellular aquaporins: clues for intracellular water transport? Pflugers Arch. 456, 701-707.

Oi, T., Hirunagi, K., Taniguchi, M. and Miyakea, H. 2013. Salt excretion from the salt glands in Rhodes grass (*Chloris gayana* Kunth) as evidenced by low-vacuum scanning electron microscopy. Flora. 208: 52-57.

Okumoto, S., Koch, W., Tegeder, M., Fischer, W.N., Biehl, A., Leister, D., Stierhof, Y.D. and Frommer, W.B. (2004). Root phloem-specific expression of the plasma membrane amino acid proton co-transporter AAP3. Journal of Experimental Botany 55: 2155-2168.

Okur, B. and Örçen, N. 2020. Climate change and soil interactions: Elsevier, Amsterdam, The Netherlands.

Oliveros, J.C. 2007-2015. Venny. An interactive tool for comparing lists with Venn's diagrams. Available online at: https://bioinfogp.cnb.csic.es/tools/venny/index.html.

Pang, Z., Chong, J., Zhou, G., de Lima Morais, D A, Chang, L., Barrette, M., Gauthier, C., Jacques, P.E., Li, S. and Xia, J. 2021. MetaboAnalyst 5.0: narrowing the gap between raw spectra and functional insights. Nucleic Acids Research 49: W388-W396.

Pankova, Y.I. and Konyushkova, M.V. 2014. Effect of global warming on soil salinity of the arid regions. Russian Agricultural Sciences 39: 464-467.

Parre, E., Ghars, M.A., Leprince, A.S., Thiery, L., Lefebvre, D., Bordenave, M., Richard, L., Mazars, C., Abdelly, C. and Savoure, A. 2007. Calcium signaling via phospholipase C is

essential for proline accumulation upon ionic but not nonionic hyperosmotic stresses in Arabidopsis. Plant Physiology 144: 503-512.

Pertea, G., Huang, X., Liang, F., Antonescu, V., Sultana, R., Karamycheva, S., Lee, Y., et al. 2003. TIGR Gene Indices clustering tools (TGICL): a software system for fast clustering of large EST datasets. Bioinformatics 19: 651-652.

Putney, J.W. and Tomita, T.-E. 2012. Phospholipase C signaling and calcium influx. Advances in Biological Regulation 52: 152-164.

Quan, R., Lin, H., Mendoza, I., Zhang, Y., Cao, W., Yang, Y., Shang, M., Chen, S., Pardo, J.M. and Guo, Y. 2007. SCABP8/CBL10, a putative calcium sensor, interacts with the protein kinase SOS2 to protect Arabidopsis shoots from salt stress. Plant Cell 19: 1415-1431.

Reddy, I.N.B.L., Kim,S.M., Kim, B.K., Yoon, I.S. and Kwon, T.R. 2017. Identification of rice accessions associated with K^+/Na^+ ratio and salt tolerance based on physiological and molecular responses. Rice Science 24: 360-364.

Ren, S., Ma, K., Lu, Z., Chen, G., Cui, J., Tong, P., Wang, L., Teng, N. and Jin, B. 2019. Transcriptomic and metabolomic analysis of the heat-stress response of *Populus tomentosa* Carr. Forests 10: 383.

Ren, Z.H., Gao, J.P., Li, L.G., Cai, X.L., Huang, W., Chao, D.Y., Zhu, M.Z., Wang, Z.Y., Luan, S. and Lin, H.X. 2005. A rice quantitative trait locus for salt tolerance encodes a sodium transporter. Nature Genetics 37: 1141-1146.

Rios, J.J., Martinez-Ballesta, M.C., Ruiz, J.M., Blasco, B. and Carvajal, M. 2017. Silicon-mediated improvement in plant salinity tolerance: the role of aquaporins. Frontiers in Plant Science 8: 948.

Roschzttardtz, H., Conejero, G., Curie, C. and Mari, S. 2009. Identification of the endodermal vacuole as the iron storage compartment in the Arabidopsis embryo. Plant Physiology 151: 1329-1338.

Sairam, R.K. and Tyagi, A. 2004. Physiology and molecular biology of salinity stress tolerance in plants. Current Science 86: 407–421.

Shabala, S., Bose, J. and Hedrich, R. 2014. Salt bladders: do they matter? Trends in Plant Science 19: 687-691.

Shahid, S.A., Zaman, M. and Heng, L. 2018. Soil salinity: historical perspectives and a world overview of the problem. In Guideline for salinity assessment, mitigation and adaptation using nuclear and related techniques. L. Heng, M. Zaman, and S. A (Eds). Shahid. Cham: Springer.

Shrivastava, P. and Kumar, R. 2015. Soil salinity: a serious environmental issue and plant growth promoting bacteria as one of the tools for its alleviation. Saudi Journal of Biological Sciences 22: 123-131.

Skalak, J., Nicolas, K. L., Vankova, R. and Hejatko, J. 2021. Signal integration in plant abiotic stress responses via multistep phosphorelay signaling. Frontiers in Plant Science 12: 644823.

Sutka, M., Li, G., Boudet, J., Boursiac, Y., Doumas, P. and Maurel, C. 2011. Natural variation of root hydraulics in Arabidopsis grown in normal and salt-stressed conditions. Plant Physiology 155: 1264-1276.

Szabados, L. and Savoure, A. 2010. Proline: a multifunctional amino acid. Trends in Plant Science 15: 89-97.

Taji, T., Seki, M., Satou, M., Sakurai, T., Kobayashi, M., Ishiyama, K., Narusaka, Y., Narusaka, M., Zhu, J.K. and Shinozaki, K. 2004. Comparative genomics in salt tolerance between Arabidopsis and Arabidopsis-related halophyte salt cress using Arabidopsis microarray. Plant Physiology 135: 1697-1709.

Tan, W.K., Lin, Q., Lim, T.M., Kumar, P. and Loh, C.S. 2013. Dynamic secretion changes in the salt glands of the mangrove tree species *Avicennia officinalis* in response to a changing saline environment. Plant, Cell & Environment 36: 1410-1422.

Tan, X., Xu, H., Khan, S., Equiza, M.A., Lee, S.H., Vaziriyeganeh, M. and Zwiazek, J.J. (2018). Plant water transport and aquaporins in oxygen-deprived environments. Journal of Plant Physiology 227: 20-30.

Trapnell, C., Williams, B.A., Pertea, G., Mortazavi, A., Kwan, G., van Baren, M.J., Salzberg, S.L., Wold, B.J. and Pachter, L. 2010. Transcript assembly and quantification by RNA-Seq reveals unannotated transcripts and isoform switching during cell differentiation. Nature Biotechnology 28: 511-515.

Vaziriyeganeh M., Carvajal M., Du N. and Zwiazek J.J. 2022. Salinity tolerance of halophytic grass *Puccinellia nuttalli*ana is associated with enhancement of aquaporin-mediated water transport by sodium. International Journal of Molecular Sciences 23: 5732.

Vaziriyeganeh, M., Lee, S.H, and Zwiazek, J.J. 2018. Water transport properties of root cells contribute to salt tolerance in halophytic grasses *Poa juncifolia* and *Puccinellia nuttalliana*. Plant Science 276: 54-62.

Voicu, M.C., Cooke, J.E. and Zwiazek, J.J. 2009. Aquaporin gene expression and apoplastic water flow in bur oak (*Quercus macrocarpa*) leaves in relation to the light response of leaf hydraulic conductance. Journal of Experimental Botany 60: 4063-4075.

Volkov, V. and Amtmann, A. 2006. *Thellungiella halophila*, a salt-tolerant relative of *Arabidopsis thaliana*, has specific root ion-channel features supporting K^+/Na^+ homeostasis under salinity stress. Plant Journal 48: 342-353.

Waidmann, S., Kusenda, B., Mayerhofer, J., Mechtler, K. and Jonak, C. 2014. A DEK domain-containing protein modulates chromatin structure and function in Arabidopsis. Plant Cell 26: 4328-4344.

Wang, J.P., Matthews, M.L., Williams, C.M., Shi, R., Yang, C., Tunlaya-Anukit, S., Chen, H.C., et al. 2018a. Improving wood properties for wood utilization through multi-omics integration in lignin biosynthesis. Nature Communications 9: 1579.

Wang, Y., Jiang, L., Chen, J., Tao, L., An, Y., Cai, H. and Guo, C. 2018b. Overexpression of the alfalfa WRKY11 gene enhances salt tolerance in soybean. PLoS One 13: e0192382.

Wang, Z.L., Li, P.H., Fredricksen, M., Gong, Z.Z., Kim, C.S., Zhang, C., Bohnert, H.J., Zhu, J.K. and Bressan, R.A. 2004. Hasegawa PM: Expressed sequence tags from *Thellungiella halophila*, a new model to study plant salt-tolerance. Plant Science 166: 609-616.

Wei, H., Li, J., Peng, Z., Lu, B., Zhao, Z. and Yang, W. 2008. Relationships of *Aegilops tauschii* revealed by DNA fingerprints: The evidence for agriculture exchange between China and the West. Progress in Natural Science 18: 1525–1531.

Wu, J., Yan, G., Duan, Z., Wang, Z., Kang, C., Guo, L., Liu, K., Tu, J., Shen, J., Yi, B., Fu, T., Li, X., Ma, C. and Dai, C. 2020. Roles of the *Brassica napus* DELLA protein BnaA6.RGA, in modulating drought tolerance by interacting with the ABA signaling component. Frontiers in Plant Science 11: 577.

Xie, M., Zhang, J., Tschaplinski, T.J., Tuskan, G.A., Chen, J.G. and Muchero, W. 2018. Regulation of lignin biosynthesis and its role in growth-defense tradeoffs. Frontiers in Plant Science 9: 1427.

Xiong, H., Guo, H., Xie, Y., Zhao, L., Gu, J., Zhao, S., Li, J. and Liu, L. 2017. RNAseq analysis reveals pathways and candidate genes associated with salinity tolerance in a spaceflight-induced wheat mutant. Scientific Reports 7: 2731.

Xiong, Y., Yan, H., Liang, H., Zhang, Y., Guo, B., Niu, M., Jian, et al. 2019. RNA-Seq analysis of *Clerodendrum inerme* (L.) roots in response to salt stress. BMC Genomics 20: 724.

Yamaguchi, M., Valliyodan, B., Zhang, J., Lenoble, M.E., Yu, O., Rogers, E.E., Nguyen, H.T. and Sharp, R.E. 2010. Regulation of growth response to water stress in the soybean primary root. I. Proteomic analysis reveals region-specific regulation of phenylpropanoid metabolism and control of free iron in the elongation zone. Plant, Cell & Environment 33: 223-243.

Yamamoto, N., Takano, T., Tanaka, K., Ishige, T., Terashima, S., Endo, C., Kurusu, T., Yajima, S., Yano, K., et al. 2015. Comprehensive analysis of transcriptome response to salinity stress in the halophytic turf grass *Sporobolus virginicus*. Frontiers in Plant Science 6: 241.

Yang, Y. and Guo, Y. 2018. Unraveling salt stress signaling in plants. Journal of Integrative Plant Biology 60: 796-804.

Yang, M.F., Song, J., and Wang, B.S. 2010. Organ-specific responses of vacuolar H-ATPase in the shoots and roots of C halophyte *Suaeda salsa* to NaCl. Journal of Integrative Plant Biology 52: 308-314.

Yao, X., Nie, J., Bai, R. and Sui, X. 2020. Amino acid transporters in plants: identification and function. Plants 9: 972.

Yokoi, S., Quintero, F. J., Cubero, B., Ruiz, M. T., Bressan, R. A., Hasegawa, P. M. and Pardo, J. M. 2002. Differential expression and function of *Arabidopsis thaliana* NHX Na^+/H^+ antiporters in the salt stress response. Plant Journal 30: 529-539.

Yu, L., Nie, J., Cao, C., Jin, Y., Yan, M., Wang, F., Liu, J., Xiao, Y., Liang, Y. and Zhang, W. 2010. Phosphatidic acid mediates salt stress response by regulation of MPK6 in *Arabidopsis thaliana*. New Phytologist 188: 762-773.

Yuan, F., Xu, Y., Leng, B. and Wang, B. 2019. Beneficial effects of salt on halophyte growth: morphology, cells, and genes. Open Life Sciences 14: 191-200.

Zhang, G.W., Xu, S.C., Hu, Q.Z., Mao, W.H. and Gong, Y.M. 2014. Putrescine plays a positive role in salt-tolerance mechanisms by reducing oxidative damage in roots of vegetable soybean. Journal of Integrative Agriculture 13: 349-357.

Zhang, L., Tan, Q., Lee, R., Trethewy, A., Lee, Y.H. and Tegeder, M. 2010. Altered xylem-phloem transfer of amino acids affects metabolism and leads to increased seed yield and oil content in Arabidopsis. Plant Cell 22: 3603-3620.

Zhao, L., Yang, Z., Guo, Q., Mao, S., Li, S., Sun, F., Wang, H. and Yang, C. 2017. Transcriptomic profiling and physiological responses of halophyte *Kochia sieversiana* provide insights into salt tolerance. Frontiers in Plant Science 8: 1985.

Zhu, J., Brown, K.M. and Lynch, J.P. 2010. Root cortical aerenchyma improves the drought tolerance of maize (*Zea mays* L.). Plant, Cell & Environment 33: 740-749.

Zhu, J.K., Liu, J. and Xiong, L. 1998. Genetic analysis of salt tolerance in Arabidopsis. Evidence for a critical role of potassium nutrition. Plant Cell 10: 1181-1191.

Zwiazek, J.J., Xu, H., Tan, X., Navarro-Rodenas, A. and Morte, A. 2017. Significance of oxygen transport through aquaporins. Scientific Reports 7: 40411.

3.6 Supplementary Material

Supplementary Table 3.1. Clean reads quality metrics

Sample	Total Raw Reads (M)	Total Clean Reads (M)	Total Clean Bases (Gb)	Clean Reads Q20 (%)	Clean Reads Q30 (%)	Clean Reads Ratio (%)
C1	52.47	51.69	5.17	97.94	91.46	98.52
C2	52.47	51.49	5.15	97.96	91.61	98.12
C3	52.47	51.56	5.16	98.08	91.94	98.26
T1	52.47	51.38	5.14	97.98	91.84	97.92
T2	52.47	51.34	5.13	97.69	90.73	97.84
T3	52.47	51.56	5.16	97.86	91.41	98.25

Supplementary Table 3.2. Primer list used for qRT-PCR validation of RNAseq data *in Puccinellia nuttalliana* to salt stress. Primer efficiency, correlation coefficient (R^2) and slope of standard curves for the genes analyzed in this study

Primer ID	Primer sequence	R^2	Slope	Efficiency (%)
PIP2;2 F	CGTCAGCTGCTACAGTTCTT	0.98	-3.51	92.71
PIP2;2 R	GACGATCACATCGAGACCATATT			
HKT1;5 F	CACCTACGTCAAGTCCAAGAAG	0.96	-3.29	101.35
HKT1;5 R	CAGGGTCGTGCATCATAGATATAG			
TIP1 F	CACCACCGACTACTAAGCTAAAG	0.98	-3.25	103.09
TIP1 R	GGTTCATGGAACGGGAAGAA			
DUF F	GTCCCGTTACAATGTGGTAGAT	0.97	-3.13	108.68
DUF R	GGTCGATCCTAGAGTCCTGAT			
HAK9 F	CGGCACGGCGTTCATAAT	0.98	-3.29	101.34
HAK9 R	GGCGCAGGAAGTTGTACC			
WRKY17 F	CGGGCATGCCTAACAACTTA	0.95	-3.19	105.82
WRKY17 R	CCTTCTTTACACGGAACAACATTC			
CBL10 F	TGCAAGCACTTGATTTACAAGA	0.99	-3.48	93.80
CBL10 R	GGAGCATTTGGACTAAAGATGTG			

MYB77 F	TCACAGACATGCTGCTTGAT	0.87	-3.56	90.94
MYB77 R	GTAGTTGTTGCTCTCTCCATCTC			
ADP F	GCAGCTGAAATCACCGATAAG	0.97	-3.22	104.43
ADP R	CCAGTCAAGTCCCTCATACAA			
ACT F	CCATGAGACCACCTACAACTC	0.88	-3.42	96.064
ACT R	TCAGCAATACCAGGGAACATAG			

Supplementary Table 3 3. Quality metrics of unigenes

Quality metrics of Unigenes. Sample	Total Number	Total Length	Mean Length	N50	N70	N90	GC(%)
C1	124476	80528211	646	982	524	268	46.97
C2	130593	85992148	658	993	544	273	46.84
C3	135411	90715457	669	1021	558	277	46.17
T1	103504	69030681	666	1062	550	268	49.18
T2	74432	59750370	802	1357	764	309	49.6
T3	83363	57997568	695	1083	621	283	50.18
All-Unigene	242833	1.8E+08	742	1223	663	289	47.15

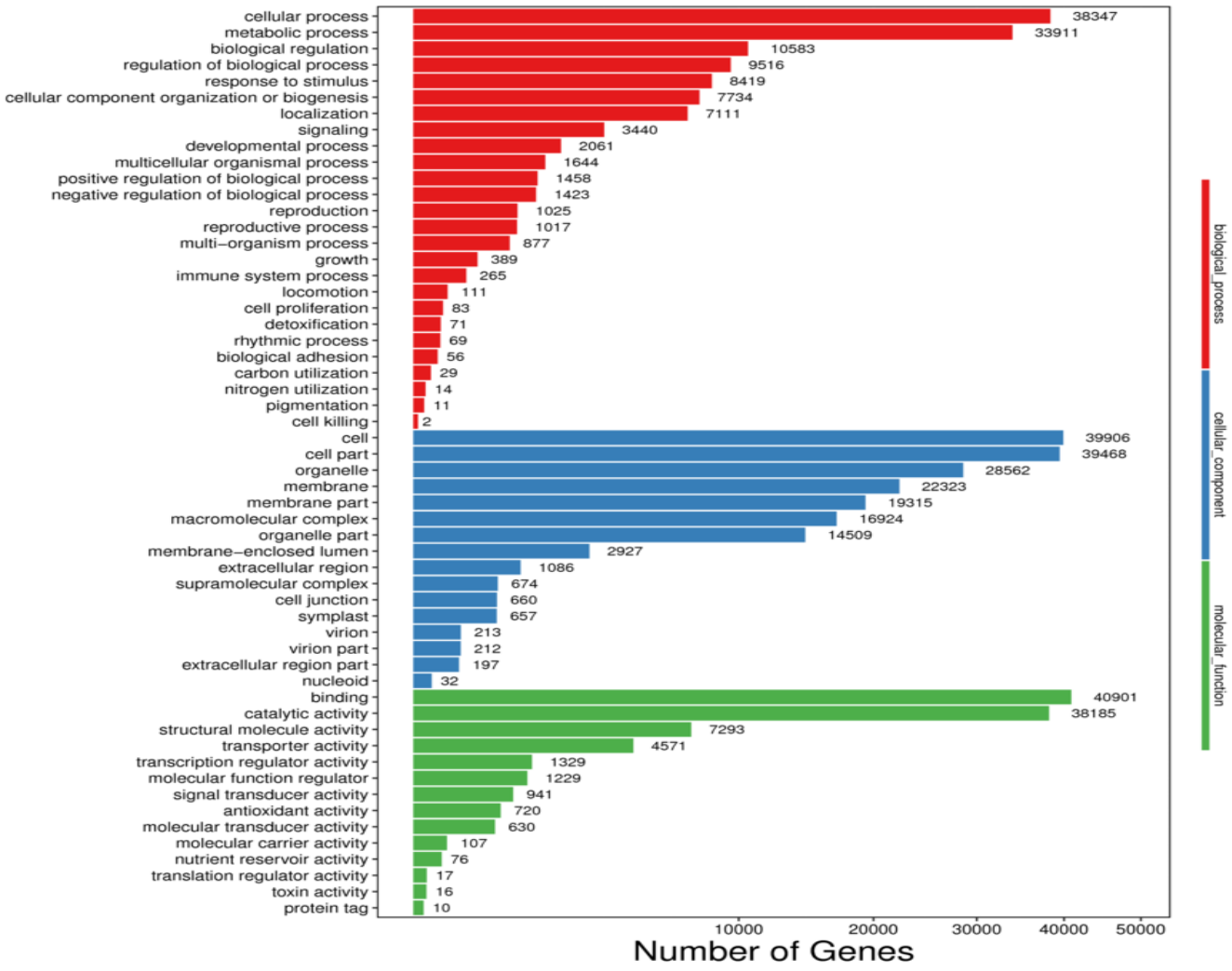

Supplementary Fig. 3.1. Functional distribution of GO annotation.

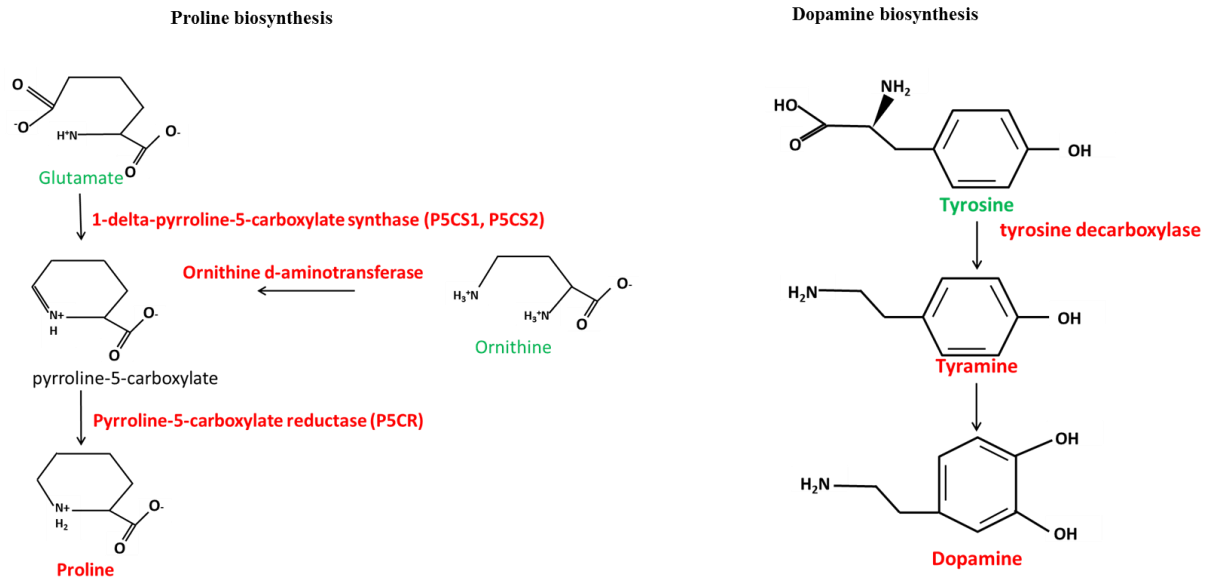

Supplementary Fig. 3.2. Proline and dopamine biosynthesis pathways identified in *Puccinellia nuttalliana.* Proline is synthesized via two pathways mainly from glutamate and alternatively ornithine. The enzymes carrying out the reactions shown in the figure are as follows: pyrroline-5-carboxylate synthase (P5CS1, P5CS2), ornithine aminotransferase (OAT); pyrroline-5-carboxylate reductase (P5CR). Red color denoted increased and green color denoted decreased. The decarboxylation of tyrosine by tyrosine decarboxylase (TYDC) produces tyramine then converted to dopamine.

Chapter 4. Structural and functional properties of PnuPIP2;2 aquaporin contribute to salt tolerance of halophytic grass *Puccinellia nuttalliana*

4.1 Introduction

Salinity exerts its effects on plants through a direct toxicity of salt ions, osmotic imbalance, altered nutrient uptake, and tissue accumulation of reactive oxygen species (ROS) (Hanin et al. 2016, Zhu et al. 2019). Salt rapidly alters water uptake and its transport in plants, which quickly leads to the loss of water balance. This further affects a wide range of processes and, eventually, contributes to plant growth inhibition and mortality (Munns and Tester 2008). Increased resistance of roots to water flow in plants affected by salt has been commonly reported for salt-sensitive glycophytic plants (Boursiac et al. 2005, Lee et al. 2010, Sutka et al. 2011) and attributed to the effects on cell hydraulic conductivity (L_{pc}) that is regulated by aquaporins (Martinez-Ballesta et al. 2003, Lee and Zwiazek 2015, Vaziriyeganeh et al. 2018). In salt-sensitive Arabidopsis plants, the aquaporin-mediated root water transport was reduced within 30 min following an exposure to NaCl concentrations as low as 10 mM (Lee and Zwiazek 2015). On the other hand, the aquaporin-mediated water transport has been reported to be either unaffected or enhanced by NaCl in salt-tolerant grasses (Vaziriyeganeh et al. 2018; 2022).

It has been well established that aquaporins play a critical role in plant water movement (Chaumont and Tyerman 2014) and affect plant responses to stress conditions (Kapilan et al. 2018). Water movement across cell membranes (transmembrane pathway) plays an essential role in regulating root and leaf hydraulic conductivity, transpiration, and cell elongation (Afzal et al. 2016). Aquaporins are highly conserved water channel proteins of the major intrinsic protein family (Pawłowicz et al. 2017), which in addition to water can also facilitate the transmembrane

transport of gases and other small charged and uncharged molecules including Na^+ and K^+ (Zwiazek et al. 2017, Liu et al., 2020, Tyerman et al. 2021). Therefore, their functionality may be especially important in plants affected by salinity (Kortenoeven and Fenton 2014). Plant aquaporins form six transmembrane helices (TM1-TM6) and have five internal loops (LA-LE) as well as highly conserved domains with the NPA (Asp-Pro-Ala) motif (Afzal et al. 2016). Based on the aquaporin subcellular localization and sequence similarities, they are divided into 5 subfamilies including the plasma membrane intrinsic proteins (PIPs), tonoplast intrinsic proteins (TIPs), Nodulin-26-like intrinsic proteins (NIPs), small basic intrinsic proteins (SIPs), and X intrinsic proteins (XIPs) (Chaumont and Tyerman 2014). Different explanations have been offered for the effects of NaCl on aquaporins including the downregulation of gene expression and membrane abundance of PIPs (Martinez-Ballesta et al. 2008, Lee et al. 2015, Knipfer et al. 2011, Kumari and Bhatla 2021), gating processes involving phosphorylation and (or) dephosphorylation (Martínez-Ballesta et al. 2008, Horie et al. 2011, Lee and Zwiazek, 2015), inhibition by ROS (Alavilli et al., 2016), and altered membrane trafficking (Luu and Maurel. 2013, Ueda et al. 2016, Yepes-Molina et al. 2020). Therefore, the functionality of aquaporins under salinity conditions may involve complex and still little characterized processes in plants.

Contrary to relatively salt-sensitive *Poa pratensis*, 150 mM NaCl and Na_2SO_4 treatments enhanced by about two-fold L_{pc} in roots of the halophytic grass *Puccinellia nuttaliana* and this increase was abolished by 50 μM $HgCl_2$ (Vaziriyeganeh et al. 2022). Mercury blocks water transport across some aquaporins (Wan and Zwiazek 1999, Maurel et al. 2015) through conformational changes in the ar/R region (Hirano et al. 2010). However, it is not considered a specific aquaporin inhibitor, and may also increase water permeability across other aquaporins through a non-cysteine-related mechanism (Frick et al. 2013). Transcriptomic and metabolomic

analyses of *P. nuttalliana* have identified several membrane transporters, including the high-affinity potassium transporter PnuHKT1;5 as well as PnuPIP2;2, and several other aquaporins, that are likely to play major roles in ion homeostasis, water balance, and water transport following plant exposure to NaCl (Vaziriyeganeh et al. 2021). TmHKT1;5 from salt tolerant *Triticum monococcum* was shown to be responsible for an effective Na^+ transport control in the xylem and its expression in durum wheat (*Triticum turgidum* ssp. *durum*) improved salt tolerance of plants (Byrt et al. 2007). This, however, likely requires an efficient water transport through the aquaporins that are not inhibited by Na^+. Increased transcript levels of aquaporin genes and aquaporin protein abundance have also been found to be associated with salinity tolerance in other plants. The gene expression levels of *PIP2;8* increased in response to NaCl treatment in shoot tissues of the salt-tolerant barley cultivar (*Hordeum vulgare*), but not in the salt-sensitive cultivar (Tran et al. 2020) and the overexpression of *PIP2;3* from the halophytic plant *Canavalia rosea* improved drought and salt tolerance when overexpressed in Arabidopsis (Lin et al. 2021). The expression of *OsTIP1;1* in rice and *ZmPIP1;1* in maize increased in response to salinity stress (Sakurai et al. 2005, Zhu et al. 2005). In Arabidopsis, TIP1;1 was re-localized into intravacuolar invaginations under salt stress (Boursiac et al. 2005). An increase in the tissue protein levels of PIPs and TIPs was also reported for salt-acclimated sunflower (*Helianthus annus*) (Kumari and Bhatla 2021) and a receptor-like cytoplasmic kinase from rice (OsRLCK311) was found to interact in Arabidopsis with AtPIP2;1 and OsPIP2;1 and induce salt tolerance (Sade et al. 2020). PIP1;3 was reported as a hypoxia-responsive gene (Zwiazek et al. 2017), but the response to salinity stress is unknown. Therefore, in the present study, I was interested in PIP2;1, PIP2;2, PIP2;3, PIP1;1, PIP1;3 and TIP1;1 as the potential aquaporins that could be involved in plant responses to NaCl. The enhancement of aquaporin-

mediated cell-to-cell water transport by NaCl in *P. nuttalliana* (Vaziriyeganeh et al., 2018; 2022) and the improved salt tolerance of Arabidopsis plants overexpressing the halophytic plant aquaporin (Sade et al., 2020) suggest that some of the aquaporins in halophytic plants may have unique properties that enable them to function under salt stress conditions. Therefore, in the present study, I cloned several PIP and TIP aquaporin genes from three related grasses varying in salt tolerance, including a halophytic grass *P. nuttalliana*, a moderately salt-tolerant *Poa juncifolia*, and a relatively salt-sensitive *Poa pratensis* (Vaziriyeganeh et al. 2018). I examined the expression levels of these genes in control and NaCl-treated plants and characterized their structural and functional properties that may have contributed to the reported differences in the responses of plant water relations to salinity (Vaziriyeganeh et al. 2018, 2022). I tested the hypothesis that the earlier reported differences in the responses of cell hydraulic conductivity to NaCl in the three grass species, including an enhancement of cell hydraulic conductivity in *P. nuttalliana* (Vaziriyeganeh et al. 2018, 2022), involve changes in the expression patterns of *PIP* and *TIP* aquaporins and direct effects of NaCl on gating properties. Since *PnuPIP2;2* expression is enhanced by NaCl, I also investigated whether this aquaporin possesses dual water and ion transport functionality when expressed in yeast and I examined the pore properties of PIP2;2 in the three grass species to shed light on its role in salt tolerance.

4.2 Materials and Methods

4.2.1 Plant growth conditions and treatments

Seeds of Kentucky bluegrass (*Poa pratensis* L.), alkali bluegrass (*Poa juncifolia* Scribn.), and Nuttall's alkali bluegrass [*Puccinellia nuttalliana* (Schult.) Hitchc.] were surface sterilized with 70% ethanol for 2 min followed by 1% sodium hypochlorite for 5 min and then rinsed in autoclaved water. The seeds were germinated in Petri plates on the sterile half-strength Murashige & Skoog solid medium (Grant et al. 2017). One week after germination, the seedlings were planted in 500 cm^3 pots containing commercial growing mix (Sunshine® Mix #4 Professional Growing Mix, Sun Gro Horticulture, Seba Beach, AB). The pots with plants were placed in a controlled-environment growth room at 22/18°C (day/night) temperature, 65 ± 10% relative humidity, and 16-h photoperiod with 350 μmol m^{-2} s^{-1} photosynthetic photon flux density. The plants were watered every two days and fertilized once a week with half-strength modified Hoagland's solution (Epstein 1972).

4.2.2 NaCl treatment

After eight weeks of growth in the soil, plants were transferred to the hydroponic set-up consisting of 12 L polyvinyl chloride containers with 50% Hoagland's mineral solution. The solution was aerated with an air pump to provide O_2 concentration of approximately 8 mg L^{-1}. Three plants of each species were randomly placed together in each of the six containers (9 plants per container) for the total of 18 plants per species. After one-week, 150 mM NaCl was gradually added (in 50 mM increments over 24 h) to three containers while plants in the other three containers remained in 50% Hoagland's solution and served as a control. Plants were harvested after 6 days of the NaCl treatment.

4.2.3 Total RNA isolation, first-strand cDNA synthesis, and RT-qPCR analysis

Total RNA was extracted from the frozen homogenized roots of *P. nutalliana, P. juncifolia,* and *P. pratensis* using the RNeasy Plant Mini Kit (Qiagen, CA, USA). The quality of total RNA was examined by gel electrophoresis and the concentration was measured with a Nano Drop 2000c spectrophotometer (Thermo Fisher Scientific Inc., Waltham, MA, USA). The RNA quality control, including the integrity value, 28S/18S, and the fragment length distribution, was carried out using a 2100 Bioanalyzer (Agilent, Mississauga, ON, Canada). The removal of genomic DNA contamination and first strand cDNAs were performed using the QuantiTect Reverse Transcription Kit (Qiagen, CA) with 500 µg total RNA according to the manufacturer's instructions. The qRT-PCR was performed using SYBR Green I dye reagent in an Applied Biosystems 7500 Fast System (Thermo Fisher) with ten-fold diluted cDNA. The relative expression of all genes was calculated using the delta-delta-Ct method. Actin (ACT) and ADP-ribosylation factor 1-like protein (ADP) were used as the reference genes for normalization.

4.2.4 Designing degenerate primers and cloning

Degenerate primers (Supplementary Table 4.2) were designed based on highly conserved regions of amino acid sequences of diverse aquaporin genes reported for *Hordeum vulgare*, *Zea mays*, *Oryza sativa*, and *Sorghum bicolor* by multiple sequence alignment. Sequences were retrieved from the GenBank database at the National Center for Biotechnology. The Consensus DEgenerate Hybrid Oligonucleotide Primer (CODEHOP) PCR strategy (Rose et al. 2003) was used to design the degenerate primers (http://blocks.fhcrc.org/codehop.html). This strategy uses multiple sequence alignment and the codon usage of the target genome in designing degenerate primers. The multiple sequence alignment was first generated with CLUSTALW, and then cut into blocks using the Block Maker server (http://blocks.fhcrc.org/codehop.html). Touchdown

PCR (Korbie and Mattick 2008) was used to amplify the aquaporin genes using cDNA templates. After examination by gel electrophoresis, reaction products were cloned into the pCR2.1-TOPO vector (Thermo Fisher). White colonies were grown overnight in a shaker incubator at 37°C (225 rpm). Verification of inserts was done by colony PCR. About 3–5 white colonies were sequenced for each PCR product using the M13 sequencing primers (Thermo Fisher). The nucleotide sequence and translation of clones have been submitted to the GenBank database (accession no. OP293057-OP293074).

4.2.5 Nomenclature of aquaporin genes

For the classification of identified putative aquaporins from *P. pratensis*, *P. juncifolia*, and *P. nuttalliana*, phylogenetic analyses were performed with the known aquaporins from *Hordeum vulgare*, *Zea mays*, *Oryza sativa*, and *Sorghum bicolor*. Amino acid sequences were aligned with the identified aquaporins using the ClustalW program. A tree was constructed using the neighbor-joining (NJ) method in the MEGA7 software suite (http://www.megasoftware.net/mega.html).

4.2.6 Rapid amplification of cDNA 3′ end and cloning

The rapid amplification of cDNA 3′ end (3’ RACE) was performed to obtain 3′-UTR sequence information that would be used for designing primers for downstream qRT-PCR analysis. The first strand cDNAs were synthesized from 1 µg of total RNA using Superscript II reverse transcriptase and an oligo (dT) primer (Thermo Fisher). Coding sequences of putative aquaporins were amplified with Phusion DNA Polymerase (Thermo Fisher) using the primers listed in Table S.2. The PCR products of the expected size were eluted from the gel and purified using The Wizard® SV Gel and PCR Clean-Up System (Promega Corporation, Madison, WI, USA). The PCR products were then cloned into the pCR2.1-TOPO vector using the Topo TA

Cloning kit and transformed into DH5α chemically competent cells (Thermo Fisher). Three to six white colonies were sequenced for each PCR product using M13 sequencing primers. The coding sequences of aquaporin genes were extended by 3′ rapid amplification of cDNA ends (RACE, Scotto-Lavino et al. 2006).

4.2.7 Plasmid construction and yeast transformation

Open reading frame (ORF) of *PnuPIPs* and *PnuTIP* aquaporins were cloned as Gateway entry clones in plasmid pDONR221 (Thermo Fisher). ORFs from the entry clones were shuttled into the galactose-inducible yeast expression plasmid pAG426Gal-ccdB-EYFP (Addgene plasmid # 14227) by Gateway LR cloning reaction to generate C-terminally tagged aquaporin-protein–YFP fusions. The S.c. EasyComp™ Transformation Kit (Thermo Fisher) was used to transform yeast with each plasmid DNA.

4.2.8 Water permeability of transformed yeast protoplasts

The water permeability of yeast protoplasts overexpressing different PIP and TIP aquaporins was measured by volume changes (Bertl and Kaldenhoff 2007). The protoplasts were prepared by enzymatically digesting cell walls in a buffer containing 50 mM KH2PO3-KOH pH 7.2, 2,4 M sorbitol, 0.2% β-mercaptoethanol, and 2 mg/mL Zymolyase 20T (to enzymatically digest the cell walls. The prepared protoplasts were suspended in an incubation buffer consisting of 1.8 M sorbitol, 50 mM NaCl, 5 mM $CaCl_2$, 10 mM Tris-HCl pH 7.0). To achieve an osmotic gradient and commence water flow, 50 µL of protoplast suspension was rapidly mixed in a 1: 1 (v/v) ratio with the protoplast suspension buffer containing 1.2 M sorbitol. The protoplast volume changes by 90^{o} light scattering at 436 nm in a SX18MV-R stopped-flow spectrophotometer (Applied Photophysics, Surrey, UK). The measurements were recorded at 400 points over 50 ms, and the signals were fitted by single-phase exponential decay functions using

the Sigmaplot 14.0 (Systat Software Inc., Chicago, IL, USA). Four to five biological replicates (n = 4 - 5), each representing a separate transformation, were used to calculate the means for each aquaporin. To evaluate the ability of Na^+ to modulate water permeability of PnuPIP2;2, 100 mM NaCl was added directly to yeast cells 5 minutes before the water transport assay. For these measurements, the incubation buffer contained 1.8 M sorbitol; 5 mM NaCl; 2 mM KCl, 1mM $MgCl_2$, 0.5 mM $CaCl_2$; 10 mM Tris-HCl pH 7.0. The mixing buffer for salt-treated yeast protoplasts contained 1.2 M sorbitol, 100 mM NaCl, 2 mM KCl, 1 mM $MgCl_2$, 0.5 mM $CaCl_2$, 10 mM Tris-HCl pH 7.0. The resulting osmolarity was 300 mosmol for both treatments.

4.2.9 Yeast elemental analysis

The full-length cDNA of PnuPIP2;2 cloned into pAG426Gal-ccdB-EYFP was transformed into *S. cerevisiae* strain. Yeast cells expressing PnuPIP2;2 and empty vector (control) were grown according to Byrt et al. (2017). In brief, yeast was grown on selective media with Yeast Nitrogen Base without amino acids, phosphates, or NaCl (MP Biomedicals) and Yeast Synthetic Drop-out Medium Supplements, without uracil (Sigma-Aldrich), 95 mg L^{-1} L-histidine-HCl, 1% (w/v) KH_2PO_4, pH 5.5 with TRIS. The treatments used in this study were 0 mM, 300 mM and 600 mM NaCl. Cells were grown at 28°C for 24 h at 200 rpm. Cells were extracted by centrifugation and then washed with a solution containing sorbitol and $MgCl_2$ of equal osmolality. Pellets were frozen at 20°C for 24 h, then re-suspended in 2 mL of MilliQ water and boiled for 30 min to lyse cells. Elemental analysis of cell extracts from four biological replicates (n = 4) was performed by the Inductively Coupled Plasma-Optical Emission Spectroscopy (Thermo iCAP6300 Duo, Thermo Fisher).

4.2.10 Live cell bioimaging

Localization of heterologously expressed EYFP-tagged aquaporins was determined by visualizing EYFP fluorescence in whole cells (Couthouis et al. 2011) with a fluorescence microscope (LSM700, Carl Zeiss, Germany).

4.2.11 Database sources

Tertiary protein structure predictions were conducted by submitting the protein sequences of PIP2;1, PIP2;2, PIP2;3, PIP1;1, PIP1;3 and TIP1;1 to the SWISS-MODEL web server (Biasini et al., 2014). The results obtained in the Protein Data Bank (PDB) format from I-TASSER were uploaded to the PoreWalker server (Pellegrini-Calace et al., 2009) to predict pore shape and cavity structure. Conserved sequences for substrate specificity of Froger's positions (P1–P5), NPA motifs, ar/Rfilters (H2, H5, LE1, LE2) were identified by manual examination of multiple sequence alignments of cloned aquaporin genes with structurally characterized aquaporins, as reported earlier (Shivaraj et al. 2017, Khan et al. 2019).

4.2.12 Statistical analyses

Statistical analyses were carried out using the SPSS 18.0 statistical package (SPSS Inc., Chicago, IL, USA). For the gene expression, one-way ANOVA was carried out followed by Tukey's test to detect significant differences between control and NaCl treatment for each plant species ($p \leq 0.05$). Duncan's Multiple Range test was used to compare the effects of NaCl on water transport in yeast transformed with different aquaporins as well as the effects of yeast transformation with PnuPIP2;2 on Na^+, K^+, and P concentrations following NaCl treatment.

4.3 Results

4.3.1 Cloning and nomenclature

The root cDNA was used as a template to clone predicted aquaporin genes from *Poa pratensis, Poa juncifolia,* and *Puccinellia nuttalliana* using degenerated primers. Six predicted aquaporin genes were cloned from each of the three plant species. A BLAST search against the NCBI database revealed their identity as the members of the plasma membrane intrinsic (PIP) and the tonoplast intrinsic protein (TIP) subfamilies, including three PIP2s, two PIP1s, and one TIP1 (Supplementary Table 4.1). The aquaporin genes identified from the three plant species were systematically named according to their phylogenetic relationship with the documented aquaporins in *Hordeum vulgare, Zea mays, Oryza sativa* and *Sorghum bicolor* (Fig.41). They included *PnuPIP1;1*, *PjPIP1;1*, *PprPIP1;1*, *PnuPIP1;3*, *PjPIP1;3*, *PprPIP1;3*, *PnuPIP2;1*, *PjPIP2;1*, *PprPIP2;1*, *PnuPIP2;2*, *PjPIP2;2*, *PprPIP2;2*, *PnuPIP2;3*, *PjPIP2;3*, *PprPIP2;3*, *PnuTIP1;1*, *PjTIP1;1*, and *PprTIP1;1*.

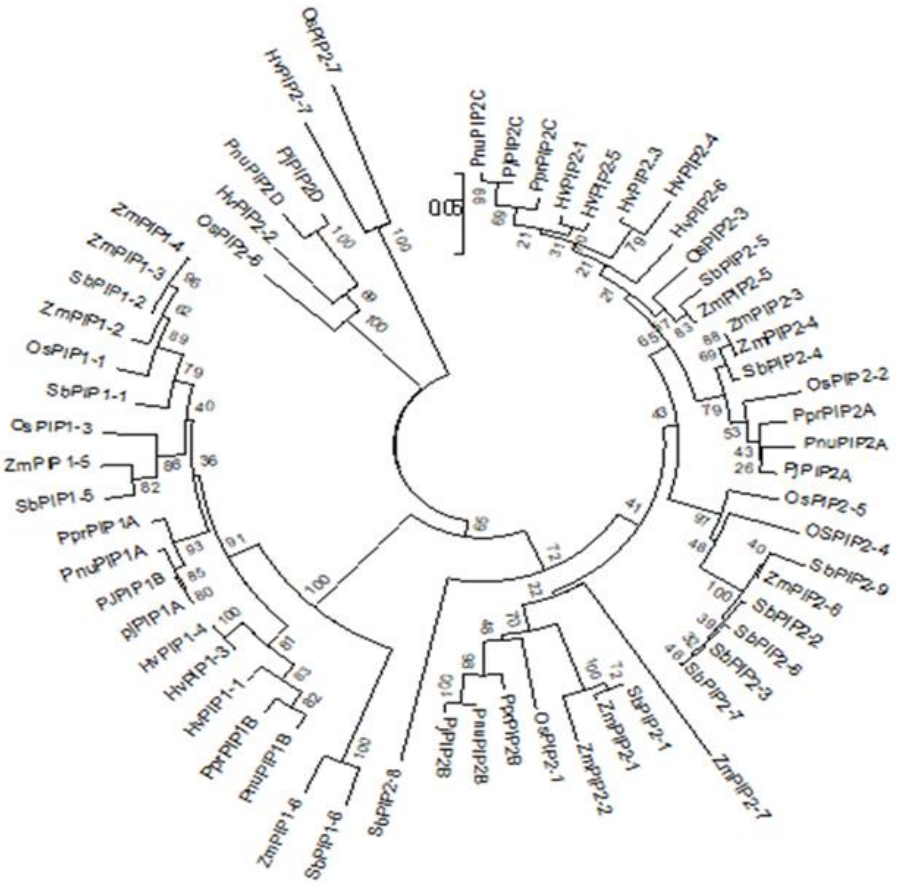

Fig. 4.1. Deduced amino acid sequences of *Poa pratensis (*Ppr*)*, *Poa juncifolia* (Pj) and *Puccinellia nuttalliana (*Pnu*)* PIPs aligned with the amino acid sequences of PIPs from *Hordeum vulgare* (Hv), *Zea mays* (Zm), *Oryza sativa* (Os) and *Sorghum bicolor* (Sb). The unrooted tree was generated with MEGA7.0 (Kumar et al., 2016) using the Neighbor Joining method (Saitou et al., 1987). Bootstrap analysis with 1000 replications was used to assess the strength of the nodes in the tree. The optimal tree with the sum of branch length of 2.99 is shown.

4.3.2 Effects of NaCl treatment on transcript abundance of *PIP* and *TIP* aquaporins

The transcript levels of *PIP2;1*, *PIP2;2*, *PIP2;3*, *PIP1;1*, *PIP1;3*, and *TIP1;1* aquaporins from the control *P. pratensis*, *P. juncifolia*, and *P. nuttalliana*, and from plants subjected to 6 days of 150 mM NaCl were determined using real-time qRT-PCR (Fig. 4.2). Changes in aquaporin expression in NaCl-treated plants showed a similar pattern in *P. juncifolia* and *P. nuttalliana* and was different from *P. pratensis*. The transcript levels of *PIP2;2* significantly increased in *P.*

nuttalliana and *P. juncifolia*, whereas it significantly decreased in *P. pratensis* in response to NaCl (Fig. 4.2). The NaCl treatment did not affect *PIP2;1* and *PIP1;1* transcript levels in the three studied plant species while it increased the transcript level of *PIP1;3* in *P. nuttalliana* (Fig. 4.2). The *TIP1;1* transcript abundance increased in *P. pratensis*, decreased in *P, nuttalliana*, and was not changed by NaCl in *P. juncifolia* (Fig. 4.2).

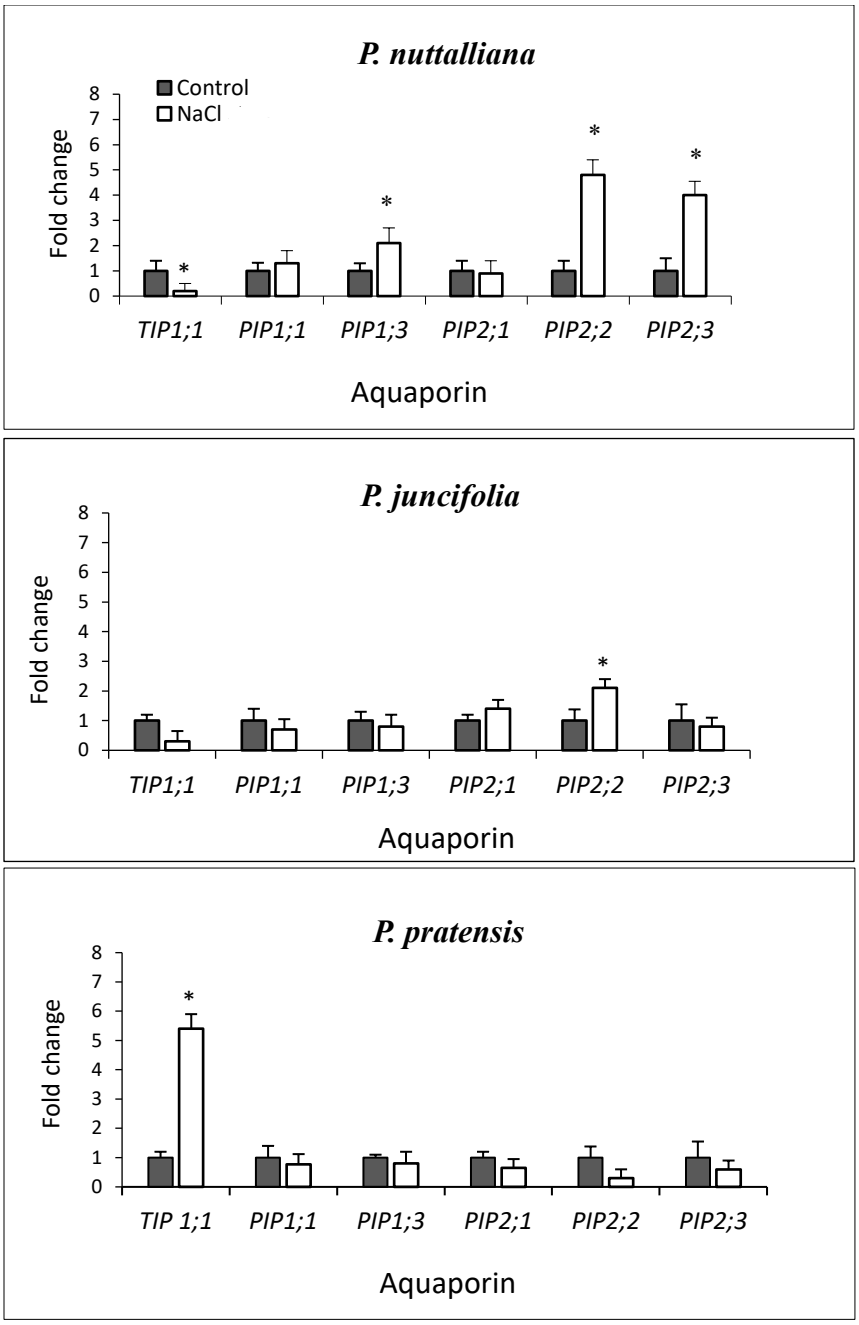

Fig. 4.2. Relative transcrtipt abundance of *PIP2;1, PIP2;2, PIP2;3 , PIP1;1, PIP1;3,* and *TIP1;1* from *Puccinellia nuttalliana* (A), *Poa juncifolia* (B), and *Poa pratensis* (C) in plants subjected for 6 days to 150 mM NaCl. The values are fold change from the means calculated for control plants (0 mM NaCl). Means (n = 4) + SE are shown. Asterisks indicate significant differences from control ($p \leq 0.05$) as determined by ANOVA, Tukey's test.

4.3.3 Structural analysis

The deduced amino acid sequences of *PIP2;1*, *PIP2;2*; *PIP2;3*, and *PIP1:1* from all three species confirmed them as the Ala-rich proteins and PIP1;3 as the Gly-rich proteins with 286-290 amino acid residues. Their estimated molecular mass is about 30 kDa and the isoelectric point ranges from 6.95 to 9.00 (Supplementary Table 4.1). Sequence analysis of the cloned aquaporins indicated that they all contain six α helices (H1-H6), two half helices (HB and HE), and five loops (LE1-LE5). All PIPs contain dual asparagine-proline-alanine (NPA) motifs and an ar/R region with phenylalanine at H2, histidine at H5, threonine, and arginine at LE position (Supplementary Fig. 4.1). The ar/R filter of *PnuPIP2;2*, *PjPIP2;2* and *PprPIP2;2* is comprised of phenylalanine, histidine, threonine, and arginine (Table 4.1). Froger's positions (P1-P5) in the PIPs are highly conserved with glutamine-serine-alanine-phenylalanine-tryptophane except in PIP1;3, which contains methionine-serine-alanine-phenylalanine-tryptophane and glycine-serine-alanine-phenylalanine-tryptophane, respectively (Supplementary Fig. 4.1). The conserved amino acid residues that were predicted to be involved in water channel regulation in PIPs are shown in Fig. 4.3. A conserved glutamic acid residue is located in PIP2s at Glu31 except for PIP2;3 at Glu32 and in PIP1;1 and PIP1;3 it is at Glu47 and Glu46, respectively (corresponds to Glu31 in SoPIP2;1; Glu34 in ZmPIP2:1 and Glu33 in McPIP2;1). In loop B, a conserved serine residue is located at Ser123 in PIP2;1 and PIP2;3, at Ser124 in PIP2;2, at Ser130 in PIP1;1, and at Ser133 in PIP1;3 (corresponds to Ser115 in SoPIP2;1, Ser126 in *ZmPIP2;1*, and Ser123 in McPIP2;1). A conserved histidine residue in loop D is located at His201 in *PIP2*s and at His208, His211 in *PIP1;1*, and *PIP1;3*, respectively (corresponds to His193 in *SoPIP2;1*, His204 in ZmPIP2;1, and His201 in *McPIP2;1*) (Fig. 4.3).

Table 4.1. Pore properties of PIP2;2 from *Puccinellia nuttalliana* (Pnu) *Poa juncifolia* (Pj) and *Poa pratensis* (Ppr). Shape string denotes pore shape identified by PoreWalker from the lowest to the highest coordinate along the pore axis. D = Decreasing diameter conical frustum. U = Increasing diameter conical frustum S = Cylinder. Commonly recognized shapes: DU = Hourglass; UD = Diamond; UDU/UDU = Hourglass-Diamond-Complex. The ar/R-region visualization and pore properties were calculated using the Mole 2.5 server (Pravda et al., 2018). The channel radii of PnuPIP2;2, PjPIP2;2 and PprPIP2;2 are shown in purple spheres

Aquaporin	**Shape String**	**Bottleneck**	**Hydropathy**	**Polarity**	ar/R-region
PnuPIP2;2	DUSU	0.7	-0.22	9.23	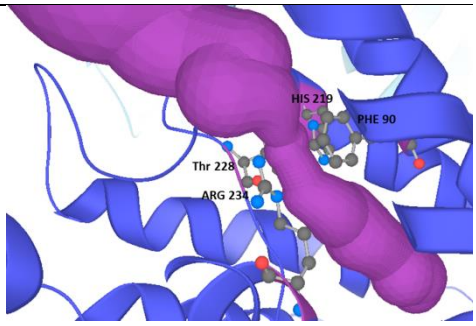
PjPIP2;2	DUDU	1.0	0.3	12.19	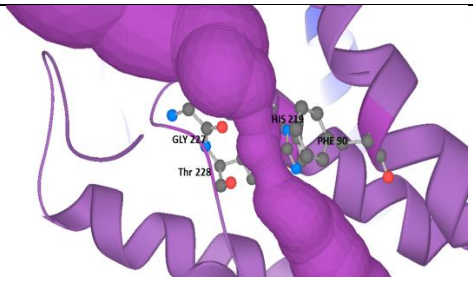
PprPIP2;2	DU	0.9	0.04	14.75	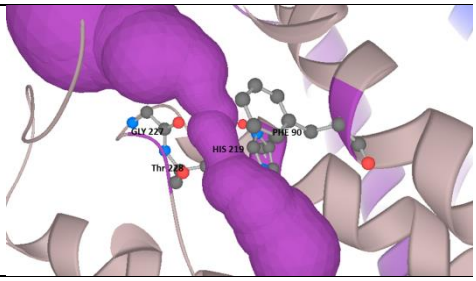

Froger's positions (P1-P5) in the PIPs are highly conserved with glutamine-serine-alanine-phenylalanine-tryptophane except in PIP1;3, which contains methionine-serine-alanine-phenylalanine-tryptophane and glycine-serine-alanine-phenylalanine-tryptophane, respectively (Supplementary Fig. 4.1). The conserved amino acid residues that were predicted to be involved

in water channel regulation in PIPs are shown in Fig. 4.3. A conserved glutamic acid residue is located in PIP2s at Glu31 except for PIP2;3 at Glu32 and in PIP1;1 and PIP1;3 it is at Glu47 and Glu46, respectively (corresponds to Glu31 in SoPIP2;1; Glu34 in ZmPIP2:1 and Glu33 in McPIP2;1). In loop B, a conserved serine residue is located at Ser123 in PIP2;1 and PIP2;3, at Ser124 in PIP2;2, at Ser130 in PIP1;1, and at Ser133 in PIP1;3 (corresponds to Ser115 in SoPIP2;1, Ser126 in ZmPIP2;1, and Ser123 in McPIP2;1). A conserved histidine residue in loop D is located at His201 in PIP2s and at His208, His211 in PIP1;1, and PIP1;3, respectively (corresponds to His193 in SoPIP2;1, His204 in ZmPIP2;1, and His201 in McPIP2;1) (Fig. 4.3).

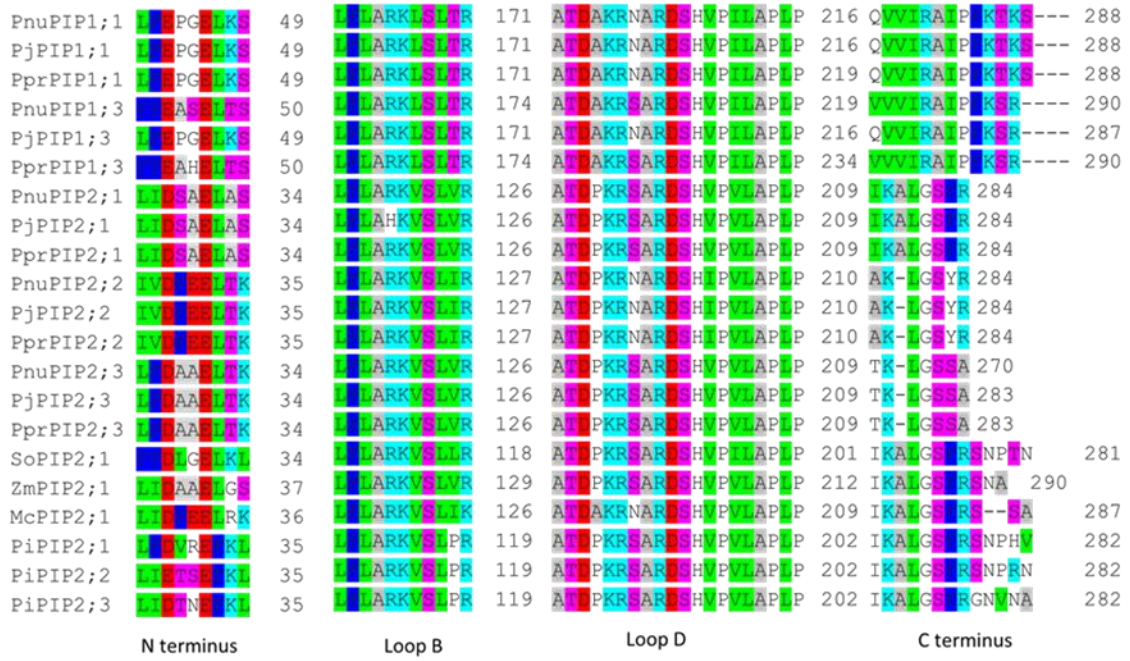

Fig. 4.3. Amino acid sequence comparisons of PIP2s and PIP1s from *Puccinellia nuttalliana* (Pnu), *Poa juncifolia* (Pj), and *Poa pratensis* (Ppr), *Spinacia oleracea* (So), *Zea mays* (Zm), *Mesembryanthemum crystallinum* (Mc), and *Pinus contorta* (Picon). The alignment of loops B and D (with six amino acid residues from helix 5) together with parts of the N- and C-terminal regions are shown. Amino acid residues are colored according to their side-chain: large aliphatic (green), small aliphatic (gray), basic (blue), acidic (red), hydroxyl non-aromatic (purple), and aromatic (royal). Amino acid residues involved in the anchoring of loop D to loop B and the N-terminus are evinced. Sequence alignment was done using MUSCLE (https://www.ebi.ac.uk/Tools/msa/muscle/).

The three-dimensional structure of the pore cavity of the cloned aquaporins showed the predicted pore diameters at 3A steps (Supplementary Fig. 4.3). Polarity, hydrophobicity and hydropathy across the pore of *PnuPIP2;2*, *PjPIP2;2* and *PprPIP2;2* revealed substantial differences between the three plant species with the hydropathy index of -0.22, 0.3 and 0.04, respectively (Table 4.1). The pore of *PrPIP2;2* has a DU-like string shape which represents an hourglass typical for most aquaporins, the pore shape of *PjPIP2;2* consists of two stacked hourglasses, and PnuPIP2;2 pore tructure is highly complex with an hourglass followed by a cylinder and increasing diameter conical frustrum (Table 4.1 and Supplementary Fig. 4.3). The amino acid residues Gly45, Thr263, Met267 and Asp166 possibly contributed to DUSU pore formation in PnuPIP2;2 because these four amino acids were different from PjPIP2;2 and PprPIP2;2 (Supplementary Fig. 4.1).

4.3.4 Water permeability of *Puccinellia nuttalliana aquaporin*s expressed in yeast

Transmembrane water flux resulted in volume changes of yeast protoplasts that were measured by 90° light scattering at 436 nm with the stopped-flow spectrophotometer. Kinetics of H_2O import into yeast protoplasts expressing PnuPIP2;2 and PnuPIP2;1 were significantly higher compared with the protoplasts expressing PnuTIP1;1, PnuPIP2;3, PnuPIP1;1 and compared to control (Fig. 4.4A). Water transport in yeast protoplasts transformed with PnuPIP1;3 was not significantly altered upon exposure to osmotic gradient of 300 mosmol (Fig. 4.4A). To verify the production and localization of *P. nuttalliana* aquaporins in the yeast cells, the localization of heterologously expressed EYFP-tagged *aquaporin* was determined by visualizing EYFP fluorescence in whole cells. The clear GFP signal was detected in the plasma membrane (Supplementary Fig. 4.2).

4.3.5 Effect of NaCl on water permeability of yeast protoplasts expressing PnuPIP2;2 and PnuPIP2;1

The effect of 100 mM NaCl on water transport was investigated in yeast protoplasts expressing PnuPIP2;1 and PnuPIP2;2 since these aquaporins transported water at high rates in the absence of NaCl (Fig. 4.4A). The NaCl solution was added to the yeast protoplasts five minutes before the water transport assay. The 100 mM NaCl treatment resulted in a 56% increase in the water transport rate in the protoplasts expressing PnuPIP2;2 compared to the 0 mM treatment (Fig. 4.4B,C). No difference in water transport rate was observed in the protoplasts expressing PnuPIP2;1 between 0 mM NaCl and 100 mM NaCl treatments (Fig. 4.4B,D).

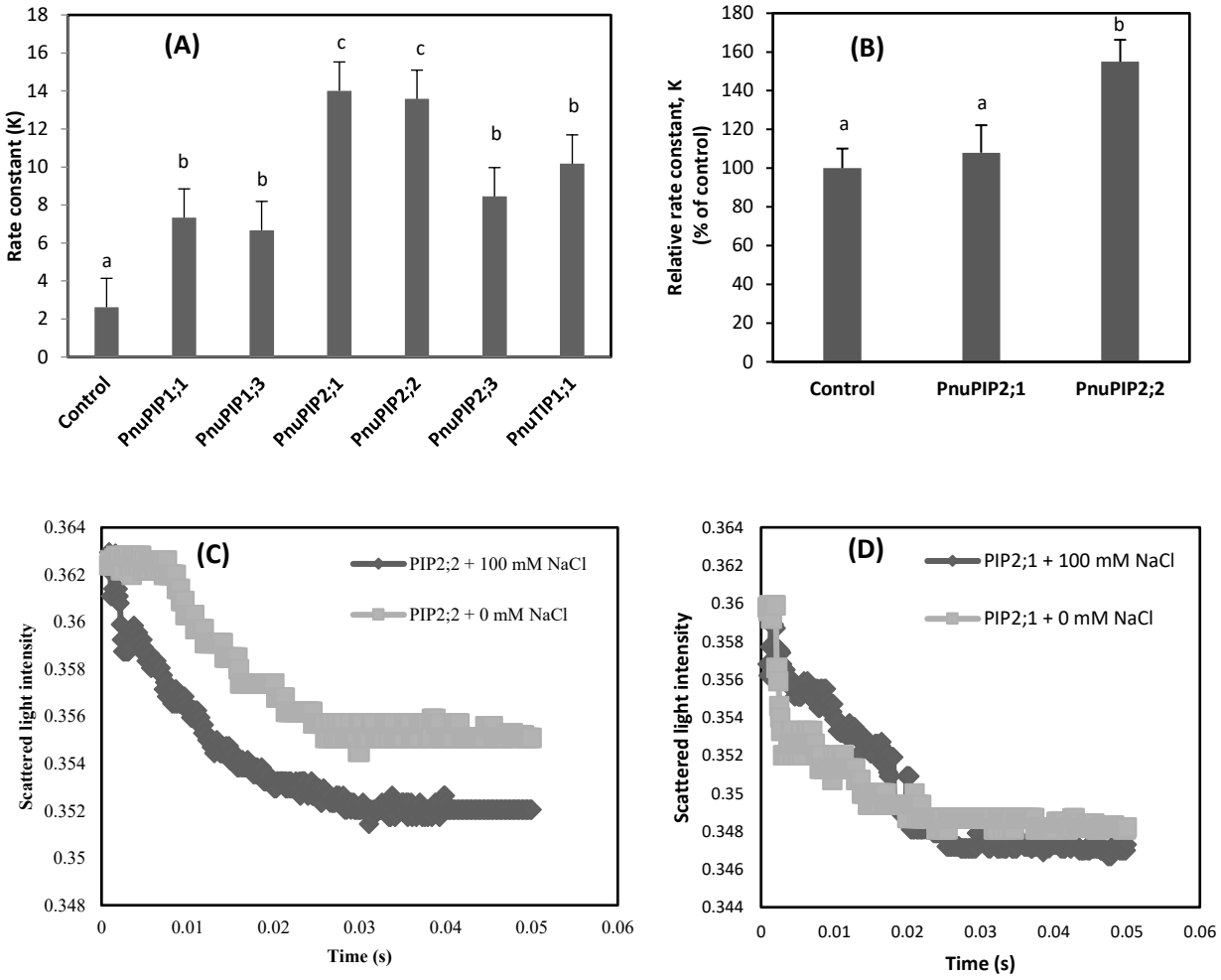

Fig. 4.4. Stopped-flow light scattering measurements of water transport activity of PnuPIP2;2 in yeast cells under osmotic stress. The water transport rate of *Saccharomyces cerevisiae* protoplasts expressing PnuPIP2;1, PnuPIP2;2, PnuPIP2;3, PnuPIP1;1, PnuPIP1;3, and PnuTIP1;1 and an empty plasmid vector as a control (A). The relative water transport rate of *Saccharomyces cerevisiae* protoplasts expressing PnuPIP2;1 and PnuPIP2;2 from *Puccinellia nuttalliana* incubated in 0 and 100 mM NaCl for 5 min prior to water transport assay (B). The water transport assay was performed by stopped-flow spectroscopy with an external osmotic gradient of 300 mosmol and the intensity of scattered light was measured at 436 nm wavelength. For each experiment, at least six traces were used. Each trace was fitted to exponential decay function (f=Y0+a*exp(-b*x)) using SigmaPlot 11 software. The reported rate constants are an average of six independent measurements of each of the four biological replicates. A higher rate constant represents faster transport of water. Changes in light scattering at 436 nm over time plotted for *Saccharomyces cerevisiae* spheroplasts expressing PnuPIP2;2 (C) and PnuPIP2;1 (D) incubated in 0 and 100 mM NaCl for 5 min before being exposed to the external osmotic gradient. Means (n = 4 - 5) + SE are shown. Different letters indicate significant differences ($P \leq 0,05$) determined by Duncan's Multiple Range Test.

4.3.6 Ion transport by yeast transformed with PnuPIP2;2

The concentrations of Na^+, K^+, and P in yeast transformed with PnuPIP2;2 were compared with the cells containing an empty vector (control) following 24 h incubation with 300 mM and 600 mM NaCl.

Compared to control cells, the cells transformed with PnuPIP2;2 had approximately 100% and 50% higher Na^+ concentrations in 300 and 600 mM NaCl treatments respectively (Fig. 4.5A). A small difference in K^+ concentration between control (empty vector) and PnuPIP2;2-transformed cells was not significant (Fig. 4.5B). No significant difference was observed in the K^+/Na^+ ratio between yeast cells expressing PnuPIP2;2 and an empty vector in control and NaCl-treated cells (Fig. 4.5C). Yeast cells expressing PnuPIP2;2 accumulated more P compared with the cells expressing an empty vector (Fig. 4.5D). Phosphorus concentration was significantly lower in cells expressing an empty vector that were subjected to 300 mM and 600 mM NaCl treatments compared to 0 mM NaCl, whereas no significant differences in P concentrations were observed in yeast cells expressing PnuPIP2;2 between 0 and 300 mM NaCl treatments (Fig. 4.5D).

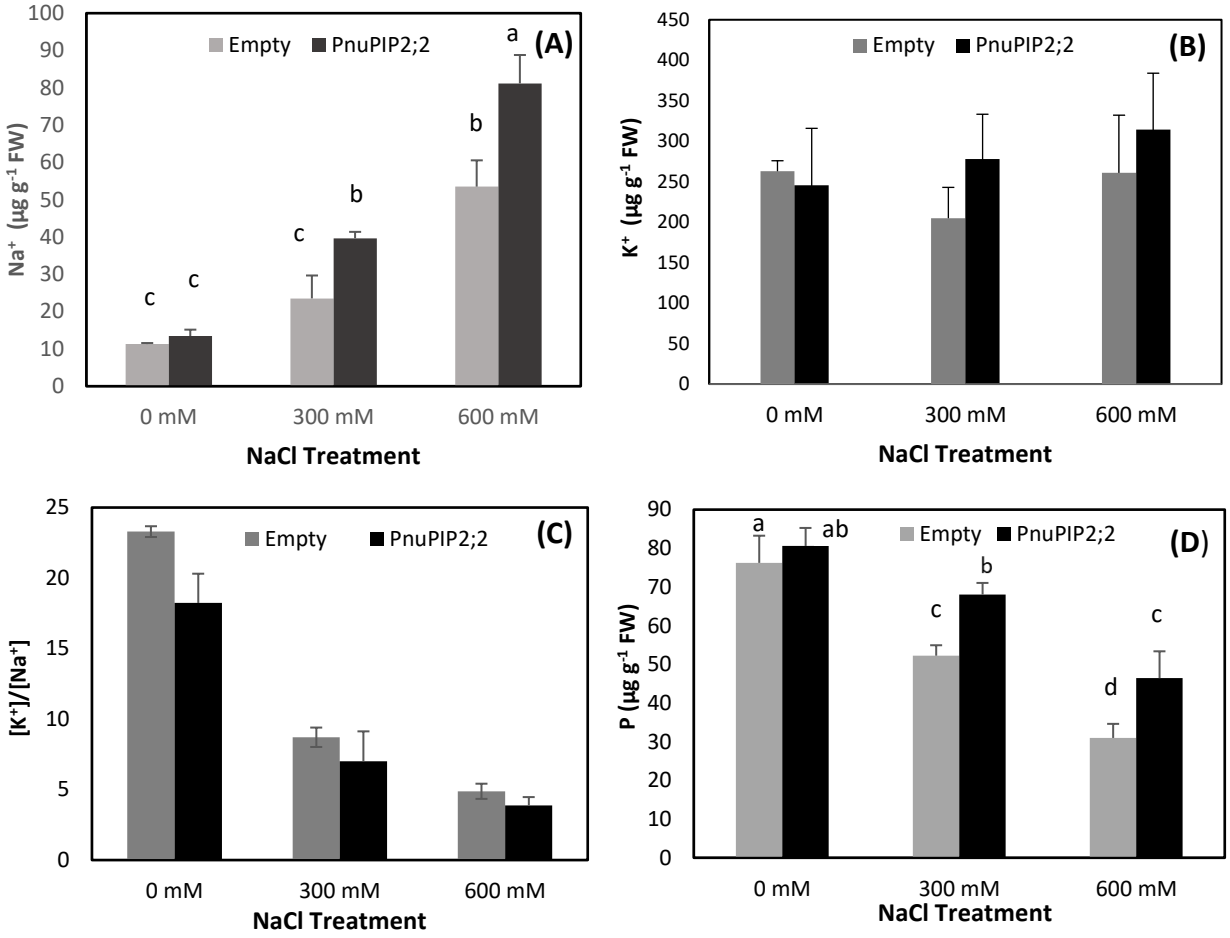

Fig. 4.5. Na^+ (A) and K^+ (B) concentrations, K^+/Na^+ ratios (C), and P concentrations (D) in *Saccharomyces cerevisiae* transformed with *PnuPIP2;2* and in control cells (empty vector) after 24 h incubation with 0, 300, and 600 mM NaCl. Bars are means (n = 4) + SE. Different letters above the bars indicate statistically significant difference ($P \leq 0.05$) determined by Duncan's Multiple Range Test.

4.4 Discussion

4.4.1 NaCl upregulates *PIP2;2* and downregulates *TIP1;1* transcript in *P. nuttalliana*

In the present study, *PIP2;2* transcripts were upregulated in both salt tolerant plant species with the highest levels measured in *P. nuttalliana*. Contrary to *PIP2;2*, *TIP1;1* was downregulated in the salt tolerant plants, especially in *P. nuttalliana*, and upregulated in the relatively salt sensitive *P. pratensis*. In the studied species of glycophytes, including salt

sensitive plants of cucumber (*Cucumis sativa*) and Arabidopsis, *PIP* and *TIP* levels were downregulated by NaCl, which was accompanied by an inhibition of root water fluxes (Boursiac et al. 2005, Lee and Zwiazek 2015, Zhu et al. 2019). However, L_{pc} in roots of Arabidopsis plants overexpressing *AtPIP2;5* was unaffected by the NaCl treatments, which caused several-fold L_{pc} reductions in the wild-type plants (Lee and Zwiazek 2015). The increased expression of *PIP2;2* in *P. nuttalliana* and *P. juncifolia* is likely linked to the enhanced water transport by NaCl (Vaziriyeganeh et al. 2018, 2022). The increase in *PIP2;2* transcript levels in NaCl-treated *P. nuttalliana* was also earlier confirmed by transcriptome analysis (Vaziriyeganeh et al. 2021). Similarly, a higher constitutive expression level of a related gene *PIP2;1* was found in the salt-tolerant species *Solanum pennellii* subjected to salt stress (Albaladejo et al. 2017).

Increased transcript levels of *PnuPIP2;2* combined with earlier reported upregulation of *HKT1;5* by NaCl (Vaziriyeganeh et al. 2021) could indicate a coordinated cation and water transport to maintain homeostatic control of water and ion balance under salt stress, especially that some of the aquaporins may also be involved in ion transport (Qui et al. 2020, Tyerman et al. 2021). Although the NaCl treatment also induced gene expression of *PIP1;3* and *PIP2;3* in *P. nuttalliana*, it only induced the expression of *PIP2;2* in the two salt tolerant grass species. Therefore, I focused mainly on PIP2;2 in the present study. *PIP2;3* was found to be upregulated under salt stress in rice and improved water deficit resistance in *PIP2;3* overexpression plants but did not affect salt tolerance (Sun et al. 2021). *PIP1;3* has been suggested to function as a water and anion channel (Tyerman et al. 2021) and was reported to transport NO_3^- in rice (Liu et al. 2020) as well as oxygen in tobacco (Zwiazek et al. 2017). The PIP1 and PIP2 heterotetramerization increases the water permeability (Bienert et al. 2018), therefore, it is also

possible that the co-expression of *PIP2;2* and *PIP1;3* in *P. nuttalliana* farther increased the membrane water permeability under salt stress.

Interestingly, contrary to the relatively salt sensitive *P. pratensis* in which *TIP1;1* was upregulated by the NaCl treatment, *TIP1;1* expression was downregulated by NaCl in *P. nuttalliana*. Compared to PIPs, relatively little is known and understood about the responses of TIPs to salinity, which could likely vary between plants depending on their salt tolerance strategy. A decrease in root *TIP*s (MIP-F) in response to NaCl was also reported for the halophytic plant *Mesembryanthemum crystallinum* (Kirch et al. 2000), which largely relies for its salt tolerance strategy on salt deposition in the epidermal bladder cells of the aerial parts of the plant (Agarie et al., 2007). Similarly to *Mesembryanthemum crystallinum*, salt is transported to leaves in *P. nuttalliana* and subsequently secreted (Vaziriyeganeh et al. 2021). The downregulation of *TIP*s by NaCl in salt tolerant plants could potentially alter the paths of water movement by affecting the water fluxes across the tonoplast (Kirch et al. 2000). The responses of *PnuTIP1;1* indicate its possible important role in maintaining water status under salt stress and warrant further attention.

4.4.2 Water permeability of PnuPIP2;2 is enhanced by Na^+

My results showed that water flux kinetics were similar for PnuPIP2;2 and PnuPIP2;1 in the absence of NaCl. However, in the presence of 100 mM NaCl, the rate constant (K) was increased by about 60% in yeast protoplasts expressing PnuPIP2;2 but not PnuPIP2;1, which can explain the earlier reported stimulating effect of NaCl on root water fluxes in *P. nuttalliana* (Vaziriyeganeh et al. 2018, 2022). Aquaporin gating can be enhanced by the divalent cations such as Cd^{2+} and Ca^{2+} (Tornroth-Horsefield et al. 2006). However, to the best of my knowledge, there are no earlier reports pointing to a possible modulation of aquaporin pore structure by Na^+

or other monovalent cations that could be responsible for the enhancement of transmembrane water fluxes.

4.4.3 Pore morphology revealed substantial differences in PnuPIP2;2 pore shape compared to PjPIP2;2 and PprPIP2;2

To assess a possibility that unique structural properties of PnuPIP2;2 could contribute to its different responses to NaCl compared with other aquaporins, I examined the three-dimensional pore structures of PIP2;2s and other aquaporins from the three grasses varying in salt tolerance using PoreWalker software (Pellegrini-Calace et al. 2009). PnuPIP2;2 constituted the DUSU pores, whereas PjPIP2;2 and PprPIP2;2 formed DU and DUDU pores, respectively. The differences in regional constriction and dilatation of pores could affect water and cation flows. In the absence of the crystal structure of PnuPIP2;2, it can only be speculated that DUSU pore shape contributed to Na^+ efflux in *P. nuttalliana*, as evident by the significant increase in Na^+ uptake of yeast cells overexpressing *PnuPIP2;2* compared with yeast cells expressing an empty vector. Moreover, ar/R filter residues, bottleneck, hydropathy, and polarity of the pores were different between PnuPIP2;2, PjPIP2;2, and PprPIP2;2. PnuPIP2;2 is more hydrophilic compared with PjPIP2;2 and PprPIP2;2. Although the functional implications of the shapes are unclear, it was identified that conical entrances with a suitable opening could result in a large increase in the channel permeability (Gravelle et al. 2013). Also, the variations in polarity and hydrophobicity of pore-forming amino acids of the aquaporins signify their functional variations under salt stress. Conserved amino acids present at ar/R, NPA domains, and Forger's residues are used to predict the solute specificity of the aquaporins. The ar/R region of all PIPs showed very high similarity to other plant species, including lodgepole pine (*Pinus contorta*) and flax (*Linum usitatissimum*) (Shivaraj et al. 2017, Khan et al. 2019). The ar/R filter consisting of

phenylalanine at H2, histidine at H5, and threonine and arginine at loop LE facilitates the selective flux of water (Amezcua-Romero et al. 2010). In lodgepole pine, PIP aquaporins containing hydrophilic aromatic/arginine selective filters were proposed to enhance drought resistance by facilitating water transport under drought stress conditions (Khan et al. 2019).

A previous study reported that phosphorylation of serine residues within the C-terminal domain is associated with water and cation transport of AtPIP2;1 (Qiu et al. 2020). The structural analysis located the conserved Ser283 but not Ser280 in PnuPIP2;2 corresponding to Ser280 and Ser283 in AtPIP2;1. Arabidopsis PIP2,2 also has conserved serine residues corresponding to Ser280 and Ser283 in AtPIP2;1 that facilitate water, but not ion, transport (Byrt et al., 2017). Conserved serine residues are also present in PIP2;1, PIP2;2 and PIP2;3 in *P. nuttalliana, P. juncifolia and P. pratensis*. This indicates that other regulatory mechanisms may play the roles that are yet to be revealed including protein networking responsible for the trafficking of PIP2;2 and gating of ion channels under salt stress. The pore shape variations found in the present study may also contribute to the reported differences in water transport properties of the three grass species in response to NaCl. Aquaporin functions have been often predicted by comparing structural details of the model aquaporin such as SoPIP2;2 from spinach, although this approach has also been criticized as prone to errors (Kitchen et al. 2019). It is crucial to find the location of specific residues in the selectivity filter, and the pore size determined by their interactions affects solute exclusion and specificity (Kitchen et al. 2019). For instance, a precise distance of 108 amino acids (AA) between NPA motifs is essential for silicon transport (Deshmukh et al. 2015). Aquaporin pore regulates the selective transport of water and solutes determined by the pore-lining amino acids and constriction.

4.4.4 PnuPIP2;2 increased accumulation of Na^+ in yeast

Saccharomyces cerevisiae cells expressing PnuPIP2;2 accumulated significantly more Na^+ compared with the yeast cells containing an empty vector after the 24 h incubation in the growth media containing 0.3 M and 0.6 M NaCl. This finding supports our hypothesis that PnuPIP2;2 may have both water and Na^+ transporting functions (Vaziriyeganeh et al. 2021). The aromatic/arginine (ar/R) selectivity filter is predicted to control solute permeability through the aquaporin pore, but a recent study found that these properties depend on complex interactions between the solute, pore size, and polarity (Kitchen et al. 2019). It is possible that PnuPIP2;2 may also transport K^+ because the majority of K^+ transporters in plants are also permeable to Na^+ (Locascio et al. 2019). In addition to the enhanced aquaporin-mediated root water transport and increased gene expression of some of the water-transporting aquaporins by NaCl, *P. nuttalliana* maintained high K^+/Na^+ ratios under salinity conditions and this was accompanied by an upregulation of *PnuHKT1;5*. (Vaziriyeganeh et al. 2018, 2021, 2022). The subclass 1 of the HKT family has been implicated in Na^+ transport (Kronzucker and Britto 2011, Ali et al. 2016, Ali et al. 2019) and HKT1;5 was shown to be involved in reducing Na^+ transport to leaves in grass species by withdrawing it from the root xylem (Byrt et al. 2007, Munns et al. 2012, Kobyashi et al. 2017, Hazzouri et al. 2018). On the other hand, knockdown of *HvHKT1;5* in barley plants, led to lower Na^+ translocation from roots to shoots (Huang et al. 2020) suggesting that HKT1;5 could be involved in either Na^+ unloading or loading into the xylem depending on the salt tolerance strategy of plants. In either case, Na^+ transport into or out of the root xylem would have a major impact on the osmotic gradient with the consequence on water fluxes. Therefore, it would be logical to expect that both Na^+ and water transporters may be simultaneously involved

in the ion and water fluxes in roots. *P. nuttalliana* requires salt for optimum growth and development (Chapman 1974, Ungar 1974).

Since, as discussed above, the excess of Na^+ is transferred by *P. nuttalliana* to leaves and secreted by salt glands (Vaziriyeganeh et al. 2021), similarly to other halophytes (Rahman et al. 2021, Palchetti et al. 2021), salt uptake restriction by roots is not among the key salt tolerance mechanisms in these plants. Therefore, PnuPIP2;2 could be helpful with Na^+ transport to leaves from which it can be secreted. Given that NaCl does not inhibit water transport through PnuPIP2;2, it is also logical that this aquaporin could also function as a non-selective cation channel (NSCC) similarly to an Arabidopsis aquaporin, AtPIP2;1 (Byrt et al. 2017, Qiu et al. 2020). The *PIP2;2* orthologous to *PnuPIP2;2* was not induced by NaCl in *Poa pratensis*, which could prevent an influx of Na^+, a salt tolerance strategy used by many glycophytes (Horie et al. 2012, Assaha et al. 2017). However, it remains to be determined whether PIP2;2 may also be involved in Na^+ transport in *P. pratensis* and *P. juncifolia*.

4.4.5 Phosphorus supply is conserved in yeast cells expressing PnuPIP2;2

Interestingly, yeast cells expressing PnuPIP2;2 maintained higher P concentrations when exposed to 300 and 600 mM NaCl compared with the yeast cells expressing an empty vector, suggesting a possible link to the PnuPIP2;2 function. Phosphorus facilitates root water uptake by modifying aquaporin expression and activity (Wang et al. 2016) since gating properties of many aquaporins are regulated by phosphorylation and dephosophorylation (Nesverova and Törnroth-Horsefield 2019, Qiu et al. 2020). Phosphorylation also influences PIP protein trafficking and localization as well as water and ion channel transport (McGaughey et al. 2018, Qiu et al. 2020), which is an important stress resistance mechanism.

4.4.6 Conclusions

In conclusion, the study demonstrated that the earlier reported increase of cell hydraulic conductivity in the roots of halophytic grass *Puccinellia nuttalliana* by NaCl can be explained by the upregulation of *PnuPIP*s with water transporting properties enhanced by NaCl when expressed in yeast. Furthermore, PnuPIP2;2 may likely function as a transporter of Na^+ and, possibly, other ions. PnuPIP2;2 has unique characteristics, including a pore that is comprised of a combination of hourglass, cylinder, and conical shapes and may offer important clues in understanding its water and ion permeability in the presence of NaCl. I suggest that maintaining the functionality of aquaporins is among the key elements of salt tolerance in halophytic plants.

4.5 References

Afzal, Z., Howton, T., Sun, Y. and Mukhtar, M. 2016. The roles of aquaporins in plant stress responses. Journal of Developmental Biology 4: 9.

Agarie, S., Shimoda, T., Shimizu, Y., Baumann, K., Sunagawa, H., Kondo, A., Ueno, O., Nakahara, T., Nose, A. and Cushman, J.C. 2007. Salt tolerance, salt accumulation, and ionic homeostasis in an epidermal bladder-cell-less mutant of the common ice plant *Mesembryanthemum crystallinum*. Journal of Experimental Botany 588: 1957-1967.

Alavilli, H., Awasthi, J.P., Rout, G.R., Sahoo, L., Lee, B.-Ha and Panda, S.K. 2016. Overexpression of a barley aquaporin gene, *HVPIP2;5* confers salt and osmotic stress tolerance in yeast and plants. Frontiers in Plant Science 7: 1566.

Albaladejo, I., Meco, V., Plasencia, F., Flores, F.B., Bolarin, M.C. and Egea, I. 2017. Unravelling the strategies used by the wild tomato species *Solanum pennellii* to confront

salt stress: From leaf anatomical adaptations to molecular responses. Environmental and Experimental Botany 135: 1-12.

Ali, A., Maggio, A., Bressan, R.A. and Yun, D.J. 2019. Role and functional differences of HKT1-type transporters in plants under salt stress. International Journal of Molecular Sciences 20: 1059.

Ali, A., Raddatz, N., Aman, R., Kim, S., Park, H.C., Jan, M., Baek, D., Khan, I.U., Oh, D.H., Lee, S.Y., Bressan, R.A., Lee, K.W., Maggio, A., Pardo, J.M., Bohnert, H.J. and Yun, D.J. 2016. A single amino-acid substitution in the sodium transporter *HKT1* is associated with plant salt tolerance. Plant Physiology 171: 2112-2126.

Amezcua-Romero, J.C., Pantoja, O. and Vera-Estrella, R. 2010. Ser123 is essential for the water channel activity of MCPIP2;1 from *Mesembryanthemum crystallinum*. Journal of Biological Chemistry 285: 16739-16747.

Apse, M.P., Blumwald, E. 2007. Na^+ transport in plants. FEBS Letters 581: 2247-2254

Assaha, D., Ueda, A., Saneoka, H., Al-Yahyai, R. and Yaish, M.W. 2017. The role of Na^+ and K^+ transporters in salt stress adaptation in glycophytes. Frontiers in Physiology 8: 509.

Bertl, A. and Kaldenhoff, R. Function of a separate NH3-pore in aquaporin TIP2;2 from wheat. FEBS Letters 581: 5413-5417.

Biasini, M., Bienert, S., Waterhouse, A., Arnold, K., Studer, G., Schmidt, T., Kiefer, F., Cassarino, T.G., Bertoni, M., Bordoli, L. and Schwede, T. 2014. Swiss-model: modelling protein tertiary and quaternary structure using evolutionary information. Nucleic Acids Research 42 (W1).

Bienert, M.D., Diehn, T.A., Richet, N., Chaumont, F. and Bienert, G.P. 2018. Heterotetramerization of plant PIP1 and PIP2 aquaporins is an evolutionary ancient feature to guide PIP1 plasma membrane localization and function. Frontiers in Plant Science: 9: 382.

Boursiac, Y., Chen, S., Luu, D.-T., Sorieul, M., van den Dries, N. and Maurel, C. 2005. Early effects of salinity on water transport in Arabidopsis roots. molecular and cellular features of aquaporin expression. Plant Physiology 139: 790-805.

Byrt, C.S., Platten, J.D., Spielmeyer, W., James, R.A., Lagudah, E.S., Dennis, E.S., Tester, M. and Munns, R. 2007. HKT1;5-like cation transporters linked to Na^+ exclusion loci in wheat, Nax2 and Kna1. Plant Physiology 143: 1918-1928.

Byrt, C. S., Zhao, M., Kourghi, M., Bose, J., Henderson, S.W., Qiu, J., Gilliham, M., Schultz, C., Schwarz, M., Ramesh, S.A., Yool, A. and Tyerman, S. 2017. Non-selective cation channel activity of aquaporin AtPIP2;1 regulated by Ca^{2+} and pH. Plant, Cell & Environment, 40: 802-815.

Chapman, V.J. 1974. Salt marshes and deserts of the world. - In: Ecology of halophytes. Edited by R.J. Reimold and W.H. Queen. Academic Press, New York, pp. 3-19.

Chaumont, F., and Tyerman, S.D. 2014. Aquaporins: highly regulated channels controlling plant water relations. Plant Physiology 164: 1600-1618.

Couthouis, J., Hart, M.P., Shorter, J., DeJesus-Hernandez, M., Erion, R., Oristano, R., Liu, A.X., Ramos, D., Jethava, N., Hosangadi, D., Epstein, J., Chiang, A., Diaz, Z., Nakaya, T., Ibrahim, F., Kim, H.J., Solski, J.A., Williams, K.L., Mojsilovic-Petrovic, J., Ingre, C., et al.

2011. A yeast functional screen predicts new candidate ALS disease genes. Proceedings of the National Academy of Sciences of the United States of America, 108: 20881-20890.

Deshmukh, R.K., Sonah, H. and Bélanger, R.R. 2016. Plant aquaporins: genome-wide identification, transcriptomics, proteomics, and advanced analytical tools. Frontiers in Plant Science 7: 1896.

Deshmukh, R.K., Vivancos, J., Ramakrishnan, G., Guérin, V., Carpentier,G., Sonah, H., Labbé, C., Isenring, P., Belzile, F.J. and Bélanger, R.R. 2015. A precise spacing between the NPA domains of aquaporins is essential for silicon permeability in plants. Plant Journal 83: 489-500.

Epstein, E.X. 1972. Mineral nutrition of plants: principles and perspectives. John Wiley, New York.

Fox, A.R., Maistriaux, L.C. and Chaumont, F. 2017. Toward understanding of the high number of plant aquaporin isoforms and multiple regulation mechanisms. Plant Science 264: 179-187.

Frick, A., Järvå, M., Ekvall, M., Uzdavinys, P., Nyblom, M. and Törnroth-Horsefield, S. 2013. Mercury increases water permeability of a plant aquaporin through a non-cysteine-related mechanism. Biochemistry Journal 15: 491-499.

Gravelle, S., Joly, L., Detcheverry, F., Ybert, C., Cottin-Bizonne, C. and Bocquet, L. 2013. Optimizing water permeability through the hourglass shape of aquaporins. Proceedings of the National Academy of Sciences 110: 16367-16372.

Hanin, M., Ebel, C., Ngom, M., Laplaze, L. and Masmoudi, K. 2016. New insights on plant salt tolerance mechanisms and their potential use for breeding. Frontiers in Plant Science 7: 1787.

Hazzouri, K.M., Khraiwesh, B., Amiri, K., Pauli, D., Blake, T., Shahid, M., Mullath, S.K., Nelson, D., Mansour, A.L., Salehi-Ashtiani, K., Purugganan, M. and Masmoudi, K. 2018. Mapping of HKT1;5 gene in barley using GWAS approach and its implication in salt tolerance mechanism. Frontiers in Plant Science 9: 156.

Hirano, Y., Okimoto, N., Kadohira, I., Suematsu, M., Yasuoka, K. and Yasui, M. 2010. Molecular mechanisms of how mercury inhibits water permeation through Aquaporin-1: understanding by molecular dynamics simulation. Biophysical Journal 98: 1512-1519.

Horie, T., Kaneko, T., Sugimoto, G., Sasano, S., Panda, S.K., Shibasaka, M. and Katsuhara, M. 2011. Mechanisms of water transport mediated by PIP aquaporins and their regulation via phosphorylation events under salinity stress in barley roots. Plant and Cell Physiology: 52: 663-675.

Horie, T., Karahara, I. and Katsuhara, M. 2012. Salinity tolerance mechanisms in glycophytes: an overview with the central focus on rice plants. Rice 5: 11.

Huang, L., Kuang, L., Wu, L., Shen, Q., Han, Y., Jiang, L., Wu, D. and Zhang, G. 2020. The HKT transporter *HvHKT1;5* negatively regulates salt tolerance. Plant Physiology 182: 584-596.

Kapilan, R., Vaziri, M. and Zwiazek, J.J. 2018. Regulation of aquaporins in plants under stress. Biological Research 51: 4.

Khan, S., Thomas, B.R., De la Mata, R., Randall, M.J., Zhang, W-Q. and Zwiazek, J.J. 2019. Variation in aquaporin and physiological responses among *Pinus contorta* families under different moisture conditions. Plants 8: 13.

Kirch, H.H., Vera-Estrella, R., Golldack, D., Quigley, F., Michalowski, C.B., Barkla, B.J. and Bohnert, H.J. 2000. Expression of water channel proteins in *Mesembryanthemum crystallinum*. Plant Physiology 123: 111-124.

Kitchen, P., Salman, M.M., Pickel, S.U., Jennings, J., Törnroth-Horsefield, S., Conner, M.T., Bill, R.M. and Conner, A.C. 2019. Water channel pore size determines exclusion properties but not solute selectivity. Scientific Reports 9: 1-14.

Knipfer, T., Besse, M., Verdeil, J.-L. and Fricke, W. 2011. Aquaporin-facilitated water uptake in barley (*Hordeum vulgare* L.) roots. Journal of Experimental Botany 62: 4115-4126.

Kobayashi, N. I., Yamaji, N., Yamamoto, H., Okubo, K., Ueno, H., Costa, A., Tanoi, K., Matsumura, H., Fujii-Kashino, M., Horiuchi, T., Nayef, M.A., Shabala, S., An, G., Ma, J. F. and Horie, T. 2017. *OsHKT1;5* mediates Na^+ exclusion in the vasculature to protect leaf blades and reproductive tissues from salt toxicity in rice. Plant Journal 91: 657-670.

Korbie, D. J. and Mattick, J.S. 2008. Touchdown PCR for increased specificity and sensitivity in PCR amplification. Nature Protocols 3: 1452-1456.

Kortenoeven, M.L. and Fenton, R.A. 2014. Renal aquaporins and water balance disorders. Biochimica et Biophysica Acta (BBA) - General Subjects 1840: 1533-1549.

Kronzucker, H.J. and Britto, D.T. 2011. Sodium transport in plants: a critical review. New Phytologist 189: 54-81.

Kumar, S., Stecher, G. and Tamura, K. 2016. Mega7: molecular evolutionary genetics analysis version 7.0 for bigger datasets. Molecular Biology and Evolution 33: 1870-1874.

Kumari, A. and Bhatla, S.C. 2021. Regulation of salt-stressed sunflower (*Helianthus annuus*) seedling's water status by the coordinated action of Na^+/K^+ accumulation, nitric oxide, and aquaporin expression. Functional Plant Biology 48: 573. Lee, S.H., Calvo-Polanco, M., Chung G.C. and Zwiazek J.J. 2010. Role of aquaporins in root water transport of ectomycorrhizal jack pine (*Pinus banksiana*) seedlings exposed to NaCl and fluoride. Plant, Cell & Environment 33: 769-780.

Lee, S.H. and Zwiazek, J.J. 2015. Regulation of aquaporin-mediated water transport in Arabidopsis roots exposed to NaCl. Plant and Cell Physiology 56: 750–758.

Lin, R., Zheng, J., Pu, L., Wang, Z., Mei, Q., Zhang, M. and Jian, S. 2021. Genome-wide identification and expression analysis of aquaporin family in *Canavalia rosea* and their roles in the adaptation to saline-alkaline soils and drought stress. BMC Plant Biology 21: 333.

Liu, S., Fukumoto, T., Gena, P., Feng, P., Sun, Q., Li, Q., Matsumoto, T., Kaneko, T., Zhang, H., Zhang, Y., Zhong, S., Zeng, W., Katsuhara, M., Kitagawa, Y., Wang, A., Calamita, G. and Ding, X. 2020. Ectopic expression of a rice plasma membrane intrinsic protein (OsPIP1;3) promotes plant growth and water uptake. Plant Journal 102: 779-796.

Locascio, A., Andrés-Colás, N., Mulet, J. M. and Yenush, L. 2019. *Saccharomyces cerevisiae* as a tool to investigate plant potassium and sodium transporters. International Journal of Molecular Sciences 20: 2133.

Luu, D.T. and Maurel, C. 2013. Aquaporin trafficking in plant cells: An emerging membrane-protein model. Traffic 14: 629-635.

Martínez-Ballesta, M.C., Aparicio, F., Pallas, V., Martínez, V. and Carvajal, M. 2003. Influence of saline stress on root hydraulic conductance and PIP expression in Arabidopsis. Journal of Plant Physiology 160: 689–697.

Martínez-Ballesta, M.C., Cabañero, F., Olmos, E., Periago, P.M., Maurel, C. and Carvajal, M. 2008. Two different effects of calcium on aquaporins in salinity-stressed pepper plants. Planta 228: 15-25.

Maurel, C., Boursiac, Y., Luu, D.-T., Santoni, V., Shahzad, Z. and Verdoucq, L. 2015. Aquaporins in plants. Physiological Reviews 95: 1321-1358.

McGaughey, S.A., Qiu, J., Tyerman, S.D. and Byrt, C.S. 2018. Regulating root aquaporin function in response to changes in salinity. Annual Plant Reviews Online 4: 381-416.

Munns, R. and Tester, M. 2008. Mechanisms of salinity tolerance. Annual Review of Plant Biology 59: 651–681.

Munns, R., James, R.A., Xu, B., Athman, A., Conn, S.J., Jordans, C., Byrt, C.S., Hare, R.A., Tyerman, S.D., Tester, M., Plett, D. and Gilliham, M. 2012. Wheat grain yield on saline soils is improved by an ancestral Na^+ transporter gene. Nature Biotechnology 30: 360-364.

Nesverova, V. and Törnroth-Horsefield, S. 2019. Phosphorylation-dependent regulation of mammalian aquaporins. Cells 8: 82.

Palchetti, M.V., Reginato, M., Llanes, A., Hornbacher, J., Papenbrock, J., Barboza, G.E., Luna, V. and Cantero, J.J. 2021. New insights into the salt tolerance of the extreme halophytic

species *Lycium humile* (Lycieae, Solanaceae). Plant Physiology and Biochemistry 163: 166–177.

Pawłowicz, I., Rapacz, M., Perlikowski, D., Gondek, K. and Kosmala, A. 2017. Abiotic stresses influence the transcript abundance of *PIP* and *TIP* aquaporins in *Festuca* species. Journal of Applied Genetics 58: 421-435.

Pellegrini-Calace, M., Maiwald, T. and Thornton, J.M. 2009. Porewalker: a novel tool for the identification and characterization of channels in transmembrane proteins from their three-dimensional structure. PLoS Computational Biology 5: e1000440

Pravda, L., Sehnal, D., Toušek, D., Navrátilová, V., Bazgier, V., Berka, K., Svobodová Vařeková, R., Koča, J. and Otyepka, M. 2018. Moleonline: a web-based tool for analyzing channels, tunnels and pores (2018 update). Nucleic Acids Research 46: W368–W373.

Qiu, J., McGaughey, S.A., Groszmann, M., Tyerman, S.D. and Byrt, C.S. 2020. Phosphorylation influences water and ion channel function of atpip2;1. Plant, Cell & Environment 43: 2428–2442.

Rahman, M.M., Mostofa, M.G., Keya, S.S., Siddiqui, M.N., Ansary, M., Das, A.K., Rahman, M.A. and Tran, L.S. 2021. Adaptive mechanisms of halophytes and their potential in improving salinity tolerance in plants. International Journal of Molecular Sciences 22: 10733.

Sade, N., Weng, F., Tajima, H., Zeron, Y., Zhang, L., del Mar Rubio Wilhelmi, M., Peleg, Z. and Blumwald, E. 2020. A cytoplasmic receptor-like kinase contributes to salinity tolerance. Plants 9: 1383.

Saitou, N. and Nei, M. 1987. The neighbor-joining method: A new method for reconstructing phylogenetic trees. Molecular Biology and Evolution, 4: 406-425.

Sakurai, J., Ishikawa, F., Yamaguchi, T., Uemura, M. and Maeshima, M. 2005. Identification of 33 rice aquaporin genes and analysis of their expression and function. Plant and Cell Physiology 46: 1568-1577.

Scotto–Lavino, E., Du, G. and Frohman, M.A. 2006. 3′ end cDNA amplification using classic race. Nature Protocols 1: 2742-2745.

Shivaraj, S.M., Deshmukh, R.K., Rai, R., Bélanger, R., Agrawal, P.K. and Dash, P.K. 2017. Genome-wide identification, characterization, and expression profile of aquaporin gene family in flax (*Linum usitatissimum*). Scientific Reports, 7: 46137.

Sun, J.Y., Liu, X.S., Khan, I.U., Wu, X.C. and Yang, Z.M. 2021. OsPIP2;3 as an aquaporin contributes to rice resistance to water deficit but not to salt stress, Environmental and Experimental Botany183: 104342.

Sutka, M., Li, G., Boudet, J., Boursiac, Y., Doumas, P. and Maurel, C. 2011. Natural variation of root hydraulics in Arabidopsis grown in normal and salt-stressed conditions. Plant Physiology 155: 1264-1276.

Törnroth-Horsefield, S., Wang, Y., Hedfalk, K., Johanson, U., Karlsson, M., Tajkhorshid, E., Neutze, R. and Kjellbom, P. 2006. Structural mechanism of plant aquaporin gating. Nature, 439: 688–694.

Tran, S.T., Horie, T., Imran, S., Qiu, J., McGaughey, S., Byrt, C.S., Tyerman, S.D. and Katsuhara, M. 2020. A survey of barley PIP aquaporin ionic conductance reveals Ca^{2+}-

sensitive *HVPIP2;8* Na^+ and K^+ conductance. International Journal of Molecular Sciences, 21: 7135.

Tyerman, S.D., McGaughey, S.A., Qiu, J., Yool, A.J. and Byrt, C.S. 2021. Adaptable and multifunctional ion-conducting aquaporins. Annual Review of Plant Biology 72: 703-736.

Ueda, M., Tsutsumi, N. and Fujimoto, M. 2016. Salt stress induces internalization of plasma membrane aquaporin into the vacuole in *Arabidopsis thaliana*. Biochemical and Biophysical Research Communications 474: 742-746.

Ungar, I.A. 1974. Inland halophytes of the United States. - In: Ecology of halophytes. Edited by R.J. Reimold and W.H. Queen. Academic Press, New York, pp. 235-305.

Vaziriyeganeh, M., Carvajal, M., Du, N. and Zwiazek, J.J. 2022. Salinity tolerance of halophytic grass *Puccinellia nuttalliana* is associated with enhancement of aquaporin-mediated water transport by Sodium. International Journal of Molecular Sciences 23: 5732.

Vaziriyeganeh, M., Khan, S. and Zwiazek, J.J. 2021. Transcriptome and metabolome analyses reveal potential salt tolerance mechanisms contributing to maintenance of water balance by the halophytic grass *Puccinellia nuttalliana*. Frontiers in Plant Science 12: 760863

Vaziriyeganeh, M., Lee, S.H. and Zwiazek, J.J. 2018. Water transport properties of root cells contribute to salt tolerance in halophytic grasses *Poa juncifolia* and *Puccinellia nuttalliana*. Plant Science 276: 54-62.

Wan, X., and Zwiazek, J.J. 1999. Mercuric chloride effects on root water transport in aspen seedlings. Plant Physiology 121: 939-946.

Wang, M., Ding, L., Gao, L., Li, Y., Shen, Q. and Guo, S. 2016. The interactions of aquaporins and mineral nutrients in higher plants. International Journal of Molecular Sciences 17:1229.

Yepes-Molina, L., Bárzana, G. and Carvajal, M. 2020. Controversial regulation of gene expression and protein transduction of aquaporins under drought and salinity stress. Plants, 9: 1662.

Zhu, Y.X., Gong, H.J. and Yin, J.L. 2019. Role of silicon in mediating salt tolerance in plants: a review. Plants 8: 147.

Zhu, C., Schraut, D., Hartung, W. and Schäffner, A.R. 2005. Differential responses of maize MIP genes to salt stress and ABA. Journal of Experimental Botany 56: 2971-2981.

Zhu, Y., Yang, L., Liu, N., Yang, J., Zhou, X., Xia, Y., He, Y., He, Y., Gong, H., Ma, D. and Yin, J. 2019. Genome-wide identification, structure characterization, and expression pattern profiling of aquaporin gene family in cucumber. BMC Plant Biology 19: 345.

Zwiazek, J.J., Xu, H., Tan, X., Navarro-Ródenas, A. and Morte, A. 2017. Significance of oxygen transport through aquaporins. Scientific Reports 7: 40411.

4.6 Supplementary Material

Supplementary Table 4.1. Properties of proteins with amino acid sequences predicted from the cloned aquaporin genes in *Poa pratensis*, *Poa juncifolia,* and *Puccinellia nuttalliana*

Aquaporin	Cloned gene name	Protein length (Amino acid)	Molecular weight (kDa)	Isoelectric point (pI)	Maximum % of residue
PIP2;1	*PjPIP2;1*	286	30.36	7.0	Ala (14.3%)
	PnuPIP2;1	286	30.32	6.95	Ala (13.3%)
	PprPIP2;1	286	30.37	6.95	Ala (14.0%)
PIP2;2	*PjPIP2;2*	287	30.25	6.15	Ala (15.0%)
	PnuPIP2;2	287	30.20	7.00	Ala (14.6%)
	PprPIP2;2	287	30.11	7.67	Ala (15.7%)
PIP2;3	*PjPIP2;3*	288	30.23	7.69	Ala (14.6%)
	PnuPIP2;3	288	30.27	8.59	Ala (14.6%)
	PprPIP2;3	288	30.19	8.28	Ala (14.9%)
PIP1;1	*PjPIP1;1*	288	30.64	9.00	Ala (12.5%)
	PnuPIP1;1	288	30.75	9.00	Ala (12.2%)
	PprPIP1;1	288	30.71	8.83	Ala (12.2%)
PIP1;3	*PjPIP1;3*	290	30.70	8.82	Gly (13.1%)
	PnuPIP1;3	290	30.70	8.82	Gly (13.1%)
	PprPIP1;3	290	30.76	8.83	Gly (13.4%)

Supplementary Table 4.2. Primer sequences for cloning the aquaporin genes from *Poa pratensis*, *Poa juncifolia* and *Puccinellia nuttalliana*

Primer name	Gene	Primer sequences
P2V1F	*PIP2-1*	5′-CCATGGATGGCSAARGACATTGAGG-3′
P2V1R		5′-GTTGGACCGGTAGGAGCCNARYTTNGC-3′
P2V2NF	*PIP2-2*	5′-ATGGSSAAGGACGAGGTGATGGAGA-3′
P2V2NR		5′-GGATCCTTACGCGTTGCTCCTGAAGG-3
PIP2degen_FG_F	*PIP2-3*	5′-CCATGGATGGCCAAGGAYATHGARGC-3
PIP2degen_FG_R		5′-CTAGYKVCTRCCGAAGGAGGC-3
P1NP1F	*PIP1-3*	5′-TACCATGGAGGGCAAGGARGARGAYGT-3′
P1NP1R		5′-CCCAAGCTTCCGGGACTTGAANGGDATNGC-3′
PP1F	*PIP1-1*	5′-TTARGACYTGSTCTTGAAYGGGATCGC-3′
PP1R		5′-TACCATGGAGGGCAAGGARGARGAYGT-3′
NSF	*TIP1-1*	5′-CCGATTCTTAGTAGTCGGTGGWGGG GAGCT-3′
SR		5′-TCCCATGGATGCCAGTGTCCMGNATHGCNGT-3′
NewAQPF	*PIP2-6*	5′-CAAGGAGGTGAGCGAGGA-3′
NewAQPR		5′-CCCGGAGGATGTACTGGTG-3′

```
PnuPIP1B      MEGKEEDVRLGANRYSEHQPIGTAAQGSNEGKDYKEPPPAPFFEASELTSWSFYRAGIAE   60
PprPIP1B      MEGKEEDVRLGANRYSEHQPIGTAAQGGNEGKDYKEPPPAPFFEAHELTSWSFYRAGIAE   60
PprPIP1A      MEGKEEDVRLGANKFSERQPIGTSAQGT-EDKDYKEPPPAPLFEPGELKSWSFYRAGIAE   59
PJPIP1B       MEGKEEDVRLGANKFSERQPIGTAAQGS-DEKDYKEPPPAPLFEPGELKSWSFYRAGIAE   59
PjPIP1A       MEGKEEDVRLGANKFSERQPIGTAAQGS-DGKDYKEPPPAPLFEPGELKSWSFYRAGIAE   59
PnuPIP1A      MEGKEEDVRLGANKFSERQPIGTAAQGS-DHKDYKEPPPAPLFEPGELKSWSFYRAGIAE   59
PnuPIP2D      -----------------KEVSEE-PEHAPVRKDYSDPPPAPLFDMGELRMWSFYRALIAE   42
PjPIP2D       ----------------------------------------------MGELRMWSFYRALIAE   16
PprPIP2B      ---------------MG-KDEVMESGGDFAAKDYTDPPPAPLIDSAELASWSLYRAVIAE   44
PnuPIP2B      ---------------MG-KDEVMETGGDFATKDYTDPPPAPLIDSAELASWSLYRAVIAE   44
PjPIP2B       ---------------MA-KDEVMETGGDFATKDYTDPPPAPLIDSAELASWSLYRAVIAE   44
PnuPIP2A      ---------------MAKDIEAAPEGGEFSAKDYSDPPPAPIVDFEELTKWSLYRAVIAG   45
PprPIP2A      ---------------MAKDIEAAPEGGEFSAKDYSDPPPAPIVDFEELTKWSLYRAVIAE   45
PjPIP2A       ---------------MAKDIEAAPEGGEFHAKDYSDPPPAPIVDFEELTKWSLYRAVIAE   45
PprPIP2C      ---------------MAKDIE-APGGGEYTAKDYSDPPPAPLFDAAELTKWSLYRAVIAE   44
PnuPIP2C      ---------------MAKDIE-APGAGEYTAKDYSDPPPAPLFDAAELTKWSLYRAVIAE   44
PjPIP2C       ---------------MAKDIE-APGAGEYTAKDYSDPPPAPLFDAAELTKWSLYRAVIAE   44
                                                          **  **:*** **

PnuPIP1B      FLATFLFLYISVLTVMGVVGDP------SGSKCGTAGIQGIAWSFGGMIFVLVYCTAGIS   114
PprPIP1B      FLATFLFLYISVLTVMGVVGDP------SGSKCGTVGIQGIAWSFGGMIFVLVYCTAGIS   114
PprPIP1A      FMATFLFLYVTILTVMGVNNSP--------SKCATVGIQGIAWSFGGMIFALVYCTAGIS   111
PJPIP1B       FMATFLFLYVTILTVMGVNNSP--------SKCATVGIQGIAWSFGGMIFALVYCTAGIS   111
PjPIP1A       FMATFLFLYVTILTVMGVNNSP--------SKCATVGIQGIAWSFGGMIFALVYCTAGIS   111
PnuPIP1A      FMATFLFLYVTILTVMGVNNSP--------SKCATVGIQGIAWSFGGMIFALVYCTAGIS   111
PnuPIP2D      FVATLLFLYITVATVIGYKVQSA------TDPCGGVGILGIAWAFGGMIFVLVYCTAGIS   96
PjPIP2D       FVATLLFLYITVATVIGYKVQSA------TDPCGGVGILGIAWAFGGMIFVLVYCTAGIS   70
PprPIP2B      FIATLLFLYITVATVIGYKHQTDAAVNGTDAACGGVGILGIAWAFGGMIFVLVYCTAGIS   104
PnuPIP2B      FIATLLFLYITVATVIGYKHQTDAGVNGTDAACGGVGVLGIAWAFGGMIFVLVYCTAGIS   104
PjPIP2B       FIATLLFLYITVATVIGYKHQTDADVNGTDAACGGVGVLGIAWAFGGMIFVLVYCTAGIS   104
PnuPIP2A      FVATLLFLYITVATVIGYKHQSDPAVNTTDAACSGVGVLGIAWAFGGMIFVLVYCTAGVS   105
PprPIP2A      FVATLLFLYITVATVIGYKHQSDPNVNTTDAACSGVGILGIAWAFGGMIFVLVYCTAGVS   105
PjPIP2A       FVATLLFLYITVATVIGYKHQSDPAVNTTDAACSGVGILGIAWAFGGMIFVLVYCTAGIS   105
PprPIP2C      FVATLLFLYITVATVIGYKHQSDPAANPTDAACSGVGILGIAWAFGGMIFVLVYCTAGVS   104
PnuPIP2C      FVATLLFLYITVATVIGYKHQSDPTVNTTDAACSGVGVLGIAWAFGGMIFVLVYCTAGVS   104
PjPIP2C       FVATLLFLYITVATVIGYKHQSDPTVNTTDAACSGVGVLGIAWAFGGMIFVLVYCTAGVS   104
              *:**:****::: **:*   .           *. .*: ****:******.**** **:*

PnuPIP1B      GGHINPAVTFGLFLARKLSLTRAVFYIVMQCLGAICGAGVVKGFGTKLYMGNGGGANSVA   174
PprPIP1B      GGHINPAVTFGLFLARKLSLTRAVFYMVMQCLGAICGAGVVKGFGTTLYMGNGGGANSVA   174
PprPIP1A      GGHINPAVTFGLFLARKLSLTRAVFYIIMQCLGAICGAGVVKGFQQGLYMTAGGGANTVA   171
PJPIP1B       GGHINPAVTFGLFLARKLSLTRAVFYIIMQCLGAICGAGVVKGFQQALYMTAGGGANSVA   171
pjPIP1A       GGHINPAVTFGLFLARKLSLTRAVFYIIMQCLGAICGAGVVKGFQQALYMTAGGGANSVA   171
PnuPIP1A      GGHINPAVTFGLFLARKLSLTRAVFYIIMQCLGAICGAGVVKGFQQTLYMTAGGGANSVA   171
PnuPIP2D      GGHINPAVTFGLLLARKVSLPRAVLYIVAQSAGAIVGVGIVKGIMKDAYEANGGGANVVA   156
PjPIP2D       GGHINPAVTFGLLLARKVSLPRAVLYIVAQSAGAIVGVGIVKGIMKDAYEANGGGANMVA   130
PprPIP2B      GGHINPAVTFGLFLARKVSLVRALLYMIAQCLGAVCGVGLVKAFQSAYFQRYGGGANTLA   164
PnuPIP2B      GGHINPAVTFGLFLARKVSLVRALLYMIAQCLGAMCGVGLVKAFQSAYFHRYGGGANTLA   164
PjPIP2B       GGHINPAVTFGLFLAHKVSLVRALLYMIAQCLGAMCGVGLVKAFQSAYFHRYGGGANTLA   164
PnuPIP2A      GGHINPAVTFGLFLARKVSLIRALLYIIAQCLGAICGVGLVKGFQSSYYVRYGGGANELS   165
PprPIP2A      GGHINPAVTFGLFLARKVSLIRALLYIIAQCLGAICGVGLVKGFQSSYYVRYGGGANELS   165
PjPIP2A       GGHINPAVTFGLFLARKVSLIRALLYIIAQCLGAICGVGLVKGFQSSYYVRYGGGANELS   165
PprPIP2C      GGHINPAVTFGLFLARKVSLVRAVLYIVAQCLGAICGVGLVKGFQSAFYVRYGGGANSLS   164
PnuPIP2C      GGHINPAVTFGLFLARKVSLVRAVLYMVAQCLGAICGVGLVKGFQSAYYVRYGGGANELS   164
PjPIP2C       GGHINPAVTFGLFLARKVSLVRAVLYMVAQCLGAICGVGLVKGFQSAYYVRYGGGANELS   164
              ************:**:*:** **::*:: *. **: *.*:**.:    :   ***** ::

PnuPIP1B      AGYTKGDGLGAEIVGTFVLVYTVFSATDAKRSARDSHVPILAPLPIGFAVFLVHLATIPI   234
PprPIP1B      PGYTKGDGLGAEIVGTFVLVYTVFSATDAKRSARDSHVPILAPLPIGFAVFLVHLATIPI   234
PprPIP1A      AGYTKGDGLGAEIVGTFVLVYTVFSATDAKRNARDSHVPILAPLPIGFAVFLVHLATIPI   231
```

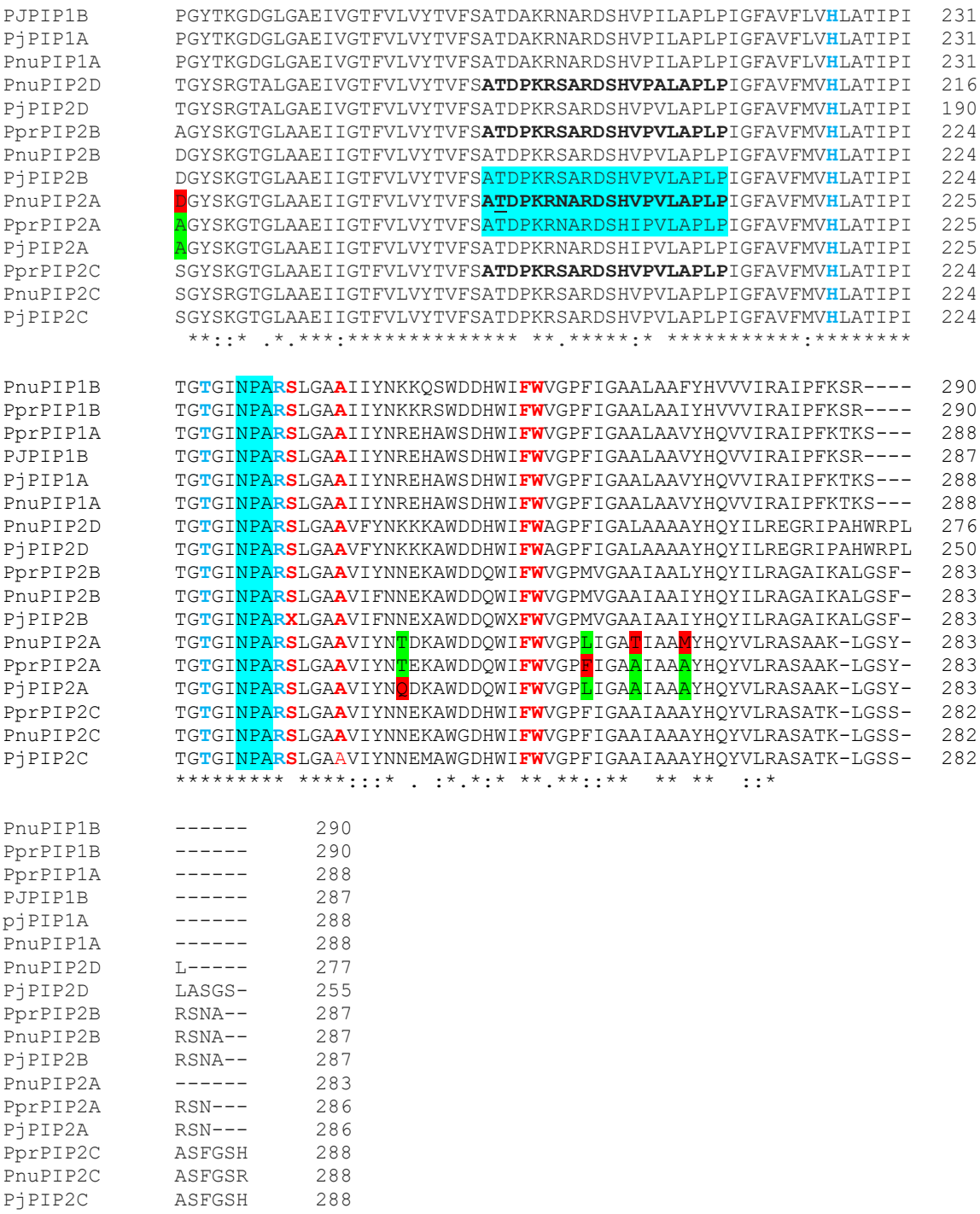

Supplementary Fig. 4.1. Protein sequence alignment of cloned aquaporins from *Poa pratensis, Poa juncifolia* and *Puccinellia nuttalliana*. Amino acids at NPA domains: blue; ar/R selectivity filters: royal blue; Froger's P1–P5 residues: red.

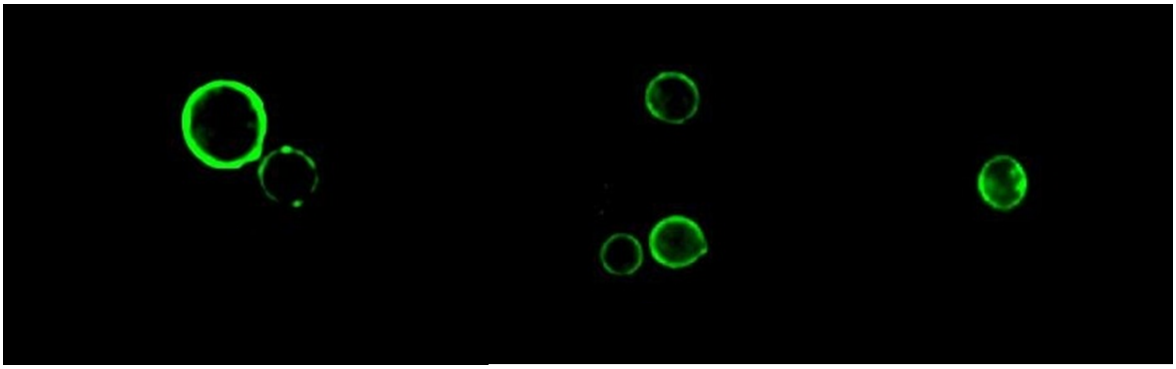

Supplementary Fig. 4.2. Images of yeast cells showing the localization of eYFP-tagged *Pnu*PIP proteins. Scale bars = 5 μm.

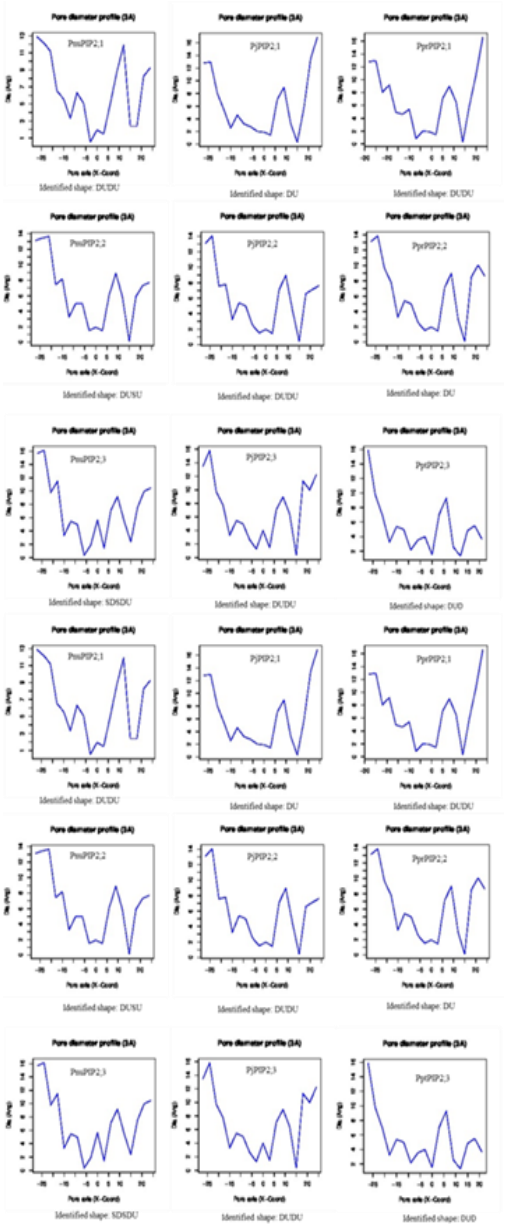

Supplementary Fig. 4.3. Pore diameter profile of PIP2;1, PIP2;2, PIP2;3 , PIP1;1, PIP1;3, and TIP1;1, from *Puccinellia nuttalliana* (Pnu), *Poa juncifolia* (Pj), and *Poa pratensis* (Ppr) at 3 Å steps. D = Decreasing diameter conical frustum. U = Increasing diameter conical frustum S = Cylinder. Commonly recognized shapes: DU = Hourglass; UD = Diamond; UDU/UDU = Hourglass-Diamond-Complex.

Chapter 5. Synthesis and Recommendations for Future Research

5.1 Synthesis

Control of water relations by plants growing in soils with elevated salinity is challenging due to the effects of salts on osmotic gradients and the toxicity of salt ions. Both factors alter water movement and its distribution in plant tissues either directly or indirectly by interfering with various processes in plants that influence water balance. To prevent plant water deficit in the soil-plant-air continuum, the rate of water loss by transpiration must be balanced by the rates of water uptake and its delivery to the transpiring areas. Therefore, in addition to efficient root water uptake, plants must maintain sufficiently high rates of water flow to deliver and distribute water in the different tissues to keep them hydrated. As reviewed in Chapter 1, the key processes in plants that are directly affected by salt and may quickly lead to upset water balance are osmotic gradients and root hydraulic conductivity, which is largely regulated at the cell level by the aquaporins (Martinzez-Ballesta et al. 2008, Munns and Tester 2008).

In my thesis research, I focused on the role of water transport and aquaporins in salinity tolerance of three species of northern grasses: *Puccinellia nuttalliana*, *Poa juncifolia*, and *Poa pratensis*. I first established that the sustained growth and measured physiological parameters in *Puccinellia nuttalliana* was associated with the presence of Na^+ in salt treatments and Na^+ was the factor responsible for the enhancement of cell hydraulic conductivity (L_{pc}) in this halophytic grass. As expected, the glycophytic grass *Poa pratensis* was the most affected by the treatments with 150 mM NaCl, 150 mM Na_2SO_4 and 150 mM KCl, while the relatively salt tolerant plants of *Poa juncifolia* showed intermediate responses to salts (Chapter 2). Since the application of 50 µM $HgCl_2$ to roots reduced L_{pc} to similar levels in all treatments and control, I concluded that the

inhibition of L_{pc} by Na^+ in *Poa pratensis* and *Poa juncifolia* and its enhancement in *Puccinellia nuttalliana* was due to the mercury-sensitive aquaporin-mediated water transport. This knowledge was important for the next phase of my research since it enabled me to conclude that Na^+, and not the osmotic effects of salts or the presence of specific anions, directly contributed to salt tolerance of water relations in this halophyte through the effect on aquaporins.

It has been long recognized that salt tolerance involves effective control of ion distribution in plant cells and tissues. The ability of plants to maintain high K^+/Na^+ ratios in cells is thought to be critical for the survival of plants under salinity conditions (Shabala and Cuin 2008). K^+ efflux from the cytoplasm could also lead to the acidification of the cytoplasm and result in the inhibition of aquaporin function and reduction of L_{pc} (Vaziriyeganeh et al. 2018). The effects of salt on root and shoot K^+ concentrations in the three studied grasses followed the same trend as their overall relative salt tolerance with decreases in K^+ concentrations measured in the salt-sensitive *Poa pratensis*, little change in the moderately-tolerant *Poa juncifolia* and increases in the halophytic *Puccinellia nuttalliana* (Chapter 2). Although there is little empirical evidence for it, it was suggested that aquaporins could function as turgor sensors to modulate the conductance of K^+ channels (Hill et al. 2004, Wang et al. 2016). Therefore, the notion that K^+ fluxes in salt-affected plants may be linked to the aquaporin function deserves future attention.

Since plant salt tolerance is a complex trait that involves multiple genes and pathways, I followed up on the findings in Chapter 2 with comprehensive transcriptomic and metabolomic analyses to characterize the molecular and functional traits that may contribute to the effective regulation of water transport in *Puccinellia nuttalliana* under salt stress conditions. I combined these analyses with microscopic observations of root and leaf structures NaCl-treated plants, which revealed that salt secretion through the salt glands in leaf epidermis was among the salt

tolerance strategies of this halophyte (Chapter 3). In addition to the responses involving SOS pathway genes, ROS scavengers, osmoprotectants, salt-responsive transcription factors, metabolic pathways, I found significant changes in the transcript levels of several aquaporins and an increase in the transcript level of the HKT1;5 high affinity potassium transporter that provided important clues for the salt tolerance strategies of *Puccinellia nuttalliana* with an impact on water transport (Chapter 3). HKT1;5 contributes to salt tolerance by reducing Na^+ transport to shoots from the xylem vessel elements, in the process that is linked to water transport (Xu et al. 2018, Munns et al. 2020). The presence of HKT1;5 from salt tolerant *Triticum monococcum* in durum wheat *Triticum turgidum* ssp. *Durum* increased plant salt tolerance and improved growth and yield by reducing leaf Na^+ concentrations (Munns et al. 2012). Therefore, it appears that *Puccinellia nuttalliana* uses several salt tolerance strategies that include maintenance of water transport and high K^+ concentrations while reducing Na^+ concentrations in shoots to less than 50% compared with *Poa pratensis* through salt secretion and restricted xylem transport.

While it is possible that Na^+ transport by PnuPIP2;2 could help with Na^+ retrieval from the xylem in the mature root parts and during the periods of slow transpiration, the effective shoot Na^+ management by *Puccinellia nuttalliana* cannot explain the reasons for the enhancement of the aquaporin-mediated water transport in roots by Na^+. The study described in Chapter 4 was designed to examine the roles of aquaporins in salt tolerance and explain possible mechanisms contributing to the increased L_{pc} in roots of *Puccinellia nuttalliana* by Na^+. Contrary to the less salt-tolerant grasses, the responses to NaCl in this halophytic plant included increases in the transcript levels of some of the examined *PIP*s and a decrease in the transcript level of the examined tonoplast aquaporin *TIP1;1*. Since the salt tolerance strategy of halophytes commonly involves sequestration of salt in the vacuoles while maintaining lower concentrations in the

cytoplasm (Oui et al. 2022), there may be steep osmotic potential gradients across the tonoplast and slowing down water influx would benefit the plant. Assuming that higher transcript levels of PIPs are indicative of their greater membrane abundance, this increase could partly explain the enhancement of aquaporin-mediated transport in roots of *Puccinellia nuttalliana*. However, the question remained whether the PIPs in salt tolerant plants have some unique properties that may enable them to function in the presence of high root Na^+ concentrations. To address this question, I first expressed several aquaporins from *Puccinellia nuttalliana* in yeast and examined their water transport characteristics in the absence and presence of 100 mM NaCl. Since I established the rate of water transport was enhanced by NaCl in yeast cells expressing *PnuPIP2;2*, I compared the structural properties of this aquaporin with PIP2;2s from *Poa juncifolia* and *Poa pratensis*. The ar/R filter residues, bottleneck, hydropathy, and polarity of the pores were different between the *PIP2;2s* from the three grass species. The PnuPIP2;2 has unique pore characteristics, which include a combination of the hourglass, cylindrical and increasing diameter conical entrance shape with pore hydropathy of - 0.22. This compared to the most common hourglass pore structure in the salt-sensitive *Poa pratensis*, with the hydropathy of 0.03 and, interestingly, an intermediate hourglass-diamond pore complex with the hydropathy of 0.3 in the relatively salt-tolerant *Poa juncifolia* (Chapter 4). While the pore shape and other structural variations could affect water and ion transport across the aquaporins, more research will be needed in the future to clearly establish the functional significance of these unique properties and to develop better understanding of the interactions between water and ion transport in halophytic plants.

In Chapter 3, I proposed a conceptual model for salt responses of the halophytic plant *Puccinellia nuttalliana* that presents a chain of events contributing to salt tolerance. The model

was developed based on the transcriptomic and metabolomic analyses that followed the study of plant physiological responses to salinity reported in Chapter 2 and it is explained in the figure legend. The model also illustrates the complexity of plant responses that ultimately lead to salt tolerance. As pointed out earlier in the discussion, salt tolerance is a multi-gene response that involves many different processes on many different levels. Over the many years of studies aimed at understanding salt tolerance, we have kept improving our knowledge of these processes with each new study providing another building block that contributes towards the final goal. My research contributed to better understanding of the roles that aquaporins may play in plant responses to salt and their importance for plant salt tolerance. It is hoped that this research contribution will have a significant impact on the future efforts to develop a comprehensive understanding of the salt tolerance processes in plants.

5.2 Recommendations for Future Research

While providing new knowledge, research studies also commonly generate new questions that need to be answered by additional research. Plant salt tolerance is a highly complex topic, and it will likely take many more years of consolidated efforts to develop good and comprehensive understanding of all the factors that must work together to produce a salt tolerant plant.

The results of my studies clearly demonstrated that maintaining the functionality of aquaporins plays an important role in the salt tolerance strategies of the salt tolerant grasses. The question remains whether this is a universal strategy in all salt-tolerant plants and how exactly it is achieved. My studies points to PIP2;2 as a likely contributor to this process, especially in the halophytic grass *Puccinellia nuttalliana*. However, there are many other PIPs, which may share

similar characteristics in this and other salt tolerant plants and which my studies did not examine. The key structural elements of *PnuPIP2;2* that may be linked to the unique characteristics of its pore. However, this needs to be validated by other studies using molecular approaches combined with comprehensive measurements of water and Na^+ transport characteristics of this protein. This could probably be accomplished through the mutation studies of the key structural areas of this aquaporin that could also help with finding answers concerning the structural properties that make it possible to enhance water transport by Na^+. The question also remains how other PIPs may affect the function of *PnuPIP2;2* when present together in forming a heterotetramer. Perhaps, the central pore could also play a role in salt responses. The other topic that needs to be addressed is the contribution of TIPs to salt tolerance strategies. The downregulation of TIP1;1 in salt tolerant grasses, contrary to the upregulation of this tonoplast aquaporin in the relatively salt sensitive *Poa pratensis* hints at a possible important strategy involving a reduction of water flow across the tonoplast, possibly slowing down the water movement due to a steep water potential gradient resulting from salt accumulation. Then, there is a question of the link between K^+ and Na^+ transporters and aquaporin-mediated water transport in the overall salt tolerance strategy. There is sufficient evidence from other studies to confirm that HKT1;5 plays a highly significant role in salt tolerance by reducing Na^+ transport to leaves in grass species by withdrawing it from the root xylem and this appears to be one of the salt tolerance strategies in *Puccinellia nuttalliana* judging from its relatively low Na^+ shoot concentrations and presence of salt glands. However, this process is likely to involve water transport and the tolerance of high Na^+ concentrations in roots, possibly explaining why root aquaporins need tolerate high Na^+ concentrations to transport water. These and many other questions, some which were also

generated through my research, will need to be answered to have better understanding of how *Puccinellia nuttaliana* and other halophytes tolerate high salinity levels.

With the advances in molecular methods, it may be possible to answer some of the above questions through genetic manipulations of plants. For example, it would be interesting to see what effect would be achieved by knocking out *PnuPIP2;2* with or without *PnuHKT1;5* or how salt sensitive grasses would respond by co-expression of these genes. Similar strategies could be used to understand the importance of *PnuTIP1;1* as well as the transcription factors, which the transcriptomics study revealed of possible importance to water transport and salt tolerance. Targeted mutations of *PnuPIP2;2* affecting the pore area would be helpful to understand the importance of individual amino acids in conferring structural characteristics of this aquaporin in relation to water and Na^+ transport. If carried out at the molecular, cell, tissue, and the whole plant level, these studies would help develop a better comprehensive understanding of plant salt tolerance and the role that aquaporin-mediated water transport plays in these processes.

Bibliography

Abbas, A., Yu, H., Cui, H. and Li, X. 2021. Genetic diversity and synergistic modulation of salinity tolerance genes in *Aegilops tauschii* Coss. Plants 10: 10071393.

Abdelkader, A.F., El-khawas, S., El-Din El-Sherif, N.A.S., Hassanein, R.A., Emam, M.A. and Hassan, R.E.-S. 2012. Expression of aquaporin gene (Os PIP1-3) in salt-stressed rice (*Oryza sativa* L.) plants pre-treated with the neurotransmitter (dopamine). Plant Omics 5: 532–541.

Abideen, Z., Koyro, H.W., Huchzermeyer, B., Ahmed, M.Z., Gul, B. and Khan, M.A. 2014. Moderate salinity stimulates growth and photosynthesis of *Phragmites karka* by water relations and tissue specific ion regulation. Environmental and Experimental Botany 105: 70-76.

Acosta-Motos, J.R., Diaz-Vivancos, P., Alvarez, S., Fernandez-Garcia, N., Sanchez-Blanco, M.J. and Hernandez, J.A. 2015. Physiological and biochemical mechanisms of the ornamental *Eugenia myrtifolia* L. plants for coping with NaCl stress and recovery. Planta 242: 829-846.

Acosta-Motos, J.R., Ortuño, M.F., Bernal-Vicente, A., Diaz-Vivancos, P., Sanchez-Blanco, M.J. and Hernandez, J.A. 2017. Plant responses to salt stress: adaptive mechanisms. Agronomy 7: 18.

Adem, G.T., Roy, S.J., Zhou, M., Bowman, J.P. and Shabala, S. 2014. Evaluating contribution of ionic, osmotic and oxidative stress components towards salinity tolerance in barley. BMC Plant Biology 14: 113.

Afzal, Z., Howton, T.C., Sun, Y. and Mukhtar, M.S. 2016. The roles of aquaporins in plant stress responses. Journal of Developmental Biology 4: db4010009.

Agarie, S., Shimoda, T., Shimizu, Y., Baumann, K., Sunagawa, H., Kondo, A., Ueno, O., Nakahara, T., Nose, A. and Cushman, J.C. 2007. Salt tolerance, salt accumulation, and ionic homeostasis in an epidermal bladder-cell-less mutant of the common ice plant *Mesembryanthemum crystallinum*. Journal of Experimental Botany 588: 1957-1967.

Ahmadi, A.J. and Ahmadikhah, A. 2022. Occurrence of simple sequence repeats in cDNA sequences of safflower (Cartamus tinctorius) reveals the importance of SSR-containing genes for cell biology and dynamic response to environmental cues. Frontiers in Plant Science 13: 991107.

Ahmed, J., Mercx, S., Boutry, M. and Chaumont, F. 2020. Evolutionary and predictive functional insights into the aquaporin gene family in the allotetraploid plant *Nicotiana tabacum*. International Journal of Molecular Sciences 21: 4743.

Akbarimoghaddam, H., Galavi, M., Ghanbari, A. and Panjehkeh, N. 2011. Salinity effects on seed germination and seedling growth of bread wheat cultivars. Trakia Journal of Sciences 9: 43-50.

Al Hassan, M., Chaura, J., Lopez-Gresa, M.P., Borsai, O., Daniso, E., Donat-Torres, M.P., Mayoral, O., Vicente, O. and Boscaiu, M. 2016. Native-invasive plants vs. halophytes in Mediterranean salt marshes: stress tolerance mechanisms in two related species. Frontiers in Plant Science 7: 473.

Alavilli, H., Awasthi, J.P., Rout, G.R., Sahoo, L., Lee, B.-Ha and Panda, S.K. 2016. Overexpression of a barley aquaporin gene, *HVPIP2;5* confers salt and osmotic stress tolerance in yeast and plants. Frontiers in Plant Science 7: 1566.

Albaladejo, I., Meco, V., Plasencia, F., Flores, F.B., Bolarin, M.C. and Egea, I. 2017. Unravelling the strategies used by the wild tomato species *Solanum pennellii* to confront salt stress: From leaf anatomical adaptations to molecular responses. Environmental and Experimental Botany 135: 1-12.

Alfarrah, N. and Walraevens, K. 2018. Groundwater overexploitation and seawater intrusion in coastal areas of arid and semi-arid regions. Water 10: 143.

Ali, A., Maggio, A., Bressan, R.A. and Yun, D.J. 2019. Role and functional differences of HKT1-type transporters in plants under salt stress. International Journal of Molecular Sciences 20: 1059.

Ali, A., Raddatz, N., Aman, R., Kim, S., Park, H.C., Jan, M., Baek, D., Khan, I.U., Oh, D.H., Lee, S.Y., Bressan, R.A., Lee, K.W., Maggio, A., Pardo, J.M., Bohnert, H.J. and Yun, D.J. 2016. A single amino-acid substitution in the sodium transporter *HKT1* is associated with plant salt tolerance. Plant Physiology 171: 2112-2126.

Aliakbari, M., Razi, H., Alemzadeh, A. and Tavakol, E. 2020. RNA-seq transcriptome profiling of the halophyte *Salicornia persica* in response to salinity. Journal of Plant Growth Regulation 40: 707-721.

Alleva, K., Niemietz, C.M/, Sutka, M., Maurel, C., Parisi, M., Tyerman, S.D. and Amodeo, G. 2006. Plasma membrane of *Beta vulgaris* storage root shows high water channel activity

regulated by cytoplasmic pH and a dual range of calcium concentrations. Journal of Experimental Botany 57: 609-621.

Allinson, G., Bui, A., Zhang, P., Rose, G., Wightwick, A.M., Allinson, M. and Pettigrove, V., 2014. Investigation of 10 herbicides in surface waters of a horticultural production catchment in southeastern Australia. Archives of Environmental Contamination and Toxicology, 67: 358-373.

Almeida-Rodriguez, A., Cooke, J.E.K., Yeh, F. and Zwiazek J.J. 2010. Functional characterization of drought-responsive aquaporins in *Populus balsamifera* and *Populus simonii* x *balsamifera* clones with different drought resistance strategies. Physiologia Plantarum 140: 321-333.

Alshammary, S.F. 2012. Effect of salinity on water relations of four turfgrasses. African Journal of Agricultural Research 7: 5498-5505.

Amezcua-Romero, J.C., Pantoja, O. and Vera-Estrella, R. 2010. Ser123 is essential for the water channel activity of MCPIP2;1 from *Mesembryanthemum crystallinum*. Journal of Biological Chemistry 285: 16739-16747.

Ampah-Korsah, H., Anderberg, H.I., Engfors, A., Kirscht A., Nordén, K., Kjellström, S., Kjellbom, P. and Johanson, U. 2016. The aquaporin splice variant NbXIP1;1α is permeable to boric acid and is phosphorylated in the N-terminal domain. Frontiers in Plant Science 7: 862.

An, Y., Zhang, M., Liu, G., Han, R. and Liang, Z. 2013. Proline accumulation in leaves of *Periploca sepium* via both biosynthesis up-regulation and transport during recovery from severe drought. PLoS One 8: e69942.

Andrés, Z., Pérez-Hormaeche, J., Leidi, E.O., Schlücking, K., Steinhorst, L., McLachlan, D.H., Schumacher, K., Hetherington, A.M., Kudla, J., Cubero, E. and Pardo, J.M. 2014. Control of vacuolar dynamics and regulation of stomatal aperture by tonoplast potassium uptake. Proceedings of the National Academy of Sciences of the United States of America 111: E1806-E1814.

Apostol, K.G. and Zwiazek, J.J. 2003. Hypoxia affects root sodium and chloride concentrations and inhibits water conductance in salt-treated jack pine (*Pinus banksiana)* seedlings. Trees: Structure and Function 17: 251-257.

Apse, M.P., Blumwald, E. 2007. Na^+ transport in plants. FEBS Letters 581: 2247-2254

Asano, T., Hakata, M., Nakamura, H., Aoki, N., Komatsu, S., Ichikawa, H., Hirochika, H. and Ohsugi, R. 2011. Functional characterisation of OsCPK21, a calcium-dependent protein kinase that confers salt tolerance in rice. Plant Molecular Biology 75: 179-191.

Ashraf, M., 2004. Some important physiological selection criteria for salt tolerance in plants. Flora-Morphology, Distribution, Functional Ecology of Plants 199: 361-376.

Ashraf, M. 2009. Biotechnological approach of improving plant salt tolerance using antioxidants as markers. Biotechnology Advances 27: 84–93.

Ashraf, M. and Harris, P.J.C. 2013. Photosynthesis under stressful conditions: an overview. Photosynthetica 51: 163-190.

Assaha, D., Ueda, A., Saneoka, H., Al-Yahyai, R. and Yaish, M.W. 2017. The role of Na^+ and K^+ transporters in salt stress adaptation in glycophytes. Frontiers in Physiology 8: 509.

Azaieh, H. Gunse, B., Steudle, E. 1992. Effects of NaCl and $CaCl_2$ on water transport across root cells of maize (*Zea mays* L.) seedlings. Plant Physiology 99: 886-894.

Baillo, E.H., Kimotho, R.N., Zhang, Z. and Xu, P. 2019. Transcription factors associated with abiotic and biotic stress tolerance and their potential for crops improvement. Genes 10: 771.

Barnetson-Moir, L., Veneklaas, E.J. and Colmer, T.D. 2016. Salinity tolerances of three succulent halophytes (*Tecticornia* spp.) differentially distributed along a salinity gradient. Functional Plant Biology 43: 739-750.

Barzegargolchini, B., Movafeghi, A., Dehestani, A. and Mehrabanjoubani, P. 2017. Increased cell wall thickness of endodermis and protoxylem in *Aeluropus littoralis* roots under salinity: The role of LAC4 and PER64 genes. Journal of Plant Physiology 218: 127-134.

Baturin, S., Galka, J.J., Piyadasa, H., Gajjeraman, S. and O'Neil, J.D. 2014. The effects of a protein osmolyte on the stability of the integral membrane protein glycerol facilitator. Biochemistry and Cell Biology 92: 564-575.

Bazihizina, N., Colmer, T.D., Cuin, T.A., Mancuso, S. and Shabala, S. 2019. Friend or foe? Chloride patterning in halophytes. Trends in Plant Science 24: 142-151.

Bellati, J., Champeyroux, C., Hem, S., Rofidal, V., Kroul, G., Maurel, C. and Santoni, V. 2016. Novel aquaporin regulatory mechanisms revealed by interactomics. Molecular and Cellular Proteomics 15: 10.1074/mcp.M116.060087, 3473– 3487.

Belujon, P. and Grace, A.A. 2017. Dopamine system dysregulation in major depressive disorders. International Journal of Neuropsychopharmacology 20: 1036-1046.

Bertl, A. and Kaldenhoff, R. Function of a separate NH3-pore in aquaporin TIP2;2 from wheat. FEBS Letters 581: 5413-5417.

Biasini, M., Bienert, S., Waterhouse, A., Arnold, K., Studer, G., Schmidt, T., Kiefer, F., Cassarino, T.G., Bertoni, M., Bordoli, L. and Schwede, T. 2014. Swiss-model: modelling protein tertiary and quaternary structure using evolutionary information. Nucleic Acids Research 42 (W1).

Biela, A., Grote, K., Otto, B., Hoth, S., Hedrich, R. and Kaldenhoff, R., 1999. The *Nicotiana tabacum* plasma membrane aquaporin NtAQP1 is mercury-insensitive and permeable for glycerol. Plant Journal 18: 565-570.

Bienert, G.P., Bienert, M.D., Jahn, T. P., Boutry, M. and Chaumont, F. 2011. Solanaceae XIPs are plasma membrane aquaporins that facilitate the transport of many uncharged substrates. Plant Journal 66: 306–317.

Bienert, M.D., Diehn, T.A., Richet, N., Chaumont, F. and Bienert, G.P. 2018. Heterotetramerization of plant PIP1 and PIP2 aquaporins is an evolutionary ancient feature to guide PIP plasma membrane localization and function. Frontiers in Plant Science 9: 382.

Bose, J., Munns, R., Shabala, S., Gilliham, M., Pogson, B. and Tyerman, S.D. 2017. Chloroplast function and ion regulation in plants growing on saline soils: lessons from halophytes. Journal of Experimental Botany 68: 3129-3143.

Bose, J., Rodrigo-Moreno, A. and Shabala, S. 2014. ROS homeostasis in halophytes in the context of salinity stress tolerance. Journal of Experimental Botany 65: 1241-1257.

Boursiac, Y., Chen, S., Luu, D.T., Sorieul, M., van den Dries, N. and Maurel, C. 2005. Early effects of salinity on water transport in Arabidopsis roots. Molecular and cellular features of aquaporin expression. Plant Physiology 139: 790-805.

Braz, L.C.C., Fernandes, P.D., Barbosa, D.D., Dutra, W.F. Silva, C.R.C., Lima, L.M., Cavalcanti, J.J.V., Farias, F.J.C. and Santos, R.C. 2019. Expression of aquaporin subtypes (GhPIP1;1, GhTIP2;1 and GhSIP1;3) in cotton (*Gossypium hirsutum*) submitted to salt stress, AoB Plants 11: plz072.

Brindha, K. and Schneider, M. 2019. Impact of urbanization on groundwater salinity. In GIS and geostatistical techniques for groundwater science. Edited by V. Senapathi, P.M. Viswanathan and S.Y. Chung. Elsevier, Oxford, pp. 179-196.

Brown, H.A., Thomas, P.G. and Lindsley, C.W. 2017. Targeting phospholipase D in cancer, infection and neurodegenerative disorders. Nature Reviews Drug Discovery16: 351-367.

Bruntz, R.C., Lindsley, C.W. and Brown, H.A. 2014. Phospholipase D signaling pathways and phosphatidic acid as therapeutic targets in cancer. Pharmacological Reviews 66, 1033-1079.

Burg, M.B. and Ferraris, J.D. 2008. Intracellular organic osmolytes: function and regulation. Journal of Biological Chemistry 283: 7309–7313.

Bushman, B.S., Amundsen, K.L., Warnke, S.E., Robins, J.G. and Johnson, P.G. 2016. Transcriptome profiling of Kentucky bluegrass (*Poa pratensis* L.) accessions in response to salt stress. BMC Genomics 17: 48.

Byrt, C.S., Platten, J.D., Spielmeyer, W., James, R.A., Lagudah, E.S., Dennis, E.S., Tester, M. and Munns, R. 2007. HKT1;5-like cation transporters linked to Na^+ exclusion loci in wheat, Nax2 and Kna1. Plant Physiology 143: 1918-1928.

Byrt, C.S., Zhao, M., Kourghi, M., Bose, J., Henderson, S.W., Qiu, J., Gilliham, M., Schultz, C., Schwarz, M., Ramesh, S.A., Yool, A. and Tyerman, S. 2017.Non-selective cation channel

activity of aquaporin AtPIP2;1 regulated by Ca^{2+} and pH. Plant, Cell & Environment 40: 802-815.

Cairns, R.R. and Bowser W.E. 1977. Solonetzic soils and their management. Agriculture Canada, Publication 1391, Ottawa, 37 pp.

Caldeira, C.F., Jeanguenin, L., Chaumont, F. and Tardieu, F., 2014. Circadian rhythms of hydraulic conductance and growth are enhanced by drought and improve plant performance. Nature Communications 5: 1-9.

Calvo-Polanco, M.C., Zwiazek, J.J. and Voicu, M.C, 2008. Responses of ectomycorrhizal American elm (*Ulmus americana*) seedlings to salinity and soil compaction. Plant and Soil 308: 189-200.

Carvajal, M., Cerda, A. and Martinez. 2000. Does calcium ameliorate the negative effect of NaCl on melon root water transport by regulating aquaporin activity? New Phytologist 145: 439-447.

Carvajal, M., Cooke, D.T. and Clarkson, D.T. 1996. Responses of wheat plants to nutrient deprivation may involve the regulation of water-channel function. Planta 199: 372-381.

Carvajal, M., Martínez, V. and Alcaraz, C.F. 1999. Physiological function of water channels as affected by salinity in roots of paprika pepper. Physiologia Plantarum 105: 95-101.

Cavill, R., Jennen, D., Kleinjans, J. and Briede, J.J. 2016. Transcriptomic and metabolomic data integration. Briefings in Bioinformatics 17: 891-901.

Chapman, V.J. 1974. Salt marshes and deserts of the world. - In: Ecology of halophytes. Edited by R.J. Reimold and W.H. Queen. Academic Press, New York, pp. 3-19.

Chaumont, F., and Tyerman, S.D. 2014. Aquaporins: highly regulated channels controlling plant water relations. Plant Physiology 164: 1600-1618Chavarria, G. and dos Santos, H.P. 2012. Plant water relations: absorption, transport, and control mechanisms. In Advances in selected plant physiology aspects. Edited by G. Montanaro. Intech Open, doi 10.5772/1874, pp. 105-132.

Chaves, M.M., Flexas, J. and Pinheiro, C. 2009. Photosynthesis under drought and salt stress: regulation mechanisms from whole plant to cell. Annals of Botany 103: 551-560.

Cheeseman, J.M. 2015. The evolution of halophytes, glycophytes and crops, and its implications for food security under saline conditions. New Phytologist 206: 557–570.

Chen, T., Cai, X., Wu, X., Karahara, I., Schreiber, L. and Lin, J. 2011. Casparian strip development and its potential function in salt tolerance. Plant Signaling and Behavior 6: 1499-1502.

Chen, Z., Pottosin, II., Cuin, T.A., Fuglsang, A.T., Tester, M., Jha, D., Zepeda-Jazo, I., Zhou, M., Palmgren, M.G., Newman, I.A. and Shabala, S. 2007. Root plasma membrane transporters controlling K^+/Na^+ homeostasis in salt-stressed barley. Plant Physiology 145: 1714-1725.

Chinnusamy, V., Jagendorf, A. and Zhu, J.-K. 2005. Understanding and improving salt tolerance in plants. Crop Science 45: 437-448.

Conesa, A., Gotz, S., Garcia-Gomez, J.M., Terol, J., Talon, M. and Robles, M. 2005. Blast2GO: a universal tool for annotation, visualization, and analysis in functional genomics research. Bioinformatics 21: 3674-3676.

Couthouis, J., Hart, M.P., Shorter, J., DeJesus-Hernandez, M., Erion, R., Oristano, R., Liu, A.X., Ramos, D., Jethava, N., Hosangadi, D., Epstein, J., Chiang, A., Diaz, Z., Nakaya, T., Ibrahim, F., Kim, H.J., Solski, J.A., Williams, K.L., Mojsilovic-Petrovic, J., Ingre, C., et al. 2011. A yeast functional screen predicts new candidate ALS disease genes. Proceedings of the National Academy of Sciences of the United States of America, 108: 20881-20890.

Cuin, T.A., Betts, S.A., Chalmandrier, R. and Shabala, S. 2008. A root's ability to retain K^+ correlates with salt tolerance in wheat. Journal of Experimental Botany 59: 2697-2706.

Cushman, J.C. 2001. Osmoregulation in plants: implications for agriculture. American Zoologist 41: 758–769.

Danielson, J.A. and Johanson U. 2008. Unexpected complexity of the aquaporin gene family in the moss *Physcomitrella patens*. BMC Plant Biology 8: 45.

Das, A.B. and Strasser, R.J. 2013. Salinity-induced genes and molecular basis of salt-tolerant strategies in Mangroves. In Molecular stress physiology of plants. Edited by G.R. Rout and A.B. Das. Springer India, pp. 53-86.

Das, A., Pramanik, K., Sharma, R., Gantait, S. and Banerjee, J. 2019. In-silico study of biotic and abiotic stress-related transcription factor binding sites in the promoter regions of rice germin-like protein genes. PLoS One 14: e0211887.

Dean, R.M., Rivers, R.L., Zeidel, M.L. and Roberts, D.M. 1999. Purification and functional reconstitution of soybean nodulin 26. An aquaporin with water and glycerol transport properties. Biochemistry 38: 347-353.

Debez, A., Hamed, K.B, Grignon, C. and Abdelly, C. 2004. Salinity effects on germination, growth, and seed production of the halophyte *Cakile maritima*. Plant and Soil 262: 179-189.

Dehaan, R.L. and Taylor, G.R. 2002. Field-derived spectra of salinized soils and vegetation as indicators of irrigation-induced soil salinization. Remote Sensing of Environment 80: 406-417.

Demidchik, V., Shabala, S., Isayenkov, S., Cuin, T.A. and Pottosin, I. 2018. Calcium transport across plant membranes: mechanisms and functions. New Phytologist 220: 49-69.

Deshmukh, R.K., Sonah, H. and Bélanger, R.R., 2016. Plant aquaporins: genome-wide identification, transcriptomics, proteomics, and advanced analytical tools. Frontiers in Plant Science 7: 1896.

Deshmukh, R.K., Vivancos, J., Ramakrishnan, G., Guérin, V., Carpentier,G., Sonah, H., Labbé, C., Isenring, P., Belzile, F.J. and Bélanger, R.R. 2015. A precise spacing between the NPA domains of aquaporins is essential for silicon permeability in plants. Plant Journal 83: 489-500.

Ding, L., Milhiet, T., Meziane, A., Tardieu, F. and Chaumont, F. 2022. The plasma membrane aquaporin ZmPIP2;5 enhances the sensitivity of stomatal closure to water deficit. Plant, Cell & Environment doi :10.1111/pce.14276.

Donaldson, L.A. and Radotic, K. 2013. Fluorescence lifetime imaging of lignin autofluorescence in normal and compression wood. Journal of Microscopy 251: 178-187.

Donohue, K., Rubio de Casas, R., Burghardt, L., Kovach, K. and Willis, C.G. 2010. Germination, post germination adaptation, and species ecological ranges. Annual Review of Ecology, Evolution and Systematics 41: 293-319.

Du, X.-Q., Wang, F.-L., Hong, L., Jing, S., Yu, M., Li, J., Wu, W-H., Kudla, J. and Wanf, Y. 201). The transcription factor MYB59 regulates K^+/NO_3^- translocation in the Arabidopsis response to low K^+ stress. Plant Cell. 31: 699–714.

Dumont, S. and Rivoal, J. 2019. Consequences of oxidative stress on plant glycolytic and respiratory metabolism. Frontiers in Plant Science 10 : 166.

El Mahi, H., Pérez-Hormaeche, J., De Luca,A., Villalta, I., Espartero, J. et al. 2019. A critical role of sodium flux via the plasma membrane Na^+/H^+ exchanger SOS1 in the salt tolerance of rice. Plant Physiology 180: 1046-1065.

Enstone, D.E., Peterson, C.A. and Ma, F. 2002. Root endodermis and exodermis: structure, function, and responses to the environment. Journal of Plant Growth Regulation, 21: 335-351.

Epstein, E.X. 1972 Mineral nutrition of plants: principles and perspectives. Wiley, New York.

Equiza, M.A., Calvo-Polanco, M., Cirelli, D., Señorans, J., Wartenbe, M., Saunders, C. and Zwiazek, J.J. 2017. Long-term impact of road salt use on soil and urban trees in Edmonton, Canada. Urban Forestry and Urban Greening 21: 16-28.

Erland, L.A., Turi, C.E. and Saxena, P.K. 2016 Serotonin: An ancient molecule and an important regulator of plant processes. Biotechnology Advances 34: 1347-1361.

FAO, 2016. Agriculture: key to achieving in the 2030. Agenda for sustainable development. Food and Agriculture Organization of the United Nations, Rome.

https://sustainabledevelopment.un.org/content/documents/2313foodandagriculture.pdf (accessed September 6, 2021).

Fatemi, F., Hashemi-Petroudi, S.H., Nematzadeh, G., Askari, H. and Abdollahi, M.R. 2019. Exploiting differential gene expression to discover ionic and osmotic-associated transcripts in the halophyte grass *Aeluropus littoralis*. Biological Procedures Online 21: 14.

Fernie, A.R., Carrari, F. and Sweetlove, L.J. 2004. Respiratory metabolism: glycolysis, the TCA cycle and mitochondrial electron transport. Current Opinion in Plant Biology 7: 254-261.

Fetter, K., Van Wilder, V., Moshelion, M. and Chaumont, F. 2004. Interactions between plasma membrane aquaporins modulate their water channel activity. Plant Cell 16: 215-228.

Fischer, M. and Kaldenhoff, R. 2008. On the pH regulation of plant aquaporins. Journal of Biological Chemistry 283: 33889 –33892.

Flowers, TJ. 2014. eHALOPH Halophytes Database. https://www.sussex.ac.uk/affiliates/halophytes (accessed January 15, 2022).

Flowers, T.J. and Colmer, T.D. 2008. Salinity tolerance in halophytes. New Phytologist 179: 945-963.

Flowers, T.J., Galal, H.K. and Bromham, L. 2010. Evolution of halophytes: multiple origins of salt tolerance in land plants. Functional Plant Biology 37: 604-612.

Flowers, T.J., Munns, R. and Colmer, T.D. 2015. Sodium chloride toxicity and the cellular basis of salt tolerance in halophytes. Annals of Botany 115: 419-431.

Flowers, T.J., Troke, P.F. and Yeo, A.R. 1977. The mechanism of salt tolerance in halophytes. Annual Review of Plant Physiology 28: 89-121.

Forest Research. 2020. Forest hydrology – how much water do forests use? https://www.forestresearch.gov.uk/research/forest-hydrology/forest-hydrology-how-much-water-do-forests-use/ (accessed June 5, 2020).

Foroutan, A., Guo, A.C., Vazquez-Fresno, R., Lipfert, M., Zhang, L., Zheng, J., et al. 2009. Chemical composition of commercial cow's milk. Journal of Agricultural and Food Chemistry 67: 4897–4914

Foroutan, A., Fitzsimmons, C., Mandal, R., Piri-Moghadam, H., Zheng, J., Guo, A., Li, C., Guan, L.L. and Wishart, D.S. 2020. The bovine metabolome. Metabolites 10: 233.

Fox, A.R., Maistriaux, L.C. and Chaumont, F. 2017. Toward understanding of the high number of plant aquaporin isoforms and multiple regulation mechanisms. Plant Science 264: 179-187.

Foyer, C.H. and Noctor, G. 2005. Oxidant and antioxidant signalling in plants: a re-evaluation of the concept of oxidative stress in a physiological context. Plant, Cell and Environment 28: 1056-1071.

Foyer, C.H. and Shigeoka, S. 2011. Understanding oxidative stress and antioxidant functions to enhance photosynthesis. Plant Physiology 155: 93-100.

Franklin, J.A. and Zwiazek, J.J. 2004. Ion uptake in *Pinus banksiana* treated with sodium chloride and sodium sulfate. Physiologia Plantarum 120: 482-490.

Fraser, C.M. and Chapple, C. 2011. The phenylpropanoid pathway in Arabidopsis. Arabidopsis Book. 9: e0152.

Frick, A., Järvå, M., Ekvall, M., Uzdavinys, P., Nyblom, M. and Törnroth-Horsefield, S. 2013. Mercury increases water permeability of a plant aquaporin through a non-cysteine-related mechanism. Biochemistry Journal 15: 491-499.

Fujiyoshi Y., Mitsuoka, K., De Groot, B.L., Philippsen, A., Grubmüller, H., Agre, P. and Engel, A. 2002. Structure and function of water channels. Current Opinion in Structural Biology 12: 509-515.

Fuglsang, A.T., Guo, Y., Cuin, T.A., Qiu, Q., Song, C., Kristiansen, K.A., Bych, K., Schulz, A., Shabala, S., Schumaker, K.S. and Palmgren M.G. 2007. Arabidopsis protein kinase PKS5 inhibits the plasma membrane H^+-ATPase by preventing interaction with 14-3-3 protein. The Plant Cell 19: 1617-1634.

Gao, T., Zhang, Z., Liu, X., Wu, Q., Chen, Q., Liu, Q., van Nocker, S., Ma, F. and Li, C. 2020. Physiological and transcriptome analyses of the effects of exogenous dopamine on drought tolerance in apple. Plant Physiology and Biochemistry 148: 260-272.

Gao, Z., He, X., Zhao, B., Zhou, C., Liang, Y., Ge, R., Shen, Y. and Huang, Z. 2010. Overexpressing a putative aquaporin gene from wheat, TaNIP, enhances salt tolerance in transgenic Arabidopsis. Plant and Cell Physiology 51: 767-775.

Geilfus, C.M. and Muehling, KH. 2012. Transient alkalinization in the leaf apoplast of *Vicia faba* L. depends on NaCl stress intensity: an *in situ* ratio imaging study. Plant, Cell & Environment 35: 578-587.

Gerbeau, P., Güçlü, J., Ripoche, P. and Maurel, C., 1999. Aquaporin Nt-TIPa can account for the high permeability of tobacco cell vacuolar membrane to small neutral solutes. Plant Journal 18: 577-587.

Glenn, E.P., Brown, J.J. and Blumwald, E. 1999. Salt tolerance and crop potential of halophytes. Critical Reviews in Plant Sciences, 18: 227-255.

Goldsmith, G.R. 2013. Changing directions: the atmosphere-plant-soil continuum. New Phytologist 199: 4-6.

Grabherr, M.G., Haas, B.J., Yassour, M., Levin, J.Z., Thompson, D.A., Amit, I., Adiconis, X., et al. 2011. Full-length transcriptome assembly from RNA-Seq data without a reference genome. Nature Biotechnology 29: 644-652.

Grant, J.N., Burris, J.N., Stewart, C.N. and Lenaghan, S.C. 2017. Improved tissue culture conditions for the emerging C4 model *Panicum hallii*. BMC Biotechnology 17: 39.

Gravelle, S., Joly, L., Detcheverry, F., Ybert, C., Cottin-Bizonne, C. and Bocquet, L. 2013. Optimizing water permeability through the hourglass shape of aquaporins. Proceedings of the National Academy of Sciences 110: 16367-16372.

Greenway, H. and Munns, R. 1980. Mechanisms of salt tolerance in nonhalophytes. Annual Review of Plant Physiology, 31: 149-190.

Grigore M.N. and Toma C. 2017. Anatomical adaptations of halophytes. Springer International Publishing AG, Cham, pp 3-28.

Groszmann, M., Osborn, H.L. and Evans, J.R. 2017. Carbon dioxide and water transport through plant aquaporins. Plant, Cell and Environment 40: 938-961.

Hachez, C. and Chaumont, F. 2010. Aquaporins: a family of highly regulated multifunctional channels. In MIPs and their role in the exchange of metalloids. Edited by T.P. Jahn and G.P. Bienert. Springer-Verlag, New York, pp. 1-17.

Hachez, C., Besserer, A., Chevalier, A.S. and Chaumont, F. 2013. Insights into plant plasma membrane aquaporin trafficking. Trends in Plant Science 18: 344-352.

Hadi, M.R. and Karimi, N. 2012. The role of calcium in plant's salt tolerance. Journal of Plant Nutrition 35: 2037-2054.

Hadi, M.R., Khiyam-Nekoie, S.M., Khavarinejad, R., Khosh, K., Sima, N.A. and Yavari, P. 2008. Accumulation and role of ions (Ca^{2+}, Mg^{2+}, SO_4^{-2}) on salt tolerance in *Triticum turgidum* L. Journal of Biological Sciences 8: 143-148.

Hanin, M., Ebel, C., Ngom, M., Laplaze, L. and Masmoudi, K. 2016. New insights on plant salt tolerance mechanisms and their potential use for breeding. Frontiers in Plant Science 7: 1787.

Harivandi, M.A., Butler, J.D. and Wu, L. 1992. Salinity and turfgrass culture. In Waddington, D.V., Carrow, R.N., Shearman, R.C. (Eds), Turfgrass. American Society of Agronomy, Madison, WI, Series No. 32., pp. 207-229.

Hasegawa, H., Zhang, R., Dohrman, A. and Verkman, A.S. 1993. Tissue-specific expression of mRNA encoding rat kidney water channel CHIP28k by in situ hybridization. American Journal of Physiology-Cell Physiology 264: C237-C245.

Hasegawa, P.M., Bressan, R.A., Zhu, J.K. and Bohnert, H.J. 2000. Plant cellular and molecular responses to high salinity. Annual Review of Plant Physiology and Plant Molecular Biology 51: 463-499.

Hastenrath, S. 1991. Climate dynamics of the tropics. Atmospheric Sciences Library, vol 8. Springer, Dordrecht.

Hauser, F. and Horie, T. 2010. A conserved primary salt tolerance mechanism mediated by HKT transporters: a mechanism for sodium exclusion and maintenance of high K^+/Na^+ ratio in leaves during salinity stress. Plant, Cell & Environment 33: 552-565.

Hazzouri, K.M., Khraiwesh, B., Amiri, K., Pauli, D., Blake, T., Shahid, M., Mullath, S.K., Nelson, D., Mansour, A.L., Salehi-Ashtiani, K., Purugganan, M. and Masmoudi, K. 2018. Mapping of HKT1;5 gene in barley using GWAS approach and its implication in salt tolerance mechanism. Frontiers in Plant Science 9: 156.

Hedrich, R. and Shabala, S. 2018. Stomata in a saline world. Current Opinion in Plant Biology 46: 87-95.

Herbert, E.R., Boon, P., Burgin, A.J., Neubauer, S.C., Franklin, R.B., Ardo´n, M., Hopfensperger, K.N., Lamers, P.M. and Gell, P. 2015. A global perspective on wetland salinization: ecological consequences of a growing threat to freshwater wetlands. Ecosphere 6: 206.

Hill, A.E., Shachar-Hill, B. and Shachar-Hill, Y. 2004. What are aquaporins for? Journal of Membrane Biology 197: 1-32.

Hirano, Y., Okimoto, N., Kadohira, I., Suematsu, M., Yasuoka, K. and Yasui, M. 2010. Molecular mechanisms of how mercury inhibits water permeation through aquaporin-1: understanding by molecular dynamics simulation. Biophysical Journal 98: 1512-1519.

Holm, L.M., Jahn, T.P., Møller, A.L., Schjoerring, J.K., Ferri, D., Klaerke, D.A. and Zeuthen, T. 2005. NH_3 and NH_4^+ permeability in aquaporin-expressing *Xenopus oocytes*. Pflügers Archiv 450: 415-428.

Hong, Y., Zhang, W. and Wang, X. 2010. Phospholipase D and phosphatidic acid signalling in plant response to drought and salinity. Plant, Cell & Environment 33: 627-635.

Horie, T., Kaneko, T., Sugimoto, G., Sasano, S., Panda, S.K., Shibasaka, M. and Katsuhara, M. 2011. Mechanisms of water transport mediated by PIP aquaporins and their regulation via phosphorylation events under salinity stress in barley roots. Plant and Cell Physiology: 52: 663-675.

Horie, T., Karahara, I. and Katsuhara, M. 2012. Salinity tolerance mechanisms in glycophytes: an overview with the central focus on rice plants. Rice 5: 11.

Hsiao, T.C. and Xu, L.K. 2000. Sensitivity of growth of roots versus leaves to water stress: biophysical analysis and relation to water transport. Journal of Experimental Botany 51: 1595-616.

Hu. L., Wang, Z. and Huang, B. 2013. Effects of cytokinin and potassium on stomatal and photosynthetic recovery of Kentucky bluegrass from drought stress. Crop Science 53: 221-231.

Hu L., Zhang P., Jiang Y., Fu J. 2015. Metabolomic analysis revealed differential adaptation to salinity and alkalinity stress in Kentucky bluegrass (*Poa pratensis*). Plant Molecular Biology Reports 33: 56–68.

Huang, C., Wei, G., Jie ,Y., Wang, L., Zhou, H., Ran, C., Huang, Z., Jia, H. and Anjum, S.A. 2014. Effects of concentrations of sodium chloride on photosynthesis, antioxidative enzymes, growth and fiber yield of hybrid ramie. Plant Physiology and Biochemistry 76: 86-93.

Huang, L., Kuang, L., Wu, L., Shen, Q., Han, Y., Jiang, L., Wu, D. and Zhang, G. 2020. The HKT transporter *HvHKT1;5* negatively regulates salt tolerance. Plant Physiology 182: 584-596.

Inan, G., Zhang, Q., Li, P., Wang, Z., Cao, Z., Zhang, H., Zhang, C., Quist, T.M., Goodwin, S.M., Zhu, J. and Shi, H. 2004. Salt cress. A halophyte and cryophyte Arabidopsis relative model system and its applicability to molecular genetic analyses of growth and development of extremophiles. Plant Physiology 135: 1718-1737.

Isayenkov, S.V. and Maathuis, F.J.M. 2019. Plant salinity stress: many unanswered questions remain. Frontiers in Plant Science 10: 80.

Ishikawa, F., Suga, S., Uemura, T., Sato, M.H. and Maeshima, M., 2005. Novel type aquaporin SIPs are mainly localized to the ER membrane and show cell-specific expression in *Arabidopsis thaliana*. FEBS Letters 579: 5814-5820.

Israel, D., Khan, S. Warren, C.R., Zwiazek, J.J., Robson, T.M. 2021. The contribution of PIP2-type aquaporins to photosynthetic response to increased vapour pressure deficit. Journal of Experimental Botany 72: 5066-5078.

Jaleel, C.A., Manivannan, P., Sankar, B., Kishorekumar, A., Gopi, R., Somasundaram, R. and Panneerselvam, R. 2007, Water deficit stress mitigation by calcium chloride in *Catharanthus roseus*: Effects on oxidative stress, proline metabolism and indole alkaloid accumulation. Colloids and Surfaces B: Biointerfaces 60: 110-116.

Javot, H. and Maurel, C. 2002. The role of aquaporins in root water uptake. Annals of Botany 90: 301-313.

Ji, H., Pardo, J.M., Batelli, G., Van Oesten M.J., Bressane R.A. and Li Xia. 2013. The salt overly sensitive (SOS) pathway: established and emerging roles. Molecular Plant 6: 275-286.

Jiménez-Arias, D., García-Machado, F.J., Morales-Sierra, S., García-García, A.L., Herrera, A.J., Valdés, F., Luis, J.C. and Borges, A.A. 2021. A beginner's guide to osmoprotection by biostimulants. Plants 10, 363.

Jimenez-Casas, M. and Zwiazek, J.J. 2014. Adventitious sprouting in *Pinus leiophylla* in response to injury caused by salt stress. Annals of Forest Science 71: 811-819.

Jogawat, A. 2019. Osmolytes and their role in abiotic stress tolerance in plants. In Molecular plant abiotic stress: biology and biotechnology. Edited by A. Roychoudhury and D. Tripathi. John Wiley & Sons Ltd., Hoboken, pp. 91-104.

Johanson, U. and Gustavsson, S. 2002. A new subfamily of major intrinsic proteins in plants. Molecular Biology and Evolution 19: 456-461.

Johanson, U., Karlsson, M., Johansson, I., Gustavsson, S., Sjövall, S., Fraysse, L., Weig, A.R. and Kjellbom, P., 2001. The complete set of genes encoding major intrinsic proteins in Arabidopsis provides a framework for a new nomenclature for major intrinsic proteins in plants. Plant Physiology 126: 1358-1369.

Joo, S., Liu, Y., Lueth, A. and Zhang, S. 2008. MAPK phosphorylation-induced stabilization of ACS6 protein is mediated by the non-catalytic C-terminal domain, which also contains the cis-determinant for rapid degradation by the 26S proteasome pathway. Plant Journal 54: 129-140.

Kamaluddin, M. and Zwiazek, J.J. 2001. Metabolic inhibition of root water transport in red-osier dogwood (*Cornus stolonifera*) seedlings. Journal of Experimental Botany 52: 739-745.

Kaneko, T., Horie, T., Nakahara, Y., Tsuji, N., Shibasaka, M. and Katsuhara, T. 2015. Dynamic regulation of root hydraulic conductivity of barley plants in response to salinity/osmotic stress. Plant, Cell & Physiology 56: 875-882.

Kant, S., Kant, P., Raveh, E. and Barak, S. 2006. Evidence that differential gene expression between the halophyte, *Thellungiella halophila*, and *Arabidopsis thaliana* is responsible for higher levels of the compatible osmolyte proline and tight control of Na^+ uptake in *T. halophila*. Plant, Cell & Environment 29: 1220-1234.

Kapilan, R., Vaziri, M. and Zwiazek, J.J., 2018. Regulation of aquaporins in plants under stress. Biological Research 51: 4.

Karahara, I., Umemura, K., Soga, Y., Akai, Y., Bando, T., Ito, Y., Tamaoki, D., et al. 2012. Demonstration of osmotically dependent promotion of aerenchyma formation at different levels in the primary roots of rice using a 'sandwich' method and X-ray computed tomography. Annals of Botany 110: 503-509.

Katsuhara, M. and Hanba, Y.T. 2008 Barley plasma membrane intrinsic proteins (PIP aquaporins) as water and CO_2 transporters. Pflugers Archiv European Journal of Physiology 456: 687-691.

Katsuhara, M., Rhee, J.Y., Sugimoto, G. and Chung, G.C. 2011. Early response in water relations influenced by NaCl reflects tolerance or sensitivity of barley plants to salinity stress via aquaporins. Soil Science and Plant Nutrition 57: 50-60.

Khan, M.S., Khan, M.A. and Ahmad, D. 2016. Assessing utilization and environmental risks of important genes in plant abiotic stress tolerance. Frontiers in Plant Science 7: 792.

Khan, S., Thomas, B.R., De la Mata, R., Randall, M.J., Zhang, W-Q. and Zwiazek, J.J. 2019. Variation in aquaporin and physiological responses among *Pinus contorta* families under different moisture conditions. Plants 8: 13.

Kim, Y.X., Ranathunge, K., Lee, S., Lee, Y., Lee, D. and Sung, J. 2018. Composite transport model and water and solute transport across plant roots: an update. Frontiers in Plant Science 9: 193.

Kirch, H.H., Vera-Estrella, R., Golldack, D., Quigley, F., Michalowski, C.B., Barkla, B.J. and Bohnert, H.J. 2000. Expression of water channel proteins in *Mesembryanthemum crystallinum*. Plant Physiology 123: 111-124.

Kitchen, P., Salman, M.M., Pickel, S.U., Jennings, J., Törnroth-Horsefield, S., Conner, M.T., Bill, R.M. and Conner, A.C. 2019. Water channel pore size determines exclusion properties but not solute selectivity. Scientific Reports 9: 1-14.

Knipfer, T. and Fricke W. 2010. Root pressure and a solute reflection coefficient close to unity exclude a purely apoplastic pathway of radial water transport in barley (*Hordeum vulgare*). New Phytologist 187: 159-170.

Knipfer, T., Danjou, M., Vionne, C. and Fricke, W. 2021. Salt stress reduces water uptake in barley (*Hordeum vulgare* L.) through modification of the transcellular path. Plant, Cell & Environment 44: 458-475.

Knipfer, T., Besse, M., Verdeil, J.-L. and Fricke, W. 2011. Aquaporin-facilitated water uptake in barley (*Hordeum vulgare* L.) roots. Journal of Experimental Botany 62: 4115-4126.

Kobayashi, N.I., Yamaji, N., Yamamoto, H., Okubo, K., Ueno, H., Costa, A., Tanoi, K., et al. 2017. OsHKT1;5 mediates Na^+ exclusion in the vasculature to protect leaf blades and reproductive tissues from salt toxicity in rice. Plant Journal 91: 657-670.

Korbie, D. J. and Mattick, J.S. 2008. Touchdown PCR for increased specificity and sensitivity in PCR amplification. Nature Protocols 3: 1452-1456.

Kortenoeven, M.L. and Fenton, R.A. 2014. Renal aquaporins and water balance disorders. Biochimica et Biophysica Acta (BBA) - General Subjects 1840: 1533-1549.

Kourghi, M., Nourmohammadi, S., Pei, J.V., Qiu, J., McGaughey, S., Tyerman, S.D., Byrt, C.S, and Yool, A. 2017. Divalent cations regulate the ion conductance properties of diverse classes of aquaporins. International Journal of Molecular Sciences 16: 2323.

Kramer, P.J. and Boyer, J.S. 1995. Water relations of plants and soils. Academic Press, New York.

Kronzucker, H.J. and Britto, D.T. 2011. Sodium transport in plants: a critical review. New Phytologist 189: 54-81.

Kulma, A. and Szopa, J. 2007. Catecholamines are active compounds in plants. Plant Science 172: 433–440.

Kumar, S., Stecher, G. and Tamura, K. 2016. Mega7: molecular evolutionary genetics analysis version 7.0 for bigger datasets. Molecular Biology and Evolution 33: 1870-1874.

Kumari, A. and Bhatla, S.C. 2021. Regulation of salt-stressed sunflower (*Helianthus annuus*) seedling's water status by the coordinated action of Na^+/K^+ accumulation, nitric oxide, and aquaporin expression. Functional Plant Biology 48: 573. Lee, S.H., Calvo-Polanco, M., Chung G.C. and Zwiazek J.J. 2010. Role of aquaporins in root water transport of

ectomycorrhizal jack pine (*Pinus banksiana*) seedlings exposed to NaCl and fluoride. Plant, Cell & Environment 33: 769-780.

Kwon, O.K., Mekapogu, M. and Kim, K.S. 2019. Effect of salinity stress on photosynthesis and related physiological responses in carnation (*Dianthus caryophyllus*). Horticulture, Environment, and Biotechnology 60: 831-839.

Lalonde, R.S., Pinno, B.D., MacKenzie, D. and Utting, N. 2020. Capping dewatered oil sands fluid fine tailings with salvaged reclamation soils at varying depths to grow woody plants. Canadian Journal of Soil Science 100: 546-557.

Lambers, H., Chapin III, F.S. and Pons, T.L. 2008. Plant physiological ecology, 2nd edition. Springer Science & Business Media, New York.

Langmead, B. and Salzberg, S.L. 2012. Fast gapped-read alignment with Bowtie 2. Nature Methods 9: 357–359.

Lee, S.H. and Zwiazek, J.J. 2015. Regulation of aquaporin-mediated water transport in Arabidopsis roots exposed to NaCl. Plant and Cell Physiology 56: 750-758.

Lee, S.H. and Zwiazek, J.J. 2019. Regulation of water transport in Arabidopsis by methyl jasmonate. Plant Physiology and Biochemistry 139: 540-547.

Lee, S.H., Calvo Polanco, M., Chung, G.C., Zwiazek, J.J. 2010. Role of aquaporins in root water transport of ectomycorrhizal (*Pinus banksiana*) seedlings exposed to NaCl and fluoride. Plant, Cell & Environment 33:769-780.

Lee, S.H., Chung, G.C. and Zwiazek, J.J. 2009. Light decreases cell hydraulic conductivity and turgor pressure in bundle sheath cells of tobacco (*Nicotiana tabacum*) leaves. Plant Science 176: 248-255.

Lee, S.H., Chung, G.C., Jang, J.Y, Ahn, S.J., Hong, S.-W. and Zwiazek J.J. 2012. Overexpression of PIP2;5 aquaporin alleviates effects of low root temperature on cell hydraulic conductivity and growth in Arabidopsis. Plant Physiology 159: 479–488.

Lewis, L.A. and McCourt, R.M. 2004. Green algae and the origin of land plants. American Journal of Botany 91: 1535-1556.

Levitt, J. 1972. Responses of Plant to Environmental Stresses. Academic Press, New York.

Li, C., Sun, X., Chang, C., Jia, D., Wei, Z., Li, C. and Ma, F. 2015. Dopamine alleviates salt-induced stress in *Malus hupehensis*. Physiologia Plantarum 153, 584-602.

Li, H.W., Zang, B.S., Deng, X.W. and Wang, X.P. 2011. Overexpression of the trehalose-6-phosphate synthase gene OsTPS1 enhances abiotic stress tolerance in rice. Planta 234: 1007-1018.

Li, T., Hu, Y.J., Hao, Z.P., Li, H. and Chen, B.D. 2013. Aquaporin genes GintAQPF1 and GintAQPF2 from *Glomus intraradices* contribute to plant drought tolerance. Plant Signaling & Behavior 8: e24030.

Liang, W., Ma, X., Wan, P. 2018. Plant salt-tolerance mechanism: a review. Biochemical and Biophysical Research Communications 495: 286-291.

Lin, R., Zheng, J., Pu, L., Wang, Z., Mei, Q., Zhang, M. and Jian, S. 2021. Genome-wide identification and expression analysis of aquaporin family in *Canavalia rosea* and their roles in the adaptation to saline-alkaline soils and drought stress. BMC Plant Biology 21: 333.

Liu, J., Equiza, M.A., Navarro-Rodenas, A., Lee, S.H. and Zwiazek, J.J. 2014. Hydraulic adjustments in aspen (*Populus tremuloides*) seedlings following defoliation involve root and leaf aquaporins. Planta 240: 553-564.

Liu, M., Tan, X., Sun, X. and Zwiazek, J.J. 2020. Properties of root water transport in canola (*Brassica napus*) subjected to waterlogging at the seedling, flowering and podding growth stages. Plant and Soil 454: 431-445.

Liu, M. and Zwiazek J.J. 2022. Oxidative stress impedes recovery of canola (*Brassica napus*) plants from waterlogging by inhibiting aquaporin-mediated root water transport. Environmental and Experimental Botany 200: 104931

Liu, S.Y., Fukumoto, T., Gena, P., Feng, P., Sun, Q., Li, Q., Matsumoto, T., Kaneko, T., Zhang, H., Zhang, J., Zhong, S., Zeng, W., Katsuhara, M., Kitagawa, Y., Wang, A., Calamita, G. and Ding, X. 2020. Ectopic expression of a rice plasma membrane intrinsic protein (OsPIP1;3) promotes plant growth and water uptake. Plant Journal 102: 779–796.

Liu, Q., Gao, T., Liu, W., Liu, Y., Zhao, Y., Liu, Y., Li, W., Ding, K., Ma, F. and Li, C. 2020a. Functions of dopamine in plants: a review. Plant. Signaling and Behavior 15: 1827782.

Liu, S., Fukumoto, T., Gena, P., Feng, P., Sun, Q., Li, Q., Matsumoto, T., Kaneko, T., Zhang, H., Zhang, Y., Zhong, S., Zeng, W., Katsuhara, M., Kitagawa, Y., Wang, A., Calamita, G. and Ding, X. 2020. Ectopic expression of a rice plasma membrane intrinsic protein (OsPIP1;3) promotes plant growth and water uptake. Plant Journal 102: 779-796.

Liu, X., Cheng, J., Jiang, F., Liang, M., Han, J., Zhang, J., Zhang, H. and Tang, X. (2020b). The tonoplast intrinsic protein gene KvTIP3 is responsive to different abiotic stresses in *Kosteletzkya virginica*. BioMed Research International 2020: 2895795.

Liu, Y. and Zhang, S. 2004) Phosphorylation of 1-aminocyclopropane-1-carboxylic acid synthase by MPK6, a stress-responsive mitogen-activated protein kinase, induces ethylene biosynthesis in Arabidopsis. Plant Cell 16: 3386-3399.

Liu, Y., Ding, X., Lv, Y., Cheng, Y., Li, C., Yan, L., Tian, S. and Zou, X. 2021. Exogenous serotonin improves salt tolerance in rapeseed (*Brassica napus* L.) seedlings. Agronomy. 11: 400.

Livak, K.J. and Schmittgen, T.D. 2001. Analysis of relative gene expression data using real-time quantitative PCR and the $2^{-\Delta\Delta C}_{\mathrm{T}}$ method. Methods 25: 402-408.

Locascio, A., Andrés-Colás, N., Mulet, J. M. and Yenush, L. 2019. *Saccharomyces cerevisiae* as a tool to investigate plant potassium and sodium transporters. International Journal of Molecular Sciences 20: 2133.

López-Berenguer, C., Garcia-Viguera, C. And Carvajal, M. 2006. Are root hydraulic conductivity responses to salinity controlled by aquaporins in broccoli plants? Plant and Soil 279: 13-23.

López-Pérez, L., Martínez-Ballesta, M.C., Maurel, C. and Carvajal, M. 2009. Changes in plasma membrane lipids, aquaporins and proton pump of broccoli roots, as an adaptation mechanism to salinity. Phytochemistry 70: 492-500.

Luu, D.T. and Maurel, C. 2013. Aquaporin trafficking in plant cells: An emerging membrane-protein model. Traffic 14: 629-635.

Luu, D.T., Martiniere, A., Sorieul, M., Runions, J. and Maurel, C. 2012. Fluorescence recovery after photobleaching reveals high cycling dynamics of plasma membrane aquaporins in Arabidopsis roots under salt stress. Plant Journal 69: 894-905.

Lux, A., Luxova, M., Abe, J. and Morita, S. 2004. Root cortex: structural and functional variability and responses to environmental stress. Root Research 13: 117-131.

Ma J.F. and Yamaji N. 2006. Silicon uptake and accumulation in higher plants. Trends in Plant Science 11: 392–397.

Ma, J.F., Tamai, K., Yamaji, N., Mitani, N., Konishi, S., Katsuhara, M., Ishiguro, M., Murata, Y. and Yano, M., 2006. A silicon transporter in rice. Nature 440: 688-691.

Machado, R.M.A. and Serralheiro, R.P. 2017. Soil salinity: effect on vegetable crop growth. Management practices to prevent and mitigate soil salinization. Horticulturae 3: 30.

Madeira, A., Moura, T.F. and Soveral, G. 2016. Detecting aquaporin function and regulation. Frontiers in Chemistry 4: 3.

Marchiosi, R., Soares, A.R., Abrahão, J., dos Santos, W.D. and Ferrarese-Filho, O. 2020. L-DOPA and dopamine in plant metabolism. In Neurotransmitters in plant signaling and communication. Signaling and communication in plants. Baluška F., Mukherjee S. and Ramakrishna A. (Eds). Cham: Springer.

Martinez-Ballesta, M.C., Aparicio, F., Pallas, V., Martinez, V. and Carvajal, M. 2003. Influence of saline stress on root hydraulic conductance and PIP expression in Arabidopsis. Journal of Plant Physiology 160: 689-697.

Martinez-Ballesta, M.C., Cabanero, F., Olmos, E., Periago, P.M., Maurel, C. and Carvajal, M. 2008. Two different effects of calcium on aquaporins in salinity-stressed pepper plants. Planta 228: 15-25.

Maurel, C. 2007. Plant aquaporins: novel functions and regulation properties. FEBS Letters, 581: 2227-2236.

Maurel, C., Boursiac, Y., Luu, D.T., Santoni, V., Shahzad, Z. and Verdoucq, L. 2015. Aquaporins in plants. Physiological Reviews 95: 1321-1358.

Maurel, C., Verdoucq, L., Luu, D.T. and Santoni, V. 2008. Plant aquaporins: membrane channels with multiple integrated functions. Annual Review of Plant Biology 59: 595-624.

Maurel, C., Verdoucq, L., Rodrigues, O. 2016. Aquaporins and plant transpiration. Plant, Cell & Environment 39: 2580-2587.

Maxwell, B.B., Andersson, C.R., Poole, D.S., Kay, S.A. and Chory, J. 2003. HY5, Circadian Clock-Associated 1, and a cis-element, DET1 dark response element, mediate DET1 regulation of chlorophyll a/b-binding protein 2 expression. Plant Physiology 133: 1565-1577.

McCully, M.E. 1999. Roots in soil: unearthing the complexities of roots and their rhizospheres. Annual Review of Plant Biology 50: 695-718.

McElrone, A.J., Choat, B., Gambetta, G.A. and Brodersen, C.R. 2013. Water uptake and transport in vascular plants. Nature Education Knowledge 4: 6.

McFarlane, D.J., George, R.J., Barrett-Lennard, E.G. and Gilfedder, M. 2016. Salinity in dryland agricultural systems: challenges and opportunities. In Innovations in dryland agriculture. Edited by M. Farook and K.H.M. Siddique. Springer Nature, Cham, pp. 521-547.

McGaughey, S.A., Qiu, J., Tyerman, S.D. and Byrt, C.S. 2018. Regulating root aquaporin function in response to changes in salinity. Annual Plant Reviews Online 4: 381-416.

McLoughlin, F. and Testerink, C. 2013. Phosphatidic acid, a versatile water-stress signal in roots. Frontiers in Plant Science 4: 525.

Miller, G., Shulaev, V. and Mittler, R. 2008. Reactive oxygen signaling and abiotic stress. Physiologia Plantarum 133: 481-489.

Mirzavand, M., Ghasemieh, H., Sadatinejad, S.J. and Bagheri, R. 2020. An overview on source, mechanism and investigation approaches in groundwater salinization studies. International Journal of Environmental Science and Technology 17: 2463-2476.

Mishra, A. and Tanna, B. 2017. Halophytes: potential resources for salt stress tolerance genes and promoters. Frontiers in Plant Science 8: 829.

Moeller, H.B., Olesen, E.T. and Fenton, R.A. 2011. Regulation of the water channel aquaporin-2 by posttranslational modification. American Journal of Physiology-Renal Physiology 300: F1062-F1073.

Morgan, S.H., Lindberg, S., Maity, P.J., Geilfus, C.M., Plieth, C. and Mühling, K.H. 2017. Calcium improves apoplastic - cytosolic ion homeostasis in salt-stressed *Vicia faba* leaves. Functional Plant Biology 44: 515-524.

Morgan, S.H., Maity, P.J., Geilfus, C.M, Lindberg, S. and Mühling, K.H. 2014 Leaf ion homeostasis and plasma membrane H^+-ATPase activity in *Vicia faba* change after extra calcium and potassium supply under salinity. Plant Physiology and Biochemistry 82: 244-253.

Morsomme, P. and Boutry, M. 2000. The plant plasma membrane H^+-ATPase: structure, function and regulation. Biochimica et Biophysica Acta (BBA)-Biomembranes 1465: 16.

Mueller-Roeber, B. and Pical, C. 2002. Inositol phospholipid metabolism in Arabidopsis. Characterized and putative isoforms of inositol phospholipid kinase and phosphoinositide-specific phospholipase C. Plant Physiology 130: 22-46.

Muhsin, T.M. and Zwiazek, J.J. 2002. Ectomycorrhizae increase water conductance and protect white spruce (*Picea glauca*) seedlings against salt stress. Plant and Soil 238: 217-225.

Müller, M., Kunz, H.H., Schroeder, J.I., Kemp, G., Young, H.S. and Neuhaus, H.E. 2014. Decreased capacity for sodium export out of Arabidopsis chloroplasts impairs salt tolerance, photosynthesis, and plant performance. Plant Journal 78: 646-658.

Munns, R. 2002. Comparative physiology of salt and water stress. Plant, Cell & Environment 25: 239-250.

Munns, R. 2005. Genes and salt tolerance: bringing them together. New Phytologist 167: 645-663.

Munns, R. and Tester, M. 2008. Mechanisms of salinity tolerance. Annual Review of Plant Biology 59: 651-681.

Munns, R., Day, D., Fricke, W., et al. 2020. Energy costs of salt tolerance in crop plants. New Phytologist 225 : 1072-1090.

Munns, R., James, R.A., Xu B., et al. 2012. Wheat grain yield on saline soils is improved by an ancestral Na^+ transporter gene. Nature Biotechnology 30: 360-364.

Murashige, T. and Skoog, F. 1962. A revised medium for rapid growth and bio assays with tobacco tissue cultures. Physiologia Plantantarum 15: 473-497.

Murata, K., Mitsuoka, K., Hirai, T., Walz, T., Agre, P., Heymann, J.B., Engel, A. and Fujiyoshi, Y. 2000. Structural determinants of water permeation through aquaporin-1. Nature 40: 599-605.

Mustafa, G., Akhtar, M.S. and Abdullah, R. 2019. Global concern for salinity on various agro-ecosystems. In Salt stress, microbes, and plant Interactions. Volume 1. Edited by S. Akhtar. Springer, Singapore, pp. 1-20.

Nardini, A., Gasco, A., Trifilo, P., Lo Gullo, M.A. and Salleo, S. 2007. Ion-mediated enhancement of xylem hydraulic conductivity is not always suppressed by the presence of Ca^{2+} in the sap. Journal of Experimental Botany 58: 2609-2615.

Nguyen, H., Calvo-Polanco, M. and Zwiazek, J.J. 2006. Gas exchange and growth responses of ectomycorrhizal *Picea mariana*, *Picea glauca*, and *Pinus banksiana* seedlings to NaCl and Na_2SO_4. Plant Biology 8: 646-652.

Nesverova, V. and Törnroth-Horsefield, S. 2019. Phosphorylation-dependent regulation of mammalian aquaporins. Cells 8: 82.

Nikalje, G.C., Mirajkar, S.J., Nikam, T.D. and Suprasanna P. 2018. Multifarious role of ROS in halophytes: signaling and defense. In Abiotic stress-mediated sensing and signaling in plants: and omics perspective. Edited by S.M. Zargar and M.Y. Zargar. Springer, Singapore, pp. 207-223.

Nikalje, G.C., Nikam, T.D. and Suprasanna, P. 2017. Looking at halophytic adaptation to high salinity through genomics landscape. Current Genomics 18: 542–552.

Nozaki, K., Ishii, D., and Ishibashi, K. (2008). Intracellular aquaporins: clues for intracellular water transport? Pflugers Arch. 456, 701-707.

Oi, T., Hirunagi, K., Taniguchi, M. and Miyakea, H. 2013. Salt excretion from the salt glands in Rhodes grass (*Chloris gayana* Kunth) as evidenced by low-vacuum scanning electron microscopy. Flora. 208: 52-57.

Okumoto, S., Koch, W., Tegeder, M., Fischer, W.N., Biehl, A., Leister, D., Stierhof, Y.D. and Frommer, W.B. (2004). Root phloem-specific expression of the plasma membrane amino acid proton co-transporter AAP3. Journal of Experimental Botany 55: 2155-2168.

Okur, B. and Örçen, N. 2020. Climate change and soil interactions: Elsevier, Amsterdam, The Netherlands.

Oliveros, J.C. 2007-2015. Venny. An interactive tool for comparing lists with Venn's diagrams. Available online at: https://bioinfogp.cnb.csic.es/tools/venny/index.html.

Oui, T., Clode, P.L., Taniguchi, M., Colmer, T.D. and Kotula, L. 2022. Salt tolerance in relation to elemental concentrations in leaf cell vacuoles and chloroplasts of a C_4 monocotyledonous halophyte. Plant, Cell & Environment 45: 1490-1506.

Palchetti, M.V., Reginato, M., Llanes, A., Hornbacher, J., Papenbrock, J., Barboza, G.E., Luna, V. and Cantero, J.J. 2021. New insights into the salt tolerance of the extreme halophytic species *Lycium humile* (Lycieae, Solanaceae). Plant Physiology and Biochemistry 163: 166–177.

Palmgren, M.G. 2001. Plant plasma membrane H^+-ATPases: powerhouses for nutrient uptake. Annual Review of Plant Biology 52: 817-845.

Pan, X., Geng, Y., Zhang, W., Li, B. and Chen, J. 2006. The influence of abiotic stress and phenotypic plasticity on the distribution of invasive *Alternanthera philoxeroides* along a riparian zone. Acta Oecologica 30: 333-341.

Pang, Z., Chong, J., Zhou, G., de Lima Morais, D A, Chang, L., Barrette, M., Gauthier, C., Jacques, P.E., Li, S. and Xia, J. 2021. MetaboAnalyst 5.0: narrowing the gap between raw spectra and functional insights. Nucleic Acids Research 49: W388-W396.

Pankova, Y.I. and Konyushkova, M.V. 2014. Effect of global warming on soil salinity of the arid regions. Russian Agricultural Sciences 39: 464-467.

Pannell, D.J. and Ewing, M.A., 2006. Managing secondary dryland salinity: options and challenges. Agricultural Water Management 80: 41-56.

Pardo, F.E., Hilal, M.B., Albornoz, P.L., Gallardo, M.G. and Ruiz, V.E. 2017. Anatomical and physiological responses of four quinoa cultivars to salinity at seedling stage. Indian Journal of Science and Technology 10: 1-12.

Parida, A.K. and Das, A.B. 2005. Salt tolerance and salinity effects on plants: a review. Ecotoxicology and Environmental Safety 60: 324-349.

Parre, E., Ghars, M.A., Leprince, A.S., Thiery, L., Lefebvre, D., Bordenave, M., Richard, L., Mazars, C., Abdelly, C. and Savoure, A. 2007. Calcium signaling via phospholipase C is essential for proline accumulation upon ionic but not nonionic hyperosmotic stresses in Arabidopsis. Plant Physiology 144: 503-512.

Patel, M.K., Mishra, A. and Jha, B. 2016. Untargeted metabolomics of halophytes. In Marine omics: principles and applications. Edited by S.-K. Kim. CRC Press, New York, pp. 309-328.

Paul, S., Roychoudhury, A., Banerjee, A. et al. 2017. Seed pre-treatment with spermidine alleviates oxidative damages to different extent in the salt (NaCl)-stressed seedlings of three indica rice cultivars with contrasting level of salt tolerance. Plant Gene 11: 112–123.

Pawłowicz, I., Rapacz, M., Perlikowski, D., Gondek, K. and Kosmala, A. 2017. Abiotic stresses influence the transcript abundance of *PIP* and *TIP* aquaporins in *Festuca* species. Journal of Applied Genetics 58: 421-435.

Pellegrini-Calace, M., Maiwald, T. and Thornton, J.M. 2009. Porewalker: a novel tool for the identification and characterization of channels in transmembrane proteins from their three-dimensional structure. PLoS Computational Biology 5: e1000440

Percey, W.J., McMinn, A., Bose, J., Breadmore, M.C., Guijt, R.M. and Shabala, S. 2016. Salinity effects on chloroplast PSII performance in glycophytes and halophytes. Functional Plant Biology 43: 1003-1015.

Pertea, G., Huang, X., Liang, F., Antonescu, V., Sultana, R., Karamycheva, S., Lee, Y., et al. 2003. TIGR Gene Indices clustering tools (TGICL): a software system for fast clustering of large EST datasets. Bioinformatics 19: 651-652.

Prak, S., Hem, S., Boudet, J., Viennois, G., Sommerer, N., Rossignol, M., Maurel, C. and Santoni, V. 2008. Multiple phosphorylations in the C-terminal tail of plant plasma membrane aquaporins: role in subcellular trafficking of AtPIP2;1 in response to salt stress. Molecular and Cellular Proteomics 7: 1019-1030.

Pravda, L., Sehnal, D., Toušek, D., Navrátilová, V., Bazgier, V., Berka, K., Svobodová Vařeková, R., Koča, J. and Otyepka, M. 2018. Moleonline: a web-based tool for analyzing channels, tunnels and pores (2018 update). Nucleic Acids Research 46: W368–W373.

Putney, J.W. and Tomita, T.-E. 2012. Phospholipase C signaling and calcium influx. Advances in Biological Regulation 52: 152-164.

Qian, Z.-J., Song, J.-J., Chaumont, F. and Ye, Q. 2015. Differential responses of plasma membrane aquaporins in mediating water transport of cucumber seedlings under osmotic and salt stresses Plant, Cell & Environment 38: 461-473.

Qiu, J., McGaughey, S.A., Groszmann, M., Tyerman, S.D. and Byrt, C.S. 2020. Phosphorylation influences water and ion channel function of AtPIP2;1. Plant, Cell & Environment 43: 2428-2442.

Quan, R., Lin, H., Mendoza, I., Zhang, Y., Cao, W., Yang, Y., Shang, M., Chen, S., Pardo, J.M. and Guo, Y. 2007. SCABP8/CBL10, a putative calcium sensor, interacts with the protein kinase SOS2 to protect Arabidopsis shoots from salt stress. Plant Cell 19: 1415-1431.

Rahman, M.M., Mostofa, M.G., Keya, S.S., Siddiqui, M.N., Ansary, M., Das, A.K., Rahman, M.A. and Tran, L.S. 2021. Adaptive mechanisms of halophytes and their potential in improving salinity tolerance in plants. International Journal of Molecular Sciences 22: 10733.

Ramos, J., Lopez, M.J. and Benlloch, M. 2004. Effect of NaCl and KCl salts on the growth and solute accumulation of the halophyte *Atriplex nummulari*a. Plant and Soil 259: 163-168.

Ranganathan, K., Cooke, J.E., El Kayal, W., Equiza, M.A., Vaziriyeganeh, M. and Zwiazek, J.J. 2017. Over-expression of PIP2; 5 aquaporin alleviates gas exchange and growth inhibition in poplars exposed to mild osmotic stress with polyethylene glycol. Acta Physiologiae Plantarum 39: 1-9.

Rasouli, F., Kiani-Pouya, A., Tahir, A., Shabala, L., Chen, Z. and Shabala, S. 2021. A comparative analysis of stomatal traits and photosynthetic responses in closely related halophytic and glycophytic species under saline conditions. Environmental and Experimental Botany 181: 104300.

Ray, P.D., Huang, B.-W. and Tsuji, Y. 2012. Reactive oxygen species (ROS) homeostasis and redox regulation in cellular signaling. Cell Signaling 24: 981-990.

Reddy, I.N.B.L., Kim,S.M., Kim, B.K., Yoon, I.S. and Kwon, T.R. 2017. Identification of rice accessions associated with K^+/Na^+ ratio and salt tolerance based on physiological and molecular responses. Rice Science 24: 360-364.

Ren, S., Ma, K., Lu, Z., Chen, G., Cui, J., Tong, P., Wang, L., Teng, N. and Jin, B. 2019. Transcriptomic and metabolomic analysis of the heat-stress response of *Populus tomentosa* Carr. Forests 10: 383.

Ren, Z.H., Gao, J.P., Li, L.G., Cai, X.L., Huang, W., Chao, D.Y., Zhu, M.Z., Wang, Z.Y., Luan, S. and Lin, H.X. 2005. A rice quantitative trait locus for salt tolerance encodes a sodium transporter. Nature Genetics 37: 1141-1146.

Rios, J.J., Martinez-Ballesta, M.C., Ruiz, J.M., Blasco, B. and Carvajal, M. 2017. Silicon-mediated improvement in plant salinity tolerance: the role of aquaporins. Frontiers in Plant Science 8: 948.

Roschzttardtz, H., Conejero, G., Curie, C. and Mari, S. 2009. Identification of the endodermal vacuole as the iron storage compartment in the Arabidopsis embryo. Plant Physiology 151: 1329-1338.

Roy, S. and Chakraborty, U. 2014. Salt tolerance mechanisms in salt tolerant grasses (STGs) and their prospects in cereal crop improvement. Botanical Studies 55: 31.

Sade, N., Weng, F., Tajima, H., Zeron, Y., Zhang, L., del Mar Rubio Wilhelmi, M., Peleg, Z. and Blumwald, E. 2020. A cytoplasmic receptor-like kinase contributes to salinity tolerance. Plants 9: 1383.

Sairam, R.K. and Tyagi, A. 2004. Physiology and molecular biology of salinity stress tolerance in plants. Current Science 86: 407–421.

Saitou, N. and Nei, M. 1987. The neighbor-joining method: A new method for reconstructing phylogenetic trees. Molecular Biology and Evolution, 4: 406-425.

Sakurai, J., Ahamed, A., Murai, M., Maeshima, M. and Uemura, M. 2008. Tissue and cell-specific localization of rice aquaporins and their water transport activities. Plant and Cell Physiology 49: 30-39.

Sakurai, J., Ishikawa, F., Yamaguchi, T., Uemura, M. and Maeshima, M. 2005. Identification of 33 rice aquaporin genes and analysis of their expression and function. Plant and Cell Physiology, 46: 1568-1577.

Saslis-Lagoudakis, C.H., Moray, C. and Bromham, L. 2014. Evolution of salt tolerance in angiosperms: a phylogenetic approach. In Plant ecology and evolution in harsh environments. Edited by N. Rajakuruna, R.S. Boyd and T.B. Harris. Nova Science Publishers, Hauppauge, NY, pp. 77-95.

Scotto–Lavino, E., Du, G. and Frohman, M.A. 2006. 3′ end cDNA amplification using classic race. Nature Protocols 1: 2742-2745.

Sengupta, S., Patra, B., Ray, S. and Majumder, A.L. 2008. Inositol methyl transferase from a halophytic wild rice, *Porteresia coarctata* Roxb. (Tateoka): regulation of pinitol synthesis under abiotic stress. Plant, Cell & Environment 31: 1442–1459.

Šesták, Z., Catský, J. and Jarvis, P.G. 1971. Plant photosynthetic production. Manual of methods. Dr. W. Junk n.v. Publishers, The Hague, Netherlands.

Shabala, S. 2013. Learning from halophytes: physiological basis and strategies to improve abiotic stress tolerance in plants. Annals of Botany 112: 1209-1221.

Shabala, S., Bose, J. and Hedrich, R. 2014. Salt bladders: do they matter? Trends in Plant Science 19: 687-691.

Shabala, S. and Cuin, T.A. 2008. Potassium transport and plant salt tolerance. Physiologia Plantarum 133: 651-669.

Shabala, S., Demidchik, V., Shabala, L., Cuin, T.A., Smith, S.J., Miller, A.J., Davies, J.M. and Newman, I.A. 2006. Extracellular Ca^{2+} ameliorates NaCl-induced K^+ loss from Arabidopsis root and leaf cells by controlling plasma membrane K^+-permeable channels. Plant Physiology 141: 1653-1665.

Shahbaz, M. and Ashraf, M. 2013. Improving salinity tolerance in cereals. Critical Reviews in Plant Sciences 32: 237-249.

Shahid, S.A., Zaman, M. and Heng, L. 2018. Soil salinity: historical perspectives and a world overview of the problem. In Guideline for salinity assessment, mitigation and adaptation using nuclear and related techniques. L. Heng, M. Zaman, and S. A (Eds). Shahid. Cham: Springer.

Shi, H., Ishitani, M., Kim, C. and Zhu, J.K. 2000. The *Arabidopsis thaliana* salt tolerance gene SOS1 encodes a putative Na^+/H^+ antiporter. Proceedings of the National Academy of Sciences of the United States of America 97: 6896-6901.

Shivaraj, S.M., Deshmukh, R.K., Rai, R., Bélanger, R., Agrawal, P.K. and Dash, P.K. 2017. Genome-wide identification, characterization, and expression profile of aquaporin gene family in flax (*Linum usitatissimum*). Scientific Reports, 7: 46137.

Shrivastava, P. and Kumar, R., 2015. Soil salinity: a serious environmental issue and plant growth promoting bacteria as one of the tools for its alleviation. Saudi Journal of Biological Sciences 22: 123-131.

Silva, C., Martínez, V. and Carvajal, M. 2008. Osmotic versus toxic effects of NaCl on pepper plants. Biologia Plantarum 52: 72-79.

Skalak, J., Nicolas, K. L., Vankova, R. and Hejatko, J. 2021. Signal integration in plant abiotic stress responses via multistep phosphorelay signaling. Frontiers in Plant Science 12: 644823.

Smith, J.L. and J.W. Doran. 1996. Measurement and use of pH and electrical conductivity for soil quality analysis. In J.W. Doran and A.J. Jones (ed.) Methods for assessing soil quality. Soil Science Society of America Spec. Publ. 49. SSSA, Madison, WI, pp. 169-185.

Smith, S.E. and Read, D.J. 2008. Mycorrhizal Symbiosis. 3rd Edition, Academic Press, Cambridge.

Sorieul, M., Santoni, V., Maurel, C. and Luu, D.T., 2011. Mechanisms and effects of retention of over-expressed aquaporin AtPIP2;1 in the endoplasmic reticulum. Traffic: 473-482.

Sparks, T.H. and Carey, P.D. 1995. The responses of species to climate over two centuries: an analysis of the Marsham phenological record, 1736-1947. Journal of Ecology 83: 321-329.

Stepien, P. and Johnson, G.N. 2009. Contrasting responses of photosynthesis to salt stress in the glycophyte Arabidopsis and the halophyte *Thellungiella*: role of the plastid terminal oxidase as an alternative electron sink. Plant Physiology 149: 1154-1165.

Steudle, E. and Meshcheryakov, A.B. 1996. Hydraulic and osmotic properties of oak roots. Journal of Experimental Botany 47: 387-401.

Steudle, E. and Peterson C.A. 1998. How does water get through roots? Journal of Experimental Botany 49: 775-788.

Sultana, N., Ikeda, T. and Kashem, M.A. 2001. Effect of foliar spray of nutrient solutions on photosynthesis, dry matter accumulation and yield in seawater-stressed rice. Environmental and Experimental Botany 46: 129-140.

Sun, J., Chen, S.L., Dai, S.X., Wang, R.G., Li, N.Y., Shen, X. and Zhang, Z.K. 2009. Ion flux profiles and plant ion homeostasis control under salt stress. Plant Signaling & Behavior 4: 261-264.

Sun, J.Y., Liu, X.S., Khan, I.U., Wu, X.C. and Yang, Z.M. 2021. OsPIP2;3 as an aquaporin contributes to rice resistance to water deficit but not to salt stress, Environmental and Experimental Botany183: 104342.

Sutka, M., Amodeo, G. and Ozu, M. 2017. Plant and animal aquaporins crosstalk: what can be revealed from distinct perspectives. Biophysical Reviews 9:545–562.

Sutka, M., Li, G., Boudet, J., Boursiac, Y., Doumas, P. and Maurel, C. 2011. Natural variation of root hydraulics in Arabidopsis grown in normal and salt-stressed conditions. Plant Physiology 155: 1264-1276.

Szabados, L. and Savoure, A. 2010. Proline: a multifunctional amino acid. Trends in Plant Science 15: 89-97.

Szabados, L., Kovács, H., Zilberstein, A. and Bouchereau, A. 2011. Plants in extreme environments: importance of protective compounds in stress tolerance. Advances in Botanical Research 57: 105-150.

Tada, Y., Komatsubara, S. and Kurusu, T. 2014. Growth and physiological adaptation of whole plants and cultured cells from a halophyte turf grass under salt stress. AoB Plants plu041.

Taji, T., Seki, M., Satou, M., Sakurai, T., Kobayashi, M., Ishiyama, K., Narusaka, Y., Narusaka, M., Zhu, J.K. and Shinozaki, K. 2004. Comparative genomics in salt tolerance between Arabidopsis and Arabidopsis-related halophyte salt cress using Arabidopsis microarray. Plant Physiology 135: 1697-1709.

Takano, J., Wada, M., Ludewig, U., Schaaf, G., Von Wirén, N. and Fujiwara, T. 2006. The Arabidopsis major intrinsic protein NIP5;1 is essential for efficient boron uptake and plant development under boron limitation. The Plant Cell 18: 1498-1509.

Tan, W.K., Lin, Q., Lim, T.M., Kumar, P. and Loh, C.S. 2013. Dynamic secretion changes in the salt glands of the mangrove tree species *Avicennia officinalis* in response to a changing saline environment. Plant, Cell & Environment 36: 1410-1422.

Tan, X., Xu, H., Khan, S., Equiza, M.A., Lee, S.H., Vaziriyeganeh, M. and Zwiazek, J.J. (2018). Plant water transport and aquaporins in oxygen-deprived environments. Journal of Plant Physiology 227: 20-30.

Tanji, K.K. 1990. Nature and extent of agricultural salinity. In Agricultural salinity assessment and management. Edited by K.K. Tanji. ASCE Manuals and Reports on Engineering Practice No. 71. American Society of Civil Engineers New York, pp. 1-17.

Tarasoff, C.S., Ball, D.A. and Mallory-Smith, C.A. 2007. Extreme ionic and temperature effects on germination of weeping alkaligrass (*Puccinellia distans*), Nuttall's alkaligrass (*Puccinellia nuttalliana*) and Kentucky bluegrass (*Poa pratensis*). Weed Science 55: 305-310.

Tester, M., Davenport, R. 2003. Na^+ tolerance and Na^+ transport in higher plants. Annals of Botany 91: 503-527.

Thomas, D.S.G. and Middleton, N.J. 1993. Salinization: new perspectives on a major desertification issue. Journal of Arid Environments 24: 95-105.

Tomos, A.D. and Leigh R.A. 1999. The pressure probe: a versatile tool in plant cell physiology. Annual Review of Plant Physiology and Plant Molecular Biology 50: 447-472.

Törnroth-Horsefield, S., Wang, Y., Hedfalk, K., Johanson, U., Karlsson, M., Tajkhorshid, E., Neutze, R. and Kjellbom, P. 2006. Structural mechanism of plant aquaporin gating. Nature, 439: 688–694.

Tran, S.T., Horie, T., Imran, S., Qiu, J., McGaughey, S., Byrt, C.S., Tyerman, S.D. and Katsuhara, M. 2020. A survey of barley PIP aquaporin ionic conductance reveals Ca^{2+}-sensitive *HVPIP2;8* Na^+ and K^+ conductance. International Journal of Molecular Sciences, 21: 7135.

Tran, S.T.H., Imran, S., Horie, T., Qiu, J., McGaughey, S., Byrt, C.S., Tyerman, S.D. and Katsuhara, M. 2020. A survey of barley PIP aquaporin ionic conductance reveals Ca^{2+}-sensitive *HvPIP2;8* Na^+ and K^+ conductance. International Journal of Molecular Sciences 21: 7135.

Trapnell, C., Williams, B.A., Pertea, G., Mortazavi, A., Kwan, G., van Baren, M.J., Salzberg, S.L., Wold, B.J. and Pachter, L. 2010. Transcript assembly and quantification by RNA-Seq reveals unannotated transcripts and isoform switching during cell differentiation. Nature Biotechnology 28: 511-515.

Turner, N.C., Abbo, S., Berger, J.D., Chaturvedi, S.K., French, R.J., Ludwig, C., Mannur, D.M., Singh, S.J. and Yadava, H.S. 2007. Osmotic adjustment in chickpea (*Cicer arietinum* L.) results in no yield benefit under terminal drought. Journal of Experimental Botany 58: 187-194.

Tyerman, S.D., McGaughey, S.A., Qiu, J., Yool, A.J. and Byrt, C.S. 2021. Adaptable and multifunctional ion-conducting aquaporins. Annual Review of Plant Biology 72: 8.1-8.34.

Ueda, M., Tsutsumi, N. and Fujimoto, M. 2016. Salt stress induces internalization of plasma membrane aquaporin into the vacuole in *Arabidopsis thaliana*. Biochemical and Biophysical Research Communications 474: 742-746.

Uehlein, N., Lovisolo, C., Siefritz, F. and Kaldenhoff, R. 2003. The tobacco aquaporin NtAQP1 is a membrane CO_2 pore with physiological functions. Nature 425: 734–737.

Ungar, I.A. 1974. Inland halophytes of the United States. - In: Ecology of halophytes. Edited by R.J. Reimold and W.H. Queen. Academic Press, New York, pp. 235-305.

United States Salinity Laboratory Staff. 1954. Diagnosis and Improvement of Saline and Alkali Soils Agriculture Handbook No. 60. United States Department of Agriculture, 159 pp.

Vaipai, M., Mukherjee, M., Sankaramakrisnan, R, 2018 Cooperativity in plasma membrane intrinsic proteins (PIPs): mechanism of increased water transport in maize PIP1 channels in hetero-tetramers. Scientific Reports 8: 12055.

Vandeleur, R.K., Sullivan, W., Athman, A., Jordans, C., Gilliham, M., Kaiser, B.N. and Tyerman, S.D. 2014. Rapid shoot-to-root signaling regulates root hydraulic conductance via aquaporins. Plant, Cell & Environment 37: 520-538.

Vaziriyeganeh, M. 2017. Physiological responses of glycophytic and halophytic grasses *Poa pratensis*, *Poa juncifolia*, and *Puccinellia nuttalliana* to salt stress. MSc Thesis, University of Alberta, Edmonton, AB, Canada, 91 pp.

Vaziriyeganeh M., Carvajal M., Du N. and Zwiazek J.J. 2022. Salinity tolerance of halophytic grass *Puccinellia nuttalli*ana is associated with enhancement of aquaporin-mediated water transport by sodium. International Journal of Molecular Sciences 23: 5732.

Vaziriyeganeh, M., Khan, S. and Zwiazek, J.J. 2021. Transcriptome and metabolome analyses reveal potential salt tolerance mechanisms contributing to maintenance of water balance by the halophytic grass *Puccinellia nuttalliana*. Frontiers in Plant Science 12: 760863.

Vaziriyeganeh, M., Lee, S.H. and Zwiazek, J.J. 2018. Water transport properties of root cells contribute to salt tolerance in halophytic grasses *Poa juncifolia* and *Puccinellia nuttalliana*. Plant Science 276:54-62.

Vera-Estrella, R., Barkla, B.J., Bohnert, H.J. and Pantoja, O. 2004. Novel regulation of aquaporins during osmotic stress. Plant Physiology, 135, pp.2318-2329.

Vicente, O., Boscaiu, M., Naranjo, M.Á., Estrelles, E., Bellés, J.M. and Soriano, P., 2004. Responses to salt stress in the halophyte *Plantago crassifolia* (Plantaginaceae). Journal of Arid Environments 58: 463-481.

Vitali, V., Bellati, J., Soto, G., Ayub, N.D. and Amodeo, G. 2015. Root hydraulic conductivity and adjustments in stomatal conductance: hydraulic strategy in response to salt stress in a halotolerant species. AoB Plants 7: plv136.

Voicu, M.C., Cooke, J.E. and Zwiazek, J.J. 2009. Aquaporin gene expression and apoplastic water flow in bur oak (*Quercus macrocarpa*) leaves in relation to the light response of leaf hydraulic conductance. Journal of Experimental Botany 60: 4063-4075.

Volkov, V. and Amtmann, A. 2006. *Thellungiella halophila*, a salt-tolerant relative of *Arabidopsis thaliana*, has specific root ion-channel features supporting K^+/Na^+ homeostasis under salinity stress. Plant Journal 48: 342-353.

Volkov, V. and Flowers, T.J. 2019, Mechanisms of ion transport in halophytes: from roots to leaves. In Gul, B., Böer, B., Khan, A., Clüsener-Godt, M., Hameed, A. (Eds). Tasks for Vegetation Science – 49. Shabkha Ecosystems, Volume VI: Asia/Pacific. Springer Nature Switzerland AG, Cham, Switzerland, pp. 125-150.

Volkov V., Wang, B., Dominy, P.J., Fricke, W. and Amtmann, A. 2004. *Thellungiella halophila*, a salt-tolerant relative of *Arabidopsis thaliana*, possesses effective mechanisms to discriminate between potassium and sodium. Plant, Cell & Environment 27: 1-14.

Waidmann, S., Kusenda, B., Mayerhofer, J., Mechtler, K. and Jonak, C. 2014. A DEK domain-containing protein modulates chromatin structure and function in Arabidopsis. Plant Cell 26: 4328-4344.

Wan, X. and Zwiazek, J.J. 1999. Mercuric chloride effects on root water transport in aspen (*Populus tremuloides*) seedlings. Plant Physiology 121: 939-946.

Wang, B., Lüttge, U. and Ratajczak, R. 2001. Effects of salt treatment and osmotic stress on V-ATPase and V-PPase in leaves of the halophyte *Suaeda salsa*. Journal of Experimental Botany 52: 2355-2365.

Wang, D., Grieve, C.M. and Suarez, D.L. 2005. Composition of irrigation water salinity affects growth characteristics and uptake of selenium and salt ions by soybean. Journal of Plant Nutrition 28: 1073-1088.

Wang, H., Schoebel, S., Schmitz, F., Dong, H. and Hedfalk, K. 2020. Characterization of aquaporin-driven hydrogen peroxide transport. BBA – Biomembranes 1862: 183065.

Wang, J.P., Matthews, M.L., Williams, C.M., Shi, R., Yang, C., Tunlaya-Anukit, S., Chen, H.C., et al. 2018a. Improving wood properties for wood utilization through multi-omics integration in lignin biosynthesis. Nature Communications 9: 1579.

Wang, M., Ding, L., Gao, L., Li, Y., Shen, Q. and Guo, S. 2016. The interactions of aquaporins and mineral nutrients in higher plants. International Journal of Molecular Sciences 17:1229.

Wang, Y., Jiang, L., Chen, J., Tao, L., An, Y., Cai, H. and Guo, C. 2018b. Overexpression of the alfalfa WRKY11 gene enhances salt tolerance in soybean. PLoS One 13: e0192382.

Wang, Z.L., Li, P.H., Fredricksen, M., Gong, Z.Z., Kim, C.S., Zhang, C., Bohnert, H.J., Zhu, J.K. and Bressan, R.A. 2004. Hasegawa PM: Expressed sequence tags from *Thellungiella halophila*, a new model to study plant salt-tolerance. Plant Science 166: 609-616.

Waszczak, C., Carmody, M. and Kangasjarvi, J. 2018. Reactive oxygen species in plant signaling. Annual Review of Plant Biology 69: 209-236.

Wei, H., Li, J., Peng, Z., Lu, B., Zhao, Z. and Yang, W. 2008. Relationships of *Aegilops tauschii* revealed by DNA fingerprints: The evidence for agriculture exchange between China and the West. Progress in Natural Science 18: 1525–1531.

Wheeler, B.D. 2005. Water and plants in freshwater wetlands. In Eco-hydrology: plants and water in terrestrial and aquatic environments. Edited by A.J. Baird and R.L. Wilby. Routledge, Milton Park, Abington, UK, pp. 127-180.

White, P.J. and Broadley, M.R. 2001. Chloride in soils and its uptake and movement within the plant: a review. Annals of Botany 88: 967-988.

Wu, J., Yan, G., Duan, Z., Wang, Z., Kang, C., Guo, L., Liu, K., Tu, J., Shen, J., Yi, B., Fu, T., Li, X., Ma, C. and Dai, C. 2020. Roles of the *Brassica napus* DELLA protein BnaA6.RGA, in modulating drought tolerance by interacting with the ABA signaling component. Frontiers in Plant Science 11: 577.

Xie, M., Zhang, J., Tschaplinski, T.J., Tuskan, G.A., Chen, J.G. and Muchero, W. 2018. Regulation of lignin biosynthesis and its role in growth-defense tradeoffs. Frontiers in Plant Science 9: 1427.

Xiong, H., Guo, H., Xie, Y., Zhao, L., Gu, J., Zhao, S., Li, J. and Liu, L. 2017. RNAseq analysis reveals pathways and candidate genes associated with salinity tolerance in a spaceflight-induced wheat mutant. Scientific Reports 7: 2731.

Xiong, Y., Yan, H., Liang, H., Zhang, Y., Guo, B., Niu, M., Jian, et al. 2019. RNA-Seq analysis of *Clerodendrum inerme* (L.) roots in response to salt stress. BMC Genomics 20: 724.

Xu, B., Waters, S., Byrt,C.S., Plett, D., Tyerman, S.D., Tester, M., Munns, R., Hrmova, M. and Gilliham, M. 2018. Structural variations in wheat HKT1;5 underpin differences in Na^+ transport capacity. Cellular and Molecular Life Sciences 75: 1133-1144.

Xu, H., Kemppainen, M., El Kayal, W., Lee, S.H., Pardo, A.G., Cooke, J.E.K. and Zwiazek J.J. 2015. Overexpression of *Laccaria bicolor* aquaporin *JQ585595* alters root water transport

properties in ectomycorrhizal white spruce (*Picea glauca*) seedlings. New Phytologist 205: 757-770.

Yamaguchi, M., Valliyodan, B., Zhang, J., Lenoble, M.E., Yu, O., Rogers, E.E., Nguyen, H.T. and Sharp, R.E. 2010. Regulation of growth response to water stress in the soybean primary root. I. Proteomic analysis reveals region-specific regulation of phenylpropanoid metabolism and control of free iron in the elongation zone. Plant, Cell & Environment 33: 223-243.

Yamamoto, N., Takano, T., Tanaka, K., Ishige, T., Terashima, S., Endo, C., Kurusu, T., Yajima, S., Yano, K., et al. 2015. Comprehensive analysis of transcriptome response to salinity stress in the halophytic turf grass *Sporobolus virginicus*. Frontiers in Plant Science 6: 241.

Yadav, S., Irfan, M., Ahmad, A. and Hayat, S. 2011. Causes of salinity and plant manifestations to salt stress: a review. Journal of Environmental Biology 32: 667-685.

Yaneff, A., Sigaut, L., Marquez, M., Alleva, K., Pietrasanta, L.I. and Amodeo, G. 2014. Heteromerization of PIP aquaporins affects their intrinsic permeability. Proceedings of the National Academy of Sciences of the United States of America 111: 231-236.

Yang, Y. and Guo, Y. 2018. Unraveling salt stress signaling in plants. Journal of Integrative Plant Biology 60: 796-804.

Yang, M.F., Song, J., and Wang, B.S. 2010. Organ-specific responses of vacuolar H-ATPase in the shoots and roots of C halophyte *Suaeda salsa* to NaCl. Journal of Integrative Plant Biology 52: 308-314.

Yao, X., Nie, J., Bai, R. and Sui, X. 2020. Amino acid transporters in plants: identification and function. Plants 9: 972.

Yepes-Molina, L., Bárzana, G. and Carvajal, M. 2020. Controversial regulation of gene expression and protein transduction of aquaporins under drought and salinity stress. Plants, 9: 1662.

Yokoi, S., Quintero, F. J., Cubero, B., Ruiz, M. T., Bressan, R. A., Hasegawa, P. M. and Pardo, J. M. 2002. Differential expression and function of *Arabidopsis thaliana* NHX Na^+/H^+ antiporters in the salt stress response. Plant Journal 30: 529-539.

Yu, L., Nie, J., Cao, C., Jin, Y., Yan, M., Wang, F., Liu, J., Xiao, Y., Liang, Y. and Zhang, W. 2010. Phosphatidic acid mediates salt stress response by regulation of MPK6 in *Arabidopsis thaliana*. New Phytologist 188: 762-773.

Yuan, F., Leng, B. and Wang B. 2016. Progress in studying salt secretion from the salt glands in recretohalophytes: how do plants secrete salt? Frontiers in Plant Science 7: 977.

Yuan, F., Xu, Y., Leng, B. and Wang, B. 2019. Beneficial effects of salt on halophyte growth: morphology, cells, and genes. Open Life Sciences 14: 191-200.

Yukutake, Y., Tsuji, S., Hirano, Y., Adachi, T., Takahashi, T., Fujihara, K., Agre, P., Yasui, M. and Suematsu, M. 2008. Mercury chloride decreases the water permeability of aquaporin-4-reconstituted proteoliposomes. Biology of the Cell, 100: 355-363.

Zaman, M., Shahid, S.A. and Heng. L. 2018. Guideline for salinity assessment, mitigation and adaptation using nuclear and related techniques. Springer Open, Cham, Switzerland.

Zelazny, E., Borst, J.W., Muylaert, M., Batoko, H., Hemminga, M.A. and Chaumont, F., 2007. FRET imaging in living maize cells reveals that plasma membrane aquaporins interact to regulate their subcellular localization. Proceedings of the National Academy of Sciences of the United States of America 104: 12359-12364.

Zhang, G.W., Xu, S.C., Hu, Q.Z., Mao, W.H. and Gong, Y.M. 2014. Putrescine plays a positive role in salt-tolerance mechanisms by reducing oxidative damage in roots of vegetable soybean. Journal of Integrative Agriculture 13: 349-357.

Zhang, L., Tan, Q., Lee, R., Trethewy, A., Lee, Y.H. and Tegeder, M. 2010. Altered xylem-phloem transfer of amino acids affects metabolism and leads to increased seed yield and oil content in Arabidopsis. Plant Cell 22: 3603-3620.

Zhang, W.-Q., Fleurial, K., Sherr, I., Vassov, R. and Zwiazek, J.J. 2020. Growth and physiological responses of tree seedlings to oil sands non-segregated tailings. Environmental Pollution 259: 113945.

Zhang, Y., Fei, S., Xu, Y., He, Y., Zhu, Z. and Liu, Y. 2022. The structure, function and expression analysis of the nodulin 26-like intrinsic protein subfamily of plant aquaporins in tomato. Scientific Reports 12: 9180.

Zhao. F., Song, C.-P., He, J. and Zhu, H. 2007. Polyamines improve K^+/Na^+ homeostasis in barley seedlings by regulating root ion channel activities. Plant Physiology 145: 1061-1072.

Zhao, L., Yang, Z., Guo, Q., Mao, S., Li, S., Sun, F., Wang, H. and Yang, C. 2017. Transcriptomic profiling and physiological responses of halophyte *Kochia sieversiana* provide insights into salt tolerance. Frontiers in Plant Science 8: 1985.

Zhu, C., Schraut, D., Hartung, W. and Schäffner, A.R. 2005. Differential responses of maize MIP genes to salt stress and ABA. Journal of Experimental Botany 56: 2971-2981.

Zhu, J.K. 2002. Salt and drought stress signal transduction in plants. Annual Review of Plant Biology 53: 247-273.

Zhu, J., Brown, K.M. and Lynch, J.P. 2010. Root cortical aerenchyma improves the drought tolerance of maize (*Zea mays* L.). Plant, Cell & Environment 33: 740-749.

Zhu, J.K., Liu, J. and Xiong, L. 1998. Genetic analysis of salt tolerance in Arabidopsis. Evidence for a critical role of potassium nutrition. Plant Cell 10: 1181-1191.

Zhu, Y., Yang, L., Liu, N., Yang, J., Zhou, X., Xia, Y., He, Y., He, Y., Gong, H., Ma, D. and Yin, J. 2019. Genome-wide identification, structure characterization, and expression pattern profiling of aquaporin gene family in cucumber. BMC Plant Biology 19: 345.

Zhu, Y.X., Gong, H.J. and Yin, J.L. 2019. Role of silicon in mediating salt tolerance in plants: a review. Plants 8: 147.

Zwiazek, J.J., Tan, X., Xu, H., Navarro-Ródenas, A. and Morte, A. 2017. Significance of oxygen transport through aquaporins. Scientific Reports 17: 40411.

Zwiazek. J.J., Equiza. M.A., Karst. J., Senorans. J., Wartenbe. M. and Calvo-Polanco M. 2019. Role of urban ectomycorrhizal fungi in improving the tolerance of lodgepole pine (*Pinus contorta*) seedlings to salt stress. Mycorrhiza 29: 303–312.

Zwiazek, J.J., Tan, X., Xu, H., Navarro-Ródenas, A. and Morte, A. 2017. Significance of oxygen transport through aquaporins. Scientific Reports 17: 40411.